IN-39
40355
P.119

NASA Contractor Report 187597

NONLINEAR DYNAMIC ANALYSIS OF FLEXIBLE MULTIBODY SYSTEMS

Olivier A. Bauchau and Nam Kook Kang

RENSSELAER POLYTECHNIC INSTITUTE
Troy, New York

Grant NAG1-1018
July 1991

National Aeronautics and
Space Administration

Langley Research Center
Hampton, Virginia 23665-5225

Abstract

Two approaches are developed to analyze the dynamic behavior of flexible multibody systems. In the first approach each body is modeled with a modal methodology in a local non-inertial frame of reference, whereas in the second approach, each body is modeled with a finite element methodology in the inertial frame. In both cases, the interaction among the various elastic bodies is represented by constraint equations. The two approaches have been compared for accuracy and efficiency: the first approach is preferable when the nonlinearities are not too strong but it becomes cumbersome and expensive to use when many modes must be used. The second approach is more general and easier to implement but could result in high computation cost for large system. The constraints should be enforced in a time derivative fashion for better accuracy and stability.

Chapter 1

Introduction.

A comprehensive analysis methodology for dynamic systems involving several elastic bodies must include a scheme to efficiently deal with the interaction between the various elastic components. For instance, in a conventional helicopter, the elastic rotor or rotors interact with the elastic fuselage, whereas in a tilt rotor configuration, the elastic rotors interact with the flexible wings and fuselage. The impact of this interaction is important to an accurate prediction of rotor loads, and essential when attempting to predict instabilities such as ground or air resonances since rigidly mounted rotors do not exhibit such instabilities. It is convenient to think of the helicopter as a multibody elastic system, i.e. a collection of elastic bodies mutually interacting at "hinges".

A fundamental difficulty in the analysis of a multibody system is the evaluation of its total kinetic energy, as it involves the calculation of the inertial velocity of each material point of the system. If the position of all material points is measured in a given inertial system, this task is trivial, however, it is often convenient to use a local coordinate system to represent the initial geometry and deformation of each elastic body. The velocity of a material point relative to this local frame is easily to obtain within the frame work of a finite element discretization or modal representation, however, the inertial velocity of this material point also involves the motion of the local frame with respect to an inertial frame of reference. This additional motion can be taken into account through various schemes, for instance hierarchical representations, or multibody schemes.

A hierarchical representation involves a hierarchy of reference frames starting with an inertial frame. The motion of each frame is described with respect to the frame that is immediately superior in the hierarchy. For a helicopter, a typical hierarchy could be as follows: inertial frame — to — airframe system — to — blade system — to — deformed blade system. Each level of the hierarchy involves a rotation matrix which gives the instantaneous position of a frame with respect to that immediately superior. Each rotation matrix is quadratic in terms of the Euler Parameters (other finite rotations parameters could be used but the rotation matrix will remain at least quadratic). Since our typical hierarchy involves four levels, the position and inertial velocity vectors of a material particle will involve nonlinear terms up to the 9th order, resulting in a kinetic energy expression with nonlinear terms up to the 18th order. Of course, some simplification could be introduced: for instance in level flight, the inertial — to — airframe transformation becomes a constant, or, if the elastic deformations of the blade are linearized, the blade — to — deformed blade transformation becomes linear. However, a general analysis methodology should be able to deal with large rotations at all levels.

This simple example points out the two major difficulties associated with hierarchical models: first, these models are difficult to handle and require advanced data base concepts for practical implementation, and second, very high order nonlinear terms appear in the analysis resulting in a very large number of coefficients. In a modal analysis, the number of coefficients is N^n, where N is the number of modes, and n the power of the

nonlinearities. For a 12 mode model involving 18th order nonlinearities $2.66\ 10^{19}$ terms will be generated, requiring $2.03\ 10^{14}$ Mbytes of storage on a computer. Of course the number of operations involved in manipulating the model grown accordingly. It is clear that such model are beyond the reach of even the most powerful computers, and would require exorbitant amounts of computation.

Two alternative approaches will be pursued in this work that avoid hierarchical representations. In both approaches, the dynamic system is modeled as a collection of flexible bodies (airframe, wings, blades, etc...) that are connected together at a number of points where kinematic constraints are enforced. Typical kinematic constraints are spherical, universal and convolute joints, or rigid links. In the first approach each elastic body is described in a local coordinate system which motion is directly related to an inertial frame through three rigid body translations and three rigid body rotations. Hence, the inertial position vector of any material particle in that elastic body involves a single rotation matrix only, allowing an easy evaluation of all inertia terms.

Since a local coordinate system is used, the elastic deformations of the body can be represented in a modal fashion, more specifically a finite element based modal analysis technique will be used which yields a Lagrangian expression involving quartic nonlinearities only.

In the second approach, all elastic bodies are described directly in a single inertial system. This is by far the simplest formulation, however, it rules out the use of a modal representation, and requires a parametrization of the finite rotation variables that allows arbitrarily large rotations (in this work the Milenkovic parameters are used.)

Chapter 2 presents a review of the beam model which will be used throughout this work. The next two chapters deals with the modeling of a single elastic body: Chapter 3 presents the modal reduction scheme for the finite element model, and chapter 4 compares the predictions of modal models with that of full finite element models. The kinematic constraints to be applied between elastic bodies is the focus of chapter 5. Chapter 6 briefly describes the full finite element modeling. Finally conclusions and recommendations are presented in chapter 7.

Chapter2

Finite Element Modeling of Rotor Blades

Section 2.1: Introduction

The kinematics involved in the nonlinear static and dynamic analysis of naturally curved and twisted blades are complex since both the deformed and undeformed configurations of a blade are three dimensional. Moreover, laminated composite materials are increasingly used for the construction of such structures, causing several non-classical effects of beam theory to become more pronounced [2–1,2].

In many applications, large displacements and rotations of the blade will occur; however, the strain level remains low. Fatigue life is indeed a major concern; hence, the operating strain level must remain well within the linear-elastic range of the material. As a result, most analyses [2–3,8] are based on a small strain assumption that considerably simplifies the formulation and resulting equations.

The small strain assumption has important implications. First, the Green-Lagrange strain components often used in the derivation of nonlinear kinematics [2–4,5] can be equated to the engineering strain components, and hence the usual stress-strain relationships of the material can be used. Second, the changes in surface area of a differential volume element due to deformation are neglible. Finally, the strain-displacement equations can be considerably simplified, since all second order terms (i.e., strain square terms) can be neglected.

In this chapter, consistent strain-displacement expressions are derived which provide the basis of the finite element approximation of the non-linear behavior of naturally curved and twisted blades undergoing arbitrarily large deflections and rotations.

Section 2.2: Geometry and Kinematics of Blade Elements

Consider a naturally curved and twisted beam depicted in Fig. 2.1.1 The triad $\vec{i}_1, \vec{i}_2, \vec{i}_3$ is fixed in space and the triad $\vec{e}_1, \vec{e}_2, \vec{e}_3$ is attached to a reference line along the axis of the beam. $\vec{e}_1$ is chosen tangent to the reference line and $\vec{e}_2$, $\vec{e}_3$ define the plane of the cross-section. The curvilinear coordinates along this triad are x_1, x_2, x_3 respectively.

The position vector of a particle of the beam in the undeformed configuration is:

$$\vec{r} = \vec{r}(x_1, x_2, x_3) \tag{2.2.1}$$

After deformation the same particle has a position vector:

$$\vec{R} = \vec{R}(x_1, x_2, x_3) \tag{2.2.2}$$

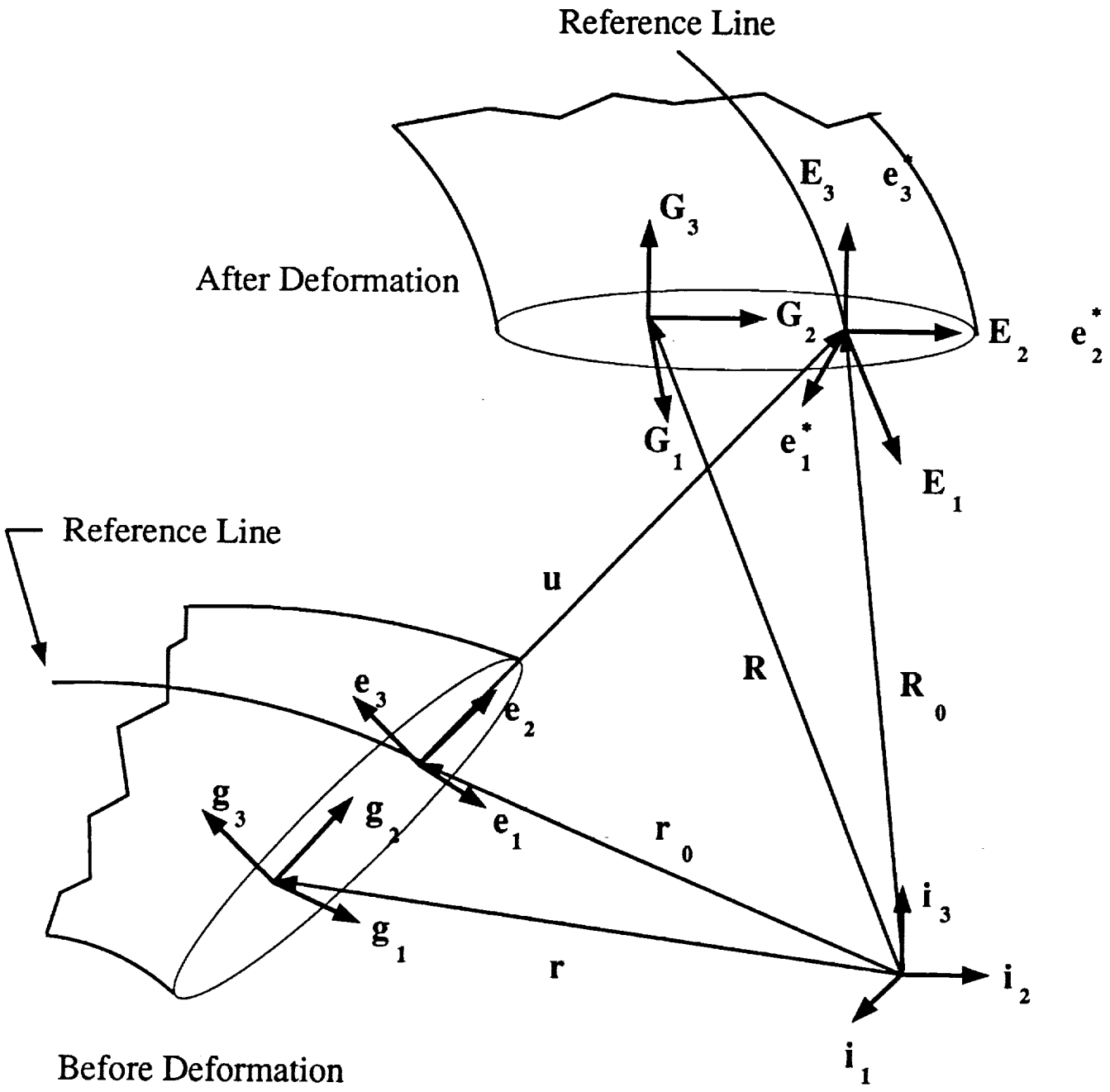

Figure 2.1.1. Geometry of the Beam Before and After Deformation

The corresponding vectors at the reference line are:

$$\begin{aligned} \vec{r_0} &= \vec{r_0}\ (x_1, 0, 0) \\ \vec{R_0} &= \vec{R_0}\ (x_1, 0, 0) \end{aligned} \tag{2.2.3}$$

and the displacement vector of the reference line is given by:

$$\vec{u} = \vec{R_0} - \vec{r_0} \tag{2.2.4}$$

The base vector [2–9,10] in the undeformed and deformed positions respectively are defined as:

$$\vec{g_i} = \vec{r_{,i}} \quad and \quad \vec{G_i} = \vec{R_{,i}} \tag{2.2.5}$$

where the notation $(.)_{,i}$ means derivative with respect to x_i. At the reference line the base vectors are:

$$\vec{e_i} = \vec{r_{0,i}} \quad and \quad \vec{E_i} = \vec{R_{0,i}} \tag{2.2.6}$$

$\vec{e_i}$ forms a triad since the derivatives in (2.2.6) are taken with respect to the natural coordinates of the beam. The triad $\vec{e_i}$ can be viewed as a rotation of the basic reference triad $\vec{i_i}$ through a given rotation matrix $t^T(x_1)$ such that :

$$\begin{bmatrix} \vec{e_1} \\ \vec{e_2} \\ \vec{e_3} \end{bmatrix} = t^T(x_1) \begin{bmatrix} \vec{i_1} \\ \vec{i_2} \\ \vec{i_3} \end{bmatrix} \tag{2.2.7}$$

The derivatives of this triad are readily calculated as :

$$\begin{bmatrix} \vec{e_1}' \\ \vec{e_2}' \\ \vec{e_3}' \end{bmatrix} = \begin{bmatrix} 0 & k_3 & -k_2 \\ -k_3 & 0 & k_1 \\ k_2 & -k_1 & o \end{bmatrix} \begin{bmatrix} \vec{e_1} \\ \vec{e_2} \\ \vec{e_3} \end{bmatrix} \tag{2.2.8}$$

where the notation $()'$ means derivative with respect to x_1; k_1 is the natural twist (or pre-twist), k_2 and k_3 are the natural curvatures (or pre-bends) of the beam. The position vector $\vec{r}$ of an arbitrary point of the beam can now be written as:

$$\vec{r} = \vec{r_0} + x_2\vec{e_2} + x_3\vec{e_3} \tag{2.2.9}$$

hence the base vectors become:

$$\begin{aligned} \vec{g_1} &= \sqrt{g}\,\vec{e}_1 - x_3k_1\vec{e_2} + x_2k_1\vec{e_3} \\ \vec{g_2} &= \vec{e_2} \\ \vec{g_3} &= \vec{e_3} \end{aligned} \tag{2.2.10}$$

where

$$\sqrt{g} = 1 - x_2\,k_3 + x_3k_2 \tag{2.2.11}$$

The metric tensor is obtained as $g_{ij} = \vec{g_i} \cdot \vec{g_j}$ and its determinant is g.

The fundamental assumption in beam theory is that the cross-section does not deform in its own plane. This means that the base vector $\vec{E}_2$ and $\vec{E}_3$ which are in the plane of the cross-section after deformation simply correspond to a translation and rotation of the base vector $\vec{e}_2$ and $\vec{e}_3$ of the original configuration. Note that arbitrarily large displacements and rotations can occur but no deformation of the cross-section is allowed i.e. $\vec{E}_2$ and $\vec{E}_3$ are mutually orthogonal unit vectors. In contrast, $\vec{E}_1$ is no longer a unit vector nor is it orthogonal to $\vec{E}_2$ and $\vec{E}_3$, as axial and shearing strains are allowed. Now a new orthogonal triad $\vec{e}_i^*$ is defined as follows:

$$\begin{aligned} \vec{e}_2^* &= \vec{E}_2 \\ \vec{e}_3^* &= \vec{E}_3 \\ \vec{e}_1^* &= \vec{e}_2^* \times \vec{e}_3^* \end{aligned} \tag{2.2.12}$$

The vector $\vec{E}_1$ can be resolved in this triad as:

$$\vec{E}_1 = (1 + \bar{e}_{11})\,\vec{e}_1^* + 2\bar{e}_{12}\vec{e}_2^* + 2\bar{e}_{13}\vec{e}_3^* \tag{2.2.13}$$

At this point, $\overline{e_{11}}$, $\overline{e_{12}}$, $\overline{e_{13}}$ are the unknowns, and they will be identified later as strain quantities. Here again the triad $\vec{e}_i^*$ can be related to the basic reference triad $\vec{i}_i$ through an unknown rotation matrix $T_e(x_1)$ such that:

$$\begin{bmatrix} \vec{e}_1^* \\ \vec{e}_2^* \\ \vec{e}_3^* \end{bmatrix} = T_e^T(x_1) \begin{bmatrix} \vec{i}_1 \\ \vec{i}_2 \\ \vec{i}_3 \end{bmatrix} \tag{2.2.14}$$

The derivatives of this triad are:

$$\begin{vmatrix} \vec{e}_1^{*\prime} \\ \vec{e}_2^{*\prime} \\ \vec{e}_3^{*\prime} \end{vmatrix} = \tilde{K}^T \begin{vmatrix} \vec{e}_1^* \\ \vec{e}_2^* \\ \vec{e}_3^* \end{vmatrix} = \begin{bmatrix} 0 & K_3 & -K_2 \\ -K_3 & 0 & K_1 \\ K_2 & -K_1 & 0 \end{bmatrix} \begin{vmatrix} \vec{e}_1^* \\ \vec{e}_2^* \\ \vec{e}_3^* \end{vmatrix} \tag{2.2.15}$$

where K_1 is the twist, K_2 and K_3 are the curvatures of the deformed beam. Since the cross-section does not deform in its own plane, the position vector $\vec{R}$ in the deformed configuration can be written as:

$$\vec{R} = \vec{R}_0 + x_2\vec{E}_2 + x_3\vec{E}_3 + \delta(x_1)\,\varphi_1(x_2, x_3)\,\vec{e}_1^* \tag{2.2.16}$$

The first three terms represent large translations and rotations of the cross-section and can be geometrically interpreted as plane sections remaining plane, but not necessarily normal to deformed axis of the beam(i.e. a Timoshenko Beam Theory). The last term represents a small displacement in the direction of $\vec{e}_1^*$, that is out of plane warping of the cross-section chosen as the torsion related warping displacement φ_1. This warping displacement is selected as the Saint-Venant torsional warping functions[2–1]. $\delta(x_1)$ is an unknown function characterizing the magnitude of the torsional warping. Combining

(2.2.5), (2.2.6), (2.2.13) and (2.2.15), the base vectors of the deformed configuration become:

$$\begin{aligned}\vec{G}_1 &= \left[(1+\bar{e}_{11}) - x_2K_3 + x_3K_2 + \delta'\varphi_1\right]\vec{e}_1^* + \left[2\bar{e}_{12} - x_3K_1\right]\vec{e}_2^* \\ &\quad + \left[2\bar{e}_{13} + x_2K_1\right]\vec{e}_3^* \\ \vec{G}_2 &= \delta\varphi_{1,2}\vec{e}_1^* + \vec{e}_2^* \\ \vec{G}_3 &= \delta\varphi_{1,3}\vec{e}_1^* + \vec{e}_3^*\end{aligned} \tag{2.2.17}$$

In (2.2.17), all higher terms containing warping quantities have been neglected.

Section 2.3: Strain Analysis

The Green-Lagrange strains f_{ij} in the curvilinear coordinate system [2–9,10] are given as $f_{ij} = \frac{1}{2}(G_{ij} - g_{ij})$ where $G_{ij} = \vec{G}_i \cdot \vec{G}_j$ is the metric tensor in the deformed configuration. It is straightforward to verify that $f_{22} = f_{33} = f_{23} = 0$ as a direct implication of the indeformability of the cross-section in its own plane. The other strain compoments are the two transverse shearing strains f_{12} and f_{13} , and the axial strain f_{11}. To relate these strains to the strains in the local rectangular coordinate system defined on the beam axis, the following transformation is needed. Define a local rectangular cartesian coordinate system y_i along $\vec{e}_i$, then the relation of this rectangular system with the material coordinate system x_j is governed by:

$$\frac{\partial y_i}{\partial x_j} = \begin{bmatrix} \sqrt{g} & 0 & 0 \\ -x_3k_1 & 1 & 0 \\ x_2k_1 & 0 & 1 \end{bmatrix} \tag{2.3.1}$$

Now, the strains e_{ij} defined in the local rectangular coordinate system $\vec{e}_i$ are obtained as:

$$e_{ij} = \frac{\partial x_k \partial x_l}{\partial y_i \partial y_j} f_{kl} \tag{2.3.2}$$

Then, the non-vanishing strain components become:

$$\begin{aligned}\sqrt{g}e_{12} &= f_{12} \\ \sqrt{g}e_{13} &= f_{13} \\ \sqrt{g}e_{11} &= f_{11} + 2x_3k_1f_{12} - 2x_2k_1f_{13}\end{aligned} \tag{2.3.3}$$

The initial curvatures of the beam k_2 and k_3 are now assumed to be small, i.e. from (2.2.11):

$$\sqrt{g} \approx 1 \tag{2.3.4}$$

In the case of helicopter blade,

$$\begin{aligned}x_2k_3 &= \frac{chord\,of\,the\,blade}{radius\,of\,the\,edgewise\,curvature} \approx 0 \\ x_3k_2 &= \frac{thickness\,of\,the\,blade}{radius\,of\,the\,flapwise\,curvature} \approx 0\end{aligned}$$

Note that $\sqrt{g} = 1$ for a straight blade. Hence, this assumption is realistic for most of the practical applications.

The strain components now become:

$$2e_{12} = 2\bar{e}_{12} - x_3\kappa_1 + \delta\varphi_{1,2} \tag{2.3.5}$$

$$2e_{13} = 2\bar{e}_{12} + x_2\kappa_1 + \delta\varphi_{1,3} \tag{2.3.6}$$

$$\begin{aligned} e_{11} =& \bar{e}_{11} + \frac{1}{2}\bar{e}_{11}^2 - x_2\left(1+\bar{e}_{11}\right)\kappa_3 + x_3\left(1+\bar{e}_{11}\right)\kappa_2 + \delta'\varphi_1 + \delta k_1\left(x_3\varphi_{1,2} - x_2\varphi_{1,3}\right) \\ &+ \frac{1}{2}\left(2\bar{e}_{12} - x_3\kappa_1\right)^2 + \frac{1}{2}\left(2\bar{e}_{13} + x_2\kappa_1\right)^2 + \frac{1}{2}\left(x_2k_3 - x_3\kappa_2\right)^2 \end{aligned} \tag{2.3.7}$$

where $\kappa_i = K_i - k_i$

To complete the formulation, the coefficients $\overline{e_{11}}$, $\overline{e_{12}}$, $\overline{e_{13}}$ in (2.2.13) must now be related to the displacements and rotations. Differentiating (2.2.4) with respect to x_1 and using (2.2.6), we obtain:

$$\vec{E}_1 = \vec{e}_1 + \vec{u}' \tag{2.3.8}$$

or

$$\vec{E}_1 = \left(u_1' + t_{11}\right)\vec{i}_1 + \left(u_2' + t_{21}\right)\vec{i}_2 + \left(u_3' + t_{31}\right)\vec{i}_3 \tag{2.3.9}$$

where u_i are the components of the displacement vector in the basic reference triad $\vec{i}_i$, and t_{ij} the components of the rotation matrix t. On the other hand, combining (2.2.13) and (2.2.14) yields another relation for $\vec{E}_1$ that can be identified with (2.3.9) to obtain

$$\begin{bmatrix} 1+\bar{e}_{11} \\ 2\bar{e}_{12} \\ 2\bar{e}_{13} \end{bmatrix} = T_e^T \begin{bmatrix} u_1' + t_{11} \\ u_2' + t_{21} \\ u_3' + t_{31} \end{bmatrix} \tag{2.3.10}$$

This completes the strain analysis. It is important to note that this development is valid for arbitrarily large displacements, rotations and strains. The unknowns of the problem are the three displacements u_i, the rotation parameters implicitly defined in the rotation matrix T_e, and torsional warping amplitude.

In the derivation of strain expressions in (2.3.5–7), no assumptions were made about the magnitudes of the displacements, rotations or strains; hence, these expressions are valid for beams with small initial curvatures undergoing arbitrarily large displacements, rotations and strains. On the other hand, later in the derivation of the total potential energy expression in (2.4.17), strain components will be assumed small enough to render negligible changes in area due to deformation, and to equate the Green-Lagrange strains to engineering strains. This requires both axial and shearing strains to be much smaller than unity, i.e. $\varepsilon << 1$, and $\gamma << 1$. However, nothing is assumed about the relative

magnitude of ε versus γ. For consistency, the same assumptions must now be introduced to the strain-displacement equations (2.3.5–7) to obtain:

$$\begin{aligned}\varepsilon_{11} =& \bar{e}_{11} - x_2\kappa_3 + x_3\kappa_2 + \delta'\varphi_1 + \delta k_1 (x_3\varphi_{1,2} - x_2\varphi_{1,3}) \\ &+ \frac{1}{2}(2\bar{e}_{12} - x_3\kappa_1)^2 + \frac{1}{2}(2\bar{e}_{13} + x_2\kappa_1)^2\end{aligned} \tag{2.3.11}$$

$$\gamma_{12} = 2\bar{e}_{12} - x_3 k_1 + \delta\varphi_{1,2} \tag{2.3.12}$$

$$\gamma_{13} = 2\bar{e}_{13} + x_2 k_1 + \delta\varphi_{1,3} \tag{2.3.13}$$

The last term appearing in (2.3.7) is negligible since it represents the square of the axial components due to bending.

If we now introduce the additional assumption that axial and shearing strains are of the same order of magnitude, then $\gamma^2 << \varepsilon$, and the two last terms in (2.3.11) can be neglected, since they are squares of the shearing strain components in (2.3.12) and (2.3.13), respectively; this yields:

$$\begin{aligned}\varepsilon_{11} &= \bar{e}_{11} - x_2\kappa_3 + x_3\kappa_2 + \delta'\varphi_1 + \delta k_1 (x_3\varphi_{1,2} - x_2\varphi_{1,3}) \\ \gamma_{12} &= 2\bar{e}_{12} - x_3\kappa_1 + \delta\varphi_{1,2} \\ \gamma_{13} &= 2\bar{e}_{13} + x_2\kappa_1 + \delta\varphi_{1,3}\end{aligned} \tag{2.3.14}$$

These expressions are often successfully used as the basis for beam models involving large displacements and rotations, but small strains [2–4 to 8, 2–11,12]. However, it is interesting to note that one additional assumption was required ($\gamma^2 << \varepsilon$), that might not be adequate when dealing with highly anisotropic composite materials [2–12].

Section 2.4: Blade Strain Energy Expression (Hellinger-Reissner Formulation)

The strain energy expression for a thin walled beam is:

$$U = \frac{1}{2}\int_0^L \int_\Gamma \underline{\varepsilon}^T A\, \underline{\varepsilon}\, ds\, dx_1 \tag{2.4.1}$$

where $\underline{\varepsilon} = (\varepsilon, \gamma)$; A is the stiffness matrix; L the length of the blade; Γ the contour of the thin-walled section, described by a curvilinear variable s (see Figure 2.4.1). Consistent with the assumption of a cross section that does not deform in its own plane, the only non-vanishing strain components are the axial strain ε and the shearing strain γ. Clearly,

$$\varepsilon = \varepsilon_{11} \quad and \quad \gamma = x_2^+\gamma_{12} + x_3^+\gamma_{13} \tag{2.4.2}$$

where $()^+$ denotes a derivative with respective to s. A set of strains $\underline{e} = \underline{\varepsilon}$ is now introduced into (2.4.1) to yied:

$$U = \int_0^L \int_\Gamma \left[\frac{1}{2}\underline{e}^T A^T \underline{e} - \underline{n}^T(\underline{e} - \underline{\varepsilon})\right] ds\, dx_1 \tag{2.4.3}$$

where the condition $\underline{e} = \underline{\varepsilon}$ was enforced by means of a set of Lagrange Multipliers $\underline{n}$. Variation over $\underline{e}$ yields $\underline{n} = A\,\underline{e}$ which yields the physical meaning of $\underline{n}$ as the internal stress flows $\underline{n} = (n, q)$, where n is the axial stress flow and q the shear stress flow. Finally the strains $\underline{e}$ are eliminated from (2.4.3) using $\underline{e} = A^{-1}\,\underline{n}$ to find:

$$U = \int_0^L \int_\Gamma \left[\underline{n^T}\,\underline{\varepsilon} - \frac{1}{2}\,\underline{n^T}\,A^{-1}\,\underline{n} \right] ds\, dx_1 \tag{2.4.4}$$

Introducing (2.3.14) into (2.4.2) yields

$$\begin{aligned} \varepsilon &= \bar{e}_{11} - x_2\kappa_3 + x_3\kappa_2 + \varphi_1\delta' - k_1 r\varphi_1^+\delta \\ \gamma &= x_2^+ 2\bar{e}_{12} + x_3^+ 2\bar{e}_{13} + r\kappa_1 + \varphi_1^+\delta \end{aligned} \tag{2.4.5}$$

where $r = x_2x_3^+ - x_3x_2^+$ is the distance from the origin to the tangent to the contour Γ (see Figure 2.4.1); $\varphi_1^+ = x_2^+\varphi_{1,2} + x_3^+\varphi_{1,3}$ and $x_3\varphi_{1,2} - x_2\varphi_{1,3} = -r\varphi_1^+$

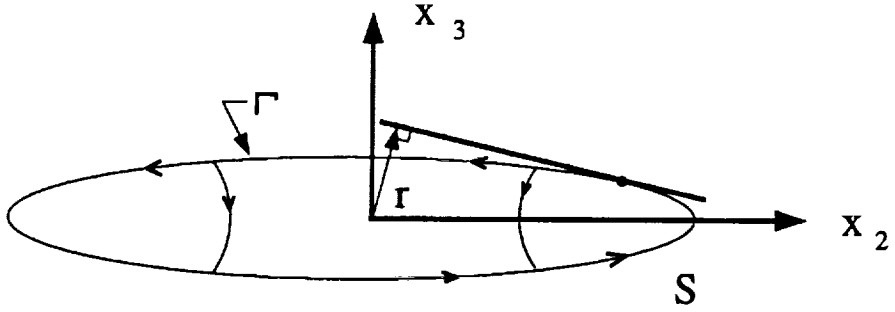

Figure 2.4.1 Geometry of the Thin-walled Cross-section

Note that equation (2.4.5) imply the small strain assumption and can be written as:

$$\begin{vmatrix} \varepsilon \\ \gamma \end{vmatrix} = \begin{bmatrix} 1 & 0 & 0 & -k_1 r\varphi_1^+ & 0 & x_3 & -x_2 & \varphi_1 \\ 0 & x_2^+ & x_3^+ & \varphi_1^+ & r & 0 & 0 & 0 \end{bmatrix} \underline{E} \tag{2.4.6}$$

where

$$\begin{aligned} &\underline{E^T} = (e_1, e_2, e_3, e_4, \kappa_1, \kappa_2, \kappa_3, \kappa_4) \\ &and \\ &e_1 = \bar{e}_{11},\ e_2 = 2\bar{e}_{12},\ e_3 = 2\bar{e}_{13},\ e_4 = \delta,\ \kappa_4 = \delta' \end{aligned} \tag{2.4.7}$$

Introducing these equations into (2.4.4) and integrating over the cross-section yields:

$$U = \int_0^L [e_1F_1 + e_2F_2 + e_3F_3 + e_4F_4 + \kappa_1M_1 + \kappa_2M_2 + \kappa_3M_3 + \kappa_4M_4]dx_1 \\ - \int_0^L \int_\Gamma \frac{1}{2}\left[\underline{n}^T A^{-1}\,\underline{n}\right] ds\, dx_1 \tag{2.4.8}$$

where

$$F_1 = \int_\Gamma n\,ds,\ F_2 = \int_\Gamma x_2^+ q\,ds,\ F_3 = \int_\Gamma x_3^+ q\,ds\ , \\ F_4 = \int_\Gamma \varphi_1^+ (q - k_1 r n)\,ds\ ,\ M_1 = \int_\Gamma rq\,ds\ , \\ M_2 = \int_\Gamma x_3 n\,ds,\ M_3 = -\int_\Gamma x_2 n\,ds,\ M_4 = \int_\Gamma \varphi_1 n\,ds \tag{2.4.9}$$

F_1 is the axial force, M_1 is the torque, F_2 and F_3 are the shear forces, M_2 and M_3 are the bending moments, and finally F_4 and M_4 are the force and moment, respectively, associated with the torsional warping induced stresses.

With Reissner's Principle independent assumptions can be made on displacements and stresses. By analogy to the strain field the stress field is assumed in the following form

$$\begin{bmatrix} n \\ q \end{bmatrix} = \begin{bmatrix} A_{nn} & A_{nq} \\ A_{nq} & A_{qq} \end{bmatrix} \begin{bmatrix} 1 & 0 & 0 & -k_1 r\varphi_1^+ & 0 & x_3 & -x_2 & \varphi_1 \\ 0 & \varphi_2^+ & \varphi_3^+ & \varphi_1^+ & r & 0 & 0 & 0 \end{bmatrix} \underline{X} \\ = \begin{bmatrix} A_{nn} & A_{nq} \\ A_{nq} & A_{qq} \end{bmatrix} B\,\underline{X} \tag{2.4.10}$$

where $\underline{X}^T = (X_1, X_2, X_3, X_4, Y_1, Y_2, Y_3, Y_4)$ is a vector of unknown stress parameters, φ_2 and φ_3 the transverse shearing related Saint-Venant warping functions[2–1]. Introducing (2.4.10) into (2.4.9) and integrating over the cross section yields

$$\underline{F} = A\,\underline{X} \tag{2.4.11}$$

where $\underline{F}^T = (F_1, F_2, F_3, F_4, M_1, M_2, M_3, M_4)$ and A is a matrix of cross-sectional coefficients. Finally the stress assumptions (2.4.10) are introduced into (2.4.8) to find:

$$U = \int_0^L [(e_1F_1 + e_2F_2 + e_3F_3 + e_4F_4 + \kappa_1M_1 + \kappa_2M_2 + \kappa_3M_3 + \kappa_4M_4) \\ - \frac{1}{2}\ \underline{F}^T H\,\underline{F}]\,dx_1 \tag{2.4.12}$$

where the compliance matrix is H given by

$$H = A^{-T}\,D\,A^{-1} \tag{2.4.13}$$

where

$$D = \int_{\Gamma} B^T \begin{bmatrix} A_{nn} & A_{nq} \\ A_{nq} & A_{qq} \end{bmatrix} B \, ds \tag{2.4.14}$$

Finally, (2.4.12) can be written as:

$$U = \int_0^L \left(\underline{e}^T \underline{F} - \frac{1}{2} \underline{F}^T H \underline{F} \right) dx_1 \tag{2.4.15}$$

where $\underline{e}^T = (e_1, e_2, e_3, e_4, \kappa_1, \kappa_2, \kappa_3, \kappa_4)$ are the sectional strains, $\underline{F}^T = (F_1, F_2, F_3, F_4, M_1, M_2, M_3, M_4, F_5)$ are internal forces, and the strain-displacement relationships are:

$$\begin{bmatrix} 1 + e_1 \\ e_2 \\ e_3 \end{bmatrix} = T_e^T \begin{bmatrix} t_{11} + u_1' \\ t_{21} + u_2' \\ t_{31} + u_3' \end{bmatrix} \tag{2.4.16}$$

$$\begin{bmatrix} \kappa_1 \\ \kappa_2 \\ \kappa_3 \end{bmatrix} = \begin{bmatrix} K_1 - k_1 \\ K_2 - k_2 \\ K_3 - k_3 \end{bmatrix}, \begin{bmatrix} K_1 \\ K_2 \\ K_3 \end{bmatrix} = 2G \begin{bmatrix} q_0' \\ q_1' \\ q_2' \\ q_3' \end{bmatrix}$$

This nonlinear strain energy expression depends on the displacements and forces:

$$U = U(\underline{u}, \underline{F}).$$

It can be expanded using a linearization procedure about a reference configuration, to yield:

$$\begin{aligned} U = \int_0^L \{ U^0 + \left[\Delta \underline{u}^T, \Delta \underline{F}^T \right] \begin{bmatrix} U_u \\ U_f \end{bmatrix} \\ + \frac{1}{2} \left[\Delta \underline{u}^T, \Delta \underline{F}^T \right] \begin{bmatrix} U_{uu} & U_{uf} \\ & U_{ff} \end{bmatrix} \begin{bmatrix} \Delta \underline{u} \\ \Delta \underline{F} \end{bmatrix} + h.o.t \} \end{aligned} \tag{2.4.17}$$

where

$$\underline{U_u} = \frac{\partial \overline{U}}{\partial \underline{u}} \; ; \qquad \underline{U_f} = \frac{\partial \overline{U}}{\partial \underline{F}} \tag{2.4.18}$$

and

$$U_{uu} = \frac{\partial^2 \overline{U}}{\partial \underline{u} \, \partial \underline{u}} \; ; \quad U_{uf} = \frac{\partial^2 \overline{U}}{\partial \underline{u} \, \partial \underline{F}} \; ; \quad U_{ff} = \frac{\partial^2 \overline{U}}{\partial \underline{F} \, \partial \underline{F}} \tag{2.4.19}$$

Section 2.5: Blade Kinetic Energy Expression (Hellinger-Reissner Formulation)

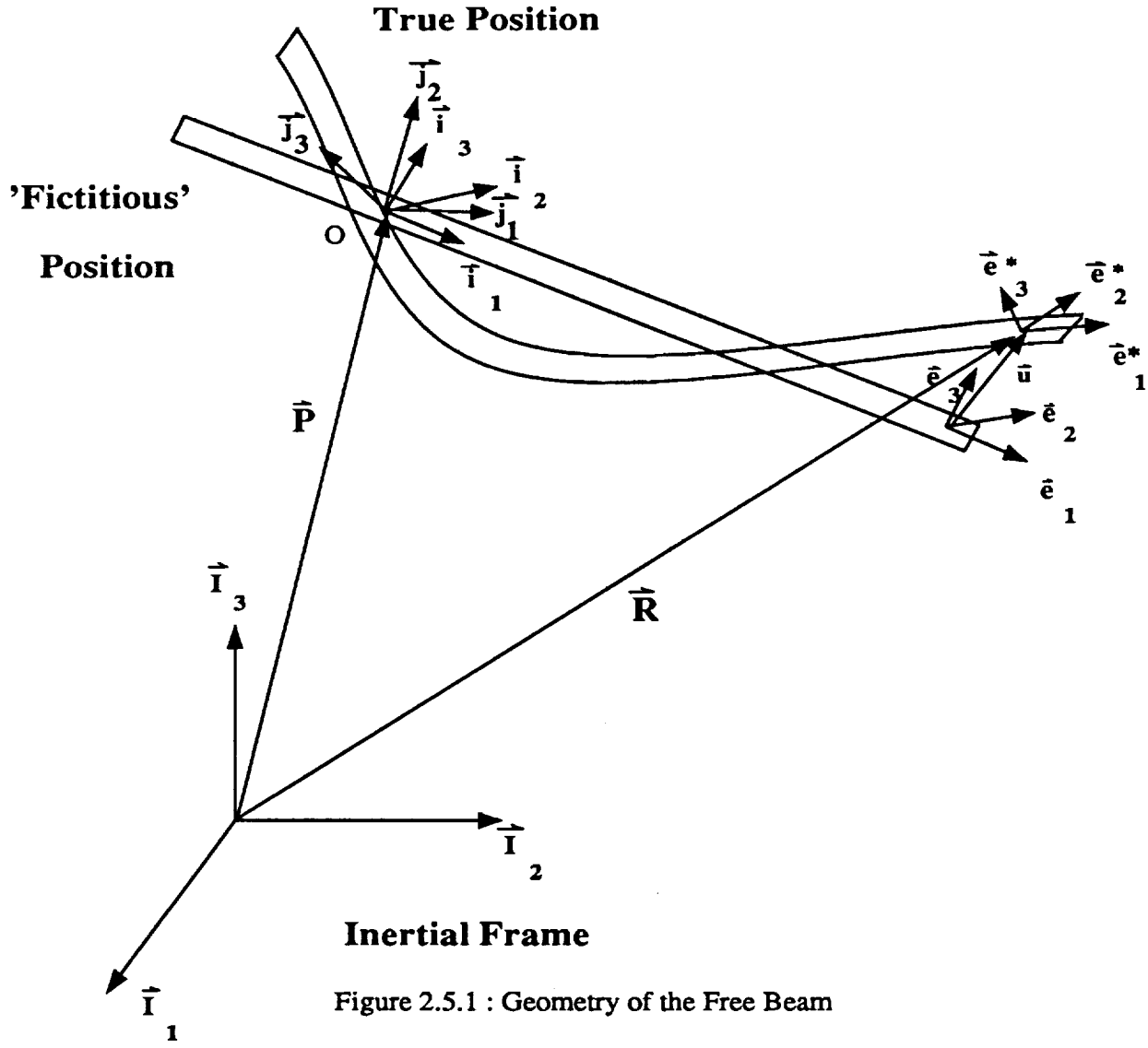

Figure 2.5.1 : Geometry of the Free Beam

Let $\vec{I}_i$ be an inertial reference frame. Consider now an unstrained structure in space with a triad $\vec{i}_i$ attached at a material point O. To locate the structure, it is convenient to separate its displacement field into rigid body displacements and elastic displacements. The rigid body motions define the position of a fictitious, rigid structure, and the elastic motions are superimposed to yield the true position of the structure. The rigid body displacement field involves three translations and three rigid body rotations. The rigid body translations are chosen as the translations of a material point O with an unknown position vector $\vec{P}(t)$. The rigid body rotations consist of two parts: first, an unknown

rigid body rotation characterized by a rotation matrix $T_r(t)$, then a known rigid body rotation with constant angular velocity charaterized by a rotation matrix $T_r^0(t)$ such that:

$$\begin{bmatrix} \vec{j}_1 \\ \vec{j}_2 \\ \vec{j}_3 \end{bmatrix} = T_r^T(t) \begin{bmatrix} \vec{I}_1 \\ \vec{I}_2 \\ \vec{I}_3 \end{bmatrix}; \quad \begin{bmatrix} \vec{i}_1 \\ \vec{i}_2 \\ \vec{i}_3 \end{bmatrix} = T_r^{0T}(t) \begin{bmatrix} \vec{j}_1 \\ \vec{j}_2 \\ \vec{j}_3 \end{bmatrix} \tag{2.5.1}$$

which yields:

$$\begin{bmatrix} \vec{i}_1 \\ \vec{i}_2 \\ \vec{i}_3 \end{bmatrix} = T_r^{0T}(t)\, T_r^T(t) \begin{bmatrix} \vec{I}_1 \\ \vec{I}_2 \\ \vec{I}_3 \end{bmatrix} \tag{2.5.2}$$

The elastic displacement field involves elastic displacements $\vec{u}(x_1, t)$ of the reference line defined in (2.2.4) and elastic rotations as defined in (2.2.14).

The sum of rigid and elastic displacement fields brings the structure to its actual position. The fictitious, rigid structure is used as a reference configuration for the described of the elastic strain field, in a manner identical to that described in section 2.2. This involves a set of material coordinates x_1, x_2, x_3, the base vectors of the reference line in the undeformed configuration $\vec{e}_1$, $\vec{e}_2$, $\vec{e}_3$, and the base vectors of the reference line in the deformed configuration $\vec{e}_1^*$, $\vec{e}_2^*$, $\vec{e}_3^*$.

The position vector of a material point is:

$$\vec{R} = \vec{P} + \vec{r_0} + \vec{u} + x_2\vec{e_2}^* + x_3\vec{e_3^*} \tag{2.5.3}$$

The instantaneous position of a material point on the blade is given by (2.2.16) where torsional warping related out-of-plane displacements were included, however the inertia forces associated with this out-of-plane motion are very small and will be neglected here, resulting in the simplified expression (2.5.3). It is clear that rigid body motions do not generate any strain field, hence the strain displacement equations (2.3.14), and the strain energy expression (2.4.12) remain unaffected. However, the kinetic energy expression is of course affected by the presence of time dependent, rigid body motions.

The time derivative, noted $\dot{()}$, of (2.5.2) yields:

$$\begin{bmatrix} \vec{i}_1 \\ \vec{i}_2 \\ \vec{i}_3 \end{bmatrix}^{\cdot} = \left(T_r^{0T} \dot{T}_r^{\,T} T_r T_r^0 + \dot{T}_r^{\,0T} T_r^0 \right) \begin{bmatrix} \vec{i}_1 \\ \vec{i}_2 \\ \vec{i}_3 \end{bmatrix} = \left(\tilde{\omega}_r^T + \tilde{\omega}_r^{0T} \right) \begin{bmatrix} \vec{i}_1 \\ \vec{i}_2 \\ \vec{i}_3 \end{bmatrix} \tag{2.5.4}$$

The time derivative of (2.2.14) yields:

$$\begin{aligned} \begin{bmatrix} \vec{e}_1^* \\ \vec{e}_2^* \\ \vec{e}_3^* \end{bmatrix}^{\cdot} &= \left(T_e^T \tilde{\omega}_r^T T_e + T_e^T \tilde{\omega}_r^{0T} T_e + \dot{T}_e^T T_e \right) \begin{bmatrix} \vec{e}_1^* \\ \vec{e}_2^* \\ \vec{e}_3^* \end{bmatrix} \\ &= \left(\tilde{\omega}_r^{*T} + \tilde{\omega}_r^{0*T} + \tilde{\omega}_e^{*T} \right) \begin{bmatrix} \vec{e}_1^* \\ \vec{e}_2^* \\ \vec{e}_3^* \end{bmatrix} \end{aligned} \tag{2.5.5}$$

The following skew symmetric angular velocity matrices have been defined: $\tilde{\omega}_r$ and $\tilde{\omega}_r^0$, the unknown and constant rigid angular velocities, respectively, resolved in the $\vec{i}_i$ system; $\tilde{\omega}_r^*$, $\tilde{\omega}_r^{0*}$ and $\tilde{\omega}_e^*$ the unknown, constant, and elastic angular velocities, respectively, resolved in the $\vec{e}_i^*$ system. The components of the corresponding angular velocity vectors can also be defined: $\underline{\omega_r} = (\omega_{r1}, \omega_{r2}, \omega_{r3})$, $\underline{\omega_r^0} = (\omega_{r1}^0, \omega_{r2}^0, \omega_{r3}^0)$; $\underline{\omega_r^*} = (\omega_{r1}^*, \omega_{r2}^*, \omega_{r3}^*)$, $\underline{\omega_r^{0*}} = (\omega_{r1}^{0*}, \omega_{r2}^{0*}, \omega_{r3}^{0*})$, and finally $\underline{\omega_e^*} = (\omega_{e1}^*, \omega_{e2}^*, \omega_{e3}^*)$. It is clear that:

$$\underline{\omega_r^*} = T_e^T \, \underline{\omega_r} \quad \text{and} \quad \underline{\omega_r^{0*}} = T_e^T \, \underline{\omega_r^0} \tag{2.5.6}$$

The position vector (2.5.3) can be resolved as follows:

$$\vec{R} = [\vec{I}_1 \quad \vec{I}_2 \quad \vec{I}_3] \begin{bmatrix} P_1 \\ P_2 \\ P_3 \end{bmatrix} + [\vec{i}_1 \quad \vec{i}_2 \quad \vec{i}_3] \begin{bmatrix} x_0 + u_1 \\ y_0 + u_2 \\ z_0 + u_3 \end{bmatrix} + [\vec{e}_1^* \quad \vec{e}_2^* \quad \vec{e}_3^*] \begin{bmatrix} 0 \\ x_2 \\ x_3 \end{bmatrix} \tag{2.5.7}$$

where $\underline{P^T} = (P_1, P_2, P_3)$ are the components of the vector $\vec{P}$ in the inertial system. The inertial velocity of a material particle is found by combining (2.5.7) with (2.5.4) and (2.5.5), to find:

$$\begin{aligned} \dot{\vec{R}} = [\vec{i}_1 \quad \vec{i}_2 \quad \vec{i}_3] \Bigg\{ & T_r^{0T} T_r^T \begin{bmatrix} \dot{P}_1 \\ \dot{P}_2 \\ \dot{P}_3 \end{bmatrix} + (\tilde{\omega}_r + \tilde{\omega}_r^0) \begin{bmatrix} x_0 + u_1 \\ y_0 + u_2 \\ z_0 + u_3 \end{bmatrix} + \begin{bmatrix} \dot{u}_1 \\ \dot{u}_2 \\ \dot{u}_3 \end{bmatrix} \Bigg\} \\ & + [\vec{e}_1^* \quad \vec{e}_2^* \quad \vec{e}_3^*] (\tilde{\omega}_r^* + \tilde{\omega}_r^{0*} + \tilde{\omega}_e^*) \begin{bmatrix} 0 \\ x_2 \\ x_3 \end{bmatrix} \end{aligned} \tag{2.5.8}$$

The following notations are introduced. First, the rigid translational velocities are defined as:

$$\underline{v_r} = \begin{bmatrix} v_{r1} \\ v_{r2} \\ v_{r3} \end{bmatrix} = T_r^{0T} T_r^T \begin{bmatrix} \dot{P}_1 \\ \dot{P}_2 \\ \dot{P}_3 \end{bmatrix} + \tilde{X}^T \, \underline{\omega_r} \tag{2.5.9}$$

$$\underline{v_e} = \begin{bmatrix} v_{e1} \\ v_{e2} \\ v_{e3} \end{bmatrix} = \begin{bmatrix} \dot{u}_1 \\ \dot{u}_2 \\ \dot{u}_3 \end{bmatrix} + \tilde{X}^T \, \underline{\omega_r^0} \tag{2.5.10}$$

where

$$\tilde{X} = \begin{vmatrix} 0 & -(z_0 + u_3) & (y_0 + u_2) \\ (z_0 + u_3) & 0 & -(x_0 + u_1) \\ -(y_0 + u_2) & (x_0 + u_1) & 0 \end{vmatrix} \tag{2.5.11}$$

The total translational velocity is now defined in the $\vec{i}_i$ system as:

$$\underline{v_t} = \underline{v_r} + \underline{v_e} \tag{2.5.12}$$

and in the $\vec{e}_i^*$ as:

$$\underline{v_t^*} = T_e^T \, \underline{v_t} \tag{2.5.13}$$

Finally, the total angular velocity vector in the $\vec{e}_i^*$ sytem is:

$$\underline{\omega_t^*} = \underline{\omega_r^*} + \underline{\omega_r^{0*}} + \underline{\omega_e^*} \tag{2.5.14}$$

For (2.5.9) to (2.5.12), the inertial velocity of a material point (2.5.8) becomes:

$$\dot{\vec{R}} = [\vec{e_1}^* \quad \vec{e_2}^* \quad \vec{e_3}^*] \begin{bmatrix} v_{t1}^* - x_2\omega_{t3}^* + x_3\omega_{t2}^* \\ v_{t2}^* \qquad\qquad - x_3\omega_{t1}^* \\ v_{t3}^* + x_2\omega_{t1}^* \end{bmatrix} \tag{2.5.15}$$

The kinetic energy of the system is:

$$T = \frac{1}{2} \int_0^L \int_\Gamma \rho \dot{\vec{R}} \cdot \dot{\vec{R}} ds dx_1 \tag{2.5.16}$$

Introducing (2.5.12) and integrating over the cross section yields:

$$T = \frac{1}{2} \int_0^L \underline{V_t^{*T}} \, M \, \underline{V_t^*} \, dx_1 \tag{2.5.17}$$

where the array of total velocities $\underline{V_t^*}$ is defined as:

$$\underline{V_t^{*T}} = (v_{t1}^*, v_{t2}^*, v_{t3}^*, \omega_{t1}^*, \omega_{t2}^*, \omega_{t3}^*) \tag{2.5.18}$$

and the mass matrix M is given by:

$$M = \begin{bmatrix} m & 0 & 0 & 0 & m_3 & -m_2 \\ 0 & m & 0 & -m_3 & 0 & 0 \\ 0 & 0 & m & m_2 & 0 & 0 \\ 0 & -m_3 & m_2 & m_{11} & 0 & 0 \\ m_3 & 0 & 0 & 0 & m_{33} & -m_{23} \\ -m_2 & 0 & 0 & 0 & -m_{23} & m_{22} \end{bmatrix} \tag{2.5.19}$$

where the mass per unit span is:

$$m = \int_\Gamma \rho ds \tag{2.5.20}$$

the inbalance per unit span is:

$$m_i = \int_\Gamma \rho x_i ds \qquad i = 2, 3 \tag{2.5.20a}$$

the moment of inertia per unit span is:

$$m_{ij} = \int_{\Gamma} \rho x_i x_j ds \qquad i,j = 2,3 \tag{2.5.20b}$$

and

$$m_{11} = m_{22} + m_{33} \tag{2.5.20c}$$

For future reference, it is convenient to write:

$$\underline{V_t^*} = A\,\underline{V_r} + \underline{V_e^*} \tag{2.5.21}$$

where the matrix A is defined as:

$$A = \begin{vmatrix} T_e^T & T_e^T \tilde{X}^T \\ 0 & T_e^T \end{vmatrix} \tag{2.5.22}$$

the rigid velocities are:

$$\underline{V_r} = \begin{vmatrix} T_r^{0T} T_r^T \underline{\dot{P}} \\ \underline{\omega_r} \end{vmatrix} = \begin{vmatrix} T_r^{0T} & 0 \\ 0 & T_r^{0T} \end{vmatrix} \begin{vmatrix} T_r^T \underline{\dot{P}} \\ 2G\,\underline{\dot{Q}} \end{vmatrix} \tag{2.5.23}$$

and the elastic velocities are:

$$\underline{V_e^*} = \begin{vmatrix} T_e^T \left(\underline{\dot{u}} + \tilde{X}^T \underline{\omega_r^0} \right) \\ T_e^T \underline{\omega_r^0} + \underline{\omega_e^*} \end{vmatrix} \tag{2.5.24}$$

A set of velocities $\underline{U} = \underline{V_t^*}$ is now introduced into the kinetic energy expression (5.2.14) to yield

$$T = \int_0^L \left[\frac{1}{2} \underline{U^T} M \underline{U} - \underline{p^{*T}} \left(\underline{U} - \underline{V_t^*} \right) \right] dx_1 \tag{2.5.25}$$

where the condition $\underline{U} - \underline{V_t^*} = 0$ was enforced by means of a set Lagrange multipliers $\underline{p^*}$. Variation over $\underline{U}$ yields $\underline{p^*} = M\,\underline{U}$ which yields the physical meaning of p^* as the momenta components, measured in the $\vec{e}_i^*$ system. Finally, the velocities $\underline{U}$ are eliminated from (2.5.18) using $\underline{U} = M^{-1}\,\underline{p^*}$, to find:

$$T = \int_0^L \left(\underline{p^*}\,\underline{V_t^*} - \frac{1}{2} \underline{p^{*T}} M^{-1} \underline{p^*} \right) dx_1 \tag{2.5.26}$$

this expression of the kinetic energy is a nonlinear function of the six rigid body velocities $\underline{V_r} = (v_{r1}, v_{r2}, v_{r3}, \omega_{r1}, \omega_{r2}, \omega_{r3})$, the elastic displacements $\underline{u}$ and their time derivatives $\underline{\dot{u}}$, and the compontents p^* i.e.:

$$T = T\left(\underline{V_r}, \underline{u}, \underline{\dot{u}}, p^* \right) \tag{2.5.27}$$

The kinetic energy will be used in two way. First, a finite element implementation of the problem to yield steady equilibrium position of the structure under applied loads and normal vibration modes. Second a modal approximation to obtain modal equations of motion. In the finite element implementation which focuses on natural vibration mode calculations, constant, rigid angular velocities are the only allowed type of rigid body motion. On the other hand, in the modal approximation the 6 rigid body motions are unknowns of the problem and describe the rigid body response of the system to the applied load. For constant rigid angular velocities we have

$$T = T\left(\underline{u}, \dot{\underline{u}}, \underline{p^*}\right) \tag{2.5.28}$$

this nonlinear expression can be expanded using a linearization procedure. This expansion is performed about a steady configuration noted $\underline{u^0}, \underline{p^{*0}}$, and the rigid angular velocities are $\omega_{r1}^0, \omega_{r2}^0, \omega_{r3}^0$, to find:

$$\begin{aligned} T = \int_0^L \Bigg\{ & T^0 + [\,\Delta\underline{u} \quad \Delta\dot{\underline{u}} \quad \Delta p^*\,] \begin{bmatrix} \underline{T_u} \\ \underline{T_{\dot{u}}} \\ \underline{T_p} \end{bmatrix} \\ & + \frac{1}{2}[\,\Delta\underline{u} \quad \Delta\dot{\underline{u}} \quad \Delta p^*\,] \begin{bmatrix} T_{uu} & T_{u\dot{u}} & T_{up} \\ T_{u\dot{u}} & T_{\dot{u}\dot{u}} & T_{\dot{u}p} \\ T_{up} & T_{\dot{u}p} & T_{pp} \end{bmatrix} \begin{bmatrix} \Delta\underline{u} \\ \Delta\dot{\underline{u}} \\ \Delta\underline{p^*} \end{bmatrix} + H.O.T. \Bigg\} dx_1 \end{aligned} \tag{2.5.29}$$

where

$$\underline{T_u} = \frac{\partial T}{\partial \underline{u}} \; ; \qquad \underline{T_{\dot{u}}} = \frac{\partial T}{\partial \dot{\underline{u}}} \; ; \qquad \underline{T_p} = \frac{\partial T}{\partial \underline{p^*}} \tag{2.5.30}$$

and

$$\begin{aligned} \underline{T_{uu}} &= \frac{\partial^2 T}{\partial \underline{u}\,\partial \underline{u}} \; ; & \underline{T_{u\dot{u}}} &= \frac{\partial^2 T}{\partial \underline{u}\,\partial \dot{\underline{u}}} \; ; & \underline{T_{up}} &= \frac{\partial^2 T}{\partial \underline{u}\,\partial \underline{p^*}} \\ \underline{T_{\dot{u}\dot{u}}} &= \frac{\partial^2 T}{\partial \dot{\underline{u}}\,\partial \dot{\underline{u}}} \; ; & \underline{T_{\dot{u}p}} &= \frac{\partial^2 T}{\partial \dot{\underline{u}}\,\partial \underline{p^*}} \; ; & \underline{T_{pp}} &= \frac{\partial^2 T}{\partial \underline{p^*}\,\partial \underline{p^*}} \end{aligned} \tag{2.5.31}$$

All these arrays are evaluated in the reference configuration.

Section 2.6: Normality Condition for Euler Parameters

In the two previous sections finite rotations were used, and to keep the formulation general, the rotation matrix T_e only appears in the equations. However, for a practical implementation, a specific set of rotation parameters must be selected. In this work the Euler Parameters (see appendixA) are used that are related through the normality condition. This normality conditon could be enforced using a penalty method, i.e. adding the following term to strain energy

$$C = \int_0^L \frac{1}{2}\alpha e_9^2 dx_1 \tag{2.6.1}$$

where α is a large penalty coefficient, and

$$e_9 = q_0^2 + q_1^2 + q_2^2 + q_3^2 - 1 \tag{2.6.2}$$

is the normality condition and q_i the Euler Parameters. Following the Hellinger-Reissner approach used in the previous sections, a variable $e = e_9$is introduced into (2.6.1) to yield

$$C = \int_0^L \left[\frac{1}{2}\alpha e^2 - \lambda(e - e_9)\right] dx_1 \tag{2.6.3}$$

where the condition $e = e_9$ was enforced by means of a Lagrange Multiplier λ. Variation over e yields $\lambda = \alpha e$, hence, the variable e can be eliminated using $e = \lambda/\alpha$, to yield

$$C = \int_0^L \left[\lambda e_9 - \frac{1}{2}\lambda^2/\alpha\right] dx_1 \tag{2.6.4}$$

It is convenient to interpret this relationship in the following physical terms : e_9 is a fictitious strain, α is fictitious stiffness, and λ a fictitious force, such that $\lambda = \alpha e_9$. By selecting a very large stiffness α we drive the strain e_9 to zero, i.e. we verify the normality condition.

The nonlinear constraint expression (2.6.4) can be expanded using a linearization technique to yield

$$\begin{aligned} C = \overline{C} &+ [\Delta \underline{u}^T \quad \Delta \underline{\lambda}^T] \begin{bmatrix} \underline{C_u} \\ \underline{C_\lambda} \end{bmatrix} \\ &+ \frac{1}{2}[\Delta \underline{u}^T \quad \Delta \underline{\lambda}^T] \begin{bmatrix} C_{uu} & C_{u\lambda} \\ C_{u\lambda} & C_{\lambda\lambda} \end{bmatrix} \begin{bmatrix} \Delta \underline{u} \\ \Delta \underline{\lambda} \end{bmatrix} + h.o.t. \end{aligned} \tag{2.6.5}$$

where

$$\begin{aligned} \underline{C_u} &= \frac{\partial \overline{C}}{\partial \underline{u}} \quad ; \qquad \underline{C_\lambda} = \frac{\partial \overline{C}}{\partial \underline{\lambda}} \\ C_{uu} &= \frac{\partial^2 \overline{C}}{\partial \underline{u} \partial \underline{u}} \quad ; \qquad C_{u\lambda} = \frac{\partial^2 \overline{C}}{\partial \underline{u} \partial \underline{\lambda}}; \qquad C_{\lambda\lambda} = \frac{\partial^2 \overline{C}}{\partial \underline{\lambda} \partial \underline{\lambda}} \end{aligned} \tag{2.6.6}$$

All derivatives are evaluated in the reference configuration.

References

2–1. Bauchau, O. A.,"A Beam Theory for Anisotrpic Materials," J. Applied Mechanics, Vol. 107, 416-422, June 1985.

2–2. Bauchau, O. A., Coffenberry, B. S. and Rehfield, L. W.,"Composite Box Beam Analysis: Theory and Experiments," J. Reinforced Plastics and Composites, Vol. 6, No. 1, Jan. 1987.

2–3. Friedmann, P. P. and Straub, F.,"Application of the Finite Element Method to Rotary-wing Aeroelasticity," J. American Helicopter Society, Vol. 25, No. 1, 36-44, Jan. 1980.

2–4. Rosen, A., Loewy, R. G., and Mathew, M. B.,"Nonlinear Analysis of Pretwisted Rods Using Principal Curvature Transformation - Part I - Theoretical Derivation, - Part II - Numerical Results," AIAA Journal, Vol. 25, No. 3, 470-478, March 1987; and Vol. 25, No. 4, 598-604.

2–5. Rosen, A. and Friedmann, P. P.,"The Nonlinear Behavior of Elastic Slender Straight Beams Undergoing Small Strains and Moderate Rotations," J. Applied Mechanics, Vol. 46, March 1979.

2–6. Sivaneri, N. T. and Chopra, I.,"Finite Element Analysis for Bearingless Rotor Blade Aeroelasticity," J. American Helicopter Society, Vol. 29, No. 2, April 1984.

2–7. Bauchau, O. A. and Hong, C. H.,"Finite Element Approach to Rotor Blade Modeling," J. American Helicopter Society, Vol. 32, No. 1, 60-67, Jan. 1987.

2–8. Bauchau, O. A. and Hong, C. H.,"Large Displacement Analysis of Naturally Curved and Twisted Beams," AIAA Journal, Vol. 25, No. 10, Oct. 1987.

2–9. Washizu, K., Variational Methods in Elasticity and Plasticity, Pergamon Press, 1975.

2–10. Wempner, G., Mechanics of Solids with Application to Thin Bodies, Sijthoff & Nordhoff, 1981.

2–11. Washizu, K.,"Some Considerations on a Naturally Curved and Twisted Slender Beam," J. Matn. and Phys., Vol. 48, No. 2, 111-116, June 1964.

2–12. Bauchau, O. A. and Hong, C. H.,"Nonlinear Composite Beam Theory," J. Applied Mechanics, Vol. 55, No. 1, 156-163, March 1988.

2–13. Reissner, E.,"On a Variational Theorem in Elasticity," J. Math. and Phys., Vol. 29, 90-95, 1950.

2–14. Reissner, E.,"On a Variational Theorem for Finite Elastic Deformations," J. Math. and Phys., Vol. 32, No. 2-3, 129-135, July 1953.

2–15. Noor, A. K. and Peters, J. M.,"Mixed Models and Reduced/Selective Integration Displacement Models for Nonlinear Analysis of Curved Beams," Int. J. for Numerical Methods in Engineering, Vol. 17, 615-631, 1981.

Chapter 3

Modal Reduction of the Finite Element Model

Section 3.1: Introduction

The versatility and efficiency of the finite element method makes it an attractive tool for the analysis of helicopter rotor blades. Hodges [3–1] has recently reviewed various finite element approaches, giving a comprehensive discussion of their assumptions and features. An analysis including moderate rotations was developed by Friedmann and Straub [2–3], as by Sivaneri and Chopra [3–2] based on the formulation of Hodges and Dowell [3–3]. Giavotto et al. [3–4] and Borri [3–5] developed an approach that includes finite rotations, as well as cross sectional warping deformations. Finally, a model for arbitrarily large displacements and rotations of naturally curved and twisted blades was developed in chapter 2.

These various approaches are very attractive because they allow accurate modeling of rotor blades. The complex kinematics resulting from the large displacements and rotations can be handled in a rational manner, and the intricate elastic behavior of composite blades can be treated realistically by introducing transverse shearing and warping deformations, as well as elastic coupling. However, the cost of such analysis can be prohibitive when realistic problem must be treated.

Consider a composite blade with varying properties along the span: 100 to 150 degrees of freedom (DOFs) are typically necessary to accurately represent its geometry and physical properties. This number must appear small, as problems involving 1,000, or even 10,000 DOFs are routinely solved with large finite element codes. However, in the case of a helicopter blade, the analyst is interested in determining its nonlinear static behavior, its dynamic characteristics i.e. its natural frequencies and mode shapes, its nonlinear, periodic dynamic response, and the stability characteristics of this periodic response. The first two analysis types are relatively straightforward to handle, but the latter ones are far more complex.

Consider the prediction of the nonlinear periodic response of the blade using the finite element in the method [3–6]: the total number of DOFs equals the number of DOFs used for the spatial model times the number of time stations. If 64 time stations are used, this will yield 6,400 to 9,600 DOFs to be solved for in an iterative manner, since the problem is nonlinear. For a gimballed rotor, all the blades must be considered simultaneously since they will interact, hence a three bladed gimballed rotor would require the nonlinear solution of 19,200 to 28,800 DOFs, rendering the analysis prohibitively expensive.

Additional problems will appear when stability analysis is performed using Floquet's theory, which is standard tool for dealing with the stability of periodic systems. In this approach, the stability of the system is assessed from the eigenvalues of the transition matrix, which is a fully populated matrix of an order equal to twice the number of spatial DOFs. Considering once again the above example, the transition matrix would be of order 200 to 300 for a single blade, and 600 to 900 for the gimballed rotor. Furthermore,

this matrix is often ill-conditioned because the characteristic frequencies of the system vary over an extremely wide range. For instance, if six DOFs are considered at each node of the blade, axial frequencies will be included in the model. Such frequencies are many orders of magnitude larger than the first flap frequency of the blade, yielding an ill-conditioned transition matrix. This limitation is inherent to the approach, and will not disappear with increased computational power.

In view of these numerical difficulties a modal representation appears as a natural way of reducing the number of degrees of freedom of the problem. In fact modal approaches have been very widely used to analyze rotor blades [3–7,11], and have the additional advantage of involving degrees of freedom that have a direct physical meaning. However, modal approaches are based on an inherent assumption: the motion of the blade is restricted to the superposition of a small number of prescribed modes. Furthermore, when applied to nonlinear problems, there is no assurance of convergence or accuracy of the procedure. The goal of this research is to develop a finite element based modal analysis for rotor blades. The expression finite element based refers to the fact that a conventional finite element model of the blade is subjacent to the modal analysis which accuracy can be assessed by reference to this complete finite element model. In the development of a nonlinear finite element based modal approach, three points are of particular importance: the type of nonlinearities, their order, and the choice of the modes. The first two point will be addressed in the present chapter and the latter in the chapter 4.

Consider for instance a nonlinearity of trigonometric type say $cos\gamma$, appearing in the strain energy expression (γ is an unknown rotation angle). In the modal approximation, this angle is expanded as $\gamma = \gamma^i\psi^i$, where γ^i are the assumed mode shapes, ψ^i the generalized coordinates, and summation over all assumed modes is implied by the repeated indices. To evaluate the strain energy, the expression $cos\gamma^i\psi^i$ must then be integrated along the span of the blade; this is of course impossible since ψ^i are as yet unknown, and due to the transcendental nature of the trigonometric functions. To avoid this problem, it is customary to expand the cosine function in a truncated series: $cos\gamma^i\psi^i \approx 1 - \frac{1}{2}\gamma^i\gamma^j\psi^i\psi^j$. This means of course that the analysis will be limited to moderate rotations. Hence, if we wish to develop a modal approximation without introducing additional assumptions, the nonlinearities must be of a simple, algebraic type.

Consider next the order of the nonlinearities, say γ^n, where n is the order of nonlinearity. In the modal expansion this becomes $\gamma^i\gamma^j\gamma^k...\psi^i\psi^j\psi^k...$. It is clear that the number of coefficients generated by such expression is proportional to N^n, where N is the number of assumed modes. Hence, for a 12 mode approximation of an expression containing sixth order nonlinearities, $2.9x10^6$ coefficients will be generated, requiring 22 megabytes of storage on a computer! From this discussion, it is clear that a modal approach must be based on expression containing simple, algebraic type of nonlinearities only, and the order of the nonlinearities must be as low as possible.

It is clear that the Reissner's Principle based formulation described in chapter 2 is ideally suited for a modal approximation since it involves nonlinearities only, of quadratic order. The details of this modal reduction are given in the following sections.

Section 3.2: Modal Approximation to The Total Lagrangian of The Structure.

When the structure is modeled using the idealizations described in chapter 2 the total Lagrangian can be written as:

$$\mathcal{L} = \int_V \left(\underline{p}_t^* \cdot \underline{V}_t^* - \frac{1}{2} \underline{p}_t^* M^{*^{-1}} \underline{p}_t^* \right) - \left(\underline{F}^T \underline{\varepsilon} - \frac{1}{2} \underline{F}^T H \underline{F} \right) \, dV \tag{3.2.1}$$

where independent approximations can be made for the displacements, momenta, and internal forces. It is convenient to distinguish between rigid and elastic velocities (2.5.21) as:

$$\underline{V}_t^* = A \underline{V}_r + \underline{V}_e^* \tag{3.2.2}$$

and correspondingly, the following momentum is chosen:

$$\underline{p}_t^* = M^* A \underline{U}_r + \underline{p}_e^* \tag{3.2.3}$$

Introducing these equations, the total Lagrangian becomes:

$$\mathcal{L} = \mathcal{L}_r + \mathcal{L}_e \tag{3.2.4}$$

where the "rigid" Lagrangian is:

$$\mathcal{L}_r = \underline{U}_r^T M \underline{V}_r - \frac{1}{2} \underline{U}_r^T M \underline{U}_r + \underline{U}_r^T (\underline{C} - \underline{D}) + V_r^T \underline{D} \tag{3.2.5}$$

with

$$M = \int_V A^T M^* A \, dV \tag{3.2.6}$$

$$\underline{C} = \int_V A^T M^* \underline{V}_e^* \, dV \tag{3.2.7}$$

$$\underline{D} = \int_V A^T \underline{p}_e^* \, dV \tag{3.2.8}$$

and the "elastic" Lagrangian is:

$$\mathcal{L}_e = \int_V \left(\underline{p}_e^* \cdot \underline{V}_e^* - \frac{1}{2} \underline{p}_e^* M^{*^{-1}} \underline{p}_e^* \right) - \left(\underline{F}^T \underline{\varepsilon} - \frac{1}{2} \underline{F}^T H \underline{F} \right) \, dV \tag{3.2.9}$$

The rigid body motions are represented in terms of physical variables

$$\underline{R}^T = \lfloor P_1 \; P_2 \; P_3 \; Q_0 \; Q_1 \; Q_2 \; Q_3 \rfloor \; ; \; \dot{\underline{R}}^T = \left\lfloor \dot{P}_1 \; \dot{P}_2 \; \dot{P}_3 \; \dot{Q}_0 \; \dot{Q}_1 \; \dot{Q}_2 \; \dot{Q}_3 \right\rfloor \tag{3.2.10}$$

where the P_i are the components of the rigid body translation (2.5.7), and Q_i the Euler Parameters of the rigid body rotation (2.5.1). In contrast, the elastic displacements,

momenta, and forces are assumed to be adequately represented by an expression in terms of known mode shapes about a given steady reference configuration.

$$u_i = u_i^0 + u_i^j \psi_u^j \tag{3.2.11}$$

where u_i^0 is the time independent reference configuration of the elastic body, u_i^j the assumed mode shapes, and ψ_u^j the generalized coordinates. A similar expansion is selected for the elastic forces and momenta, respectively.

$$F_i = F_i^0 + F_i^j \psi_f^j \tag{3.2.12}$$

$$p_i^* = p_i^{*0} + p_i^{*j} \psi_p^j \tag{3.2.13}$$

Section 3.3: Elastic Lagrangian for Beam Elements.

Introducing the modal expansion described in section 3.2 into the expressions for matrices G and H (Appendix A.6) yields:

$$G = G^0 + G^k \psi_u^k \;\; ; \;\; H = H^0 + H^k \psi_u^k \tag{3.3.1}$$

where

$$G^0 = \begin{bmatrix} -q_1^0 & q_1^0 & q_3^0 & -q_2^0 \\ -q_2^0 & -q_3^0 & q_0^0 & q_1^0 \\ -q_3^0 & q_2^0 & -q_1^0 & q_0^0 \end{bmatrix} \tag{3.3.2}$$

and

$$G^k = \begin{bmatrix} -q_1^k & q_1^k & q_3^k & -q_2^k \\ -q_2^k & -q_3^k & q_0^k & q_1^k \\ -q_3^k & q_2^k & -q_1^k & q_0^k \end{bmatrix} \tag{3.3.3}$$

H^0 and H^k are defined similarly. The elastic rotation matrix becomes

$$T = T^0 + T^k \psi_u^k + T^{kl} \psi_u^k \psi_u^l \tag{3.3.4}$$

where

$$T_e^0 = H^0 G^{0T} \; ; \; T_e^k = H^0 G^{kT} + H^k G^{0T} \; ; \; T_e^{kl} = H^k G^{lT} \tag{3.3.5}$$

The strains (2.4.16) become

$$\underline{e} = \underline{e^0} + \underline{e^k} \psi_u^k + \underline{e^{kl}} \psi_u^k \psi_u^l + \underline{e^{klm}} \psi_u^k \psi_u^l \psi_u^m \tag{3.3.6}$$

where:

$$\underline{e^0} = T_e^{0T} \underline{u'^0}; \; \underline{e^k} = T_e^{0T} \underline{u'^k} + T_e^{kT} \underline{u'^0}; \; \underline{e^{kl}} = T_e^{kT} \underline{u'^l} \; ; \; \underline{e^{klm}} = T^{klT} \underline{u'^m} \tag{3.3.7}$$

with

$$\underline{u'^0} = \begin{bmatrix} u_1'^0 + t_{11} \\ u_2'^0 + t_{21} \\ u_3'^0 + t_{31} \end{bmatrix}; \; \underline{u'^k} = \begin{bmatrix} u_1'^k \\ u_2'^k \\ u_3'^k \end{bmatrix}. \tag{3.3.8}$$

and

$$T_e^{0^T} = \begin{bmatrix} q_{11}^0 & q_{12}^0 & q_{13}^0 \\ q_{21}^0 & q_{22}^0 & q_{23}^0 \\ q_{31}^0 & q_{32}^0 & q_{33}^0 \end{bmatrix}; \; T_e^{kT} = \begin{bmatrix} q_{11}^k & q_{12}^k & q_{13}^k \\ q_{21}^k & q_{22}^k & q_{23}^k \\ q_{31}^k & q_{32}^k & q_{33}^k \end{bmatrix} \tag{3.3.9}$$

Similarly the curvature (2.4.16) become:

$$\underline{\kappa} = \underline{\kappa}^0 + \underline{\kappa}^k \psi_u^k + \underline{\kappa}^{kl} \psi_u^k \psi_u^l \tag{3.3.10}$$

where

$$\underline{\kappa_0} = 2G^0 \underline{q}'^0; \; \underline{\kappa}^k = 2G^0 \underline{q}'^k + 2G^k \underline{q}'^0; \; \underline{\kappa}^{kl} = 2G^k \underline{q}'^l \tag{3.3.11}$$

the warping strains become:

$$e_4 = e_4^0 + e_4^k \psi_u^k \tag{3.3.12}$$

Finally the fictitious strains are expanded as:

$$e_9 = \underline{q}^T \underline{q} - 1 = e_9^0 + e_9^k \psi_u^k + e_9^{kl} \psi_u^k \psi_u^l \tag{3.3.13}$$

where

$$e_9^0 = \underline{q}^{0T} \cdot \underline{q}^0 - 1; \; e_9^k = 2\underline{q}^{0T} \cdot \underline{q}^k; \; e_9^{kl} = \underline{q}^{kT} \cdot \underline{q}^l \tag{3.3.14}$$

The strain expressions (3.3.1) to (3.3.4) can be written in a generic form

$$\underline{\epsilon} = \underline{\epsilon}^0 + \underline{\epsilon}^k \psi_u^k + \underline{\epsilon}^{kl} \psi_u^k \psi_u^l + \underline{\epsilon}^{klm} \psi_u^k \psi_u^l \psi_u^m \tag{3.3.15}$$

We now turns to the expression of the elastic translation velocity (2.5.10)

$$\begin{aligned} \underline{v_e^*} = \underline{v_e^{*0}} + \underline{v_e^{*k}} \psi_u^k + \underline{\dot{v}_e^{*k}} \psi_u^k + \underline{v_e^{kl}} \psi_u^k \psi_u^l + \underline{\dot{v}_e^{*kl}} \dot{\psi}_u^k \psi_u^l \\ + \underline{v_e^{klm}} \psi_u^k \psi_u^l \psi_u^m + \underline{\dot{v}_e^{*klm}} \dot{\psi}_u^k \psi_u^l \psi_u^m \end{aligned} \tag{3.3.16}$$

where

$$\begin{aligned} &\underline{v_e^{*0}} = T_e^{0^T} \tilde{X}^{0^T} \underline{\omega_r^0}; \; \underline{v_e^{*k}} = \left(T_e^{0^T} \tilde{X}^{k^T} + T_e^{k^T} \tilde{X}^{0^T} \right) \underline{\omega_r^0}; \; \underline{\dot{v}_e}^{*k} = T^{0^T} \underline{u}^k \\ &\underline{v_e^{*kl}} = T_e^{k^T} \tilde{X}^{l^T} \underline{\omega_r^0}; \; \underline{\dot{v}_e}^{*kl} = T^{l^T} \underline{u}^k; \; \underline{v_e^{*klm}} = T_e^{kl^T} \tilde{X}^{m^T} \underline{\omega_r^0}; \; \underline{\dot{v}_e}^{*klm} = T^{lm^T} \underline{u}^k \end{aligned} \tag{3.3.17}$$

with

$$\tilde{X}^0 = \begin{bmatrix} 0 & -(z_0 + u_3^0) & (y_0 + u_2^0) \\ (z_0 + u_3^0) & 0 & -(x_0 + u_1^0) \\ -(y_0 + u_2^0) & (x_0 + u_1^0) & 0 \end{bmatrix}$$

and

$$\tilde{X}^k = \begin{bmatrix} 0 & -u_3^k & u_2^k \\ u_3^k & 0 & -u_1^k \\ -u_2^k & u_1^k & 0 \end{bmatrix} \tag{3.3.18}$$

The elastic angular velocities are found:

$$\underline{w}_e^* = \underline{w}_e^{*0} + \underline{w}_e^{*k}\psi_u^k + \underline{\dot{\omega}}^{*k}\dot{\psi}_u^k + \underline{w}_e^{*kl}\psi_u^k\psi_u^l + \underline{\dot{\omega}}^{*kl}\dot{\psi}_u^k\psi_u^l \tag{3.3.19}$$

where

$$\underline{\omega}_e^{*0} = T_e^{0T}\underline{\omega}_r^0 \; ; \; \underline{\omega}_e^{*k} = T_e^{kT}\underline{\omega}_r^0 \; ; \; \dot{\tilde{\omega}}_e^{*k} = 2G^0\underline{q}^k \; ; \; \underline{\omega}_e^{*kl} = T_e^{kT}\underline{\omega}_r^l; \;\; \dot{\tilde{\omega}}_e^{*kl} = 2G^k\underline{q}^k \tag{3.3.20}$$

The velocity expressions can be combined as:

$$\begin{aligned}\underline{V_e^*} = \underline{V_e^{*o}} + \underline{V_e^{*k}}\psi_u^k + \underline{\dot{V}_e^{*k}}\dot{\psi}_u^k + \underline{V_e^{*kl}}\psi_u^k\psi_u^l + \underline{\dot{V}_e^{*kl}}\dot{\psi}_u^k\psi_u^l \\ + \underline{V_e^{*klm}}\psi_u^k\psi_u^l\psi_u^m + \underline{\dot{V}_e^{*klm}}\dot{\psi}_u^k\psi_u^l\psi_u^m\end{aligned} \tag{3.3.21}$$

The elastic Lagrangian now becomes:

$$\begin{aligned}\mathcal{L}_e = \mathcal{L}^0 + \mathcal{L}_u^k\psi_u^k + \mathcal{L}_d^k\dot{\psi}_u^k + \mathcal{L}_f^k\psi_f^k + \mathcal{L}_p^k\psi_p^k + \mathcal{L}_{uu}^{kl}\psi_u^k\psi_u^l + \mathcal{L}_{du}^{kl}\dot{\psi}_u^k\psi_u^l \\ + \mathcal{L}_{fu}^{kl}\psi_f^k\psi_u^l + \mathcal{L}_{pu}^{kl}\psi_p^k\psi_u^l + \mathcal{L}_{pd}^{kl}\psi_p^k\dot{\psi}_u^l + \mathcal{L}_{ff}^{kl}\psi_f^k\psi_f^l + \mathcal{L}_{pp}^{kl}\psi_p^k\psi_p^l \\ + \mathcal{L}_{fuu}^{klm}\psi_f^k\psi_u^l\psi_u^m + \mathcal{L}_{puu}^{klm}\psi_p^k\psi_u^l\psi_u^m + \mathcal{L}_{pdu}^{klm}\psi_p^k\dot{\psi}_u^l\psi_u^m \\ + \mathcal{L}_{fuuu}^{klmn}\psi_f^k\psi_u^l\psi_u^m\psi_u^n + \mathcal{L}_{puuu}^{klmn}\psi_p^k\psi_u^l\psi_u^m\psi_u^n + \mathcal{L}_{pduu}^{klmn}\psi_p^k\dot{\psi}_u^l\psi_u^m\psi_u^n\end{aligned} \tag{3.3.22}$$

where

$$\begin{aligned}&\mathcal{L}_u^k = \underline{p}_e^{*0^T}\underline{V}_e^{*k} - \underline{F}^{0^T}\underline{\epsilon}^k \; ; \; \mathcal{L}_d^k = \underline{p}_e^{*0^T}\dot{\underline{V}}_e^{\;*k} \; ; \; \mathcal{L}_f^k = -\underline{F}^{k^T}\left(\underline{\epsilon}^0 - H\underline{F}^0\right) ; \\ &\mathcal{L}_p^k = \underline{p}_e^{*k^T}\left(\underline{V}_e^{*0} - M^{*^{-1}}\underline{p}_e^{*0}\right); \mathcal{L}_{uu}^{kl} = \underline{p}_e^{*0^T}\underline{V}_e^{*kl} - \underline{F}^{0^T}\underline{\epsilon}^{kl} \; ; \; \mathcal{L}_{du}^{kl} = \underline{p}_e^{*0^T}\dot{\underline{V}}_e^{\;*kl} \; ; \\ &\mathcal{L}_{fu}^{kl} = -F^{k^T}\underline{\epsilon}^l \; ; \; \mathcal{L}_{ff}^{kl} = \frac{1}{2}\underline{F}^{k^T}H\underline{F}^l \; ; \; \mathcal{L}_{pu}^{kl} = \underline{p}_e^{*k^T}\underline{V}_e^{*l} \; ; \; \mathcal{L}_{pd}^{kl} = \underline{p}_e^{*k^T}\dot{\underline{V}}_e^{\;*l} \; ; \\ &\mathcal{L}_{pp}^{kl} = -\frac{1}{2}\underline{p}_e^{*k^T}M^{*^{-1}}\underline{p}_e^{*l} \; ; \; \mathcal{L}_{uuu}^{klm} = \underline{p}_e^{*0^T}\underline{V}_e^{*klm} - \underline{F}^{0^T}\underline{\epsilon}^{klm}; \; \mathcal{L}_{duu}^{klm} = \underline{p}_e^{*0^T}\dot{\underline{V}}_e^{\;*klm} \; ; \\ &\mathcal{L}_{fuu}^{klm} = -F^{k^T}\underline{\epsilon}^{lm} \; ; \; \mathcal{L}_{puu}^{klm} = \underline{p}_e^{*k^T}\underline{V}_e^{*lm} \; ; \; \mathcal{L}_{pdu}^{klm} = \underline{p}_e^{*k}\dot{\underline{V}}_e^{\;*lm}; \\ &\mathcal{L}_{fuuu}^{klmn} = -F^{k^T}\underline{\epsilon}^{lmn} \; ; \; \mathcal{L}_{puuu}^{klmn} = \underline{p}_e^{*k^T}\underline{V}_e^{*lmn} \; ; \; \mathcal{L}_{pduu}^{klmn} = \underline{p}_e^{*k^T}\dot{\underline{V}}_e^{\;*lmn}\end{aligned} \tag{3.3.23}$$

Section 3.4: Rigid Lagrangian for Beam Elements

The matrix M^* defined in 2.5.19 can be partitioned as:

$$M^* = \begin{bmatrix} mI & \tilde{m}^{*T} \\ \tilde{m}^* & J^* \end{bmatrix} \tag{3.4.1}$$

The matrix M (3.2.6) can then be written as

$$M = \begin{bmatrix} mI & \tilde{m}^T \\ \tilde{m} & J \end{bmatrix} \tag{3.4.2}$$

where

$$\tilde{m} = m\tilde{X} + T_e\tilde{m}^* T_e^T \tag{3.4.3}$$

and

$$J = \tilde{X}\tilde{m}^T + \tilde{m}\tilde{X}^T - m\tilde{X}\tilde{X}^T + T_e J^* T_e^T \tag{3.4.4}$$

The modal expansion of $\tilde{m}$ gives:

$$\underline{m} = \underline{m}^0 + \underline{m}^k\psi_u^k + \underline{m}^{kl}\psi_u^k\psi_u^l \tag{3.4.5}$$

where

$$\underline{m}^0 = m\underline{u}^0 + T_e^0\underline{m}^* \;;\; \underline{m}^k = m\underline{u}^k + T_e^k\underline{m}^*;\; \underline{m}^{kl} = T_e^{kl}\underline{m}^* \tag{3.4.6}$$

The modal expansion of J becomes:

$$J = J^0 + J^k\psi_u^k + J^{kl}\psi_u^k\psi_u^l + J^{klm}\psi_u^k\psi_u^l\psi_u^m + J^{klmn}\psi_u^k\psi_u^l\psi_u^m\psi_u^n \tag{3.4.7}$$

with

$$\begin{aligned}
J^0 =& \tilde{X}^0\tilde{m}^{0T} + \tilde{m}^0\tilde{X}^{0T} - m\tilde{X}^0\tilde{X}^{0T} + T_e^0 J^* T_e^{0T} \\
J^k =& \tilde{X}^0\tilde{m}^{kT} + \tilde{X}^k\tilde{m}^{0T} + \tilde{m}^0\tilde{X}^{kT} + \tilde{m}^k\tilde{X}^{0T} - m\tilde{X}^0\tilde{X}^{kT} - m\tilde{X}^k\tilde{X}^{0T} \\
&+ T_e^0 J^* T_e^{kT} + T_e^k J^* T_e^{0T} \\
J^{kl} =& \tilde{X}^0\tilde{m}^{klT} + \tilde{X}^k\tilde{m}^{lT} + \tilde{m}^k\tilde{X}^{lT} + \tilde{m}^{kl}\tilde{X}^{0T} - m\tilde{X}^k\tilde{X}^{lT} \\
&+ T_e^0 J^* T_e^{klT} + T_e^{kl} J^* T_e^{0T} + T_e^k J^* T_e^{lT} \\
J^{klm} =& \tilde{X}^k\tilde{m}^{lmT} + \tilde{m}^{kl}\tilde{X}^{mT} + T_e^k J^* T_e^{lmT} + T_e^{kl} J^* T_e^{mT} \\
J^{klm} =& T_e^{kl} J^* T_e^{mnT}
\end{aligned} \tag{3.4.8}$$

The vector $\underline{C}^T = \left\lfloor \underline{CA}^T, \underline{CB}^T \right\rfloor$ becomes:

$$\begin{aligned}
\underline{CA} &= m\dot{\underline{u}} + \tilde{m}^T\underline{\omega}_r^0 + \dot{T}_e\underline{m}^* \\
&= \underline{CA}^0 + \underline{CA}_u^k\psi_u^k + \underline{CA}_d^k\dot{\psi}_u^k + \underline{CA}_{uu}^{kl}\psi_u^k\psi_u^l + \underline{CA}_{du}^{kl}\dot{\psi}_u^k\psi_u^l
\end{aligned} \tag{3.4.9}$$

$$\begin{aligned}
\underline{CB} &= \tilde{m}\dot{\underline{u}} + J\underline{\omega}_r^0 + \tilde{X}\dot{T}_e\underline{m}^* + T_e J^*\underline{\omega}_e^* \\
&= \underline{CB}^0 + \underline{CB}_u^k\psi_u^k + \underline{CB}_d^k\dot{\psi}_u^k + \underline{CB}_{uu}^{kl}\psi_u^k\psi_u^l + \underline{CB}_{du}^{kl}\dot{\psi}_u^k\psi_u^l \\
&+ \underline{CB}_{uuu}^{klm}\psi_u^k\psi_u^l\psi_u^m + \underline{CB}_{duu}^{klm}\dot{\psi}_u^k\psi_u^l\psi_u^m + \underline{CB}_{uuuu}^{klmn}\psi_u^k\psi_u^l\psi_u^m\psi_u^n + \underline{CB}_{duuu}^{klmn}\dot{\psi}_u^k\psi_u^l\psi_u^m\psi_u^n
\end{aligned} \tag{3.4.10}$$

where

$$\begin{aligned}
&\underline{CA}^0 = \tilde{m}^{0T}\underline{\omega}_r^0 \;;\; \underline{CA}_u^k = \tilde{m}^{kT}\underline{\omega}_r^0 \;;\; \underline{CA}_d^k = m\underline{u}^k + T_e^k\underline{m}^* = \underline{m}^k \\
&\underline{CA}_{uu}^{kl} = \tilde{m}^{klT}\underline{\omega}_r^0 \;;\; \underline{CA}_{du}^{kl} = \left(T^{kl} + T^{lk}\right)\underline{m}^*
\end{aligned} \tag{3.4.11}$$

and

$$\begin{aligned}
&\underline{CB}^0 = J^0\underline{\omega}_r^0 \;;\; \underline{CB}_u^k = J^k\underline{\omega}_r^0 \;;\; \underline{CB}_d^k = \tilde{m}^0\underline{u}^k + \tilde{X}^0 T_e^k\underline{m}^* + T_e^0 J^*\dot{\underline{\omega}}_e^{*k} \\
&\underline{CB}_{uu}^{kl} = J^{kl}\underline{\omega}_r^0 \;;\; \underline{CB}_{du}^{kl} = \tilde{m}^l\underline{u}^k + \tilde{X}^l T_e^k\underline{m}^* + \tilde{X}^l\left(T_e^{kl} + T_e^{lk}\right)\underline{m}^* + T_e^0 J^*\dot{\underline{\omega}}_e^{*kl} + T_e^l J^*\dot{\underline{\omega}}_e^{*k} \\
&\underline{CB}_{uuu}^{klm} = J^{klm}\underline{\omega}_r^0 \;;\; \underline{CB}_{duu}^{klm} = \tilde{m}^{lm}\underline{u}^k + \tilde{X}^m\left(T_e^{kl} + T_e^{lk}\right)\underline{m}^* + T_e^m J^*\dot{\underline{\omega}}_e^{*kl} + T_e^{lm} J^*\dot{\underline{\omega}}_e^{*k} \\
&\underline{CB}_{uuuu}^{klmn} = J^{klmn}\underline{\omega}_r^0 \;;\; \underline{CB}_{duuu}^{klmn} = T_e^{lm} J^*\dot{\underline{\omega}}_e^{*kl}
\end{aligned} \tag{3.4.12}$$

Finally the vector $\underline{D}^T = \left\lfloor \underline{DA}^T, \underline{DB}^T \right\rfloor$ becomes:

$$\begin{aligned}\underline{DA} &= T_e \underline{p}_a^* \\ &= \underline{DA}^0 + \underline{DA}_u^k \psi_u^k + \underline{DA}_p^k \psi_p^k + \underline{DA}_{uu}^{kl} \psi_u^k \psi_u^l + \underline{DA}_{pu}^{kl} \psi_p^k \psi_u^l + \underline{DA}_{puu}^{klm} \psi_p^k \psi_u^l \psi_u^m\end{aligned} \tag{3.4.13}$$

and

$$\begin{aligned}\underline{DB} &= \tilde{X} T_e \underline{p}_a^* + T_e \underline{p}_b^* \\ &= \underline{DB}^0 + \underline{DB}_u^k \psi_u^k + \underline{DB}_p^k \psi_p^k + \underline{DB}_{uu}^{kl} \psi_u^k \psi_u^l + \underline{DB}_{pu}^{kl} \psi_p^k \psi_u^l \\ &+ \underline{DB}_{uuu}^{klm} \psi_u^k \psi_u^l \psi_u^m + \underline{DB}_{puu}^{klm} \psi_p^k \psi_u^l \psi_u^m + \underline{DB}_{puuu}^{klmn} \psi_p^k \psi_u^l \psi_u^m \psi_u^n\end{aligned} \tag{3.4.14}$$

where

$$\begin{gathered}\underline{DA}^0 = T_e^0 \underline{p}_a^{*0} \; ; \; \underline{DA}_u^k = T_e^k \underline{p}_a^{*0} \; ; \; \underline{DA}_p^k = T_e^0 \underline{p}_a^{*k} \; ; \; \underline{DA}_{uu}^{kl} = T_e^{kl} \underline{p}_a^{*0} \; ; \\ \underline{DA}_{pu}^{kl} = T_e^l \underline{p}_a^{*k} \; ; \; \underline{DA}_{puu}^{klm} = T_e^{lm} \underline{p}_a^{*k}\end{gathered} \tag{3.4.15}$$

and

$$\begin{aligned}&\underline{DB}^0 = \tilde{X}^0 T_e^0 \underline{p}_a^{*0} + T_e^0 \underline{p}_b^{*0} \; ; \; \underline{DB}_u^k = \left(\tilde{X}^0 T_e^k + \tilde{X}^k T_e^0\right) \underline{p}_a^{*0} + T_e^k \underline{p}_b^{*0} \\ &\underline{DB}_p^k = \tilde{X}^0 T_e^0 \underline{p}_a^{*k} + T_e^0 \underline{p}_b^{*k} \; ; \\ &\underline{DB}_{uu}^{kl} = \left(\tilde{X}^0 T_e^{kl} + \tilde{X}^k T_e^l\right) \underline{p}_a^{*0} + T_e^{kl} \underline{p}_b^{*0} \; ; \; \underline{DB}_{pu}^{kl} = \left(\tilde{X}^0 T_e^l + \tilde{X}^l T_e^0\right) \underline{p}_a^{*k} + T_e^l \underline{p}_b^{*k} \\ &\underline{DB}_{uuu}^{klm} = \tilde{X}^k T_e^{lm} \underline{p}_a^{*0} \; ; \; \underline{DB}_{puu}^{klm} = \left(\tilde{X}^0 T_e^{lm} + \tilde{X}^l T_e^m\right) \underline{p}_a^{*k} + T_e^{lm} \underline{p}_b^{*k} \\ &\underline{DB}_{puuu}^{klmn} = \tilde{X}^l T_e^{mn} \underline{p}_a^{*k}\end{aligned} \tag{3.4.16}$$

Section 3.5: Linearization of The Lagrangian

As a result of the modal expression described in the previous section, the total Lagrangian can be written as:

$$\mathcal{L} = \underline{U}_r^T M \underline{V}_r - \frac{1}{2} \underline{U}_r^T M \underline{U}_r + \underline{U}_r^T (\underline{C} - \underline{D}) + \underline{V}_r^T \underline{D} + \mathcal{L}_e \tag{3.5.1}$$

where

$$\begin{aligned}M &= M^0 + M^k \phi^k + M^{kl} \phi^k \phi^l + M^{klm} \phi^k \phi^l \phi^m + M^{klmn} \phi^k \phi^l \phi^m \phi^n \\ \underline{C} &= \underline{C}^0 + \underline{C}^k \phi^k + \underline{C}^{kl} \phi^k \phi^l + \underline{C}^{klm} \phi^k \phi^l \phi^m + \underline{C}^{klmn} \phi^k \phi^l \phi^m \phi^n \\ \underline{D} &= \underline{D}^0 + \underline{D}^k \phi^k + \underline{D}^{kl} \phi^k \phi^l + \underline{D}^{klm} \phi^k \phi^l \phi^m + \underline{D}^{klmn} \phi^k \phi^l \phi^m \phi^n \\ \mathcal{L}_e &= \mathcal{L}_e^0 + \mathcal{L}_e^k \phi^k + \mathcal{L}_e^{kl} \phi^k \phi^l + \mathcal{L}_e^{klm} \phi^k \phi^l \phi^m + \mathcal{L}_e^{klmn} \phi^k \phi^l \phi^m \phi^n\end{aligned} \tag{3.5.2}$$

The state vector $\phi = \left\lfloor \underline{\psi}_u, \dot{\underline{\psi}}_u, \underline{\psi}_f, \underline{\psi}_p \right\rfloor$ has been used to simplify the notation. The quasi-linearization procedure is used to expand the Lagrangian about a known configuration:

$$\mathcal{L} = \overline{\mathcal{L}} + \left\lfloor \Delta \underline{R}^T, \Delta \dot{\underline{R}}^T, \Delta U^T, \Delta \underline{\phi}^T \right\rfloor \left\{ \begin{vmatrix} \underline{\mathcal{L}}_R \\ \underline{\mathcal{L}}_{\dot{R}} \\ \underline{\mathcal{L}}_U \\ \underline{\mathcal{L}}_\phi \end{vmatrix} + \frac{1}{2} \begin{bmatrix} \mathcal{L}_{RR} & & & \\ \mathcal{L}_{\dot{R}R} & 0 & & \\ \mathcal{L}_{UR} & \mathcal{L}_{U\dot{R}} & \mathcal{L}_{UU} & \\ \mathcal{L}_{\phi R} & \mathcal{L}_{\phi \dot{R}} & \mathcal{L}_{\phi U} & \mathcal{L}_{\phi\phi} \end{bmatrix} \begin{vmatrix} \Delta \underline{R} \\ \Delta \dot{\underline{R}} \\ \Delta U \\ \Delta \underline{\phi} \end{vmatrix} \right\} + h.o.t \tag{3.5.3}$$

where the first derivatives of the Lagrangian are:

$$\begin{aligned}
&\mathcal{L}_R = Z(M\underline{U}_r + \underline{D})\ ;\ \mathcal{L}_{\dot{R}} = \dot{Z}(M\underline{U}_r + \underline{D})\ ; \\
&\mathcal{L}_U = (M\underline{V}_r + \underline{C}) - (M\underline{U}_r + \underline{D}) \\
&\mathcal{L}_\phi = \underline{U}_r^T M_i \underline{V}_r - \frac{1}{2}\underline{U}_r^T M_i \underline{U}_r + \underline{U}_r^T \underline{C}_i + \left(\underline{V}_r^T - \underline{U}_r^T\right)\underline{D}_i + \mathcal{L}_{ei}
\end{aligned} \tag{3.5.4}$$

The second derivatives of the Lagrangian are:

$$\begin{aligned}
&\mathcal{L}_{RR} = W\ ;\ \mathcal{L}_{\dot{R}R} = \dot{W}\ ;\ \mathcal{L}_{UR} = MZ^T\ ;\ \mathcal{L}_{U\dot{R}} = M\dot{Z}^T\ ;\ \mathcal{L}_{UU} = -M \\
&\mathcal{L}_{\phi R} = \left(\underline{U}_r^T M_i + \underline{D}_i^T\right) Z^T\ ;\ \mathcal{L}_{\phi\dot{R}} = \left(\underline{U}_r^T M_i + \underline{D}_i^T\right)\dot{Z}^T\ ; \\
&\mathcal{L}_{\phi U} = (M_i\underline{V}_r + \underline{C}_i) - (M_i\underline{U}_r + \underline{D}_i)\ ; \\
&\mathcal{L}_{\phi\phi} = \underline{U}_r^T M_{ij}\underline{V}_r - \frac{1}{2}\underline{U}_r^T M_{ij}\underline{U}_r + \underline{U}_r^T \underline{C}_{ij} + \left(\underline{V}_r^T - \underline{U}_r^T\right)\underline{D}_{ij} + \mathcal{L}_{eij}
\end{aligned} \tag{3.5.5}$$

Increments in the rigid velocities can be related to increments in the rigid body parameters as:

$$\Delta\underline{V}_r = Z^T\Delta\underline{R} + \dot{Z}^T\Delta\underline{\dot{R}} \tag{3.5.6}$$

where

$$Z^T = \begin{bmatrix} T_r^{0^T} & 0 & 0 \\ 0 & T_r^{0^T} & 0 \\ 0 & 0 & 1 \end{bmatrix} \begin{bmatrix} 0 & 0 & 0 & 2F_1 & 2F_0 & -2F_3 & 2F_2 \\ 0 & 0 & 0 & 2F_2 & 2F_3 & 2F_0 & -2F_1 \\ 0 & 0 & 0 & 2F_3 & -2F_2 & 2F_1 & 2F_0 \\ 0 & 0 & 0 & 2\dot{Q}_1 & -2\dot{Q}_0 & -2\dot{Q}_3 & 2\dot{Q}_2 \\ 0 & 0 & 0 & 2\dot{Q}_2 & 2\dot{Q}_3 & -2\dot{Q}_0 & -2\dot{Q}_1 \\ 0 & 0 & 0 & 2\dot{Q}_1 & -2\dot{Q}_2 & 2\dot{Q}_1 & -2\dot{Q}_0 \\ 0 & 0 & 0 & 2\dot{Q}_0 & 2\dot{Q}_1 & 2\dot{Q}_2 & 2\dot{Q}_3 \end{bmatrix} \tag{3.5.7}$$

$$\dot{Z}^T = \begin{bmatrix} T_r^{0^T} & 0 & 0 \\ 0 & T_r^{0^T} & 0 \\ 0 & 0 & 1 \end{bmatrix} \begin{bmatrix} T_{11} & T_{21} & T_{31} & 0 & 0 & 0 & 0 \\ T_{12} & T_{22} & T_{32} & 0 & 0 & 0 & 0 \\ T_{13} & T_{23} & T_{33} & 0 & 0 & 0 & 0 \\ 0 & 0 & 0 & -2Q_1 & 2Q_0 & 2Q_3 & -2Q_2 \\ 0 & 0 & 0 & -2Q_2 & -2Q_3 & 2Q_0 & 2Q_1 \\ 0 & 0 & 0 & -2Q_3 & 2Q_2 & -2Q_1 & 2Q_0 \\ 0 & 0 & 0 & 2Q_0 & 2Q_1 & 2Q_2 & 2Q_3 \end{bmatrix} \tag{3.5.8}$$

with

$$\begin{vmatrix} F_0 \\ F_1 \\ F_2 \\ F_3 \end{vmatrix} = \begin{bmatrix} Q_1 & Q_2 & Q_3 \\ Q_0 & Q_3 & -Q_2 \\ -Q_3 & Q_0 & Q_1 \\ Q_2 & -Q_1 & Q_0 \end{bmatrix} \begin{vmatrix} \dot{P}_1 \\ \dot{P}_2 \\ \dot{P}_3 \end{vmatrix} \tag{3.5.9}$$

The following quantities are now defined:

$$\tilde{\mathcal{L}}_e^k = \mathcal{L}_e^k + \underline{U}_r^T M^k \underline{V}_r - \frac{1}{2}\underline{U}_r^T M^k \underline{U}_r + \underline{U}_r^T \underline{C}^k + \left(\underline{V}_r^T - \underline{U}_r^T\right)\underline{D}^k$$

$$\tilde{\mathcal{L}}_e^{kl} = \mathcal{L}_e^{kl} + \underline{U}_r^T M^{kl} \underline{V}_r - \frac{1}{2}\underline{U}_r^T M^{kl} \underline{U}_r + \underline{U}_r^T \underline{C}^{kl} + \left(\underline{V}_r^T - \underline{U}_r^T\right)\underline{D}^{kl}$$

$$\tilde{\mathcal{L}}_e^{klm} = \mathcal{L}_e^{klm} + \underline{U}_r^T M^{klm} \underline{V}_r - \frac{1}{2}\underline{U}_r^T M^{klm} \underline{U}_r + \underline{U}_r^T \underline{C}^{klm} + \left(\underline{V}_r^T - \underline{U}_r^T\right)\underline{D}^{klm}$$

$$\tilde{\mathcal{L}}_e^{klmn} = \mathcal{L}_e^{klmn} + \underline{U}_r^T M^{klmn} \underline{V}_r - \frac{1}{2}\underline{U}_r^T M^{klmn} \underline{U}_r + \underline{U}_r^T \underline{C}^{klmn} + \left(\underline{V}_r^T - \underline{U}_r^T\right)\underline{D}^{klmn} \tag{3.5.10}$$

and

$$\begin{aligned}
\underline{\tilde{C}}^0 &= M^0 \underline{V}_r + \underline{C}^0; \quad & \underline{\tilde{D}}^0 &= M^0 \underline{U}_r + \underline{D}^0 \\
\underline{\tilde{C}}^k &= M^k \underline{V}_r + \underline{C}^k; \quad & \underline{\tilde{D}}^k &= M^k \underline{U}_r + \underline{D}^k \\
\underline{\tilde{C}}^{kl} &= M^{kl} \underline{V}_r + \underline{C}^{kl}; \quad & \underline{\tilde{D}}^{kl} &= M^{kl} \underline{U}_r + \underline{D}^{kl} \\
\underline{\tilde{C}}^{klm} &= M^{klm} \underline{V}_r + \underline{C}^{klm}; \quad & \underline{\tilde{D}}^{klm} &= M^{klm} \underline{U}_r + \underline{D}^{klm} \\
\underline{\tilde{C}}^{klmn} &= M^{klmn} \underline{V}_r + \underline{C}^{klmn}; \quad & \underline{\tilde{D}}^{klmn} &= M^{klmn} \underline{U}_r + \underline{D}^{klmn}
\end{aligned} \tag{3.5.11}$$

The first derivative becomes:

$$\mathcal{L}_R = Z\underline{Y}\ ;\ \mathcal{L}_{\dot{R}} = \dot{Z}\underline{Y}\ ;\mathcal{L}_U = \underline{X} - \underline{Y}\ ;\ \mathcal{L}_{\phi i} = \tilde{\mathcal{L}}_{ei} \tag{3.5.12}$$

The second derivative becomes:

$$\begin{aligned}
&\mathcal{L}_{RR} = W\ ;\ \mathcal{L}_{\dot{R}R} = \dot{W}\ ;\ \mathcal{L}_{UR} = MZ^T\ ;\ \mathcal{L}_{U\dot{R}} = M\dot{Z}^T\ ;\ \mathcal{L}_{UU} = -M \\
&\mathcal{L}_{\phi R} = \underline{Y}_i Z^T\ ;\ \mathcal{L}_{\phi \dot{R}} = \underline{Y}_i \dot{Z}^T\ ;\ \mathcal{L}_{\phi U} = \underline{X}_i - \underline{Y}_i \\
&\mathcal{L}_{\phi\phi} = \tilde{\mathcal{L}_{eij}}
\end{aligned} \tag{3.5.13}$$

where

$$\begin{aligned}
\underline{X} &= \underline{\tilde{C}}^0 + \underline{\tilde{C}}^k \phi^k + \underline{\tilde{C}}^{kl} \phi^k \phi^l + \underline{\tilde{C}}^{klm} \phi^k \phi^l \phi^m + \underline{\tilde{C}}^{klmn} \phi^k \phi^l \phi^m \phi^n \\
\underline{Y} &= \underline{\tilde{D}}^0 + \underline{\tilde{D}}^k \phi^k + \underline{\tilde{D}}^{kl} \phi^k \phi^l + \underline{\tilde{D}}^{klm} \phi^k \phi^l \phi^m + \underline{\tilde{D}}^{klmn} \phi^k \phi^l \phi^m \phi^n
\end{aligned} \tag{3.5.14}$$

The following arrays were defined

$$W = \begin{bmatrix}
0 & & & & & & \\
0 & 0 & & & & & \\
0 & 0 & 0 & & & & \\
0 & 0 & 0 & R_0 & & & \\
0 & 0 & 0 & S_1 & R_1 & & \\
0 & 0 & 0 & S_2 & T_3 & R_2 & \\
0 & 0 & 0 & S_3 & T_2 & T_1 & R_3
\end{bmatrix}$$

$$\dot{W} = \begin{bmatrix}
0 & 0 & 0 & H_1 & H_0 & H_3 & -H_2 \\
0 & 0 & 0 & H_2 & -H_3 & H_0 & H_1 \\
0 & 0 & 0 & H_3 & H_2 & -H_1 & H_0 \\
0 & 0 & 0 & \alpha U_7 & -2Y_4^* & -2Y_5^* & -2Y_6^* \\
0 & 0 & 0 & 2Y_4^* & \alpha U_7 & 2Y_6^* & -2Y_5^* \\
0 & 0 & 0 & 2Y_5^* & -2Y_6^* & \alpha U_7 & 2Y_4^* \\
0 & 0 & 0 & 2Y_6^* & 2Y_5^* & -2Y_4^* & \alpha U_7
\end{bmatrix} \tag{3.5.15}$$

and

$$\begin{vmatrix} R_0 \\ R_1 \\ R_2 \\ R_3 \end{vmatrix} = 2 \begin{bmatrix} \dot{P}_1 & \dot{P}_2 & \dot{P}_3 \\ \dot{P}_1 & -\dot{P}_2 & -\dot{P}_3 \\ -\dot{P}_1 & \dot{P}_2 & -\dot{P}_3 \\ -\dot{P}_1 & -\dot{P}_2 & \dot{P}_3 \end{bmatrix} \begin{vmatrix} Y_1^* \\ Y_2^* \\ Y_3^* \end{vmatrix} \; ; \; \begin{vmatrix} S_1 \\ S_2 \\ S_3 \end{vmatrix} = 2 \begin{bmatrix} 0 & \dot{P}_3 & -\dot{P}_2 \\ -\dot{P}_3 & 0 & \dot{P}_1 \\ \dot{P}_2 & -\dot{P}_1 & 0 \end{bmatrix} \begin{vmatrix} Y_1^* \\ Y_2^* \\ Y_3^* \end{vmatrix}$$

$$\begin{vmatrix} H_0 \\ H_1 \\ H_2 \\ H_3 \end{vmatrix} = 2 \begin{bmatrix} Q_1 & Q_2 & Q_3 \\ Q_0 & -Q_3 & Q_2 \\ Q_3 & Q_0 & -Q_1 \\ -Q_2 & Q_1 & Q_0 \end{bmatrix} \begin{vmatrix} Y_1^* \\ Y_2^* \\ Y_3^* \end{vmatrix} \; ; \; \begin{vmatrix} T_1 \\ T_2 \\ T_3 \end{vmatrix} = 2 \begin{bmatrix} 0 & \dot{P}_3 & \dot{P}_2 \\ \dot{P}_3 & 0 & \dot{P}_1 \\ \dot{P}_2 & \dot{P}_1 & 0 \end{bmatrix} \begin{vmatrix} Y_1^* \\ Y_2^* \\ Y_3^* \end{vmatrix}$$

$$\underline{Y}^* = \begin{bmatrix} T_r^0 & 0 & 0 \\ 0 & T_r^0 & 0 \\ 0 & 0 & 1 \end{bmatrix} \underline{Y} \tag{3.5.16}$$

References

3–1. Hodges, D. H.,"A Review of Composite Rotor Blade Modeling," to appear in J. American Helicopter Society.

3–2. Sivaneri, N. T. and Chopra, I."Finite Element Analysis for Bearingless Rotor Blade Aeroelasticity," J. American Helicopter Society, Vol. 29, No. 2, 42-51, April 1984.

3–3. Hodges, D, H. and Dowell, E. H.,"Nonlinear Equations of Motion for the Elastic Bending and Torsion of Twisted Nonuniform Blades," NASA TN D-7818, Dec. 1974.

3–4. Giavotto, V., Borri, M., Mantegazza, P., Ghiringhelli, G., Carmschi, V., Maffioli, G., and Mussi, F.,"Anistropic Beam Theory and Applications," Computer and Structures, Vol. 16, 403-413, 1983.

3–5. Borri, M. and Merlini, T.,"A Large Displacement Formulation for Anisotropic Beam Analysis," Meccanica, Vol. 21, 30-37, 1986.

3–6. Baucahu, O. A. and Hong, C. H.,"Nonlinear Response and Stability Analysis of Beams Using Finite Elements in Time," AIAA Sept. 1988.

3–7. Loewy, R.G.,"Review of Rotary-wing V/STOL Dynamic and Aeroelastic Problems," J. American Helicopter Society. Vol. 14, 3-23, July 1969.

3–8. Friedmann, P. P.,"Recent Developments in Rotary-wing Aeroelasticity," J. Aircraft Vol. 14, No. 11, 1027-1041, Nov. 1977.

3–9. Friedmann, P. P.,"Formulation and Solutions of Rotary-wing Aeroelastic Stability and Response Problems," Vertica Vol. 7, 101-104, 1983.

3–10. Friedmann, P. P., "Recent Trends in Rotary-wing Aeroelasticity," Vertica Vol. 11, No. 1/2, 139-170, 1987.

Chapter 4

Comparisons of Modal and Finite Element Methods

Section 4.1 Introduction

The appropriate choice of modes is crucial to achieve accuracy in the modal analysis. In general, natural vibration modes have been selected in modal analysis of rotor blades. The relative merits of various sets of modes have been investigated, for instance, coupled or uncoupled free vibration modes of a rotating or non-rotating blade [4–1,3]. It is important to note that natural vibration modes characterize the linearized dynamic behavior of the blade, i.e. the dynamic behavior of small, time dependent perturbations about a given, steady equilibrium position of the blade. Even though it is natural to use such modes in the analysis of nonlinear problem, it is well known that the accuracy and efficiency of a modal method depends on the "quality" of the assumed modes, i.e. the ability of the assumed modes to represent the actual response of the blade.

When natural vibration modes are used in conjunction with a displacement based energy formulation that includes axial displacement as an independent variable, the performance of the modal approximation is extremely poor. Consider the lateral deflection of a blade in the nonlinear range, under a simple tip oscillatory load. If flapping modes are used in the modal approximation, the lateral deflection is found to be much smaller than that predicted by the full finite element model. This can be explained by the fact that flapping modes contain no axial component (since they are linearized modes), hence foreshortening of the blade is not allowed in the modal approximation and this results in large axial loads which in turn, stiffen the blade considerably. The situation is somewhat improved by adding axial vibration modes, but a large number of these modes is required to obtained a good solution.

The reason for this behavior is twofold. First, in a displacement based formulation, the stress-strain relationships are strongly enforced (i.e. they are satisfied on a point by point basis), therefore, a very small error in the estimation of the axial strain (as should be expected from a modal approximation) will result in very large axial forces, because of the very large axial stiffness of the blade. In fact, the inextensibility assumption is often made to avoid this problem, however, the formulation is then restricted to single load path blades. This problem can be overcome when using the mixed formulation described in Chapter 2. Indeed, in a mixed formulation, the stress-strain relationships are only enforced in a weak sense (i.e. in an integral sense); hence, small errors in strain do not necessarily result in large errors in the forces.

Second, the actual axial displacement of the blade is due to foreshortening (a nonlinear kinematic phenomena), whereas axial vibration modes characterize true axial vibrations (a purely linear vibratory phenomenon). In other words, we are trying to "synthesize" a nonlinear kinematic mode shape, with linear vibratory mode. Since these two phenomena are not physically related, we should hardly expect to obtain good results in predicting axial displacements. This discussion has focussed on axial displacements

due to foreshortening however, the above arguments equally apply to any nonlinear behavior of the blade. For instance, transverse loads applied to the blade create a torque due to the blade's transverse deflections. This nonlinear kinematic coupling is very important for helicopter blade response, as it can change its angle of attack.

This clearly indicates the need for selecting alternate mode shapes that contain information about the nonlinear behavior of the structure. Several concepts have been proposed to improve the quality of the modal bases when dealing with nonlinear problems. The conceptually simplest method it to recalculate a new set of natural vibration modes every once in a while as the deformations of the blade become significant [4–7]. In fact, the natural vibration frequencies and associated mode shapes of a helicopter blade are known to vary significantly around the azimuth [4–3]. Even though this approach might give good results, it does so at a tremendous computational cost, since the modal basis must be updated during the response calculation, and the modal reduction scheme must be repeated at each update. Another approach is to include in the modal basis natural vibration modes about various different equilibrium configurations of the structure. This method is attractive since only a modest increase in computation cost is required to evaluate the various equilibrium configurations. Furthermore, this method appears to give accurate results, see for instance [4–7].

Finally, the concept of perturbation modes seems to hold promise for improving the accuracy of modal methods. It was introduced by Thompson and Walker [4–4] as an analytical tool for the study of the nonlinear behavior of beam structures, and later the same concept was used by Noor et al [4–5,6] in the nonlinear static analysis of beam and shell structures in conjunction with the finite element method. The very same concept will be used here to study nonlinear dynamic problems.

Section 4.2 Perturbation Modes.

Static perturbation modes can be evaluated from a finite element model according to the following procedure. The incremental form of the finite element equation is:

$$K(\bar{\underline{u}})\Delta\underline{u} = \underline{Q} - \underline{F}(\bar{\underline{u}}), \tag{4.2.1}$$

where $\underline{u}$ is the vector of nodal unknown that includes both nodal displacements and forces, K the stiffness matrix linearized about a reference configuration $\bar{\underline{u}}$, Q the vector of externally applied loads, and $\underline{F}$ the vector of equivalent nodal forces. Equilibrium is achieved when $\Delta\underline{u} = 0$, or

$$\underline{F}(\underline{u}^*) - \underline{Q} = 0, \tag{4.2.2}$$

which simply states that at equilibrium, the equivalent nodal forces are equal to the applied loads. The equilibrium configuration$\underline{u}^*$ is of course a function of the applied load. Consider now an applied load of the form $\lambda\underline{Q}$ (λ is a scalar), the equilibrium condition is:

$$F_i(\underline{u}(\lambda)) - \lambda Q_i = 0. \tag{4.2.3}$$

Since F_i is a nonlinear function of the displacements, equation (4.2.3) can not be solved easily, however, taking the first derivative of this relation with respect to λ yields:

$$\frac{\partial F_i}{\partial u_j} u_j^{(1)} = Q_i, \tag{4.2.4}$$

where $\frac{\partial F_i}{\partial u_j} = K_{ij}$ is the linearized stiffness matrix, and$u_j^{(1)}$ is the first perturbation mode which is clearly nothing else but the solution of the linearized problem. The second and higher order derivatives become:

$$K_{ij} u_j^{(2)} = -\frac{\partial^2 F_i}{\partial u_j \partial u_k} u_j^{(1)} u_k^{(1)}; \tag{4.2.5}$$

$$\begin{aligned} K_{ij} u_j^{(3)} &= -3 \frac{\partial^2 F_i}{\partial u_j \partial u_k} u_j^{(2)} u_k^{(1)} \\ &\quad - \frac{\partial^3 F_i}{\partial u_j \partial u_k \partial u_l} u_j^{(1)} u_k^{(1)} u_l^{(1)}; \end{aligned} \tag{4.2.6}$$

$$\begin{aligned} K_{ij} u_j^{(4)} &= -\frac{\partial^2 F_i}{\partial u_j \partial u_k} \left(4 u_j^{(3)} u_k^{(1)} + 3 u_j^{(2)} u_k^{(2)} \right) \\ &\quad -6 \frac{\partial^3 F_i}{\partial u_j \partial u_k \partial u_l} u_j^{(2)} u_k^{(1)} u_l^{(1)}; \end{aligned} \tag{4.2.7}$$

$$\begin{aligned} K_{ij} u_j^{(5)} &= -\frac{\partial^2 F_i}{\partial u_j \partial u_k} \left(5 u_j^{(4)} u_k^{(1)} + 10 u_j^{(3)} u_k^{(2)} \right) \\ &\quad - \frac{\partial^3 F_i}{\partial u_j \partial u_k \partial u_l} \left(10 u_j^{(3)} u_k^{(1)} u_l^{(1)} + 15 u_j^{(2)} u_k^{(2)} u_l^{(1)} \right). \end{aligned} \tag{4.2.8}$$

These relationships are recursive, and involve a single inversion of the linearized stiffness matrix. They also involve higher order derivatives of the equivalent load vector F_i. This task is relatively simple when dealing with the finite element formulation described in Section 2, since the energy expressions are purely algebraic, quartic expressions. This also explains why fourth and higher order derivatives vanish and are thus absent in (4.2.7) and (4.2.8). In a perturbation theory approach, the solution would be written as:

$$u_i = \bar{u}_i + \lambda u_i^{(1)} + \frac{1}{2!} \lambda^2 u_i^{(2)} + \frac{1}{3!} \lambda^3 u_i^{(3)} + \cdots\cdots, \tag{4.2.9}$$

however, the convergence characteristics of this expansion are extremely poor. A much better approach is that proposed by Noor et al. [4–5,6] where the perturbation modes are simply added to the modal basis of a standard modal analysis as described in Chapter 3.

The above formulation is limited to static problems; however, it can be readily extended to accommodate dynamic situations. Let $\underline{Q}$ be the inertia forces associated with a natural vibration mode shape $\underline{u}_i$, i.e. $\underline{Q} = \omega_i^2 M \underline{u}_i$, where M is the mass matrix, and ω_i, the associated natural frequency. The recursive relations (4.2.4) to (4.2.8) can be used to obtain perturbations of these natural vibration mode shapes. Such modes will be termed

here "dynamic perturbation modes." In this case the stiffness matrix is the sum of the structural stiffness matrix, and the centrifugal stiffness matrix.

Section 4.3 Numerical results and discussion.

The purpose of this chapter is to assess the accuracy of modal analysis methodologies. This will be done by computing the dynamic response of structures obtained on one hand from the full finite element procedure, which will be taken as a "reference" solution, and on the other hand, from the modal analysis procedure , with various modal bases. The computation proceeds with the following steps. First, the physical structure is discretized into a number of beam elements and the corresponding finite element equations are integrated in time using the finite element in time procedure to obtain the reference solution. The second step is the selection of a modal basis consisting of a mixture of the following types of modes: natural vibration mode shapes about the reference configuration, natural vibration mode shapes about any other configuration, and static or dynamic perturbation mode shapes. The third step consists of the modal reduction. It is important to note that the full finite element model, the modal basis, and the modal reduction are all based on the identical finite element discretization of the physical problem. In the last step, the modal equations are integrated in time to obtain the modal response. In all cases, both full finite element and modal equations are integrated using two noded elements in time (i.e. a linear approximation for the displacements within each time step), and identical time step size are selected.

It is important to note that all the models discussed here are based on the exact same equations, namely the Euler equations resulting from the minimization of the Lagrangian expression. The only difference among the various solutions is the description of the solution fields: in the full finite element model, the solution is represented by polynomial expressions defined within each finite element, whereas in the modal analysis, the solution is represented by the modal superposition. Hence, all the responses presented in this work are based on the exact same equations, with different spatial discretization of the solution.

The first test case consists of a straight, cantilevered blade, with a thin-walled, rectangular cross-section. The blade has a length of 3 m, a width of 0.15 m, and a height of 0.02 m. The wall thickness is 1mm, and the material is aluminum (Young's Modulus 73 GPa, density 2700 kg/m^3). The overall geometry of the blade is depicted in Figure 4.2. The blade does not rotate, and is subjected to a tip load of 250 N oscillating with a period of 1 second. The blade is modelled with four cubic beam elements, for a total of 96 displacement degrees of freedom. Forty time steps are used to model the 1 second period. Table 4.1 details the three different modal bases used for correlation. Figure 4.3 compares the flapping deflections of the tip of the beam for the various modal bases and the full finite element model. A good correlation is obtained for all modal bases, even though very large transverse deflections occur (1.3 m compared to the 3m length of the beam). Figure 4.4 shows the correlation for the axial displacement, i.e. the foreshortening of the tip of the beam. Note that a single perturbation about the first flap mode yields an excellent correlation, whereas adding the first 3 or 5 axial vibration modes do not achieve this level of accuracy (bases 2 and 3, respectively).

Table 4.1 Description of the Modal Bases for the 0° Nonrotating Blade

	Basis 1.	Basis 2.	Basis 3.
Flap Modes	1	1	1
Flap Perturbations	1	0	0
Lead-Lag Modes	1	1	1
Axial Modes	0	3	5

In the second test case, the blade's cross section is tilted at a 45° angle with respect to the loading axis. Table 4. 2 summarizes the various modal bases used here for the modal analysis. Note that basis 4 involves modes which were taken about the deformed configuration of the blade under the static load of 250 N at the tip. Figures 4.5 and 4.6 show the in-plane and out-of-plane deflections of the blade, which are all in reasonable agreement with the reference solution. Figure 4.7 shows the tip twist of the blade, a nonlinear kinematic phenomenon due to the offset of the tip load creating a torsion moment arm. Basis 4, which contains the natural vibration modes about a predeformed configuration of the blade performs well when the dynamic response of the blade is in the same direction as that of the predeformation (the first half of the period), however it performs very poorly when the dynamic response is in the opposite direction of the predeformation (the second half of the period). This clearly shows that modes about a predeformed configuration should be avoided when the dynamic response involves complete reversals, as is the case for a helicopter blade. Basis 3 contains natural vibration mode shapes only, and performs very poorly, missing the tip elastic twist by over a factor of two, even though 5 torsion modes were used in an attempt to capture this kinematic phenomenon. The reason for this poor correlation is that the observed twisting of the blade is due to a nonlinear coupling effect, whereas the natural vibration mode shapes characterize true torsion vibrations. These two phenomena are not physically related, and this explains the poor correlation. Finally, Figure 4.8 depicts the amplitude of the torsional warping deformation. Only basis 1 provides a good correlation for this quantity that is directly related to the torsional loading in the blade. Clearly the perturbation modes of basis 1 outperform all other bases, even though it only includes a total of 5 modes. Note that a static perturbation mode was included in this basis to provide the proper nonlinear coupling between transverse loading and twisting.

Table 4.2 Description of the Modal Bases for the 45° Nonrotating Blade

	Basis 1.	Basis 2.	Basis 3.	Basis 4.
Flap Modes	1	1	1	1
Flap Perturbations	1	1	0	1
Lead-Lag Modes	1	1	1	1
Axial Modes	0	0	5	0
Torsion Modes	0	5	5	0
Static Modes	1	0	0	0
Static Perturbations	1	0	0	0

In the third test case, the 45° blade is now spinning at an angular velocity of 6.28 rad/sec, and is subjected to a 350 N oscillating tip load. Table 4.3 summarizes the various modal bases used in this case. Figures 4.9 and 4.10 show the in-plane and out-of-plane deflections, which are all in good agreement with the reference solution. Figures 4.11 and 4.12 show the tip twist and torsional warping amplitudes. Once again, basis 1, which involves perturbation modes, clearly outperforms the other bases, even though it includes 5 modes only.

Table 4.3 Description of the Modal bases for the 45° Rotating Blade

	Basis 1.	Basis 2.	Basis 3.
Flap Modes	1	1	1
Flap Perturbations	1	1	0
Lead-Lag Modes	1	1	1
Axial Modes	0	0	5
Torsion Modes	0	5	5
Static Modes	1	0	0
Static Perturbations	1	0	0

The last test case involves an actual helicopter blade: Sikorsky Aircraft's Blackhawk blade. This 27 ft long blade is modelled with 16 cubic elements, for a total of 336 degrees of freedom. Forty time steps are used to model a single period of 0.23 seconds. The aerodynamic loading is approximated by a concentrated lift (1000 lb) and drag

(250 lb) forces applied at 92% span. Figures 4.13 and 4.14 show the in-plane and out-of-plane deflections of the blade, which are in excellent agreement with the reference solution. Figure 4.15 shows the tip twist (i.e., the tip angle of attack) of the blade, and large discrepancies are observed between the reference solution and the various modal responses. Several bases are examined, but produce only marginal improvement. The reason for this discrepancy is probably the presence of nonlinear coupling between the twisting of the blade and rotational dynamic effects. Such nonlinear couplings are non properly represented by natural vibration modes, nor by perturbation modes. Indeed, when calculating the perturbation modes, gyroscopic terms are ignored.

It is important to note that all the test cases examined in this effort involve a prescribed loading. In actual problems, the loading is of an aerodynamic origin, and hence dependant on the response of the blade, most noticeably on the angle of attack. Were the above modal analysis used in an actual coupled problem (aerodynamics coupled with structural dynamics), the discrepancy observed in the angle of attack (Figure 4.15) would generate different loading conditions, which in turn would further change the blade's response. This would generate different responses for flapping, lead-lag, and twisting.

Table 4.4 Description of the Modal bases for the Blackhawk Blade

	Basis 1.	Basis 2.	Basis 3.
Flap Modes	3	3	3
Flap Perturbations	0	0	1
Lead-Lag Modes	2	2	2
Axial Modes	0	1	1
Torsion Modes	5	5	5
Static Modes	1	0	0
Static Perturbations	1	0	0

Finally, it is interesting to compare the computational times for the various approaches. Table 4.5 summarizes the CPU times for the full finite element analysis and the various modal approaches, normalized by the CPU time for the full finite element analysis. It is interesting to note that even though the 5 mode modal analysis only requires a small fraction of the full finite element CPU time, the cost of the modal analysis drastically increases with the number of modes. In fact, the 12 mode analysis is more expensive than the full finite element model. As the complexity of the full finite element model increases, its cost will increase as well, however, Table 4.5 clearly indicates that the costs of dealing with modal or full finite element models become comparable as the number of modes increases. Since the accuracy of the modal analysis is questionable even when using an increasing number of modes, the full finite element model is preferable.

Table 4.5 Normalized CPU times for the 45° rotating blade

Analysis Method	Normalized CPU Time
Full FEM (96 DOFs)	1.00
Basis 1. (5 Modes)	0.090
Basis 2. (8 Modes)	0.261
Basis 3. (12 Modes)	1.22

References

4–1. Friedmann, P. P. and Kottapalli, S. B. R., "Coupled Flap-Lag-Torsional Dynamics of Hingeless Rotor Blades in Forward Flight," **J. American Helicopter Society**, Vol. 27, No. 4, pp. 28-36, Oct. 1982.

4–2. Peters, D. A., "An Approximate Solution for the Free Vibration of Rotating Uniform Cantilevered Beams," **NASA TM** X-62, p. 299, Sept. 1973.

4–3. Rosen, A., Loewy, R. G., and Mathew, M. B., "Nonlinear Analysis of Pretwisted Rods Using Principal Curvature Transformation - Part I - Theoretical Derivation, - Part II - Numerical Results," **AIAA Journal**, Vol. 25, No. 3, pp. 470-478, March, 1987, and Vol. 25, No. 4, pp. 598-604.

4–4. Thompson, J. M. T. and Walker, A. C., "The Nonlinear Perturbation Analysis of Discrete Structural Systems," **Int. J. Solids and Structures**, Vol. 4, pp. 757-768, 1968.

4–5. Noor, A. K. and Peters, J. M., "Reduced Basis Technique for Nonlinear Analysis of Structures," **AIAA Journal**, Vol. 19, No. 4, pp. 455-462, April, 1980.

4–6. Noor, A. K., "Recent Advances in Reduction Methods for Nonlinear Problems," **Computers and Structures**, Vol. 13, pp. 31-44, 1981.

4–7. Nickell, R. E., "Nonlinear Dynamics by Mode Superposition," **Computer Methods in Applied Mechanics and Engineering**, Vol. 7, pp. 107-129, 1976.

4–8. Kane, T. R., Likins, P. W., and Levinson, D. A., **Spacecraft Dynamics**, McGraw Hill Book Company, 1983.

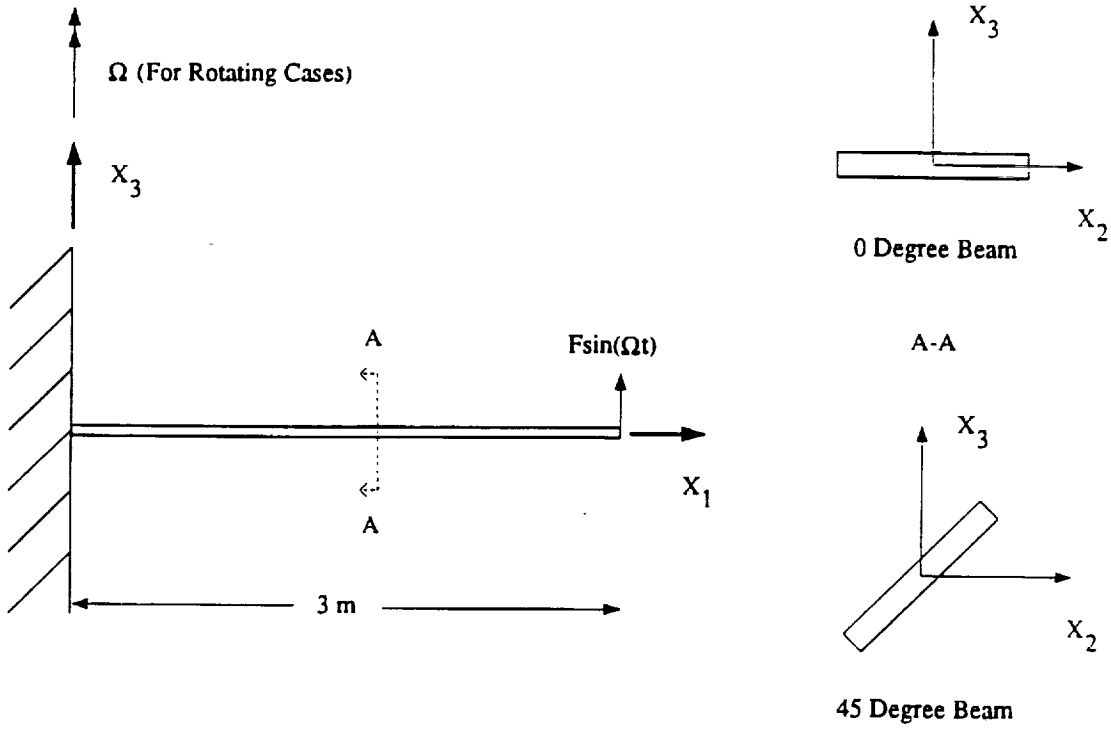

Fig 4.1 Thin Walled Rectangular Blade

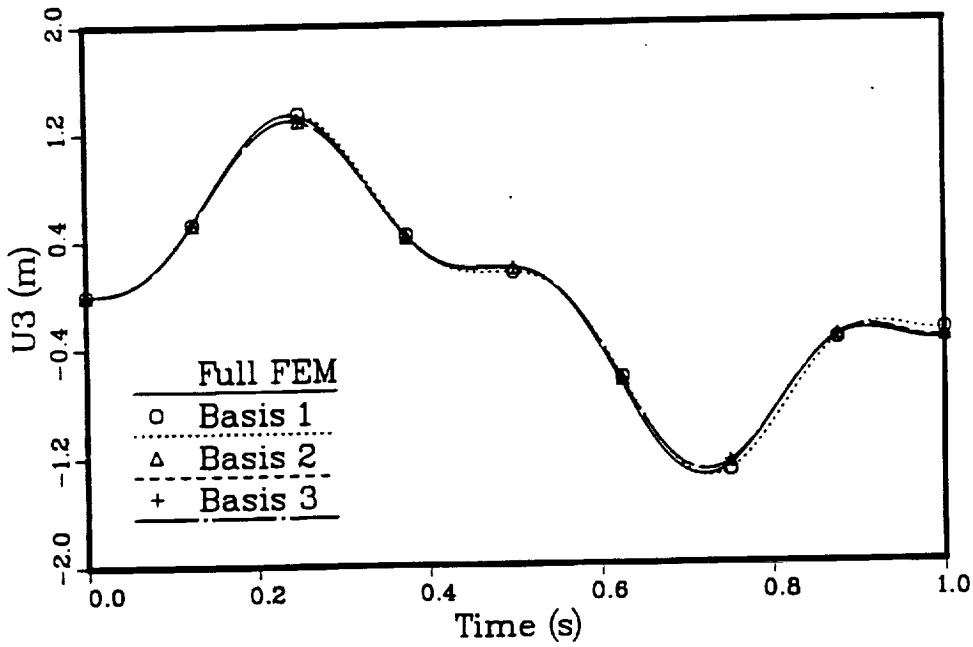

Fig 4.2. Out-of-Plane Tip Deflection vs. Time for the Nonrotating 0^o Blade.

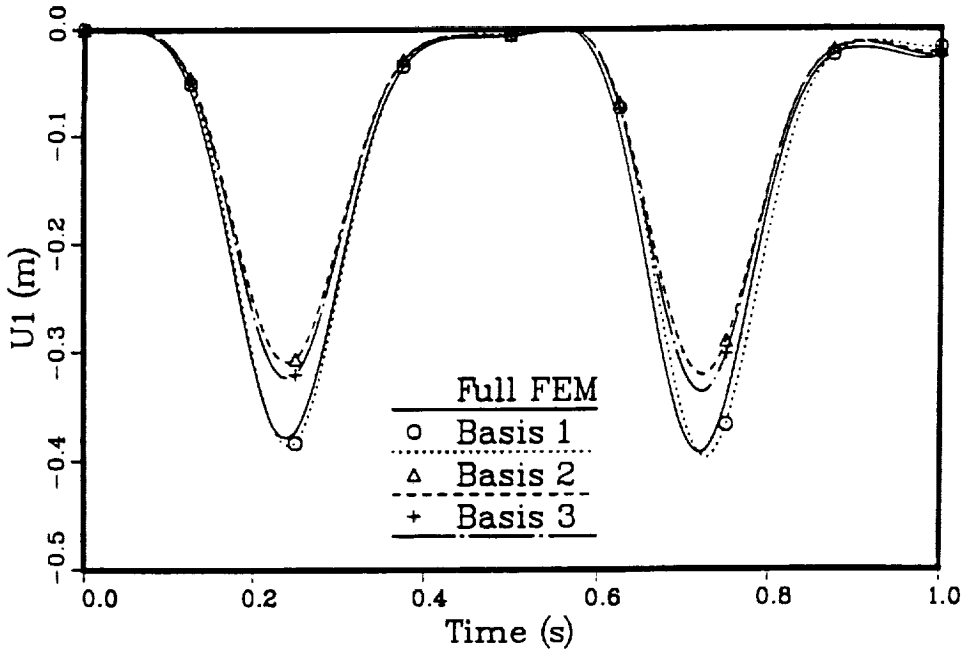

Fig 4.3. Axial Tip Displacement vs. Time for the Nonrotating 0^o Blade.

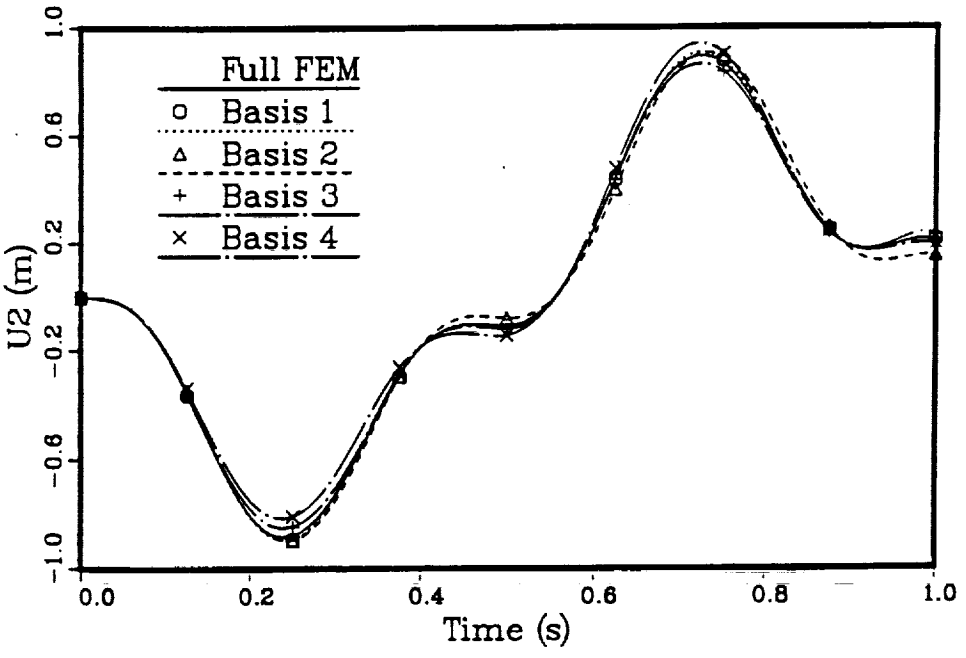

Fig 4.4. In-Plane Tip Displacement vs. Time for the Nonrotating 45^o Blade.

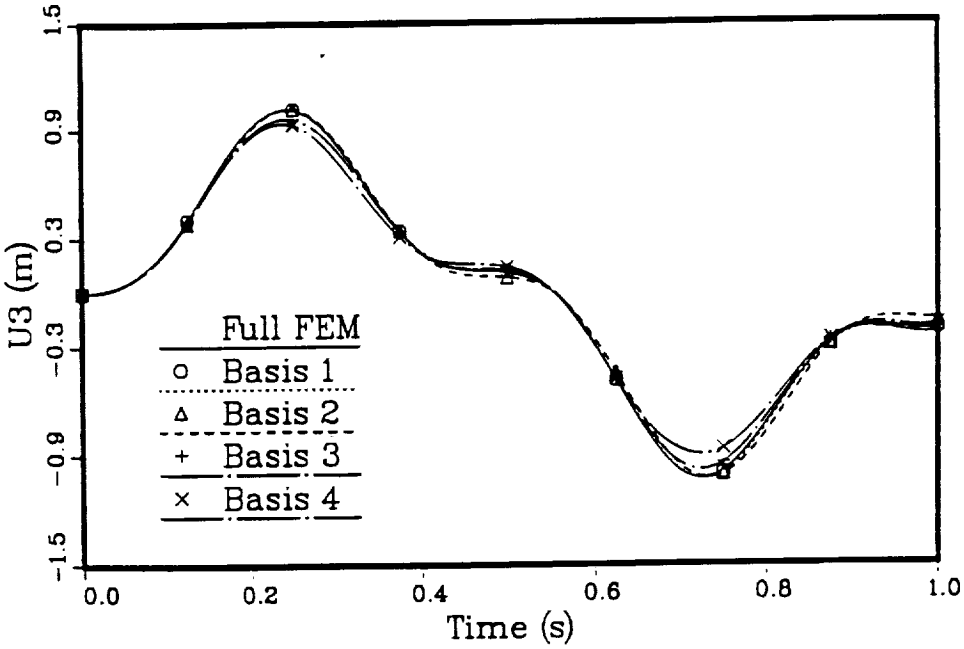

Fig 4.5. Out–of-Plane Tip Displacement vs. Time for the Nonrotating 45^o Blade.

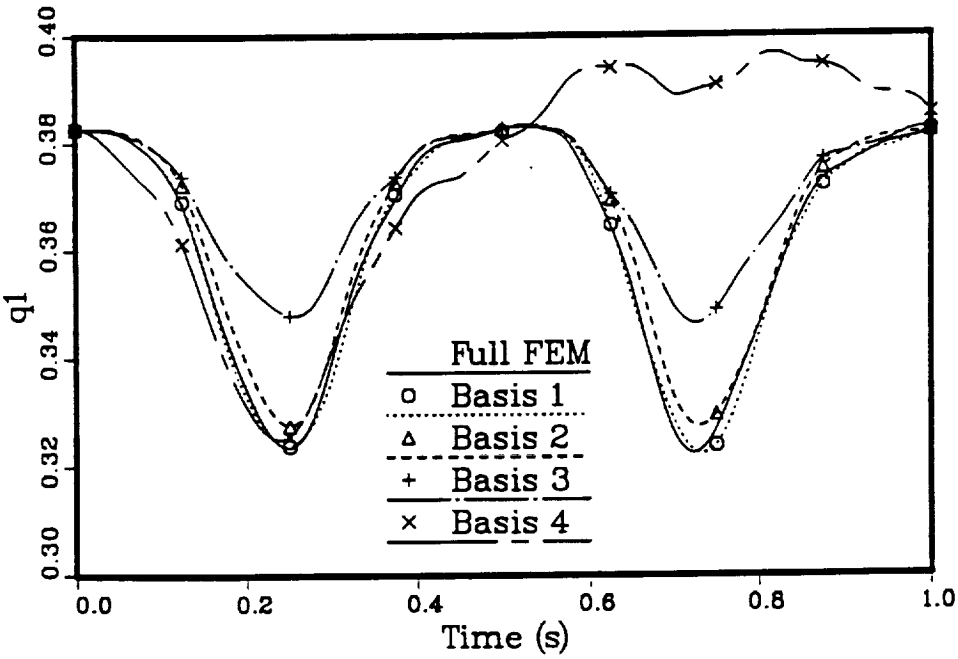

Fig 4.6. Tip Twist vs. Time for the Nonrotating 45^o Blade.

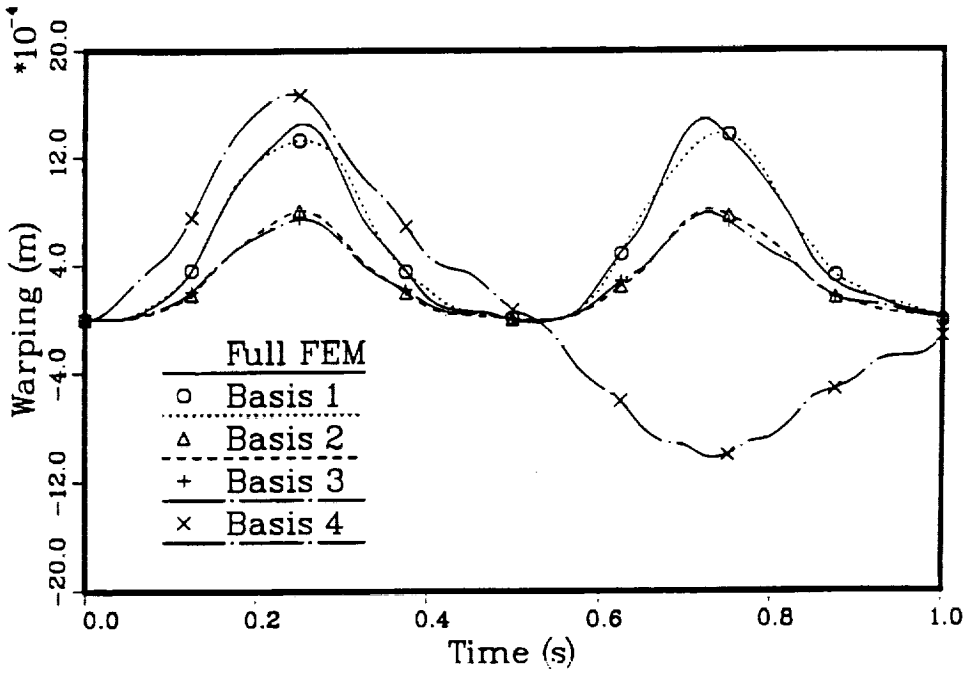

Fig 4.7. Tip Torsional Warping vs. Time for the Nonrotating 45^o Blade.

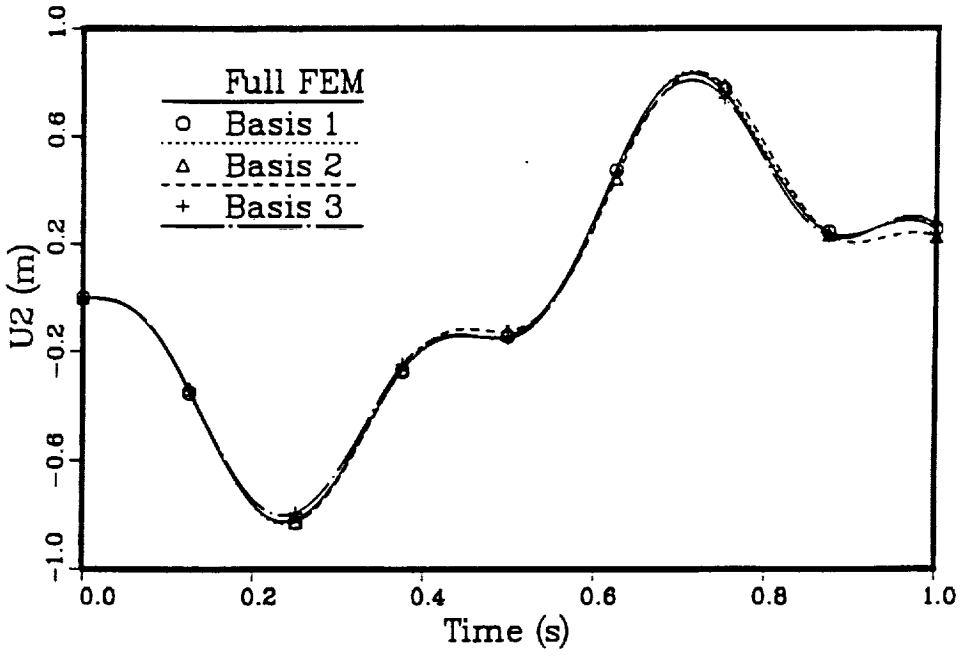

Fig 4.8. In-Plane Tip Displacement vs. Time for the Rotating 45^o Blade.

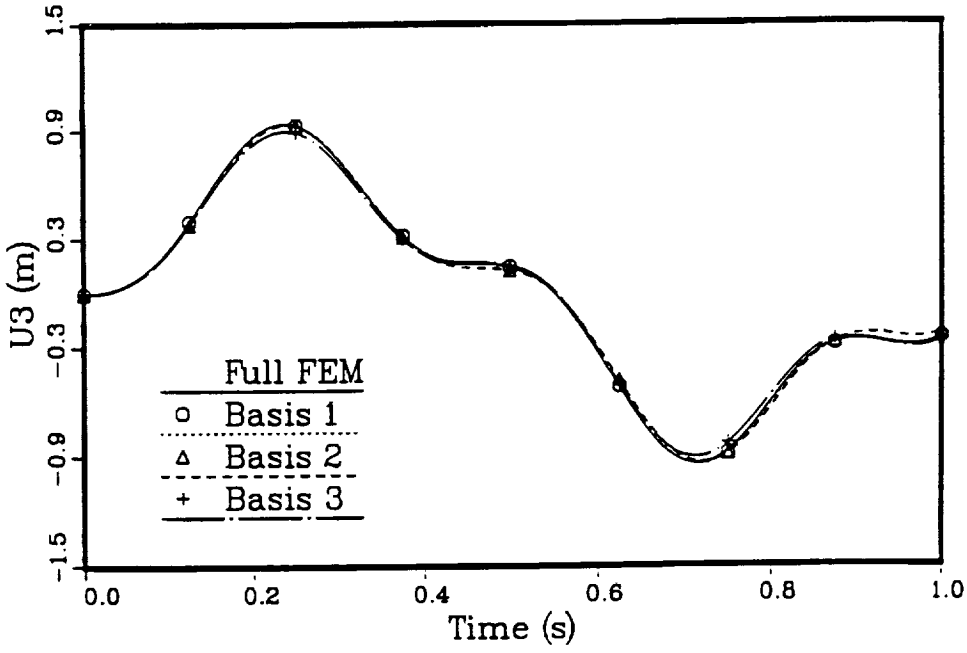

Fig 4.9. Out-of-Plane Tip Displacement vs. Time for the Rotating 45^o Blade.

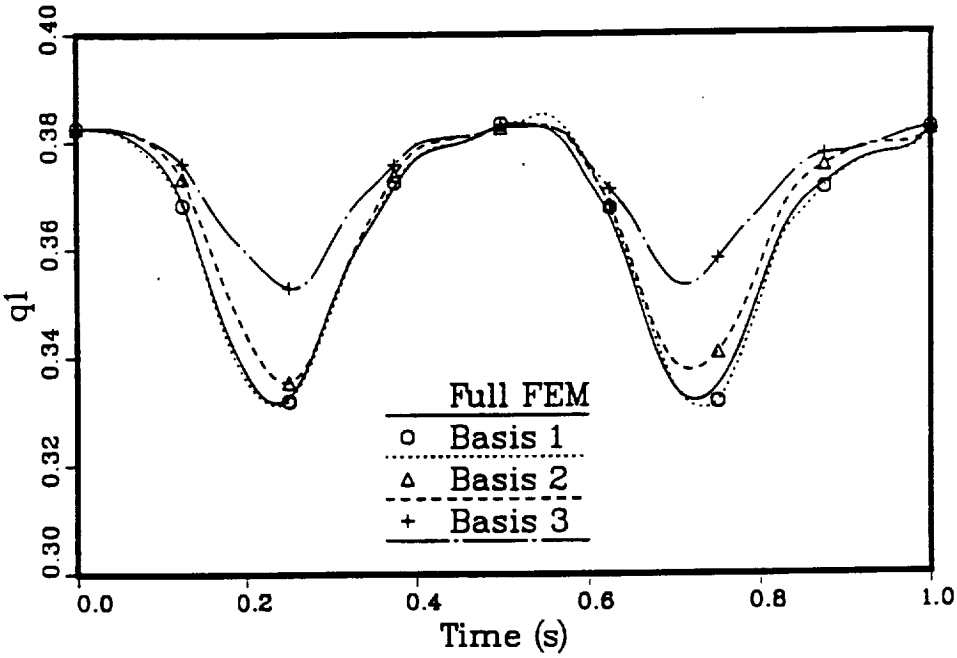

Fig 4.10. Tip Twist vs. Time for the Rotating 45^o Blade.

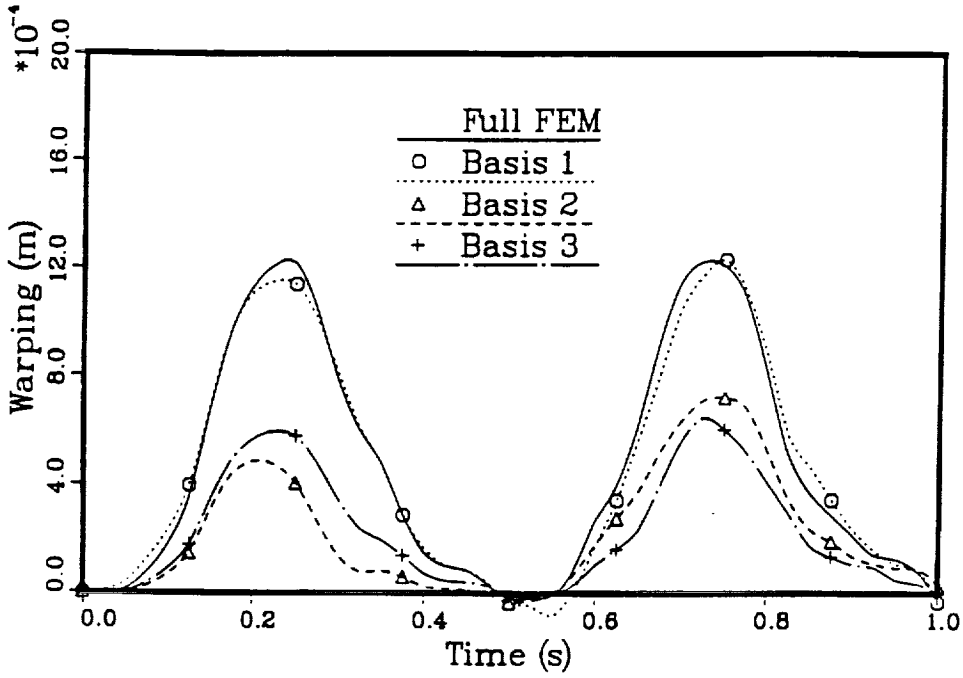

Fig 4.11. Tip Torsional Warping vs. Time for the Rotating 45^o Blade.

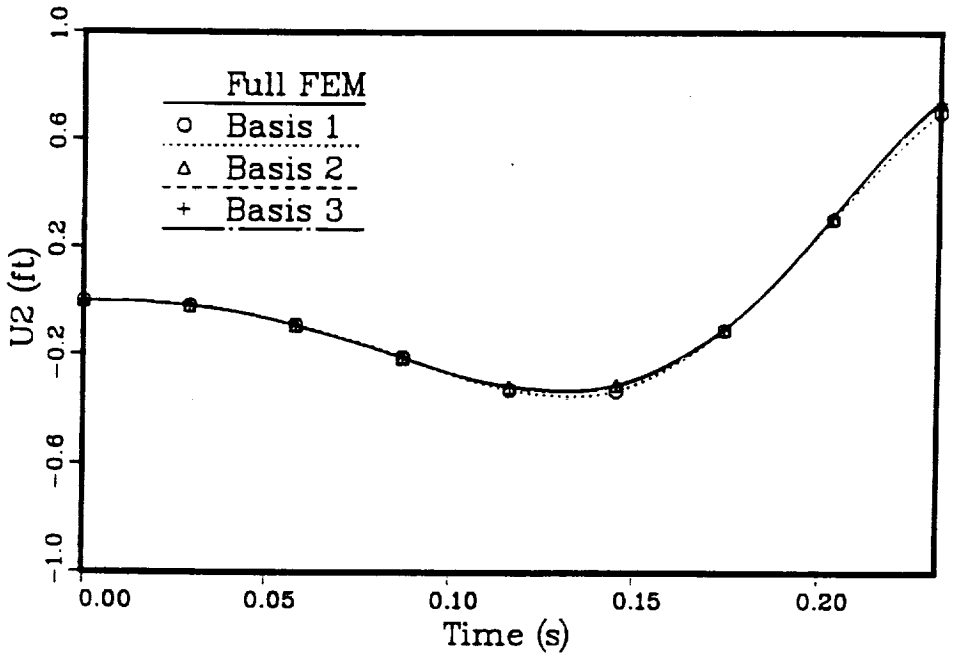

Fig 4.12. In-Plane Tip Displacement vs. Time for the Blackhawk Blade.

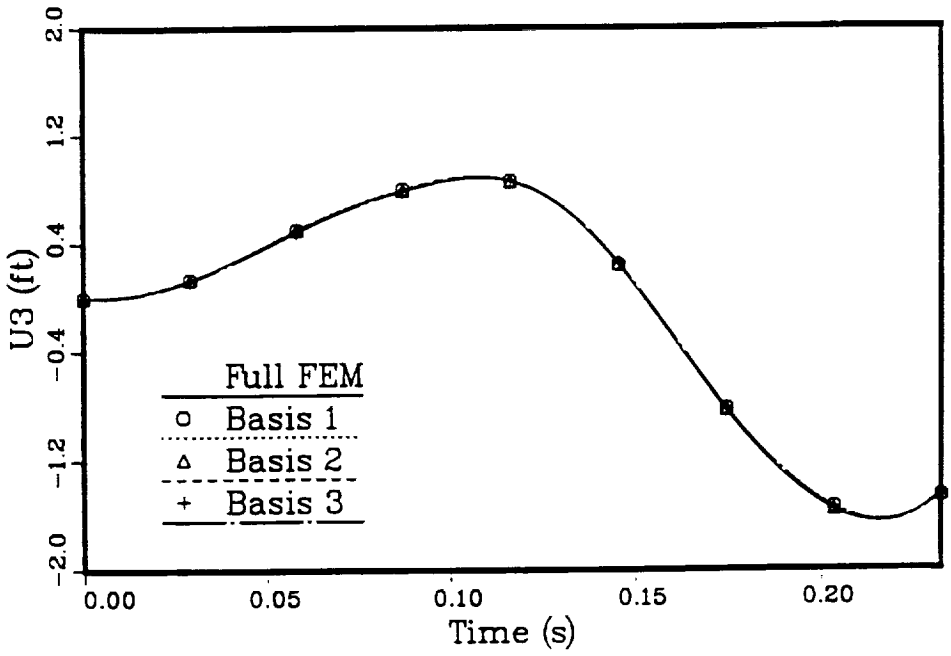

Fig 4.13. Out-of-Plane Tip Displacement vs. Time for the Blackhawk Blade.

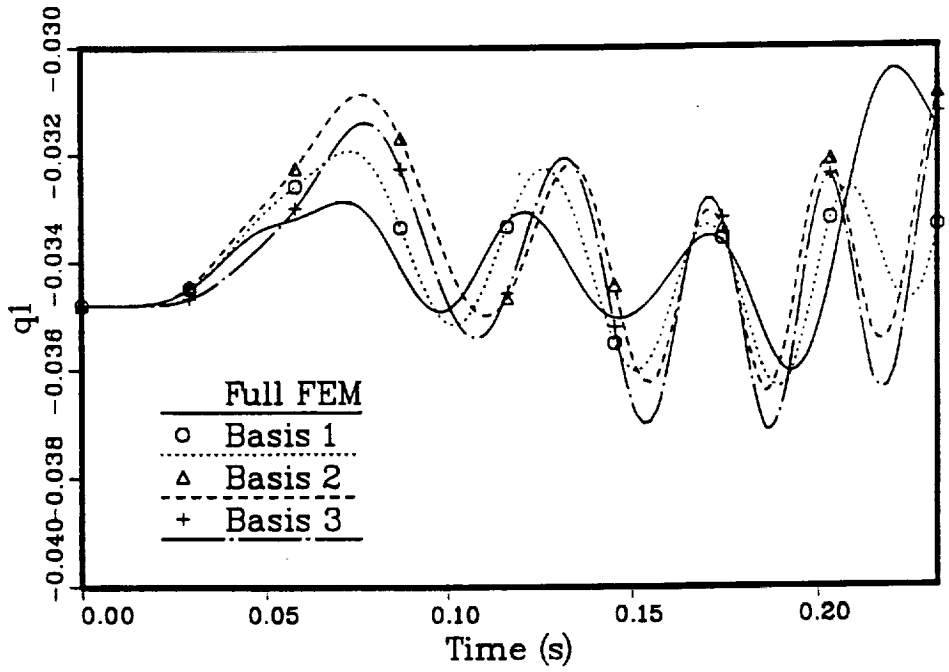

Fig 4.14. Tip Twist vs. Time for the Blackhawk Blade.

Chapter 5

Kinematic Constraints between Elastic Bodies.

Section 5.1: Introduction

This chapter deals with the formulation of the kinematic constraints between the elastic bodies of a multibody system.

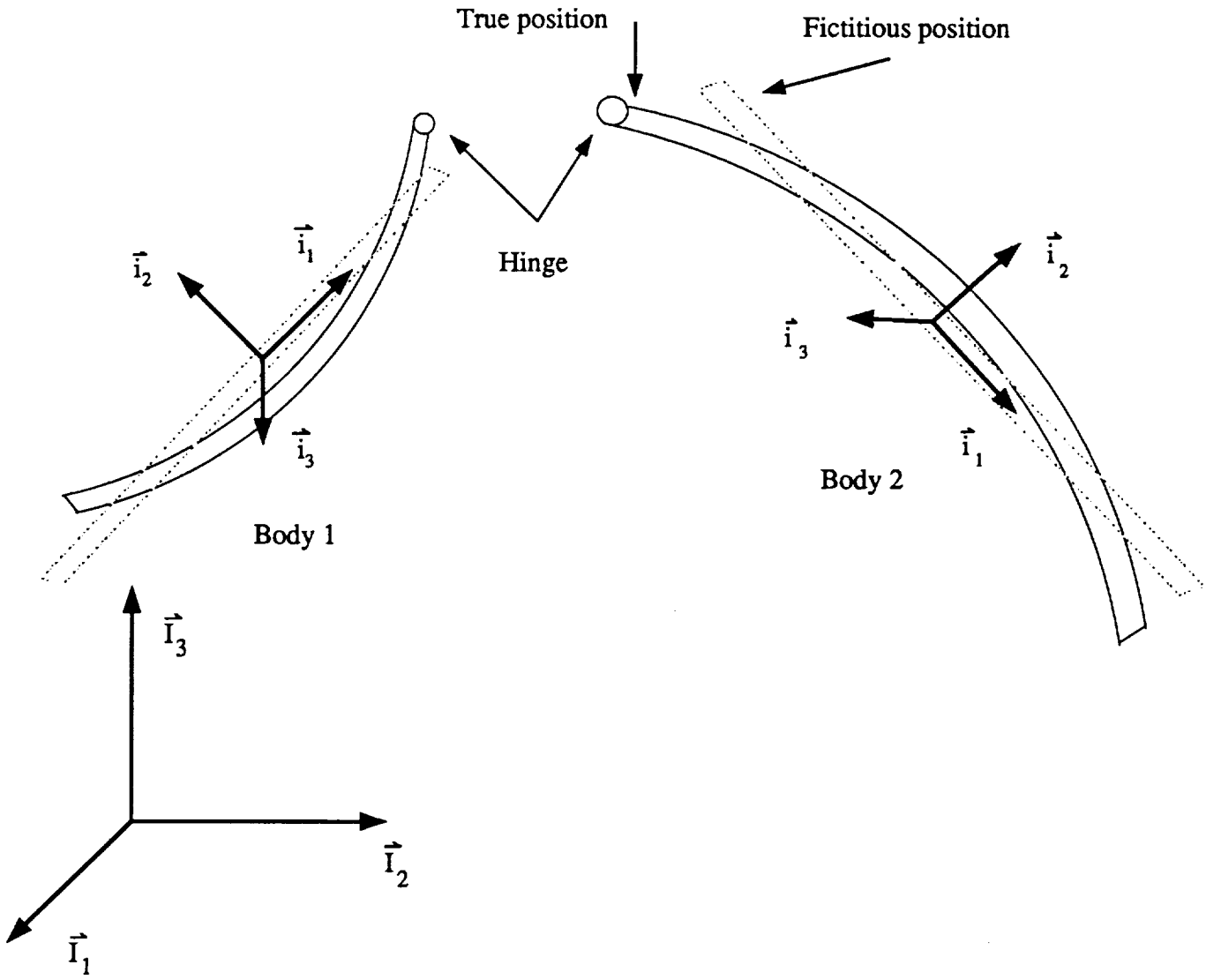

To define the multibody system, the initial position and orientation of the various elastic bodies must be given, i.e. $\vec{P}^{(i)}(t=0)$ the inertial position of the material point O (2.5.7), and $T_r^{(i)}(t=0)$ the inertial orientation of the body (2.5.1) are specified. It is

assumed that $T_r^{0\langle i\rangle}(t=0)$ is an identity matrix. The notation $(.)^{\langle i\rangle}$ is used to identify the body i whenever the distinction is necessary.

Section 5.2: Displacement constraint hinge

A hinge corresponds to a set of kinematic constraints on the relative displacements and rotations of two distinct bodies, and involves the degrees of freedom of two nodes, one in each body. A set of orientation vectors $\vec{d}_i$ is also associated with each hinge to allow for the definition of the relative rotation constraints.

Consider first the kinematic constraint corresponding to the continuity of displacements across the "hinge" which can be written as:

$$\vec{R}_h^{\langle 1\rangle} = \vec{R}_h^{\langle 2\rangle} \tag{5.2.1}$$

where $\vec{R}_h^{\langle i\rangle}$ is the position of the hinge calculated in body i. In this section we examine the formulation on the problem when constraint 5.2.1 is enforced. However, it is also possible to enforce the time derivative of this constraint, this approach will be discussed in section 5.4. When the constraint conditions are adequately formulated, the Lagrange multipliers become the unknown forces transmitted at the "hinge". Equation (5.2.1) can be expanded as:

$$\left(\vec{P}^{\langle 1\rangle} + \vec{r}_{0h}^{\langle 1\rangle} + \vec{u}_h^{\langle 1\rangle}\right) - \left(\vec{P}^{\langle 2\rangle} + \vec{r}_{0h}^{\langle 2\rangle} + \vec{u}_h^{\langle 2\rangle}\right) = 0 \tag{5.2.2}$$

where $\vec{P}$ is the position of the reference frame (see (2.5.3), $\vec{r}_{0h}$ the position of the hinge in the undeformed body, and $\vec{u}_h$ the elastic displacement of the hinge. The vector relationship (5.2.2) can be expanded in component form as:

$$\begin{aligned} &\lfloor \vec{I}_1 \quad \vec{I}_2 \quad \vec{I}_3 \rfloor \begin{vmatrix} P_1^{\langle 1\rangle} \\ P_2^{\langle 1\rangle} \\ P_3^{\langle 1\rangle} \end{vmatrix} + \lfloor \vec{i}_1^{\langle 1\rangle} \quad \vec{i}_2^{\langle 1\rangle} \quad \vec{i}_3^{\langle 1\rangle} \rfloor \begin{vmatrix} x_{0h}^{\langle 1\rangle} + u_{1h}^{\langle 1\rangle} \\ y_{0h}^{\langle 1\rangle} + u_{2h}^{\langle 1\rangle} \\ z_{0h}^{\langle 1\rangle} + u_{3h}^{\langle 1\rangle} \end{vmatrix} \\ &- \lfloor \vec{I}_1 \quad \vec{I}_2 \quad \vec{I}_3 \rfloor \begin{vmatrix} P_1^{\langle 2\rangle} \\ P_2^{\langle 2\rangle} \\ P_3^{\langle 2\rangle} \end{vmatrix} - \lfloor \vec{i}_1^{\langle 2\rangle} \quad \vec{i}_2^{\langle 2\rangle} \quad \vec{i}_3^{\langle 2\rangle} \rfloor \begin{vmatrix} x_{0h}^{\langle 2\rangle} + u_{1h}^{\langle 2\rangle} \\ x_{0h}^{\langle 2\rangle} + u_{1h}^{\langle 2\rangle} \\ z_{0h}^{\langle 2\rangle} + u_{3h}^{\langle 2\rangle} \end{vmatrix} = 0 \end{aligned} \tag{5.2.3}$$

The reference triad of each elastic body is related to the inertial triad through (2.5.2), hence the constraint condition becomes:

$$\left\lfloor \vec{I}_1, \vec{I}_2, \vec{I}_3 \right\rfloor \left\{ \begin{vmatrix} P_1^{\langle 1\rangle} - P_1^{\langle 2\rangle} \\ P_2^{\langle 1\rangle} - P_2^{\langle 2\rangle} \\ P_3^{\langle 1\rangle} - P_3^{\langle 2\rangle} \end{vmatrix} + T_r^{\langle 1\rangle} T_r^{0\langle 1\rangle} \begin{vmatrix} x_{0h}^{\langle 1\rangle} + u_{1h}^{\langle 1\rangle} \\ y_{0h}^{\langle 1\rangle} + u_{2h}^{\langle 1\rangle} \\ z_{0h}^{\langle 1\rangle} + u_{3h}^{\langle 1\rangle} \end{vmatrix} - T_r^{\langle 2\rangle} T_r^{0\langle 2\rangle} \begin{vmatrix} x_{0h}^{\langle 2\rangle} + u_{1h}^{\langle 2\rangle} \\ y_{0h}^{\langle 2\rangle} + u_{2h}^{\langle 2\rangle} \\ z_{0h}^{\langle 2\rangle} + u_{3h}^{\langle 2\rangle} \end{vmatrix} \right\} = 0 \tag{5.2.4}$$

or, in component terms:

$$\underline{P}^{\langle 1\rangle} + T_r^{\langle 1\rangle} T_r^{0\langle 1\rangle} \underline{u}_h^{\langle 1\rangle} - \underline{P}^{\langle 2\rangle} - T_r^{\langle 2\rangle} T_r^{0\langle 2\rangle} \underline{u}_h^{\langle 2\rangle} = 0 \tag{5.2.5}$$

Consider now the kinematic constraints on the relative rotations of the two bodies. At time t = 0, the orientation of the hinge is given as:

$$\begin{vmatrix} \vec{d}_1^{\langle 1\rangle} \\ \vec{d}_2^{\langle 1\rangle} \\ \vec{d}_3^{\langle 1\rangle} \end{vmatrix} = \begin{vmatrix} \vec{d}_1^{\langle 2\rangle} \\ \vec{d}_2^{\langle 2\rangle} \\ \vec{d}_3^{\langle 2\rangle} \end{vmatrix} = T_d^T \begin{vmatrix} \vec{I}_1 \\ \vec{I}_2 \\ \vec{I}_3 \end{vmatrix} \tag{5.2.6}$$

This orientation triad can be related to the base vectors in each body using (2.5.2) and (2.2.7):

$$\begin{vmatrix} \vec{d}_1^{\langle \alpha\rangle} \\ \vec{d}_2^{\langle \alpha\rangle} \\ \vec{d}_3^{\langle \alpha\rangle} \end{vmatrix} = T_d^T T_r^{\langle \alpha\rangle}(t=0) t_h^{\langle \alpha\rangle} \begin{vmatrix} \vec{e}_1^{\langle \alpha\rangle} \\ \vec{e}_2^{\langle \alpha\rangle} \\ \vec{e}_3^{\langle \alpha\rangle} \end{vmatrix} = t_d^{\langle \alpha\rangle T} \begin{vmatrix} \vec{e}_1^{\langle \alpha\rangle} \\ \vec{e}_2^{\langle \alpha\rangle} \\ \vec{e}_3^{\langle \alpha\rangle} \end{vmatrix} \tag{5.2.7}$$

At time t, the two bodies have now rotated with respect to each other: $\vec{d}_i^{\langle \alpha\rangle}$ becomes $\vec{d}_i^{*\langle \alpha\rangle}$, however, $\vec{d}_i^{*\langle 1\rangle}$ is attached to body 1, and $\vec{d}_i^{*\langle 2\rangle}$ is attached to body 2, hence:

$$\begin{vmatrix} \vec{d}_1^{*\langle \alpha\rangle} \\ \vec{d}_2^{*\langle \alpha\rangle} \\ \vec{d}_3^{*\langle \alpha\rangle} \end{vmatrix} = t_d^{\langle \alpha\rangle T} \begin{vmatrix} \vec{e}_1^{*\langle \alpha\rangle} \\ \vec{e}_2^{*\langle \alpha\rangle} \\ \vec{e}_3^{*\langle \alpha\rangle} \end{vmatrix} \tag{5.2.8}$$

With the help of (2.2.14) and (2.5.2), we find:

$$\begin{vmatrix} \vec{d}_1^{*\langle \alpha\rangle} \\ \vec{d}_2^{*\langle \alpha\rangle} \\ \vec{d}_3^{*\langle \alpha\rangle} \end{vmatrix} = t_d^{\langle \alpha\rangle T} T_e^{\langle \alpha\rangle T} T_r^{0\langle \alpha\rangle T} T_r^{\langle \alpha\rangle T} \begin{vmatrix} \vec{I}_1 \\ \vec{I}_2 \\ \vec{I}_3 \end{vmatrix} = R^{\langle \alpha\rangle T} \begin{vmatrix} \vec{I}_1 \\ \vec{I}_2 \\ \vec{I}_3 \end{vmatrix} \tag{5.2.9}$$

Let $d_i^{\langle \alpha\rangle}$, $q_i^{\langle \alpha\rangle}, Q_i^{0\langle \alpha\rangle}, Q_i^{\langle \alpha\rangle}$, *and* $r_i^{\langle \alpha\rangle}$ be the Euler Parameters associated with the rotation matrices $t_d^{\langle \alpha\rangle}$, $T_e^{\langle \alpha\rangle}, T_r^{0\langle \alpha\rangle}, T_r^{\langle \alpha\rangle}$, *and* $R^{\langle \alpha\rangle}$ respectively. The relative rotation rule (A36–37) yields:

$$\underline{r}^{\langle \alpha\rangle} = A\left(Q^{\langle \alpha\rangle}\right) A\left(Q^{0\langle \alpha\rangle}\right) B\left(d^{\langle \alpha\rangle}\right) \underline{q}^{\langle \alpha\rangle} \tag{5.2.10}$$

The relative rotation at the hinge is now:

$$\begin{vmatrix} \vec{d}_1^{*\langle 1\rangle} \\ \vec{d}_2^{*\langle 1\rangle} \\ \vec{d}_3^{*\langle 1\rangle} \end{vmatrix} = R^{\langle 1\rangle T} R^{\langle 2\rangle} \begin{vmatrix} \vec{d}_1^{*\langle 2\rangle} \\ \vec{d}_2^{*\langle 2\rangle} \\ \vec{d}_3^{*\langle 2\rangle} \end{vmatrix} = S \begin{vmatrix} \vec{d}_1^{*\langle 2\rangle} \\ \vec{d}_2^{*\langle 2\rangle} \\ \vec{d}_3^{*\langle 2\rangle} \end{vmatrix} \tag{5.2.11}$$

and the relative rotation rule (A38) now yields the Euler parameters associated with S as:

$$s_i = \underline{r}^{\langle 1\rangle T} S^i \underline{r}^{\langle 2\rangle} \tag{5.2.12}$$

where

$$S^1 = \begin{vmatrix} 0 & 1 & 0 & 0 \\ -1 & 0 & 0 & 0 \\ 0 & 0 & 0 & -1 \\ 0 & 0 & 1 & 0 \end{vmatrix} \tag{5.2.13}$$

$$S^2 = \begin{vmatrix} 0 & 0 & 1 & 0 \\ 0 & 0 & 0 & 1 \\ -1 & 0 & 0 & 0 \\ 0 & -1 & 0 & 0 \end{vmatrix} \tag{5.2.14}$$

$$S^3 = \begin{vmatrix} 0 & 0 & 0 & 1 \\ 0 & 0 & -1 & 0 \\ 0 & 1 & 0 & 0 \\ -1 & 0 & 0 & 0 \end{vmatrix} \tag{5.2.15}$$

The appropriate relative rotation can be constrained by enforcing the corresponding Euler Parameter to vanish, i.e.

$$s_i = 0 \tag{5.2.16}$$

The kinematic constraints (5.2.5) or (5.2.16) can be enforced by means of the Lagrange multiplier technique. Since a Hellinger-Reissner formulation is used for the other components of the Lagrangian, it is convenient to use a similar formulation for the constraints, namely:

$$\begin{aligned} H = & \underline{f}^T \left(\underline{P}^{\langle 1 \rangle} + T_r^{\langle 1 \rangle} T_r^{0\langle 1 \rangle} \underline{u}_h^{\langle 1 \rangle} - \underline{P}^{\langle 2 \rangle} - T_r^{\langle 2 \rangle} T_r^{0\langle 2 \rangle} \underline{u}_h^{\langle 2 \rangle} \right) \\ & + \underline{r}^{\langle 1 \rangle T} S \underline{r}^{\langle 2 \rangle} - \frac{1}{2\alpha} \left(\underline{f}^T . \underline{f} + \underline{g}^T . \underline{g} \right) \end{aligned} \tag{5.2.17}$$

where

$$S = g_1 S^1 + g_2 S^2 + g_3 S^3 = \begin{bmatrix} 0 & g_1 & g_2 & g_3 \\ -g_1 & 0 & -g_3 & g_2 \\ -g_2 & g_3 & 0 & -g_1 \\ -g_3 & -g_2 & g_1 & 0 \end{bmatrix} \tag{5.2.18}$$

f_i *and* g_i are the Lagrange multipliers, and α is a large number.

Section 5.3: Modal approximation of the kinematic constraint at a displacement hinge.

In this section the kinematic constraint at a hinge (5.2.17) is expanded using the modal approximation described in section 3.2. The elastic displacement of the hinge (5.2.5) is expanded as:

$$\underline{u}_h^{\langle \alpha \rangle} = \underline{u}_h^{0\langle \alpha \rangle} + \underline{u}_h^{k\langle \alpha \rangle} \psi_u^{k\langle \alpha \rangle} \tag{5.3.1}$$

and

$$\underline{v}^{\langle \alpha \rangle} = T_r^{0\langle \alpha \rangle} \underline{u}_h^{\langle \alpha \rangle} = \underline{v}^{0\langle \alpha \rangle} + \underline{v}^{k\langle \alpha \rangle} \psi_u^{k\langle \alpha \rangle} \tag{5.3.2}$$

where

$$\underline{v}^{0\langle\alpha\rangle} = T_r^{0\langle\alpha\rangle}\underline{u}_h^{0\langle\alpha\rangle};\ \underline{v}^{k\langle\alpha\rangle} = T_r^{0\langle\alpha\rangle}\underline{u}_h^{k\langle\alpha\rangle} \tag{5.3.3}$$

and finally:

$$\underline{v}^{*\langle\alpha\rangle} = T_r^{\langle\alpha\rangle}\underline{v}^{\langle\alpha\rangle} = \underline{v}^{*0\langle\alpha\rangle} + \underline{v}^{*k\langle\alpha\rangle}\psi_u^{k\langle\alpha\rangle} \tag{5.3.4}$$

where

$$\underline{v}^{*0\langle\alpha\rangle} = T_r^{\langle\alpha\rangle}\underline{v}^{0\langle\alpha\rangle};\ \underline{v}^{*k\langle\alpha\rangle} = T_r^{\langle\alpha\rangle}\underline{v}^{k\langle\alpha\rangle} \tag{5.3.5}$$

Similarly, the array $\underline{r}^{\langle\alpha\rangle}$ (5.2.10) is expanded as:

$$\underline{r}^{\langle\alpha\rangle} = \underline{r}^{0\langle\alpha\rangle} + \underline{r}^{k\langle\alpha\rangle}\psi_u^{k\langle\alpha\rangle} \tag{5.3.6}$$

where:

$$\begin{aligned}\underline{r}^{0\langle\alpha\rangle} &= A\left(Q^{\langle\alpha\rangle}\right)A\left(Q^{0\langle\alpha\rangle}\right)B\left(d^{\langle\alpha\rangle}\right)\underline{q}^{0\langle\alpha\rangle};\\ \underline{r}^{k\langle\alpha\rangle} &= A\left(Q^{\langle\alpha\rangle}\right)A\left(Q^{0\langle\alpha\rangle}\right)B\left(d^{\langle\alpha\rangle}\right)\underline{q}^{k\langle\alpha\rangle}.\end{aligned} \tag{5.3.7}$$

With the help of (5.2.1) to (5.2.7) the constraint condition (5.2.17) becomes:

$$H = \underline{f}^T\left(\underline{P}^{\langle1\rangle} - \underline{P}^{\langle2\rangle} + \underline{v}^{*\langle1\rangle} - \underline{v}^{*\langle2\rangle}\right) + \underline{r}^{\langle1\rangle T}S\underline{r}^{\langle2\rangle} - \frac{1}{2\alpha}\left(\underline{f}^T.\underline{f} + \underline{g}^T.\underline{g}\right) \tag{5.3.8}$$

The constraint expression is a nonlinear funtions of the rigid body parameters and generalized elastic coordinates of the two bodies. The quasilinearization procedure can be used to expand this expression about a known configuration to find:

$$\begin{aligned}H = \overline{H} + \lfloor \Delta\underline{R}^{\langle1\rangle T} \quad \Delta\underline{\psi}_u^{\langle1\rangle T} \quad \Delta\underline{R}^{\langle2\rangle T} \quad \Delta\underline{\psi}_u^{\langle2\rangle T} \quad \Delta\underline{f}^T \rfloor \{ \begin{vmatrix} \underline{H}_{R^{\langle1\rangle}} \\ \underline{H}_{u^{\langle1\rangle}} \\ \underline{H}_{R^{\langle2\rangle}} \\ \underline{H}_{u^{\langle2\rangle}} \\ \underline{H}_f \end{vmatrix}\\ + \frac{1}{2}\begin{vmatrix} H_{R^{\langle1\rangle}R^{\langle1\rangle}} & & & & & \\ H_{u^{\langle1\rangle}R^{\langle1\rangle}} & 0 & & & & \\ H_{R^{\langle2\rangle}R^{\langle1\rangle}} & H_{R^{\langle2\rangle}u^{\langle1\rangle}} & H_{R^{\langle2\rangle}R^{\langle2\rangle}} & & & \\ H_{u^{\langle2\rangle}R^{\langle1\rangle}} & H_{u^{\langle2\rangle}u^{\langle1\rangle}} & H_{u^{\langle2\rangle}R^{\langle2\rangle}} & 0 & & \\ H_{fR^{\langle1\rangle}} & H_{fu^{\langle1\rangle}} & H_{fR^{\langle2\rangle}} & H_{fu^{\langle2\rangle}} & H_{ff} & \end{vmatrix} \begin{vmatrix} \Delta\underline{R}^{\langle1\rangle} \\ \Delta\underline{\psi}_u^{\langle1\rangle} \\ \Delta\underline{R}^{\langle2\rangle} \\ \Delta\underline{\psi}_u^{\langle2\rangle} \\ \Delta\underline{f} \end{vmatrix} \} + h.o.t.\end{aligned} \tag{5.3.9}$$

The derivative with respect to $\underline{R}^{\langle\alpha\rangle}$ is:

$$\underline{H}_{R^{\langle\alpha\rangle}} = sign\langle\alpha\rangle \begin{bmatrix} f_1 \\ f_2 \\ f_3 \\ f_1 b_1^{\langle\alpha\rangle} + f_2 b_2^{\langle\alpha\rangle} + f_3 b_3^{\langle\alpha\rangle} + \underline{r}_0^{\langle\alpha\rangle T} S\underline{r}^{\langle\beta\rangle} \\ f_1 b_0^{\langle\alpha\rangle} - f_2 b_3^{\langle\alpha\rangle} + f_3 b_2^{\langle\alpha\rangle} + \underline{r}_1^{\langle\alpha\rangle T} S\underline{r}^{\langle\beta\rangle} \\ f_1 b_3^{\langle\alpha\rangle} + f_2 b_0^{\langle\alpha\rangle} - f_3 b_1^{\langle\alpha\rangle} + \underline{r}_2^{\langle\alpha\rangle T} S\underline{r}^{\langle\beta\rangle} \\ -f_1 b_2^{\langle\alpha\rangle} + f_2 b_1^{\langle\alpha\rangle} + f_3 b_0^{\langle\alpha\rangle} + \underline{r}_3^{\langle\alpha\rangle T} S\underline{r}^{\langle\beta\rangle} \end{bmatrix} \tag{5.3.10}$$

where the following notation is used:

$$sign\langle 1\rangle = +1;\ sign\langle 2\rangle = -1 \tag{5.3.11}$$

$$\langle\beta\rangle = 2\ when\ \langle\alpha\rangle = 1;\ \langle\beta\rangle = 1\ when\ \langle\alpha\rangle = 2 \tag{5.3.12}$$

$\underline{r}_i^{\langle\alpha\rangle}$ denotes the derivative of $\underline{r}^{\langle\alpha\rangle}$ with respect to $Q_i^{\langle\alpha\rangle}$, and

$$\begin{vmatrix} b_0^{\langle\alpha\rangle} \\ b_1^{\langle\alpha\rangle} \\ b_2^{\langle\alpha\rangle} \\ b_3^{\langle\alpha\rangle} \end{vmatrix} = 2 \begin{vmatrix} Q_1^{\langle\alpha\rangle} & Q_2^{\langle\alpha\rangle} & Q_3^{\langle\alpha\rangle} \\ Q_0^{\langle\alpha\rangle} & -Q_3^{\langle\alpha\rangle} & Q_2^{\langle\alpha\rangle} \\ Q_3^{\langle\alpha\rangle} & Q_0^{\langle\alpha\rangle} & -Q_1^{\langle\alpha\rangle} \\ -Q_2^{\langle\alpha\rangle} & Q_1^{\langle\alpha\rangle} & Q_0^{\langle\alpha\rangle} \end{vmatrix} \underline{v}^{\langle\alpha\rangle} \tag{5.3.13}$$

The derivative with respect to $\psi_u^{\langle\alpha\rangle}$ is:

$$\underline{H}_{u^{i\langle\alpha\rangle}} = sign\langle\alpha\rangle \left(\underline{f}^T \underline{v}^{*i\langle\alpha\rangle} + \underline{r}^{i\langle\alpha\rangle T} S \underline{r}^{\langle\beta\rangle} \right) \tag{5.3.14}$$

The derivative with respect to $\underline{f}$ is:

$$\underline{H}_f = \begin{vmatrix} P_1^{\langle 1\rangle} + v_1^{*\langle 1\rangle} - P_1^{\langle 2\rangle} - v_1^{*\langle 2\rangle} - f_1/\alpha \\ P_2^{\langle 1\rangle} + v_2^{*\langle 1\rangle} - P_2^{\langle 2\rangle} - v_2^{*\langle 2\rangle} - f_2/\alpha \\ P_3^{\langle 1\rangle} + v_3^{*\langle 1\rangle} - P_3^{\langle 2\rangle} - v_3^{*\langle 2\rangle} - f_3/\alpha \\ \underline{r}^{\langle 1\rangle T} S^1 \underline{r}^{\langle 2\rangle} - g_1/\alpha \\ \underline{r}^{\langle 1\rangle T} S^2 \underline{r}^{\langle 2\rangle} - g_2/\alpha \\ \underline{r}^{\langle 1\rangle T} S^3 \underline{r}^{\langle 2\rangle} - g_3/\alpha \end{vmatrix} \tag{5.3.15}$$

The derivative with respect to $\underline{R}^{\langle\alpha\rangle}, \underline{R}^{\langle\alpha\rangle}$ is:

$$H_{R^{\langle\alpha\rangle}R^{\langle\alpha\rangle}} = sign\langle\alpha\rangle \begin{vmatrix} 0 & & & & & & & \\ 0 & 0 & & & & & & \\ 0 & 0 & 0 & & & & & \\ 0 & 0 & 0 & R_0^{\langle\alpha\rangle} & & & & \\ 0 & 0 & 0 & S_1^{\langle\alpha\rangle} & R_1^{\langle\alpha\rangle} & & & \\ 0 & 0 & 0 & S_2^{\langle\alpha\rangle} & T_3^{\langle\alpha\rangle} & R_2^{\langle\alpha\rangle} & & \\ 0 & 0 & 0 & S_3^{\langle\alpha\rangle} & T_2^{\langle\alpha\rangle} & T_1^{\langle\alpha\rangle} & R_3^{\langle\alpha\rangle} \end{vmatrix} \tag{5.3.16}$$

where

$$\begin{vmatrix} R_0^{\langle\alpha\rangle} \\ R_1^{\langle\alpha\rangle} \\ R_2^{\langle\alpha\rangle} \\ R_3^{\langle\alpha\rangle} \end{vmatrix} = 2 \begin{vmatrix} v_1^{\langle\alpha\rangle} & v_2^{\langle\alpha\rangle} & v_3^{\langle\alpha\rangle} \\ v_1^{\langle\alpha\rangle} & -v_2^{\langle\alpha\rangle} & -v_3^{\langle\alpha\rangle} \\ -v_1^{\langle\alpha\rangle} & v_2^{\langle\alpha\rangle} & -v_3^{\langle\alpha\rangle} \\ -v_1^{\langle\alpha\rangle} & -v_2^{\langle\alpha\rangle} & v_3^{\langle\alpha\rangle} \end{vmatrix} \begin{vmatrix} f_1 \\ f_2 \\ f_3 \end{vmatrix}$$

$$\begin{vmatrix} S_1^{\langle\alpha\rangle} \\ S_2^{\langle\alpha\rangle} \\ S_3^{\langle\alpha\rangle} \end{vmatrix} = 2 \begin{vmatrix} 0 & -v_3^{\langle\alpha\rangle} & v_2^{\langle\alpha\rangle} \\ v_3^{\langle\alpha\rangle} & 0 & -v_1^{\langle\alpha\rangle} \\ -v_2^{\langle\alpha\rangle} & v_1^{\langle\alpha\rangle} & 0 \end{vmatrix} \begin{vmatrix} f_1 \\ f_2 \\ f_3 \end{vmatrix} \tag{5.3.17}$$

$$\begin{vmatrix} T_1^{\langle\alpha\rangle} \\ T_2^{\langle\alpha\rangle} \\ T_3^{\langle\alpha\rangle} \end{vmatrix} = 2 \begin{vmatrix} 0 & v_3^{\langle\alpha\rangle} & v_2^{\langle\alpha\rangle} \\ v_3^{\langle\alpha\rangle} & 0 & v_1^{\langle\alpha\rangle} \\ v_2^{\langle\alpha\rangle} & v_1^{\langle\alpha\rangle} & 0 \end{vmatrix} \begin{vmatrix} f_1 \\ f_2 \\ f_3 \end{vmatrix}$$

The derivative with respect to $\psi_u^{i\langle\alpha\rangle}, \underline{R}^{\langle\alpha\rangle}$ is:

$$H^T_{u^{i\langle\alpha\rangle}R^{\langle\alpha\rangle}} = sign\langle\alpha\rangle \begin{bmatrix} 0 \\ 0 \\ 0 \\ f_1 b_1^{i\langle\alpha\rangle} + f_2 b_2^{i\langle\alpha\rangle} + f_3 b_3^{i\langle\alpha\rangle} + \underline{r}_0^{i\langle\alpha\rangle T} S \underline{r}^{\langle\beta\rangle} \\ f_1 b_0^{i\langle\alpha\rangle} - f_2 b_3^{i\langle\alpha\rangle} + f_3 b_2^{i\langle\alpha\rangle} + \underline{r}_1^{i\langle\alpha\rangle T} S \underline{r}^{\langle\beta\rangle} \\ f_1 b_3^{i\langle\alpha\rangle} + f_2 b_0^{i\langle\alpha\rangle} - f_3 b_1^{i\langle\alpha\rangle} + \underline{r}_2^{i\langle\alpha\rangle T} S \underline{r}^{\langle\beta\rangle} \\ -f_1 b_2^{i\langle\alpha\rangle} + f_2 b_1^{i\langle\alpha\rangle} + f_3 b_0^{i\langle\alpha\rangle} + \underline{r}_3^{i\langle\alpha\rangle T} S \underline{r}^{\langle\beta\rangle} \end{bmatrix} \tag{5.3.18}$$

where

$$\begin{vmatrix} b_0^{i\langle\alpha\rangle} \\ b_1^{i\langle\alpha\rangle} \\ b_2^{i\langle\alpha\rangle} \\ b_3^{i\langle\alpha\rangle} \end{vmatrix} = 2 \begin{vmatrix} Q_1^{\langle\alpha\rangle} & Q_2^{\langle\alpha\rangle} & Q_3^{\langle\alpha\rangle} \\ Q_0^{\langle\alpha\rangle} & -Q_3^{\langle\alpha\rangle} & Q_2^{\langle\alpha\rangle} \\ Q_3^{\langle\alpha\rangle} & Q_0^{\langle\alpha\rangle} & -Q_1^{\langle\alpha\rangle} \\ -Q_2^{\langle\alpha\rangle} & Q_1^{\langle\alpha\rangle} & Q_0^{\langle\alpha\rangle} \end{vmatrix} \underline{v}^{i\langle\alpha\rangle} \tag{5.3.19}$$

The derivative with respect to $\underline{f}, \underline{R}^{\langle\alpha\rangle}$ is:

$$H_{fR^{\langle\alpha\rangle}} = sign\langle\alpha\rangle \begin{bmatrix} 1 & 0 & 0 & b_1^{\langle\alpha\rangle} & b_0^{\langle\alpha\rangle} & b_3^{\langle\alpha\rangle} & -b_2^{\langle\alpha\rangle} \\ 0 & 1 & 0 & b_2^{\langle\alpha\rangle} & -b_3^{\langle\alpha\rangle} & b_0^{\langle\alpha\rangle} & b_1^{\langle\alpha\rangle} \\ 0 & 0 & 1 & b_3^{\langle\alpha\rangle} & b_2^{\langle\alpha\rangle} & -b_1^{\langle\alpha\rangle} & b_0^{\langle\alpha\rangle} \\ 0 & 0 & 0 & \underline{r}_0^{\langle\alpha\rangle T} S^1 \underline{r}^{\langle\beta\rangle} & \underline{r}_1^{\langle\alpha\rangle T} S^1 \underline{r}^{\langle\beta\rangle} & \underline{r}_2^{\langle\alpha\rangle T} S^1 \underline{r}^{\langle\beta\rangle} & \underline{r}_3^{\langle\alpha\rangle T} S^1 \underline{r}^{\langle\beta\rangle} \\ 0 & 0 & 0 & \underline{r}_0^{\langle\alpha\rangle T} S^2 \underline{r}^{\langle\beta\rangle} & \underline{r}_1^{\langle\alpha\rangle T} S^2 \underline{r}^{\langle\beta\rangle} & \underline{r}_2^{\langle\alpha\rangle T} S^2 \underline{r}^{\langle\beta\rangle} & \underline{r}_3^{\langle\alpha\rangle T} S^2 \underline{r}^{\langle\beta\rangle} \\ 0 & 0 & 0 & \underline{r}_0^{\langle\alpha\rangle T} S^3 \underline{r}^{\langle\beta\rangle} & \underline{r}_1^{\langle\alpha\rangle T} S^3 \underline{r}^{\langle\beta\rangle} & \underline{r}_2^{\langle\alpha\rangle T} S^3 \underline{r}^{\langle\beta\rangle} & \underline{r}_3^{\langle\alpha\rangle T} S^3 \underline{r}^{\langle\beta\rangle} \end{bmatrix} \tag{5.3.20}$$

The derivative with respect to $\underline{f}, \psi_u^{i\langle\alpha\rangle}$ is:

$$H_{fu^{i\langle\alpha\rangle}} = sign\langle\alpha\rangle \begin{vmatrix} v_1^{*i\langle\alpha\rangle} \\ v_2^{*i\langle\alpha\rangle} \\ v_3^{*i\langle\alpha\rangle} \\ \underline{r}^{i\langle\alpha\rangle T} S^1 \underline{r}^{\langle\beta\rangle} \\ \underline{r}^{i\langle\alpha\rangle T} S^2 \underline{r}^{\langle\beta\rangle} \\ \underline{r}^{i\langle\alpha\rangle T} S^3 \underline{r}^{\langle\beta\rangle} \end{vmatrix} \tag{5.3.21}$$

The derivative with respect to $\underline{R}^{\langle 2\rangle}, \underline{R}^{\langle 1\rangle}$ is:

$$H_{R^{\langle 2\rangle}R^{\langle 1\rangle}} = \begin{vmatrix} 0 & 0 & 0 & 0 & 0 & 0 & 0 \\ 0 & 0 & 0 & 0 & 0 & 0 & 0 \\ 0 & 0 & 0 & 0 & 0 & 0 & 0 \\ 0 & 0 & 0 & \underline{r}_0^{\langle 1\rangle T} S \underline{r}_0^{\langle 2\rangle} & \underline{r}_1^{\langle 1\rangle T} S \underline{r}_0^{\langle 2\rangle} & \underline{r}_2^{\langle 1\rangle T} S \underline{r}_0^{\langle 2\rangle} & \underline{r}_3^{\langle 1\rangle T} S \underline{r}_0^{\langle 2\rangle} \\ 0 & 0 & 0 & \underline{r}_0^{\langle 1\rangle T} S \underline{r}_1^{\langle 2\rangle} & \underline{r}_1^{\langle 1\rangle T} S \underline{r}_1^{\langle 2\rangle} & \underline{r}_2^{\langle 1\rangle T} S \underline{r}_1^{\langle 2\rangle} & \underline{r}_3^{\langle 1\rangle T} S \underline{r}_1^{\langle 2\rangle} \\ 0 & 0 & 0 & \underline{r}_0^{\langle 1\rangle T} S \underline{r}_2^{\langle 2\rangle} & \underline{r}_1^{\langle 1\rangle T} S \underline{r}_2^{\langle 2\rangle} & \underline{r}_2^{\langle 1\rangle T} S \underline{r}_2^{\langle 2\rangle} & \underline{r}_3^{\langle 1\rangle T} S \underline{r}_2^{\langle 2\rangle} \\ 0 & 0 & 0 & \underline{r}_0^{\langle 1\rangle T} S \underline{r}_3^{\langle 2\rangle} & \underline{r}_1^{\langle 1\rangle T} S \underline{r}_3^{\langle 2\rangle} & \underline{r}_2^{\langle 1\rangle T} S \underline{r}_3^{\langle 2\rangle} & \underline{r}_3^{\langle 1\rangle T} S \underline{r}_3^{\langle 2\rangle} \end{vmatrix} \tag{5.3.22}$$

The derivative with respect to $\psi_u^{i\langle 2\rangle}, \underline{R}^{\langle 1\rangle}$ is:

$$H_{u^{i\langle 2\rangle}R^{\langle 1\rangle}} = \begin{bmatrix} 0 & 0 & 0 & \underline{r}^{i\langle 2\rangle T} S\underline{r}_0^{\langle 1\rangle} & \underline{r}^{i\langle 2\rangle T} S\underline{r}_1^{\langle 1\rangle} & \underline{r}^{i\langle 2\rangle T} S\underline{r}_2^{\langle 1\rangle} & \underline{r}^{i\langle 2\rangle T} S\underline{r}_3^{\langle 1\rangle} \end{bmatrix} \quad (5.3.23)$$

The derivative with respect to $\underline{R}^{\langle 2\rangle}, \psi_u^{i\langle 1\rangle}$ is:

$$H_{R^{\langle 2\rangle}u^{i\langle 1\rangle}} = \begin{bmatrix} 0 \\ 0 \\ 0 \\ \underline{r}^{i\langle 1\rangle T} S\underline{r}_0^{\langle 2\rangle} \\ \underline{r}^{i\langle 1\rangle T} S\underline{r}_1^{\langle 2\rangle} \\ \underline{r}^{i\langle 1\rangle T} S\underline{r}_2^{\langle 2\rangle} \\ \underline{r}^{i\langle 1\rangle T} S\underline{r}_3^{\langle 2\rangle} \end{bmatrix} \quad (5.3.24)$$

The derivative with respect to $\psi_u^{i\langle 2\rangle}, \psi_u^{j\langle 1\rangle}$ is:

$$H_{u^{i\langle 2\rangle}u^{j\langle 1\rangle}} = \underline{r}^{j\langle 1\rangle T} S\underline{r}^{i\langle 2\rangle} \quad (5.3.25)$$

Finally, the derivative with respect to $\underline{f}, \underline{f}$ is:

$$H_{ff} = -\frac{1}{\alpha}\begin{vmatrix} I & 0 \\ & I \end{vmatrix} \quad (5.3.26)$$

Section 5.4: Velocity constraint hinge

The second constraint is the continuity of velocities across the "hinge" which can be written as:

$$\dot{\vec{R}}_h^{<1>} = \dot{\vec{R}}_h^{<2>} \quad (5.4.1)$$

where $\dot{\vec{R}}_h^{\langle i\rangle}$ is the velocity of the hinge calculated in body i. When the constraint conditions are adequately formulated, the Lagrange multipliers become the unknown impulses transmitted at the "hinges". Equation (5.4.1) can be expanded as:

$$\left(\dot{\vec{P}}^{\langle 1\rangle} + \dot{\vec{r}}_{0h}^{\langle 1\rangle} + \dot{\vec{u}}_h^{\langle 1\rangle}\right) - \left(\dot{\vec{P}}^{\langle 2\rangle} + \dot{\vec{r}}_{0h}^{\langle 2\rangle} + \dot{\vec{u}}_h^{\langle 2\rangle}\right) = 0 \quad (5.4.2)$$

The vector relationship (5.4.2) can be expanded in component form as:

$$\begin{bmatrix} \vec{I}_1 & \vec{I}_2 & \vec{I}_3 \end{bmatrix} \begin{vmatrix} \dot{P}_1^{\langle 1\rangle} \\ \dot{P}_2^{\langle 1\rangle} \\ \dot{P}_3^{\langle 1\rangle} \end{vmatrix} + \begin{bmatrix} \dot{\vec{i}}_1^{\langle 1\rangle} & \dot{\vec{i}}_2^{\langle 1\rangle} & \dot{\vec{i}}_3^{\langle 1\rangle} \end{bmatrix} \begin{vmatrix} \dot{x}_{0h}^{\langle 1\rangle} + \dot{u}_{1h}^{\langle 1\rangle} \\ \dot{y}_{0h}^{\langle 1\rangle} + \dot{u}_{2h}^{\langle 1\rangle} \\ \dot{z}_{0h}^{\langle 1\rangle} + \dot{u}_{3h}^{\langle 1\rangle} \end{vmatrix} + \begin{bmatrix} \dot{\vec{i}}_1^{\langle 1\rangle} & \dot{\vec{i}}_2^{\langle 1\rangle} & \dot{\vec{i}}_3^{\langle 1\rangle} \end{bmatrix} \begin{vmatrix} \dot{u}_{1h}^{\langle 1\rangle} \\ \dot{u}_{2h}^{\langle 1\rangle} \\ \dot{u}_{3h}^{\langle 1\rangle} \end{vmatrix}$$

$$- \begin{bmatrix} \vec{I}_1 & \vec{I}_2 & \vec{I}_3 \end{bmatrix} \begin{vmatrix} \dot{P}_1^{\langle 2\rangle} \\ \dot{P}_2^{\langle 2\rangle} \\ \dot{P}_3^{\langle 2\rangle} \end{vmatrix} - \begin{bmatrix} \dot{\vec{i}}_1^{\langle 2\rangle} & \dot{\vec{i}}_2^{\langle 2\rangle} & \dot{\vec{i}}_3^{\langle 2\rangle} \end{bmatrix} \begin{vmatrix} \dot{x}_{0h}^{\langle 2\rangle} + \dot{u}_{1h}^{\langle 2\rangle} \\ \dot{y}_{0h}^{\langle 2\rangle} + \dot{u}_{2h}^{\langle 2\rangle} \\ \dot{z}_{0h}^{\langle 2\rangle} + \dot{u}_{3h}^{\langle 2\rangle} \end{vmatrix} - \begin{bmatrix} \dot{\vec{i}}_1^{\langle 2\rangle} & \dot{\vec{i}}_2^{\langle 2\rangle} & \dot{\vec{i}}_3^{\langle 2\rangle} \end{bmatrix} \begin{vmatrix} \dot{u}_{1h}^{\langle 2\rangle} \\ \dot{u}_{2h}^{\langle 2\rangle} \\ \dot{u}_{2h}^{\langle 2\rangle} \end{vmatrix} = 0 \quad (5.4.3)$$

The reference triad of each elastic body is related to the inertial triad through (2.5.2), hence the constraint condition becomes:

$$\left[\vec{I}_1, \vec{I}_2, \vec{I}_3\right] \{ \begin{vmatrix} \dot{P}_1^{\langle 1\rangle} - \dot{P}_1^{\langle 2\rangle} \\ \dot{P}_2^{\langle 1\rangle} - \dot{P}_2^{\langle 2\rangle} \\ \dot{P}_3^{\langle 1\rangle} - \dot{P}_3^{\langle 2\rangle} \end{vmatrix} + \dot{T}_r^{\langle 1\rangle} T_r^{0\langle 1\rangle} \begin{vmatrix} x_{0h}^{\langle 1\rangle} + u_{1h}^{\langle 1\rangle} \\ y_{0h}^{\langle 1\rangle} + u_{2h}^{\langle 1\rangle} \\ z_{0h}^{\langle 1\rangle} + u_{3h}^{\langle 1\rangle} \end{vmatrix} + T_r^{\langle 1\rangle} \dot{T}_r^{0\langle 1\rangle} \begin{vmatrix} x_{0h}^{\langle 1\rangle} + u_{1h}^{\langle 1\rangle} \\ y_{0h}^{\langle 1\rangle} + u_{2h}^{\langle 1\rangle} \\ z_{0h}^{\langle 1\rangle} + u_{3h}^{\langle 1\rangle} \end{vmatrix} + T_r^{\langle 1\rangle} T_r^{0\langle 1\rangle} \begin{vmatrix} \dot{u}_{1h}^{\langle 1\rangle} \\ \dot{u}_{2h}^{\langle 1\rangle} \\ \dot{u}_{3h}^{\langle 1\rangle} \end{vmatrix}$$
$$- \dot{T}_r^{\langle 2\rangle} T_r^{0\langle 2\rangle} \begin{vmatrix} x_{0h}^{\langle 2\rangle} + u_{1h}^{\langle 2\rangle} \\ y_{0h}^{\langle 2\rangle} + u_{2h}^{\langle 2\rangle} \\ z_{0h}^{\langle 2\rangle} + u_{3h}^{\langle 2\rangle} \end{vmatrix} - T_r^{\langle 2\rangle} \dot{T}_r^{0\langle 2\rangle} \begin{vmatrix} x_{0h}^{\langle 2\rangle} + u_{1h}^{\langle 2\rangle} \\ y_{0h}^{\langle 2\rangle} + u_{2h}^{\langle 2\rangle} \\ z_{0h}^{\langle 2\rangle} + u_{3h}^{\langle 2\rangle} \end{vmatrix} - T_r^{\langle 2\rangle} T_r^{0\langle 2\rangle} \begin{vmatrix} \dot{u}_{1h}^{\langle 2\rangle} \\ \dot{u}_{2h}^{\langle 2\rangle} \\ \dot{u}_{3h}^{\langle 2\rangle} \end{vmatrix} \} = 0 \tag{5.4.4}$$

or, in component terms:

$$\begin{aligned} &\dot{\underline{P}}^{\langle 1\rangle} + \left(\dot{T}_r^{\langle 1\rangle} T_r^{0\langle 1\rangle} + T_r^{\langle 1\rangle} \dot{T}_r^{0\langle 1\rangle} \right) \underline{u}_h^{\langle 1\rangle} + T_r^{\langle 1\rangle} T_r^{0\langle 1\rangle} \dot{\underline{u}}_h^{\langle 1\rangle} \\ &- \dot{\underline{P}}^{\langle 2\rangle} - \left(\dot{T}_r^{\langle 2\rangle} T_r^{0\langle 2\rangle} + T_r^{\langle 2\rangle} \dot{T}_r^{0\langle 2\rangle} \right) \underline{u}_h^{\langle 2\rangle} - T_r^{\langle 2\rangle} T_r^{0\langle 2\rangle} \dot{\underline{u}}_h^{\langle 2\rangle} = 0 \end{aligned} \tag{5.4.5}$$

The kinematic constraints (5.4.4) or (5.4.5) can be enforced by means of the Lagrange multiplier technique. Since a Hellinger-Reissner formulation is used for the other components of the Lagrangian, it is convenient to use a similar formulation for the constraints, namely:

$$\begin{aligned} H = f^T \{ &\dot{\underline{P}}^{\langle 1\rangle} + \left(\dot{T}_r^{\langle 1\rangle} T_r^{0\langle 1\rangle} + T_r^{\langle 1\rangle} \dot{T}_r^{0\langle 1\rangle} \right) \underline{u}_h^{\langle 1\rangle} + T_r^{\langle 1\rangle} T_r^{0\langle 1\rangle} \dot{\underline{u}}_h^{\langle 1\rangle} \\ &- \dot{\underline{P}}^{\langle 2\rangle} - \left(\dot{T}_r^{\langle 2\rangle} T_r^{0\langle 2\rangle} + T_r^{\langle 2\rangle} \dot{T}_r^{0\langle 2\rangle} \right) \underline{u}_h^{\langle 2\rangle} - T_r^{\langle 2\rangle} T_r^{0\langle 2\rangle} \dot{\underline{u}}_h^{\langle 2\rangle} \} \\ &- \frac{1}{2\alpha} \left(f^T . f \right) = 0 \end{aligned} \tag{5.4.6}$$

Section 5.5: Modal Approximation of the kinematic constraint at a velocity hinge.

In this section the kinematic constraint at a hinge (5.4.6) is expanded using the modal approximation described in section 3.2. The elastic displacement of the hinge (5.4.5) is expanded as:

$$\begin{aligned} \underline{u}_h^{\langle \alpha\rangle} &= \underline{u}_h^{0\langle \alpha\rangle} + \underline{u}_h^{k\langle \alpha\rangle} \psi_u^{k\langle \alpha\rangle} \\ \dot{\underline{u}}_h^{\langle \alpha\rangle} &= \underline{u}_h^{k\langle \alpha\rangle} \dot{\psi}_u^{k\langle \alpha\rangle} \end{aligned} \tag{5.5.1}$$

and

$$\begin{aligned}
\underline{v}_1^{\langle\alpha\rangle} &= T_r^{0\langle\alpha\rangle}\underline{u}_h^{\langle\alpha\rangle} = \underline{v}_1^{0\langle\alpha\rangle} + \underline{v}_1^{k\langle\alpha\rangle}\psi_u^{k\langle\alpha\rangle} \\
\underline{v}_2^{\langle\alpha\rangle} &= T_r^{\dot{0}\langle\alpha\rangle}\underline{u}_h^{\langle\alpha\rangle} = \underline{v}_2^{0\langle\alpha\rangle} + \underline{v}_2^{k\langle\alpha\rangle}\psi_u^{k\langle\alpha\rangle} \\
\underline{v}_3^{\langle\alpha\rangle} &= T_r^{0\langle\alpha\rangle}\underline{\dot{u}}_h^{\langle\alpha\rangle} = \underline{v}_1^{k\langle\alpha\rangle}\dot{\psi}_u^{k\langle\alpha\rangle}
\end{aligned} \tag{5.5.2}$$

where

$$\begin{aligned}
\underline{v}_1^{0\langle\alpha\rangle} &= T_r^{0\langle\alpha\rangle}\underline{u}_h^{0\langle\alpha\rangle};\ \underline{v}_1^{k\langle\alpha\rangle} = T_r^{0\langle\alpha\rangle}\underline{u}_h^{k\langle\alpha\rangle} \\
\underline{v}_2^{0\langle\alpha\rangle} &= T_r^{\dot{0}\langle\alpha\rangle}\underline{u}_h^{0\langle\alpha\rangle};\ \underline{v}_2^{k\langle\alpha\rangle} = T_r^{\dot{0}\langle\alpha\rangle}\underline{u}_h^{k\langle\alpha\rangle}
\end{aligned} \tag{5.5.3}$$

and finally:

$$\begin{aligned}
\underline{v}_1^{*\langle\alpha\rangle} &= \dot{T}_r^{\langle\alpha\rangle}\underline{v}_1^{\langle\alpha\rangle} = \underline{v}_1^{*0\langle\alpha\rangle} + \underline{v}_1^{*k\langle\alpha\rangle}\psi_u^{k\langle\alpha\rangle} \\
\underline{v}_2^{*\langle\alpha\rangle} &= T_r^{\langle\alpha\rangle}\underline{v}_2^{\langle\alpha\rangle} = \underline{v}_2^{*0\langle\alpha\rangle} + \underline{v}_2^{*k\langle\alpha\rangle}\psi_u^{k\langle\alpha\rangle} \\
\underline{v}_3^{*\langle\alpha\rangle} &= T_r^{\langle\alpha\rangle}\underline{v}_3^{\langle\alpha\rangle} = \underline{v}_3^{*k\langle\alpha\rangle}\dot{\psi}_u^{k\langle\alpha\rangle}
\end{aligned} \tag{5.5.4}$$

where

$$\begin{aligned}
\underline{v}_1^{*0\langle\alpha\rangle} &= \dot{T}_r^{\langle\alpha\rangle}\underline{v}_1^{0\langle\alpha\rangle};\ \underline{v}_1^{*k\langle\alpha\rangle} = \dot{T}_r^{\langle\alpha\rangle}\underline{v}_1^{k\langle\alpha\rangle} \\
\underline{v}_2^{*0\langle\alpha\rangle} &= T_r^{\langle\alpha\rangle}\underline{v}_2^{0\langle\alpha\rangle};\ \underline{v}_2^{*k\langle\alpha\rangle} = T_r^{\langle\alpha\rangle}\underline{v}_2^{k\langle\alpha\rangle} \\
\underline{v}_3^{*k\langle\alpha\rangle} &= T_r^{\langle\alpha\rangle}\underline{v}_1^{k\langle\alpha\rangle}
\end{aligned} \tag{5.5.5}$$

With the help of (5.5.1) to (5.5.5) the constraint condition (5.4.6) becomes:

$$H = \underline{f}^T\left(\underline{\dot{P}}^{\langle 1\rangle} - \underline{\dot{P}}^{\langle 2\rangle} + \underline{v}_1^{*\langle 1\rangle} - \underline{v}_1^{*\langle 2\rangle} + \underline{v}_2^{*\langle 1\rangle} - \underline{v}_2^{*\langle 2\rangle} + \underline{v}_3^{*\langle 1\rangle} - \underline{v}_3^{*\langle 2\rangle}\right) - \frac{1}{2\alpha}\left(\underline{f}^T\underline{f}\right) \tag{5.5.6}$$

The constraint expression is a nonlinear funtions of the rigid body parameters and generalized elastic coordinates of the two bodies. The quasilinearization procedure can be used to expand this expression about a known configuration to find:

$$\begin{aligned}
H = \overline{H} + \left\lfloor \Delta\underline{\Phi}^{\langle 1\rangle T} \quad \Delta\underline{\Psi}_u^{\langle 1\rangle T} \quad \Delta\underline{\Phi}^{\langle 2\rangle T} \quad \Delta\underline{\Psi}_u^{\langle 2\rangle T} \quad \Delta\underline{f}^T \right\rfloor \left\{ \begin{vmatrix} \underline{H}_{\Phi^{\langle 1\rangle}} \\ \underline{H}_{\Psi^{\langle 1\rangle}} \\ \underline{H}_{\Phi^{\langle 2\rangle}} \\ \underline{H}_{\Psi^{\langle 2\rangle}} \\ \underline{H}_f \end{vmatrix} \right. \\
\left. + \frac{1}{2} \begin{vmatrix} H_{\Phi^{\langle 1\rangle}\Phi^{\langle 1\rangle}} & & & & & \\ H_{\Psi^{\langle 1\rangle}\Phi^{\langle 1\rangle}} & 0 & & & & \\ H_{\Phi^{\langle 2\rangle}\Phi^{\langle 1\rangle}} & H_{\Phi^{\langle 2\rangle}\Psi^{\langle 1\rangle}} & H_{\Phi^{\langle 2\rangle}\Psi^{\langle 2\rangle}} & & & \\ H_{\Psi^{\langle 2\rangle}\Phi^{\langle 1\rangle}} & H_{\Psi^{\langle 2\rangle}\Psi^{\langle 1\rangle}} & H_{\Psi^{\langle 2\rangle}\Psi^{\langle 2\rangle}} & 0 & & \\ H_{f\Phi^{\langle 1\rangle}} & H_{f\Psi^{\langle 1\rangle}} & H_{f\Psi^{\langle 2\rangle}} & H_{f\Psi^{\langle 2\rangle}} & H_{ff} & \end{vmatrix} \left\| \begin{vmatrix} \Delta\underline{\Phi}^{\langle 1\rangle} \\ \Delta\underline{\Psi}_u^{\langle 1\rangle} \\ \Delta\underline{\Phi}^{\langle 2\rangle} \\ \Delta\underline{\Psi}_u^{\langle 2\rangle} \\ \Delta\underline{f} \end{vmatrix} \right\} + h.o.t.
\end{aligned} \tag{5.5.7}$$

where $\Phi^T = \left\lfloor \underline{R}^T \quad \dot{\underline{R}}^T \right\rfloor$ and $\underline{\Psi}^T = \left\lfloor \underline{\psi}^T \quad \dot{\underline{\psi}}^T \right\rfloor$.

The derivative with respect to $\underline{R}^{\langle\alpha\rangle}$ is:

$$\underline{H}_{R^{\langle\alpha\rangle}} = sign\langle\alpha\rangle \begin{bmatrix} 0 \\ 0 \\ 0 \\ f_1 e_1^{\langle\alpha\rangle} + f_2 e_2^{\langle\alpha\rangle} + f_3 e_3^{\langle\alpha\rangle} \\ f_1 e_0^{\langle\alpha\rangle} - f_2 e_3^{\langle\alpha\rangle} + f_3 e_2^{\langle\alpha\rangle} \\ f_1 e_3^{\langle\alpha\rangle} + f_2 e_0^{\langle\alpha\rangle} - f_3 e_1^{\langle\alpha\rangle} \\ -f_1 e_2^{\langle\alpha\rangle} + f_2 e_1^{\langle\alpha\rangle} + f_3 e_0^{\langle\alpha\rangle} \end{bmatrix} \tag{5.5.8}$$

where,

$$\begin{vmatrix} b_0^{\langle\alpha\rangle} \\ b_1^{\langle\alpha\rangle} \\ b_2^{\langle\alpha\rangle} \\ b_3^{\langle\alpha\rangle} \end{vmatrix} = 2 \begin{vmatrix} Q_1^{\langle\alpha\rangle} & Q_2^{\langle\alpha\rangle} & Q_3^{\langle\alpha\rangle} \\ Q_0^{\langle\alpha\rangle} & -Q_3^{\langle\alpha\rangle} & Q_2^{\langle\alpha\rangle} \\ Q_3^{\langle\alpha\rangle} & Q_0^{\langle\alpha\rangle} & -Q_1^{\langle\alpha\rangle} \\ -Q_2^{\langle\alpha\rangle} & Q_1^{\langle\alpha\rangle} & Q_0^{\langle\alpha\rangle} \end{vmatrix} \underline{v}_2^{\langle\alpha\rangle} \tag{5.5.9}$$

$$\begin{vmatrix} c_0^{\langle\alpha\rangle} \\ c_1^{\langle\alpha\rangle} \\ c_2^{\langle\alpha\rangle} \\ c_3^{\langle\alpha\rangle} \end{vmatrix} = 2 \begin{vmatrix} Q_1^{\langle\alpha\rangle} & Q_2^{\langle\alpha\rangle} & Q_3^{\langle\alpha\rangle} \\ Q_0^{\langle\alpha\rangle} & -Q_3^{\langle\alpha\rangle} & Q_2^{\langle\alpha\rangle} \\ Q_3^{\langle\alpha\rangle} & Q_0^{\langle\alpha\rangle} & -Q_1^{\langle\alpha\rangle} \\ -Q_2^{\langle\alpha\rangle} & Q_1^{\langle\alpha\rangle} & Q_0^{\langle\alpha\rangle} \end{vmatrix} \underline{v}_3^{\langle\alpha\rangle} \tag{5.5.10}$$

and

$$\begin{vmatrix} d_0^{\langle\alpha\rangle} \\ d_1^{\langle\alpha\rangle} \\ d_2^{\langle\alpha\rangle} \\ d_3^{\langle\alpha\rangle} \end{vmatrix} = 2 \begin{vmatrix} \dot{Q}_1^{\langle\alpha\rangle} & \dot{Q}_2^{\langle\alpha\rangle} & \dot{Q}_3^{\langle\alpha\rangle} \\ Q_0^{\langle\alpha\rangle} & -Q_3^{\langle\alpha\rangle} & Q_2^{\langle\alpha\rangle} \\ \dot{Q}_3^{\langle\alpha\rangle} & Q_0^{\langle\alpha\rangle} & -\dot{Q}_1^{\langle\alpha\rangle} \\ -\dot{Q}_2^{\langle\alpha\rangle} & Q_1^{\langle\alpha\rangle} & Q_0^{\langle\alpha\rangle} \end{vmatrix} \underline{v}_1^{\langle\alpha\rangle} \tag{5.5.11}$$

finally

$$e_i^{<\alpha>} = b_i^{<\alpha>} + c_i^{<\alpha>} + d_i^{<\alpha>} \qquad for \quad i = 0, 3 \tag{5.5.12}$$

The derivative with respect to $\underline{\dot{R}}^{\langle\alpha\rangle}$ is:

$$\underline{H}_{\dot{R}^{\langle\alpha\rangle}} = sign\langle\alpha\rangle \begin{bmatrix} f_1 \\ f_2 \\ f_3 \\ f_1 h_1^{\langle\alpha\rangle} + f_2 h_2^{\langle\alpha\rangle} + f_3 h_3^{\langle\alpha\rangle} \\ f_1 h_0^{\langle\alpha\rangle} - f_2 h_3^{\langle\alpha\rangle} + f_3 h_2^{\langle\alpha\rangle} \\ f_1 h_3^{\langle\alpha\rangle} + f_2 h_0^{\langle\alpha\rangle} - f_3 h_1^{\langle\alpha\rangle} \\ -f_1 h_2^{\langle\alpha\rangle} + f_2 h_1^{\langle\alpha\rangle} + f_3 h_0^{\langle\alpha\rangle} \end{bmatrix} \tag{5.5.13}$$

where

$$\begin{vmatrix} h_0^{<\alpha>} \\ h_1^{<\alpha>} \\ h_2^{<\alpha>} \\ h_3^{<\alpha>} \end{vmatrix} = 2 \begin{vmatrix} Q_1^{\langle\alpha\rangle} & Q_2^{\langle\alpha\rangle} & Q_3^{\langle\alpha\rangle} \\ Q_0^{\langle\alpha\rangle} & -Q_3^{\langle\alpha\rangle} & Q_2^{\langle\alpha\rangle} \\ Q_3^{\langle\alpha\rangle} & Q_0^{\langle\alpha\rangle} & -Q_1^{\langle\alpha\rangle} \\ -Q_2^{\langle\alpha\rangle} & Q_1^{\langle\alpha\rangle} & Q_0^{\langle\alpha\rangle} \end{vmatrix} \underline{v}_1^{\langle\alpha\rangle} \tag{5.5.14}$$

The following notation is used:

$$sign\langle 1\rangle = +1;\ sign\langle 2\rangle = -1 \tag{5.5.15}$$

$$\langle\beta\rangle = 2\ when\ \langle\alpha\rangle = 1;\ \langle\beta\rangle = 1\ when\ \langle\alpha\rangle = 2 \tag{5.5.16}$$

The derivative with respect to $\psi_u^{\langle\alpha\rangle}$ is:

$$\underline{H}_{u^{i\langle\alpha\rangle}} = sign\langle\alpha\rangle \underline{f}^T \left(\underline{v}_1^{*i\langle\alpha\rangle} + \underline{v}_2^{*i\langle\alpha\rangle}\right) \tag{5.5.17}$$

The derivative with respect to $\dot{\psi}_u^{\langle\alpha\rangle}$ is:

$$\underline{H}_{\dot{u}^{i\langle\alpha\rangle}} = sign\langle\alpha\rangle \left(\underline{f}^T \underline{v}_3^{*i\langle\alpha\rangle}\right) \tag{5.5.18}$$

The derivative with respect to $\underline{f}$ is:

$$\underline{H}_f = \left|\dot{\underline{P}}^{<1>} - \dot{\underline{P}}^{<2>} + \underline{v}_1^{*<1>} - \underline{v}_1^{*<1>} + \underline{v}_2^{*<1>} - \underline{v}_2^{*<1>} + \underline{v}_3^{*<1>} - \underline{v}_3^{*<1>} - \underline{f}/\underline{\alpha}\right| \tag{5.5.19}$$

The derivative with respect to $\underline{R}^{\langle\alpha\rangle}, \underline{R}^{\langle\alpha\rangle}$ is:

$$H_{R^{\langle\alpha\rangle}R^{\langle\alpha\rangle}} = sign\langle\alpha\rangle \begin{vmatrix} 0 & & & & & & \\ 0 & 0 & & & & & \\ 0 & 0 & 0 & & & & \\ 0 & 0 & 0 & R_0^{\langle\alpha\rangle} & & & \\ 0 & 0 & 0 & S_1^{\langle\alpha\rangle} & R_1^{\langle\alpha\rangle} & & \\ 0 & 0 & 0 & S_2^{\langle\alpha\rangle} & T_3^{\langle\alpha\rangle} & R_2^{\langle\alpha\rangle} & \\ 0 & 0 & 0 & S_3^{\langle\alpha\rangle} & T_2^{\langle\alpha\rangle} & T_1^{\langle\alpha\rangle} & R_3^{\langle\alpha\rangle} \end{vmatrix} \tag{5.5.20}$$

where

$$\begin{vmatrix} R_0^{\langle\alpha\rangle} \\ R_1^{\langle\alpha\rangle} \\ R_2^{\langle\alpha\rangle} \\ R_3^{\langle\alpha\rangle} \end{vmatrix} = 2\left\{ \begin{vmatrix} v_2^{1\langle\alpha\rangle} & v_2^{2\langle\alpha\rangle} & v_2^{3\langle\alpha\rangle} \\ v_2^{1\langle\alpha\rangle} & -v_2^{2\langle\alpha\rangle} & -v_2^{3\langle\alpha\rangle} \\ -v_2^{1\langle\alpha\rangle} & v_2^{2\langle\alpha\rangle} & -v_2^{3\langle\alpha\rangle} \\ -v_2^{1\langle\alpha\rangle} & -v_2^{2\langle\alpha\rangle} & v_2^{3\langle\alpha\rangle} \end{vmatrix} + \begin{vmatrix} v_3^{1\langle\alpha\rangle} & v_3^{2\langle\alpha\rangle} & v_3^{3\langle\alpha\rangle} \\ v_3^{1\langle\alpha\rangle} & -v_3^{2\langle\alpha\rangle} & -v_3^{3\langle\alpha\rangle} \\ -v_3^{1\langle\alpha\rangle} & v_3^{2\langle\alpha\rangle} & -v_3^{3\langle\alpha\rangle} \\ -v_3^{1\langle\alpha\rangle} & -v_3^{2\langle\alpha\rangle} & v_3^{3\langle\alpha\rangle} \end{vmatrix} \right\} \begin{vmatrix} f_1 \\ f_2 \\ f_3 \end{vmatrix}$$

$$\begin{vmatrix} S_1^{\langle\alpha\rangle} \\ S_2^{\langle\alpha\rangle} \\ S_3^{\langle\alpha\rangle} \end{vmatrix} = 2\left\{ \begin{vmatrix} 0 & -v_2^{3\langle\alpha\rangle} & v_2^{2\langle\alpha\rangle} \\ v_2^{3\langle\alpha\rangle} & 0 & -v_2^{1\langle\alpha\rangle} \\ -v_2^{2\langle\alpha\rangle} & v_2^{1\langle\alpha\rangle} & 0 \end{vmatrix} + \begin{vmatrix} 0 & -v_3^{3\langle\alpha\rangle} & v_3^{2\langle\alpha\rangle} \\ v_3^{3\langle\alpha\rangle} & 0 & -v_3^{1\langle\alpha\rangle} \\ -v_3^{2\langle\alpha\rangle} & v_3^{1\langle\alpha\rangle} & 0 \end{vmatrix} \right\} \begin{vmatrix} f_1 \\ f_2 \\ f_3 \end{vmatrix}$$

$$\begin{vmatrix} T_1^{\langle\alpha\rangle} \\ T_2^{\langle\alpha\rangle} \\ T_3^{\langle\alpha\rangle} \end{vmatrix} = 2\left\{ \begin{vmatrix} 0 & v_2^{3\langle\alpha\rangle} & v_2^{2\langle\alpha\rangle} \\ v_2^{3\langle\alpha\rangle} & 0 & v_2^{1\langle\alpha\rangle} \\ v_2^{2\langle\alpha\rangle} & v_2^{1\langle\alpha\rangle} & 0 \end{vmatrix} + \begin{vmatrix} 0 & v_3^{3\langle\alpha\rangle} & v_3^{2\langle\alpha\rangle} \\ v_3^{3\langle\alpha\rangle} & 0 & v_3^{1\langle\alpha\rangle} \\ v_3^{2\langle\alpha\rangle} & v_3^{1\langle\alpha\rangle} & 0 \end{vmatrix} \right\} \begin{vmatrix} f_1 \\ f_2 \\ f_3 \end{vmatrix} \tag{5.5.21}$$

The derivative with respect to $\underline{R}^{\dot{\langle\alpha\rangle}}, \underline{R}^{\langle\alpha\rangle}$ is:

$$H_{R^{\langle\alpha\rangle}R^{\langle\alpha\rangle}} = sign\langle\alpha\rangle \begin{vmatrix} 0 & 0 & 0 & 0 & 0 & 0 & 0 \\ 0 & 0 & 0 & 0 & 0 & 0 & 0 \\ 0 & 0 & 0 & 0 & 0 & 0 & 0 \\ 0 & 0 & 0 & U_0^{\langle\alpha\rangle} & V_1^{\langle\alpha\rangle} & V_2^{\langle\alpha\rangle} & V_3^{\langle\alpha\rangle} \\ 0 & 0 & 0 & V_1^{\langle\alpha\rangle} & U_1^{\langle\alpha\rangle} & W_3^{\langle\alpha\rangle} & W_2^{\langle\alpha\rangle} \\ 0 & 0 & 0 & V_2^{\langle\alpha\rangle} & W_3^{\langle\alpha\rangle} & U_2^{\langle\alpha\rangle} & W_1^{\langle\alpha\rangle} \\ 0 & 0 & 0 & V_3^{\langle\alpha\rangle} & W_2^{\langle\alpha\rangle} & W_1^{\langle\alpha\rangle} & U_3^{\langle\alpha\rangle} \end{vmatrix} \tag{5.5.22}$$

where

$$\begin{aligned} \begin{vmatrix} U_0^{\langle\alpha\rangle} \\ U_1^{\langle\alpha\rangle} \\ U_2^{\langle\alpha\rangle} \\ U_3^{\langle\alpha\rangle} \end{vmatrix} &= 2 \begin{vmatrix} v_1^{1\langle\alpha\rangle} & v_1^{2\langle\alpha\rangle} & v_1^{3\langle\alpha\rangle} \\ v_1^{1\langle\alpha\rangle} & -v_1^{2\langle\alpha\rangle} & -v_1^{3\langle\alpha\rangle} \\ -v_1^{1\langle\alpha\rangle} & v_1^{2\langle\alpha\rangle} & -v_1^{3\langle\alpha\rangle} \\ -v_1^{1\langle\alpha\rangle} & -v_1^{2\langle\alpha\rangle} & v_1^{3\langle\alpha\rangle} \end{vmatrix} \begin{vmatrix} f_1 \\ f_2 \\ f_3 \end{vmatrix} \\ \begin{vmatrix} V_1^{\langle\alpha\rangle} \\ V_2^{\langle\alpha\rangle} \\ V_3^{\langle\alpha\rangle} \end{vmatrix} &= 2 \begin{vmatrix} 0 & -v_1^{3\langle\alpha\rangle} & v_1^{2\langle\alpha\rangle} \\ v_1^{3\langle\alpha\rangle} & 0 & -v_1^{1\langle\alpha\rangle} \\ -v_1^{2\langle\alpha\rangle} & v_1^{1\langle\alpha\rangle} & 0 \end{vmatrix} \begin{vmatrix} f_1 \\ f_2 \\ f_3 \end{vmatrix} \\ \begin{vmatrix} W_1^{\langle\alpha\rangle} \\ W_2^{\langle\alpha\rangle} \\ W_3^{\langle\alpha\rangle} \end{vmatrix} &= 2 \begin{vmatrix} 0 & v_1^{3\langle\alpha\rangle} & v_1^{2\langle\alpha\rangle} \\ v_1^{3\langle\alpha\rangle} & 0 & v_1^{1\langle\alpha\rangle} \\ v_1^{2\langle\alpha\rangle} & v_1^{1\langle\alpha\rangle} & 0 \end{vmatrix} \begin{vmatrix} f_1 \\ f_2 \\ f_3 \end{vmatrix} \end{aligned} \tag{5.5.23}$$

The derivative with respect to $\psi_u^{i\langle\alpha\rangle}, \underline{R}^{\langle\alpha\rangle}$ is:

$$H^T_{u^{i\langle\alpha\rangle}R^{\langle\alpha\rangle}} = sign\langle\alpha\rangle \begin{bmatrix} 0 \\ 0 \\ 0 \\ f_1\left(b_1^{i\langle\alpha\rangle} + d_1^{i\langle\alpha\rangle}\right) + f_2\left(b_2^{i\langle\alpha\rangle} + d_2^{i\langle\alpha\rangle}\right) + f_3\left(b_3^{i\langle\alpha\rangle} + d_3^{i\langle\alpha\rangle}\right) \\ f_1\left(b_0^{i\langle\alpha\rangle} + d_0^{i\langle\alpha\rangle}\right) - f_2\left(b_3^{i\langle\alpha\rangle} + d_3^{i\langle\alpha\rangle}\right) + f_3\left(b_2^{i\langle\alpha\rangle} + d_2^{i\langle\alpha\rangle}\right) \\ f_1\left(b_3^{i\langle\alpha\rangle} + d_3^{i\langle\alpha\rangle}\right) + f_2\left(b_0^{i\langle\alpha\rangle} + d_0^{i\langle\alpha\rangle}\right) - f_3\left(b_1^{i\langle\alpha\rangle} + d_1^{i\langle\alpha\rangle}\right) \\ -f_1\left(b_2^{i\langle\alpha\rangle} + d_2^{i\langle\alpha\rangle}\right) + f_2\left(b_1^{i\langle\alpha\rangle} + d_1^{i\langle\alpha\rangle}\right) + f_3\left(b_0^{i\langle\alpha\rangle} + d_0^{i\langle\alpha\rangle}\right) \end{bmatrix} \tag{5.5.24}$$

where

$$\begin{aligned} \begin{vmatrix} b_0^{i<\alpha>} \\ b_1^{i<\alpha>} \\ b_2^{i<\alpha>} \\ b_3^{i<\alpha>} \end{vmatrix} &= 2 \begin{vmatrix} Q_1^{\langle\alpha\rangle} & Q_2^{\langle\alpha\rangle} & Q_3^{\langle\alpha\rangle} \\ Q_0^{\langle\alpha\rangle} & -Q_3^{\langle\alpha\rangle} & Q_2^{\langle\alpha\rangle} \\ Q_3^{\langle\alpha\rangle} & Q_0^{\langle\alpha\rangle} & -Q_1^{\langle\alpha\rangle} \\ -Q_2^{\langle\alpha\rangle} & Q_1^{\langle\alpha\rangle} & Q_0^{\langle\alpha\rangle} \end{vmatrix} \underline{v}_2^{i\langle\alpha\rangle} \\ \begin{vmatrix} d_0^{i<\alpha>} \\ d_1^{i<\alpha>} \\ d_2^{i<\alpha>} \\ d_3^{i<\alpha>} \end{vmatrix} &= 2 \begin{vmatrix} Q_1^{\langle\alpha\rangle} & Q_2^{\langle\alpha\rangle} & Q_3^{\langle\alpha\rangle} \\ Q_0^{\langle\alpha\rangle} & -Q_3^{\langle\alpha\rangle} & Q_2^{\langle\alpha\rangle} \\ Q_3^{\langle\alpha\rangle} & Q_0^{\langle\alpha\rangle} & -Q_1^{\langle\alpha\rangle} \\ -Q_2^{\langle\alpha\rangle} & Q_1^{\langle\alpha\rangle} & Q_0^{\langle\alpha\rangle} \end{vmatrix} \underline{v}_1^{i\langle\alpha\rangle} \end{aligned} \tag{5.5.25}$$

The derivative with respect to $\psi_u^{i\langle\alpha\rangle}, \underline{R}^{\langle\alpha\rangle}$ is:

$$H^T_{u^{i\langle\alpha\rangle}R^{\langle\alpha\rangle}} = sign\langle\alpha\rangle \begin{bmatrix} 0 \\ 0 \\ 0 \\ f_1 c_1^{i\langle\alpha\rangle} + f_2 c_2^{i\langle\alpha\rangle} + f_3 c_3^{i\langle\alpha\rangle} \\ f_1 c_0^{i\langle\alpha\rangle} - f_2 c_3^{i\langle\alpha\rangle} + f_3 c_2^{i\langle\alpha\rangle} \\ f_1 c_3^{i\langle\alpha\rangle} + f_2 c_0^{i\langle\alpha\rangle} - f_3 c_1^{i\langle\alpha\rangle} \\ -f_1 c_2^{i\langle\alpha\rangle} + f_2 c_1^{i\langle\alpha\rangle} + f_3 c_0^{i\langle\alpha\rangle} \end{bmatrix} \tag{5.5.26}$$

where

$$\begin{vmatrix} c_0^{i\langle\alpha\rangle} \\ c_1^{i\langle\alpha\rangle} \\ c_2^{i\langle\alpha\rangle} \\ c_3^{i\langle\alpha\rangle} \end{vmatrix} = 2 \begin{vmatrix} Q_1^{\langle\alpha\rangle} & Q_2^{\langle\alpha\rangle} & Q_3^{\langle\alpha\rangle} \\ Q_0^{\langle\alpha\rangle} & -Q_3^{\langle\alpha\rangle} & Q_2^{\langle\alpha\rangle} \\ Q_3^{\langle\alpha\rangle} & Q_0^{\langle\alpha\rangle} & -Q_1^{\langle\alpha\rangle} \\ -Q_2^{\langle\alpha\rangle} & Q_1^{\langle\alpha\rangle} & Q_0^{\langle\alpha\rangle} \end{vmatrix} \underline{v}_1^{i\langle\alpha\rangle} \tag{5.5.27}$$

$$H^T_{u^{i\langle\alpha\rangle}\dot{R}^{\langle\alpha\rangle}} = H^T_{u^{i\langle\alpha\rangle}R^{\langle\alpha\rangle}} \tag{5.5.28}$$

The derivative with respect to $\underline{f}, \underline{R}^{\langle\alpha\rangle}$ is:

$$H_{fR^{\langle\alpha\rangle}} = sign\langle\alpha\rangle \begin{bmatrix} 0 & 0 & 0 & e_1^{\langle\alpha\rangle} & e_0^{\langle\alpha\rangle} & e_3^{\langle\alpha\rangle} & -e_2^{\langle\alpha\rangle} \\ 0 & 0 & 0 & e_2^{\langle\alpha\rangle} & -e_3^{\langle\alpha\rangle} & e_0^{\langle\alpha\rangle} & e_1^{\langle\alpha\rangle} \\ 0 & 0 & 0 & e_3^{\langle\alpha\rangle} & e_2^{\langle\alpha\rangle} & -e_1^{\langle\alpha\rangle} & e_1^{\langle\alpha\rangle} \end{bmatrix} \tag{5.5.29}$$

The derivative with respect to $\underline{f}, \dot{\underline{R}}^{\langle\alpha\rangle}$ is:

$$H_{fR^{\langle\alpha\rangle}} = sign\langle\alpha\rangle \begin{bmatrix} 1 & 0 & 0 & h_1^{\langle\alpha\rangle} & h_0^{\langle\alpha\rangle} & h_3^{\langle\alpha\rangle} & -h_2^{\langle\alpha\rangle} \\ 0 & 1 & 0 & h_2^{\langle\alpha\rangle} & -h_3^{\langle\alpha\rangle} & h_0^{\langle\alpha\rangle} & h_1^{\langle\alpha\rangle} \\ 0 & 0 & 1 & h_3^{\langle\alpha\rangle} & h_2^{\langle\alpha\rangle} & -h_1^{\langle\alpha\rangle} & h_0^{\langle\alpha\rangle} \end{bmatrix} \tag{5.5.30}$$

The derivative with respect to $\underline{f}, \psi_u^{i\langle\alpha\rangle}$ is:

$$H_{fu^{i\langle\alpha\rangle}} = sign\langle\alpha\rangle \begin{vmatrix} v_1^{1*i\langle\alpha\rangle} + v_2^{1*i\langle\alpha\rangle} \\ v_1^{2*i\langle\alpha\rangle} + v_2^{2*i\langle\alpha\rangle} \\ v_1^{3*i\langle\alpha\rangle} + v_2^{3*i\langle\alpha\rangle} \end{vmatrix} \tag{5.5.31}$$

The derivative with respect to $\underline{f}, \dot{\psi}_u^{i\langle\alpha\rangle}$ is:

$$H_{fu^{i\langle\alpha\rangle}} = sign\langle\alpha\rangle \begin{vmatrix} v_3^{1*i\langle\alpha\rangle} \\ v_3^{2*i\langle\alpha\rangle} \\ v_3^{3*i\langle\alpha\rangle} \end{vmatrix} \tag{5.5.32}$$

Finally, the derivative with respect to $\underline{f}, \underline{f}$ is:

$$H_{ff} = -\frac{1}{\alpha}\begin{vmatrix} I & 0 \\ & I \end{vmatrix} \tag{5.5.33}$$

Section 5.6: Finite Element in Time Discretization of a Single Elastic Body.

The finite element in time procedure will be used to derive the governing equations of the problem. In the modal formulation, the time varying unknowns of the problem are the dispacement variables $\underline{\mathcal{U}}$, the force variables $\underline{\mathcal{F}}$, the momenta variables $\underline{\mathcal{P}}$, and Λ. The displacement variables are interpolated as follows:

$$\underline{\mathcal{U}}(t) = \sum_{k=1}^{N_u} g_u^k(\tau)\underline{\hat{\mathcal{U}}}_k \tag{5.6.1}$$

where g_u^k are the interpolation functions, and $\underline{\hat{\mathcal{U}}^k}$ the nodal displacements. If t_i and t_f are the initial and final times of the period under investigation, the nondimensional time τ is given as:

$$\tau = \frac{2}{\Delta t}\left(t - \frac{t_i - t_f}{2}\right) \tag{5.6.2}$$

where $\Delta t = t_f - t_i$. The shape function will be chosen as follows:

$$\begin{aligned} g_u^1 &= \frac{1}{2}(P_0 - P_1) \\ g_u^2 &= \frac{1}{2}(P_0 + P_1) \\ g_u^k &= \frac{P_{k-1} - P_{k-3}}{2k-3} = S_{k-2} \quad k = 3, 4, ...N_u \end{aligned} \tag{5.6.3}$$

where the P_i are the Legendre Polynomials, and the S_i their integrals. In view of the properties of Legendre polynomials, these interpolation functions are such that:

$$\begin{aligned} &g_u^1(-1) = 1.0;\ g_u^2(-1) = 0.0;\ g_u^k(-1) = 0.0,\ k = 3, ...N_u \\ &g_u^1(+1) = 0.0;\ g_u^2(+1) = 1.0;\ g_u^k(+1) = 0.0,\ k = 3, ...N_u \end{aligned} \tag{5.6.4}$$

which means that:

$$\underline{\mathcal{U}}(t_i) = \underline{\hat{\mathcal{U}}}_1, \text{and } \underline{\mathcal{U}}(t_f) = \underline{\hat{\mathcal{U}}}_2 \tag{5.6.5}$$

The time derivative of the displacement generalized coordinates are now:

$$\dot{\underline{\mathcal{U}}}(t) = \sum_{k=1}^{N_u} \dot{g}_u^k(\tau)\underline{\hat{\mathcal{U}}}_k \tag{5.6.6}$$

where

$$\begin{aligned} \dot{g}_u^1 &= -\frac{1}{2} \\ \dot{g}_u^2 &= \frac{1}{2} \\ \dot{g}_u^k &= P_{k-2} \quad k = 3, 4, \ldots N_u \end{aligned} \tag{5.6.7}$$

The force and momentum variables are interpolated with the help of the Legendre polynomials as well:

$$\underline{\mathcal{F}}(t) = \sum_{k=1}^{N_f} g_f^k(\tau)\underline{\hat{\mathcal{F}}}_k \tag{5.6.8}$$

and

$$\underline{\mathcal{P}}(t) = \sum_{k=1}^{N_p} g_p^k(\tau)\underline{\hat{\mathcal{P}}}_k \tag{5.6.9}$$

where

$$g_f^k = P_{k-1} \quad k = 1, 2, \ldots N_f \tag{5.6.10}$$

and

$$g_p^k = P_{k-1} \quad k = 1, 2, \ldots N_p \tag{5.6.11}$$

These various interpolation functions are conveniently written in matrix form, for instance (5.6.1) can be written as:

$$\begin{aligned} \underline{\mathcal{U}}(t) &= B_u\underline{\hat{\mathcal{U}}};\ \underline{\dot{\mathcal{U}}}(t) = B_v\underline{\hat{\mathcal{U}}}; \\ \underline{\mathcal{F}}(t) &= B_f\underline{\hat{\mathcal{F}}};\ \underline{\mathcal{P}}(t) = B_p\underline{\hat{\mathcal{P}}} \end{aligned} \tag{5.6.12}$$

where

$$\underline{\hat{\mathcal{U}}}^T = \left\lfloor \underline{\hat{\mathcal{U}}}_1^T, \underline{\hat{\mathcal{U}}}_2^T, \ldots, \underline{\hat{\mathcal{U}}}_{N_u}^T \right\rfloor \tag{5.6.13}$$

The complete Lagrangian for a single elastic body was derived in chapter 3, equation (3.5.3), introducing the interpolation functions we find:

$$\begin{aligned} \mathcal{L} = \overline{\mathcal{L}} + \lfloor\, \Delta\underline{\hat{\mathcal{U}}}^T \quad \Delta\underline{\hat{\mathcal{F}}}^T \quad \Delta\underline{\hat{\mathcal{P}}}^T \,\rfloor \{ & \begin{vmatrix} \underline{\hat{\mathcal{L}}}_{\mathcal{U}} \\ \underline{\hat{\mathcal{L}}}_{\mathcal{F}} \\ \underline{\hat{\mathcal{L}}}_{\mathcal{P}} \end{vmatrix} \\ + \frac{1}{2} & \begin{vmatrix} \hat{\mathcal{L}}_{uu} & \hat{\mathcal{L}}_{u\mathcal{F}} & \hat{\mathcal{L}}_{u\mathcal{P}} \\ & \hat{\mathcal{L}}_{\mathcal{F}\mathcal{F}} & 0 \\ & & \hat{\mathcal{L}}_{\mathcal{P}\mathcal{P}} \end{vmatrix} \begin{vmatrix} \Delta\underline{\hat{\mathcal{U}}} \\ \Delta\underline{\hat{\mathcal{F}}} \\ \Delta\underline{\hat{\mathcal{P}}} \end{vmatrix} \} + h.o.t \end{aligned} \tag{5.6.14}$$

where

$$\underline{\hat{\mathcal{L}}}_{\mathcal{U}} = \int_{t_i}^{t_f} \left(B_u^T \underline{\mathcal{L}}_{\mathcal{U}} + B_d^T \underline{\mathcal{L}}_{\mathcal{D}} \right) dt;$$

$$\underline{\hat{\mathcal{L}}}_{\mathcal{F}} = \int_{t_i}^{t_f} B_f^T \underline{\mathcal{L}}_{\mathcal{F}} dt; \tag{5.6.15}$$

$$\underline{\hat{\mathcal{L}}}_{\mathcal{P}} = \int_{t_i}^{t_f} B_p^T \underline{\mathcal{L}}_{\mathcal{P}} dt$$

and

$$\hat{\mathcal{L}}_{uu} = \int_{t_i}^{t_f} \left(B_u^T \mathcal{L}_{uu} B_u + B_u^T \mathcal{L}_{u\mathcal{V}} B_v + B_v^T \mathcal{L}_{u\mathcal{V}}^T B_u \right) dt;$$

$$\hat{\mathcal{L}}_{u\mathcal{F}} = \int_{t_i}^{t_f} B_u^T \mathcal{L}_{u\mathcal{F}} B_f dt; \tag{5.6.16}$$

$$\hat{\mathcal{L}}_{u\mathcal{P}} = \int_{t_i}^{t_f} \left(B_u^T \mathcal{L}_{u\mathcal{P}} B_p + B_v^T \mathcal{L}_{\mathcal{V}\mathcal{P}} B_p \right) dt;$$

$$\hat{\mathcal{L}}_{\mathcal{F}\mathcal{F}} = \int_{t_i}^{t_f} B_f^T \mathcal{L}_{\mathcal{F}\mathcal{F}} B_f dt; \; \hat{\mathcal{L}}_{\mathcal{P}\mathcal{P}} = \int_{t_i}^{t_f} B_p^T \mathcal{L}_{\mathcal{P}\mathcal{P}} B_p dt$$

In the case of mutually interacting bodies, kinematic constraints such as (5.2.2) will couple the behavior of the various bodies. However, these constraints are purely kinematic, i.e. they do not involve forces and momenta, hence, forces and momenta are independent variables within each body. The stationarity condition with respect to these variables yields:

$$\begin{aligned} \Delta \underline{\hat{\mathcal{F}}} &= -\hat{\mathcal{L}}_{\mathcal{F}\mathcal{F}}^{-1} \underline{\hat{\mathcal{L}}}_{\mathcal{F}} - \hat{\mathcal{L}}_{\mathcal{F}\mathcal{F}}^{-1} \hat{\mathcal{L}}_{u\mathcal{F}}^T \Delta \underline{\hat{\mathcal{U}}} \\ \Delta \underline{\hat{\mathcal{P}}} &= -\hat{\mathcal{L}}_{\mathcal{P}\mathcal{P}}^{-1} \underline{\hat{\mathcal{L}}}_{\mathcal{P}} - \hat{\mathcal{L}}_{\mathcal{P}\mathcal{P}}^{-1} \hat{\mathcal{L}}_{u\mathcal{P}}^T \Delta \underline{\hat{\mathcal{U}}} \end{aligned} \tag{5.6.17}$$

Introducing these results into (5.6.14) yields a reduced Lagrangian expression:

$$\mathcal{L} = \overline{\mathcal{L}} + \Delta \underline{\hat{\mathcal{U}}}^T \underline{\mathsf{L}}_u + \frac{1}{2} \Delta \underline{\hat{\mathcal{U}}}^T \mathsf{L}_{uu} \Delta \underline{\hat{\mathcal{U}}} + h.o.t \tag{5.6.18}$$

where

$$\underline{\mathsf{L}}_u = \underline{\hat{\mathcal{L}}}_u - \hat{\mathcal{L}}_{u\mathcal{F}} \hat{\mathcal{L}}_{\mathcal{F}\mathcal{F}}^{-1} \underline{\hat{\mathcal{L}}}_{\mathcal{F}} - \hat{\mathcal{L}}_{u\mathcal{P}} \hat{\mathcal{L}}_{\mathcal{P}\mathcal{P}}^{-1} \underline{\hat{\mathcal{L}}}_{\mathcal{P}} \tag{5.6.19}$$

and

$$\mathsf{L}_{uu} = \hat{\mathcal{L}}_{uu} - \hat{\mathcal{L}}_{u\mathcal{F}} \hat{\mathcal{L}}_{\mathcal{F}\mathcal{F}}^{-1} \hat{\mathcal{L}}_{u\mathcal{F}}^T - \hat{\mathcal{L}}_{u\mathcal{P}} \hat{\mathcal{L}}_{\mathcal{P}\mathcal{P}}^{-1} \hat{\mathcal{L}}_{u\mathcal{P}}^T \tag{5.6.20}$$

Section 5.7: Finite Element in Time Discretization of a Hinge Constraint.

Consider a single hinge joining two elastic bodies. The corresponding kinematic constraint is in the form of (5.2.1). The Finite Element in Time discretization of the displacement variables was given in section 5.6, and the Lagrange multipliers are interpolated as:

$$\underline{\mu}(t) = \sum_{k=1}^{N_\mu} g_\mu^k(\tau)\underline{\hat{\mu}_k} \tag{5.7.1}$$

where

$$g_\mu^k(\tau) = P_{k-1} \qquad k = 1, ...N_\mu \tag{5.7.2}$$

and the corresponding interpolation matrix isB_μ.

With the help of these interpolation functions, the constraint condition (5.2.9) becomes:

$$\begin{aligned} H = \overline{H} + \lfloor \Delta\underline{\hat{\mathcal{U}}^{\langle 1\rangle T} \quad \Delta\underline{\hat{\mathcal{U}}^{\langle 2\rangle T} \quad \Delta\underline{\hat{\mu}}^T} \rfloor \{ & \left| \begin{array}{c} \hat{\mathcal{H}}_{\mathcal{U}^{\langle 1\rangle}} \\ \hat{\mathcal{H}}_{\mathcal{U}^{\langle 2\rangle}} \\ \hat{\mathcal{H}}_\mu \end{array} \right| \\ + \frac{1}{2} \left| \begin{array}{ccc} \hat{\mathcal{H}}_{\mathcal{U}^{\langle 1\rangle}\mathcal{U}^{\langle 1\rangle}} & \hat{\mathcal{H}}_{\mathcal{U}^{\langle 1\rangle}\mathcal{U}^{\langle 2\rangle}} & \hat{\mathcal{H}}_{\mathcal{U}^{\langle 1\rangle}\mu} \\ & \hat{\mathcal{H}}_{\mathcal{U}^{\langle 2\rangle}\mathcal{U}^{\langle 2\rangle}} & \hat{\mathcal{H}}_{\mathcal{U}^{\langle 2\rangle}\mu} \\ & & \hat{\mathcal{H}}_{\mu\mu} \end{array} \right| \left| \begin{array}{c} \Delta\underline{\hat{\mathcal{U}}^{\langle 1\rangle}} \\ \Delta\underline{\hat{\mathcal{U}}^{\langle 2\rangle}} \\ \Delta\underline{\hat{\mu}} \end{array} \right| \} + h.o.t. \end{aligned} \tag{5.7.3}$$

where

$$\underline{\hat{\mathcal{H}}_{\mathcal{U}^{\langle i\rangle}}} = \int_{t_i}^{t_f} B_u^T \underline{\mathcal{H}_{\mathcal{U}^{\langle i\rangle}}} dt; \quad \underline{\hat{\mathcal{H}}_\mu} = \int_{t_i}^{t_f} B_\mu^T \underline{\mathcal{H}_\mu} dt \tag{5.7.4}$$

and

$$\begin{aligned} \hat{\mathcal{H}}_{\mathcal{U}^{\langle i\rangle}\mathcal{U}^{\langle j\rangle}} &= \int_{t_i}^{t_f} B_u^T \mathcal{H}_{\mathcal{U}^{\langle i\rangle}\mathcal{U}^{\langle j\rangle}} B_u dt; \; \hat{\mathcal{H}}_{\mathcal{U}^{\langle i\rangle}\mu} = \int_{t_i}^{t_f} B_u^T \mathcal{H}_{\mathcal{U}^{\langle i\rangle}\mu} B_\mu dt; \\ \hat{\mathcal{H}}_{\mu\mu} &= \int_{t_i}^{t_f} B_\mu^T \mathcal{H}_{\mu\mu} B_\mu dt \end{aligned} \tag{5.7.5}$$

The Lagrange multipliers are independent variables for each hinge. The stationarity condition with respect to these variables yields:

$$\Delta\underline{\hat{\mu}} = -\hat{\mathcal{H}}_{\mu\mu}^{-1}\underline{\hat{\mathcal{H}}_\mu} - \hat{\mathcal{H}}_{\mu\mu}^{-1}\hat{\mathcal{H}}_{\mathcal{U}^{\langle 1\rangle}\mu}^T \Delta\underline{\hat{\mathcal{U}}^{\langle 1\rangle}} - \hat{\mathcal{H}}_{\mu\mu}^{-1}\hat{\mathcal{H}}_{\mathcal{U}^{\langle 2\rangle}\mu}^T \Delta\underline{\hat{\mathcal{U}}^{\langle 2\rangle}} \tag{5.7.6}$$

Introducing these results into (5.7.3) yields a reduced constraint expression:

$$\begin{aligned} H = \overline{H} + \lfloor \Delta\underline{\hat{\mathcal{U}}^{\langle 1\rangle T} \quad \Delta\underline{\hat{\mathcal{U}}^{\langle 2\rangle T}} \rfloor \{ & \left| \begin{array}{c} \mathbf{H}_{\mathcal{U}^{\langle 1\rangle}} \\ \mathbf{H}_{\mathcal{U}^{\langle 2\rangle}} \end{array} \right| \\ + \frac{1}{2} \left| \begin{array}{cc} \mathbf{H}_{\mathcal{U}^{\langle 1\rangle}\mathcal{U}^{\langle 1\rangle}} & \mathbf{H}_{\mathcal{U}^{\langle 1\rangle}\mathcal{U}^{\langle 2\rangle}} \\ & \mathbf{H}_{\mathcal{U}^{\langle 2\rangle}\mathcal{U}^{\langle 2\rangle}} \end{array} \right| \left| \begin{array}{c} \Delta\underline{\hat{\mathcal{U}}^{\langle 1\rangle}} \\ \Delta\underline{\hat{\mathcal{U}}^{\langle 2\rangle}} \end{array} \right| \} + h.o.t \end{aligned} \tag{5.7.7}$$

where

$$\underline{\mathsf{H}_{U^{(i)}}} = \left(\underline{\hat{\mathcal{H}}_{U^{(i)}}} - \hat{\mathcal{H}}_{U^{(i)}\mu}\hat{\mathcal{H}}_{\mu\mu}^{-1}\underline{\hat{\mathcal{H}}_{\mu}}\right) \tag{5.7.8}$$

and

$$\mathsf{H}_{U^{(i)}U^{(j)}} = \left(\hat{\mathcal{H}}_{U^{(i)}U^{(j)}} - \hat{\mathcal{H}}_{U^{(i)}\mu}\hat{\mathcal{H}}_{\mu\mu}^{-1}\hat{\mathcal{H}}_{U^{(j)}\mu}^{T}\right) \tag{5.7.9}$$

Section 5.8: Governing Equations of Multibody Systems.

Consider now a problem involving N_b elastic bodies interacting through N_h hinges. Hamilton's Principle writes:

$$\delta\mathsf{L} + \delta W + \delta\left\{\underline{\mathsf{P}_i^T}\left[\underline{\mathsf{U}}(t_i) - \underline{\mathsf{U}_i}\right] - \underline{\mathsf{P}_f^T}\left[\underline{\mathsf{U}}(t_f) - \underline{\mathsf{U}_f}\right]\right\} = 0 \tag{5.8.1}$$

where L is the total Lagrangian of the system given by:

$$\mathsf{L} = \sum_{i=1}^{N_b}\mathcal{L}^{(i)} + \sum_{\alpha=1}^{N_h}H^{(\alpha)} \tag{5.8.2}$$

δW is the virtual work done by the applied loads; $\underline{\mathsf{P}_i}$ and $\underline{\mathsf{P}_f}$ are the initial and final momenta vectors, respectively; $\underline{\mathsf{U}_i}$ and $\underline{\mathsf{U}_f}$ the initial and final values of the displacement vector $\underline{\mathsf{U}}(t)$; and finally t_i and t_f the initial and final times of the period under consideration. The unknowns of the problem are the displacements in each of the N_b elastic bodies, i.e.

$$\underline{\mathsf{U}^T}(t) = \left[\underline{\hat{\mathcal{U}}^{\langle 1\rangle T}}(t), \underline{\hat{\mathcal{U}}^{\langle 2\rangle T}}(t), \ldots \underline{\hat{\mathcal{U}}^{\langle N_b\rangle T}}(t)\right] \tag{5.8.3}$$

With the help of the finite element in time discretization described in the previous sections, the unknown nodal values are:

$$\underline{\hat{\mathsf{U}}^T} = \left[\underline{\hat{\mathsf{U}}_1^T}, \underline{\hat{\mathsf{U}}_2^T}, \ldots, \underline{\hat{\mathsf{U}}_{N_u}^T},\right] \tag{5.8.4}$$

where

$$\underline{\hat{\mathsf{U}}_i^T} = \left[\underline{\hat{\mathcal{U}}_i^{\langle 1\rangle T}}, \underline{\hat{\mathcal{U}}_i^{\langle 2\rangle T}}, \ldots \underline{\hat{\mathcal{U}}_i^{\langle N_b\rangle T}}\right] \quad i = 1, 2, \ldots N_u \tag{5.8.5}$$

The variations of (5.8.1) with respect to the unknown initial and final momenta yields:

$$\underline{\hat{\mathsf{U}}_1} = \underline{\hat{\mathsf{U}}_i} \qquad ; \underline{\hat{\mathsf{U}}_2} = \underline{\hat{\mathsf{U}}_f} \tag{5.8.6}$$

and the variation with respect to $\underline{\hat{\mathsf{U}}}$ yields:

$$\underline{\mathsf{U}}(t_i) = \underline{\mathsf{U}_i} \text{ and } \underline{\mathsf{U}}(t_f) = \underline{\mathsf{U}_f} \tag{5.8.7}$$

which, in view of (5.6.5) is simply:

$$\underline{\hat{\mathsf{U}}_1} = \underline{\mathsf{U}_i} \text{ and } \underline{\hat{\mathsf{U}}_2} = \underline{\mathsf{U}_f} \tag{5.8.8}$$

The variation of (5.8.1) with respect to the unknown displacements yields:

$$\underline{F} + \mathbf{K}\Delta\underline{U} + \underline{P} + \underline{Q} = 0 \tag{5.8.9}$$

where $\underline{F}$ is the equivalent load vector and $\mathbf{K}$ the stiffness matrix, both obtained from the appropriate assembly of the Lagrangian (5.6.20) of each elastic body and the constraint (5.7.7) of each hinge. The momentum vector is:

$$\underline{P}^T = \left[\underline{P_i}^T, -\underline{P_f}^T, 0, \ldots 0\right] \tag{5.8.10}$$

and $\mathbf{Q}$ is the vector of applied loads.

The intermediate nodal variables can be evaluated and eliminated from (5.8.9) to give:

$$\begin{vmatrix} \mathbf{K}_{ii} & \mathbf{K}_{if} \\ & \mathbf{K}_{ff} \end{vmatrix} \begin{vmatrix} \Delta\hat{\underline{U}}_i \\ \Delta\underline{\hat{U}}_f \end{vmatrix} = \begin{vmatrix} -\underline{P_i} \\ +\underline{P_f} \end{vmatrix} - \begin{vmatrix} \underline{F_i} + \underline{Q_i} \\ \underline{F_f} + \underline{Q_f} \end{vmatrix} \tag{5.8.11}$$

In a step by step integration scheme the initial displacement and momentum are known quantities, hence $\Delta\underline{U_i} = 0$ and the corresponding quantities at the end of the time step are:

$$\begin{aligned} \Delta\underline{U_f} &= -\mathbf{K}_{if}^{-1}\left[\underline{P_i} + \underline{F_i} + \underline{Q_i}\right] \\ \underline{P_f} &= \mathbf{K}_{ff}\Delta\underline{U_f} + \underline{F_f} + \underline{Q_f} \end{aligned} \tag{5.8.12}$$

Section 5.9: Numerical results and discussions

Section 5.9.1 Spinning Top

The spinning top will be investigated to test the modeling of rigid body motions and constraint equations. The base point of the spinning top is not free to translate but rotations are allowed. As discussed in the previous sections, this constraint can be applied in two ways: the displacement of the base point can be constrained (we will refer to this case as the "D-hinge".), or the velocity of the base point can be constrained (the "V-hinge"). The numerical accuracy and stability of these two models will be addressed here.

The analytical solution of the spinning top case is obtained by using Euler angles $\theta, \phi, \ and \ \psi$. The Lagrangian of the system writes:

$$\begin{aligned} L &= T - U \\ &= \frac{1}{2}\bar{I}_1\omega_1^2 + \frac{1}{2}\bar{I}_2\omega_2^2 + \frac{1}{2}\bar{I}_3\omega_3^2 - \mu g d\cos\theta \end{aligned} \tag{5.9.1}$$

where $\bar{I}_i, \ and \ \omega_i$ are the moments of inertia and angular velocities in 1,2 and 3 coordinates respectively. $\mu, g, \ and \ d$ represents mass density, gravitational acceleration and the distance from the origin to the center of gravity of the body respectively. By using the Euler angles $\theta, \phi, \ and \ \psi$ Eq. (5.9.1) can be rewritten as:

$$L = \frac{1}{2}\bar{I}_1\dot{\phi}^2\sin^2\theta + \frac{1}{2}\bar{I}_2\dot{\theta}^2 + \frac{1}{2}\bar{I}_3\left(\dot{\phi}\cos\theta + \dot{\psi}\right)^2 - \mu g d\cos\theta \tag{5.9.2}$$

Hamilton's Principle writes:

$$\delta \int_{t_i}^{t_f} \left(\frac{1}{2}\bar{I}_1 \dot{\phi}^2 \sin^2\theta + \frac{1}{2}\bar{I}_2 \dot{\theta}^2 + \frac{1}{2}\bar{I}_3 \left(\dot{\phi}\cos\theta + \dot{\psi} \right)^2 - \mu g d \cos\theta \right) dt = [\hat{p}\delta x]_{t_i}^{t_f} \tag{5.9.3}$$

Variations with respect to $\theta, \phi,$ *and* ψ yield to three equations of motions.

$$\begin{aligned}
\delta\theta: &\quad \frac{1}{2}\bar{I}_1 \dot{\phi}^2 \sin 2\theta - \bar{I}_2 \ddot{\theta} - \bar{I}_3 \dot{\phi} \sin\theta \left(\dot{\phi}\cos\theta + \dot{\psi} \right) + \mu g d \cos\theta = 0 \\
\delta\phi: &\quad \bar{I}_1 \dot{\phi} \sin^2\theta + \bar{I}_3 \left(\dot{\phi}\cos\theta + \dot{\psi} \right) \cos\theta = P_\phi = Constant \\
\delta\psi: &\quad \bar{I}_3 \left(\dot{\phi}\cos\theta + \dot{\psi} \right) = P_\psi = Constant
\end{aligned} \tag{5.9.4}$$

These equations are solved by Gear's method in IMSL routine. The error tolerance is assigned as 10^{-10}. The solutions obtained by this method will be called as "analytical solution".

Three sets of initial conditions were investigated and compared with another numerical solution obtained by F.J. Mello [5–1]. The initial conditions are chosen to yield three different types of motions.

Case 1 exhibits precession which is always in the same direction throughout in the motion; Case 2 exhibits precession which changes sign during the motion; and Case 3 exhibits precession which does not reverse its direction but it does stop at points in its motion (cuspidal motion).

The input data for each case is the same as Ref [5–1] given as:

Case 1:

The mass is 1.0. The axial moment of inertia is .40

The transverse moment of inertia is .75.

The initial orientation is in the yz plane +10 degrees from vertical.

The initial angular velocity is (0., .9888, 7.5167) rad/sec.

The distance from the mass center to the support is .2

Gravity is 3.0

Case 2:

The initial angular velocity is (0., .20905, 6.2964) rad/sec.

All other data are the same.

Case 3:

Initial angular velocity is (0., 0., 6.3794) rad/sec.

All other data are the same.

In this work the constraints are imposed via a Lagrange multiplier technique, and uses a fictitious stiffnesses (5.3.8, 5.4.6). The results are sensitive to the choice of these Lagrange multipliers. α_1 is the fictitious stiffness associated with the normality condition of the Euler parameters representing the rigid body motion, and α_2 that the hinge constraint. Several values were in uses as shown in table 5.1.

Table 5.1 Choices of fictitious stiffness

	Fictitious stiffness for Euler Parameters(α_1)	Fictitious stiffness for Hinge Constraint(α_2)
Case (A)	10^5	10^7
Case (B)	10^6	10^8
Case (C)	10^8	10^{10}

The motion of the spinning top was analyzed with 2,3, and 4 noded elements in time for the various motion types, and for the different values fictitious stiffness. The accuracy of the results is assessed by comparing the analytical solution with the numerical predictions for the x, y, and z coordinates of the center of mass of the spinning top. Table 5.2 presents the results for the case 1 type motion. 100 time steps of Δt=0.06 sec were performed. For the two noded time element the D-hinge solution diverged for all values of the fictitious stiffnesses, the V-hinge solution was stable, but its accuracy was poor when compared to the results of ref [5–1]. For the three noded element, the D-hinge gave stable solutions but its accuracy is rather poor when compare to that of V-hinge which gave answers comparable to that of ref [5–1]. Finally the four noded element gave poor answers for the D-hinge, and very accurate predictions for the V-hinge.

These results also clearly show the need to select appropriate values of the fictitious stiffnesses: high enough values should be selected as to properly enforce the constraint. Fig 5.1 shows the motion of the center of mass projected in the xy plane, for the two noded element. It is that the numerical results are ahead of the analytical solution, in other words, the top "spins faster" in the numerical model. Fig 5.2 shows the result for the D-hinge, however, at Δt=0.02 sec was selected, as Δt=0.06 sec yield unstable results.

Fig 5.3 and 5.4 present the results of the three and four noded elements with time increment. Fig 5.5 through 5.9 present the results for case 2 and 3 motions. It is clear that the D-hinge shows oscillations of increasing amplitude, typical of numerically unstable behavior, whereas the V-hinge yields a numerically stable solution.

Fig 5.10 to 5.12 show the distance between the actual position of the base of the spinning top, and the position it is constrained to be. Surprisingly, the V-hinge results maintains this distance to a zero value, as it should, whereas the D-hinge results oscillate about the zero value and eventually become unstable. Fig 5.14 through 17 show similar results for the case 2 and 3 motion types.

Table 5.2 Relative Displacement errors of The Top Case 1.

2–noded Element

Relative Errors (%)		X	Y	Z
Ref [1]		0.976	1.345	0.0539
V-Hinge	(A)	88.90	6.636	2.844
	(B)	129.3	-7.130	2.692
	(C)	130.0	-9.196	2.672

3–noded Element

Relative Errors (%)		X	Y	Z
Ref [1]		0.308	0.176	0.0068
D-Hinge	(A)	44.96	-10.15	2.947
	(B)	10.91	4.687	1.611
	(C)	6.133	5.235	1.345
V-Hinge	(A)	38.06	14.98	0.056
	(B)	4.422	-1.221	0.040
	(C)	0.350	-0.103	-0.0048

4–noded element

Relative Errors (%)		X	Y	Z
Ref [1]		0.068	0.095	0.0022
D-Hinge	(A)	-27.36	21.75	-12.46
	(B)	-77.03	35.66	-15.45
	(C)	-76.51	34.22	-14.94
V-Hinge	(A)	38.05	14.96	1.0025
	(B)	4.124	-1.129	0.045
	(C)	0.048	-0.017	0.0005

Section 5.9.2 Pendulum Problem

The characteristics of the rigid link constraint will be assessed by studying the single and double pendulum problems. Rigid link imposes the constraint of a fixed distance between two points. For instance the pendulum problem can be seen as the motion of a point mass in a two dimensional space subjected to the constraint of a given distance between the origin and the mass point. In the D-link the constraint condition is that of this fixed distance whereas in the V-link the constraint condition is the orthogonality of the position and velocity vector for the mass point.

The analytical solution for the single and double pendulum are readily obtained and integrated. Three problems were analyzed with the following characteristics.

Problem I : μg= 1.0 N, V_i = 1.0 m/sec, L = 0.2m

Problem II : μg = 10.0 N, V_i = 1.0 m/sec, L = 0.2m

Problem III: $\mu_1 g = \mu_2 g$=1.0 N, V_{i1} = 1.0 m/sec,V_{i2} = 0.0 m/sec,

L_1=0.2 m,L_2=0.1 m.

where μg is the gravity forces, V_i the initial velocity, and L the length of the pendulum.

Table 5.3 Choices of fictitious stiffness

	Fictitious stiffness for Velocity Link(α_v)	Fictitious stiffness for Displacement Link(α_d)
Case (A)	10^5	10^{10}
Case (B)	10^7	10^{12}
Case (C)	10^{10}	10^{14}

Table 5.4 Relative Displacement errors

Problem I

Relative Errors (%)		X	Y
D-Link	(A)	58.79	22.46
	(B)	19.06	38.67
	(C)	18.53	37.15
V-Link	(A)	2.61	4.60
	(B)	0.40	0.51
	(C)	0.43	-0.56

Problem II

Relative Errors (%)		X	Y
D-Link	(A)	***	***
	(B)	22.62	15.13
	(C)	21.95	14.62
V-Link	(A)	2.27	4.95
	(B)	0.28	0.09
	(C)	0.30	0.15

Problem III

Relative Errors (%)		X	Y
D-Link	(A)	***	***
	(B)	25.48	5.50
	(C)	23.18	5.08
V-Link	(A)	23.84	0.95
	(B)	1.27	0.28
	(C)	1.53	0.30

Table 5.3 shows the three different cases of fictitious stiffnesses. From a number of trial and error reasonable ranges of fictitious stiffnesses are obtained. For D-link solutions for the single pendulum are going to be unstable in the case of $\alpha_d \leq 10^9$. In the range of $10^{10} - 10^{14}$ the solutions of D-link are converging for the single pendulum even though not converging for the double pendulum. But all the solutions are not accurate. On the other hand V-link does not seem to be sensitive to the values of fictitious stiffness α_v if α_v is large enough. The fictitious stiffness α_v is investigated in the range of $10^5 - 10^{10}$.

Table 5.4 shows the accuracies of the displacements for 2 different links. Again V-link has much more accurate solutions than D-link. In all 3 cases V-link has solutions with a reasonable accuracy. For problem I and II which is for the single pendulum D-link of case (C) yields the convergent solutions though not accurate. But for problem III which is for the double pendulum D-link cannot obtain the convergent solution while V-link (B) and (C) has a quite accurate solution.

Fig 5.18 — 5.20 show the results of problem I. Fig 5.17 shows the displacements of the pendulum along the time history with D-link. From fig 5.18 the solutions are quite sensitive to the values of α_d. All three cases the solutions are oscillating. The best result is from case(C) the accuracy of which is at most 18%. Fig 5.19 shows the results with V-link. All three results are quite accurate and the best results are from case(B) the accuracy of which is as good as 0.5%. Those best results from D-link and V-link are investigated from now on. Fig 5.20 is the best result of problem I from D-link and V-link. Even though it looks identical the difference of the accuracies between the two links is large as seen from the table 5.4. Fig 5.21 shows the results of problem II. After 200 time steps the pendulum oscillates for 5 periods. Fig 5.22 and 5.23 show the results of problem III which is for double pendulum. From fig 5.22 displacements of D-link are diverging after 165 time steps in all three cases. With this Δt=0.01 secs no convergent solution was obtained. Fig 5.23 shows the results with V-link which are quite accurate even after 400 time steps. In this double pendulum problem $\alpha_v = 10^5$ is not large enough to obtain the accurate solutions. But once $\alpha_v \geq 10^7$ the accuracies are within 1.5 %.

Fig 5.24 shows how well the link preserves the distance from the mass point from the origin. Again the length of V-link remains the same as accurate as 10^{-5} error while the length of D-link is oscillating in the range of 5 % for problem I and 3 % for problem II.

References

5–1. Mello, F.J., "Weak Formulations in Analytical dynamics, with Applications to Multi-rigid-body Systems, using Time Finite Elements.", Doctoral Thesis at GIT, 1989.

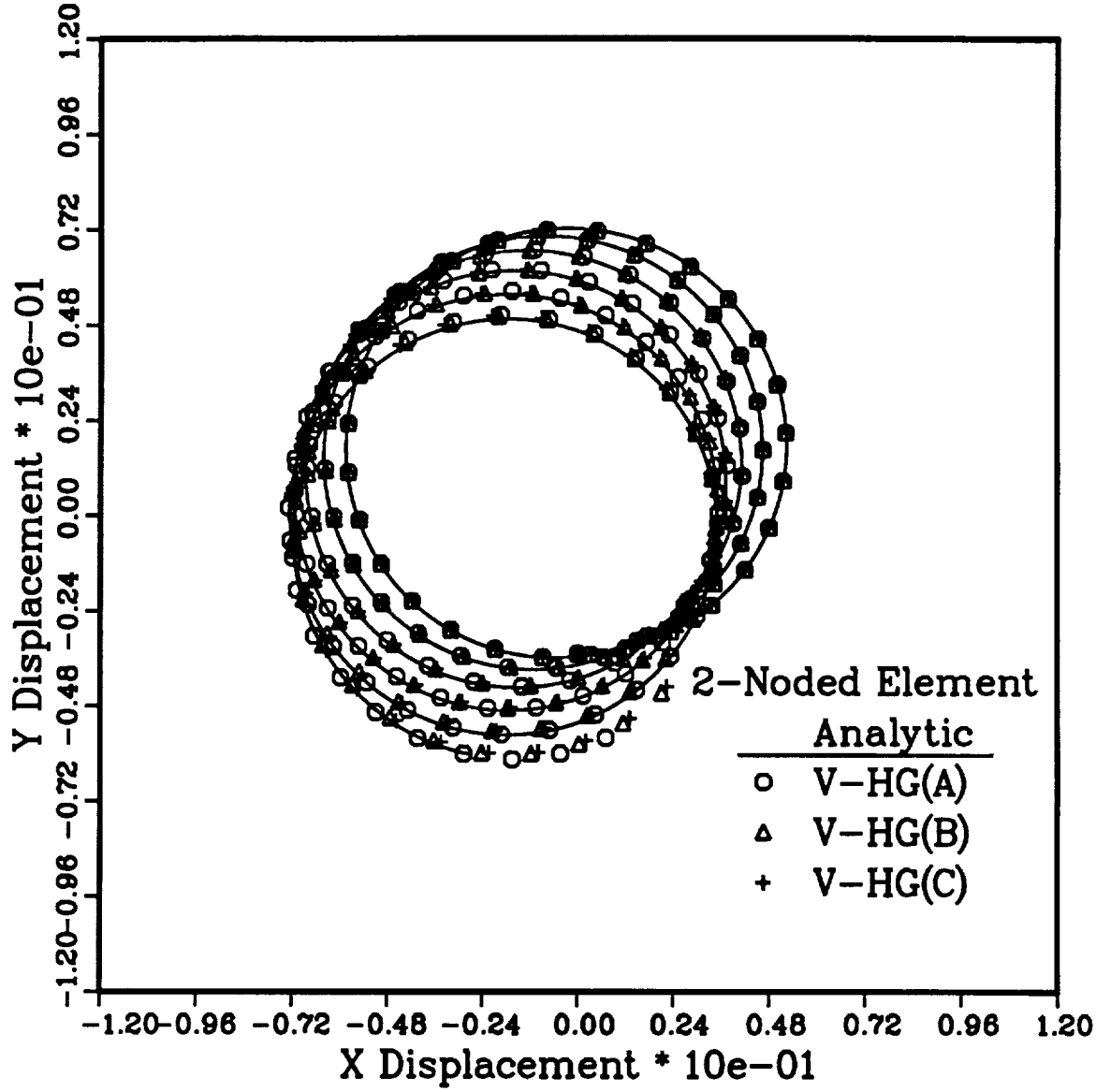

Fig 5.1 Spinning Top Case 1: $\Delta T = .06$ sec

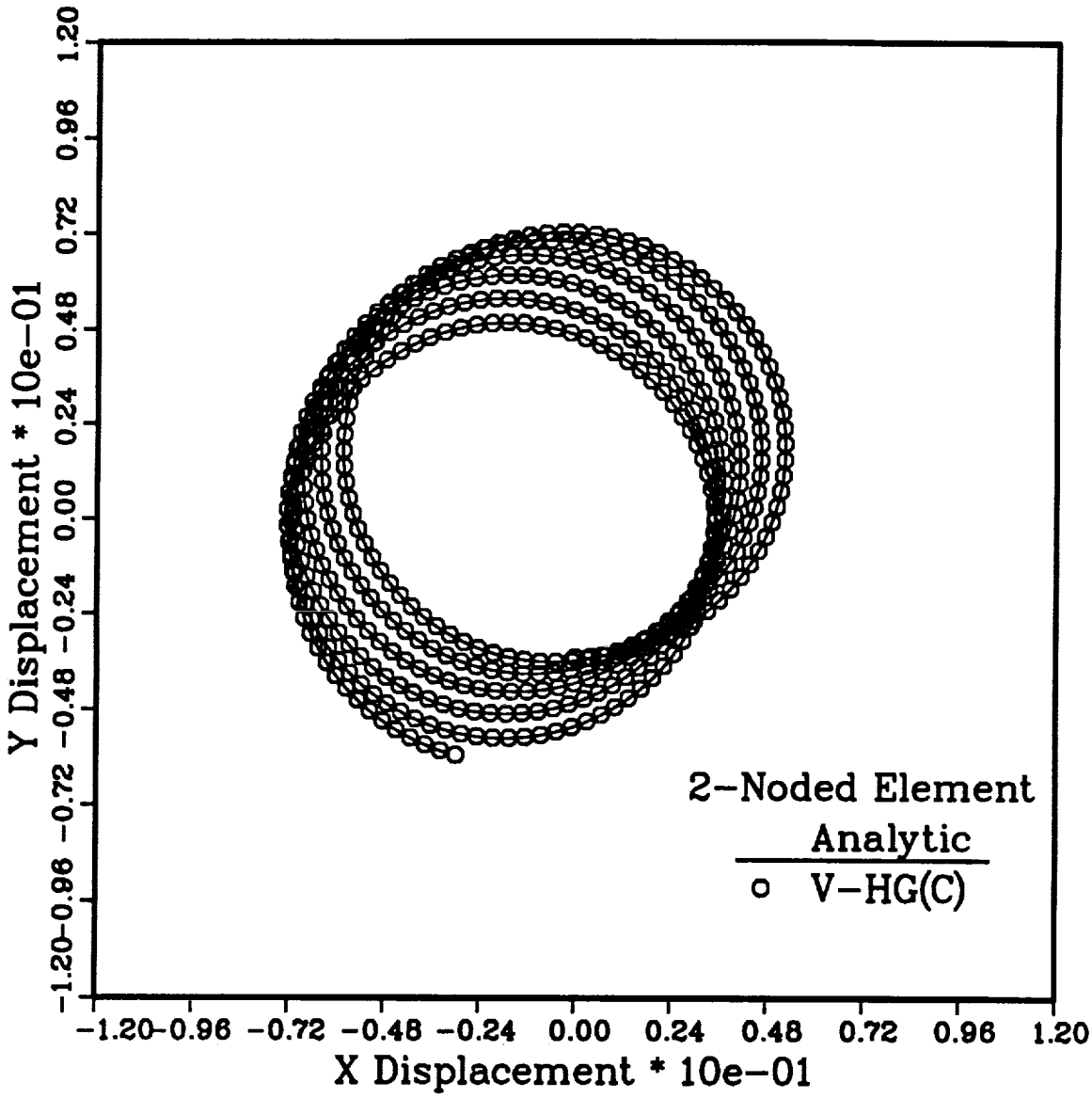

Fig 5.2 Spinning Top Case 1: $\Delta T = .02$ sec

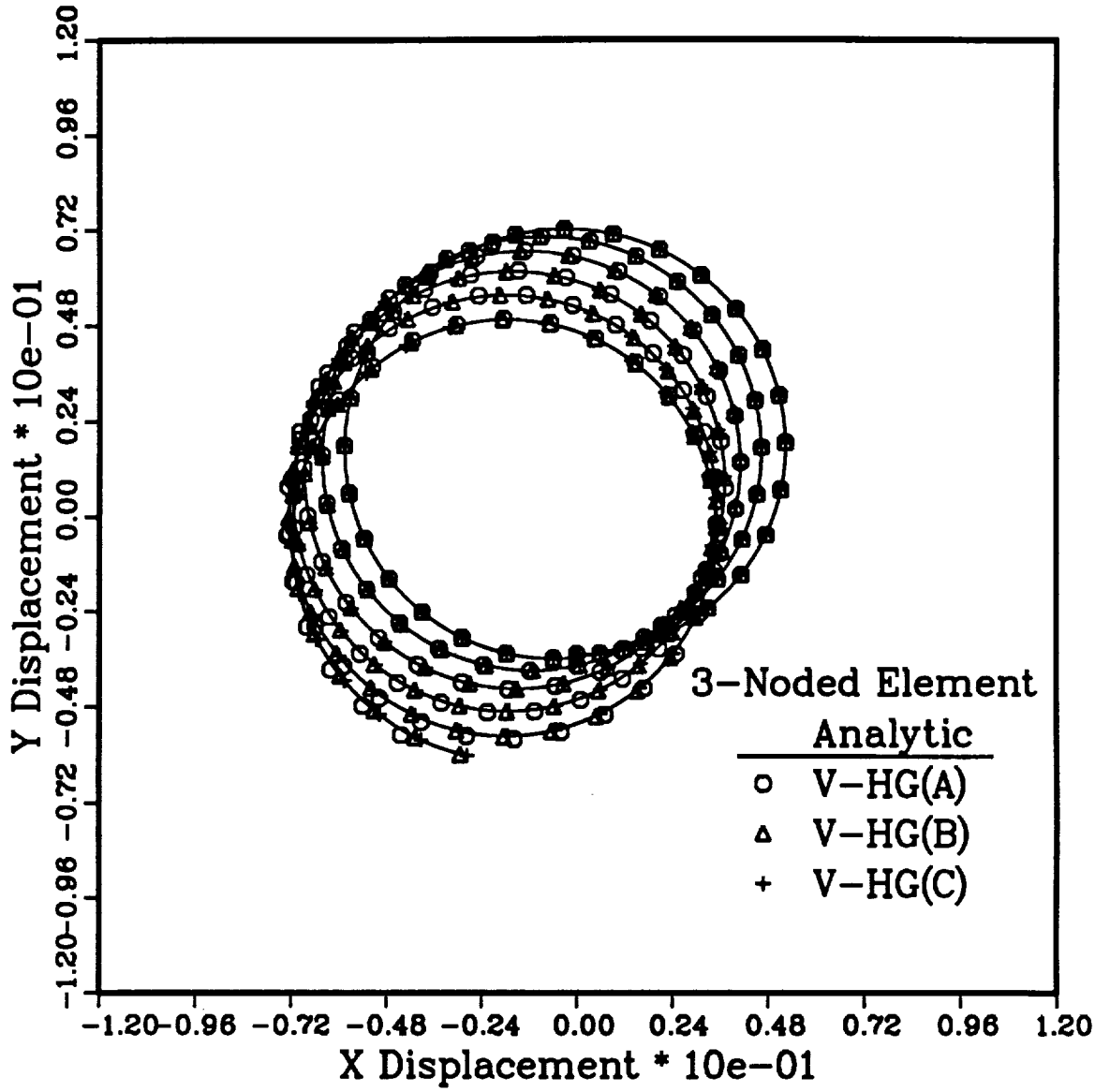

Fig 5.3 Spinning Top Case 1: $\Delta T = .06$ sec

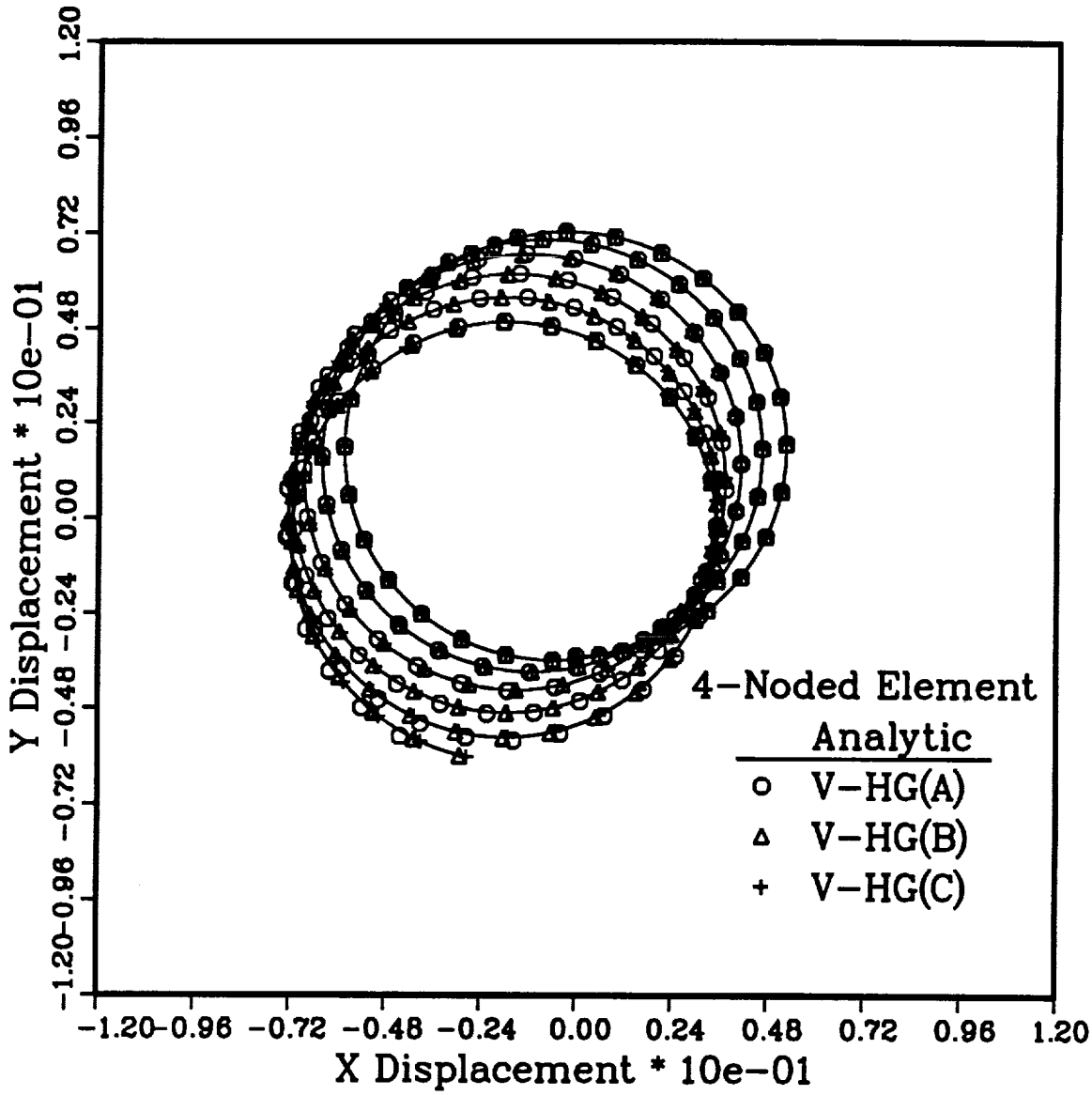

Fig 5.4 Spinning Top Case 1: $\Delta T = .06$ sec

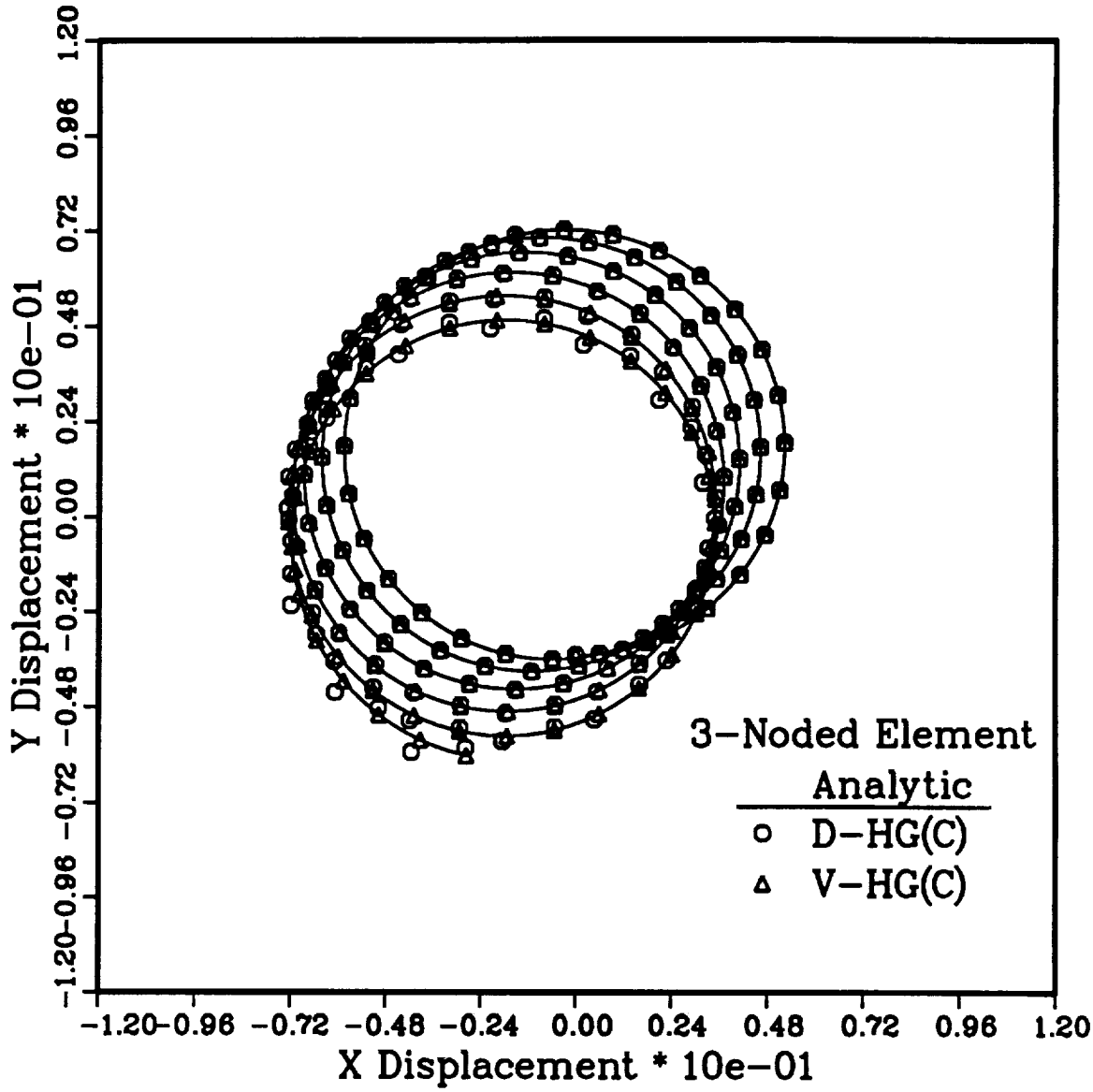

Fig 5.5 Spinning Top Case 1: $\Delta T = .06$ sec

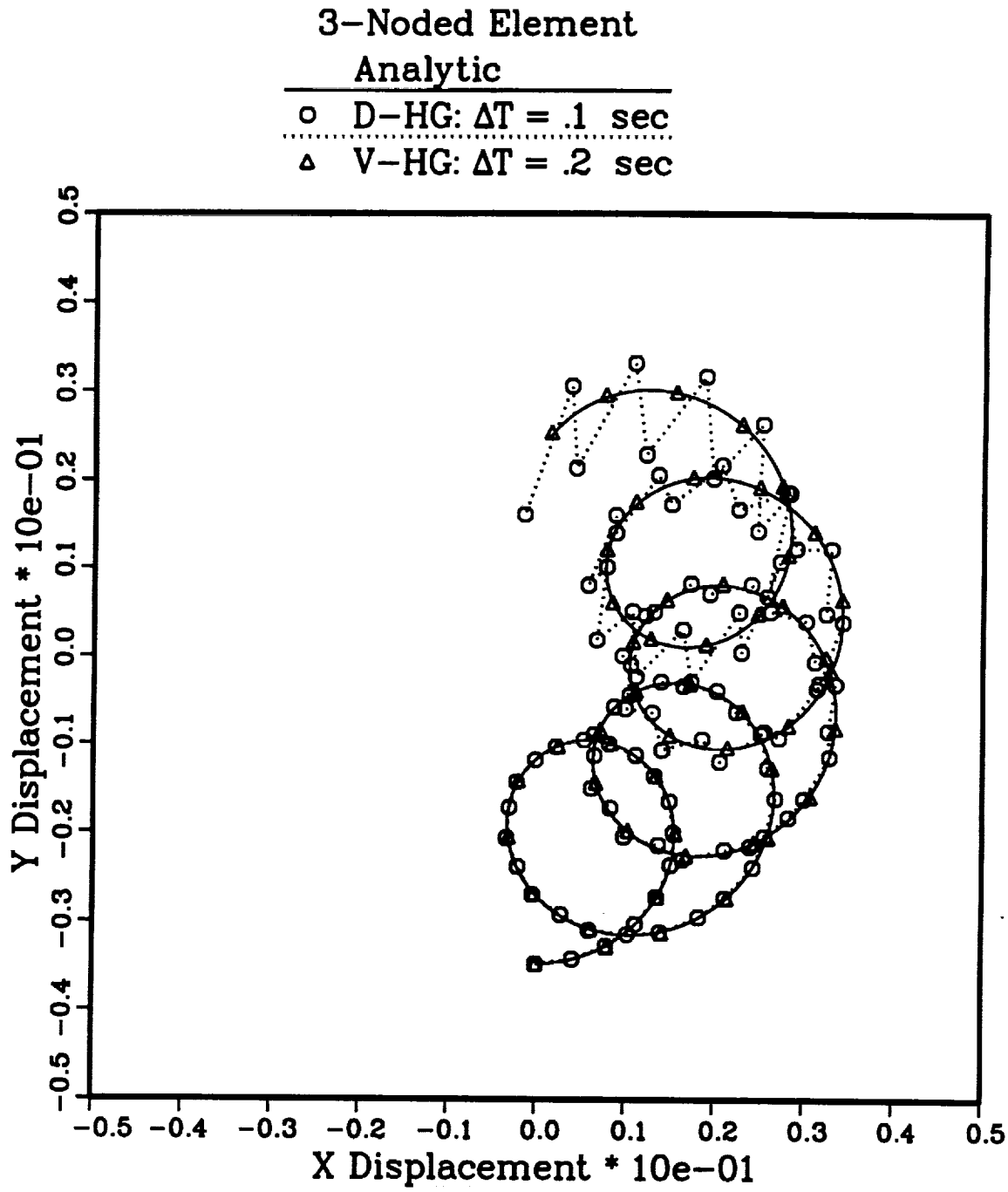

Fig 5.6 Spinning Top Case 2

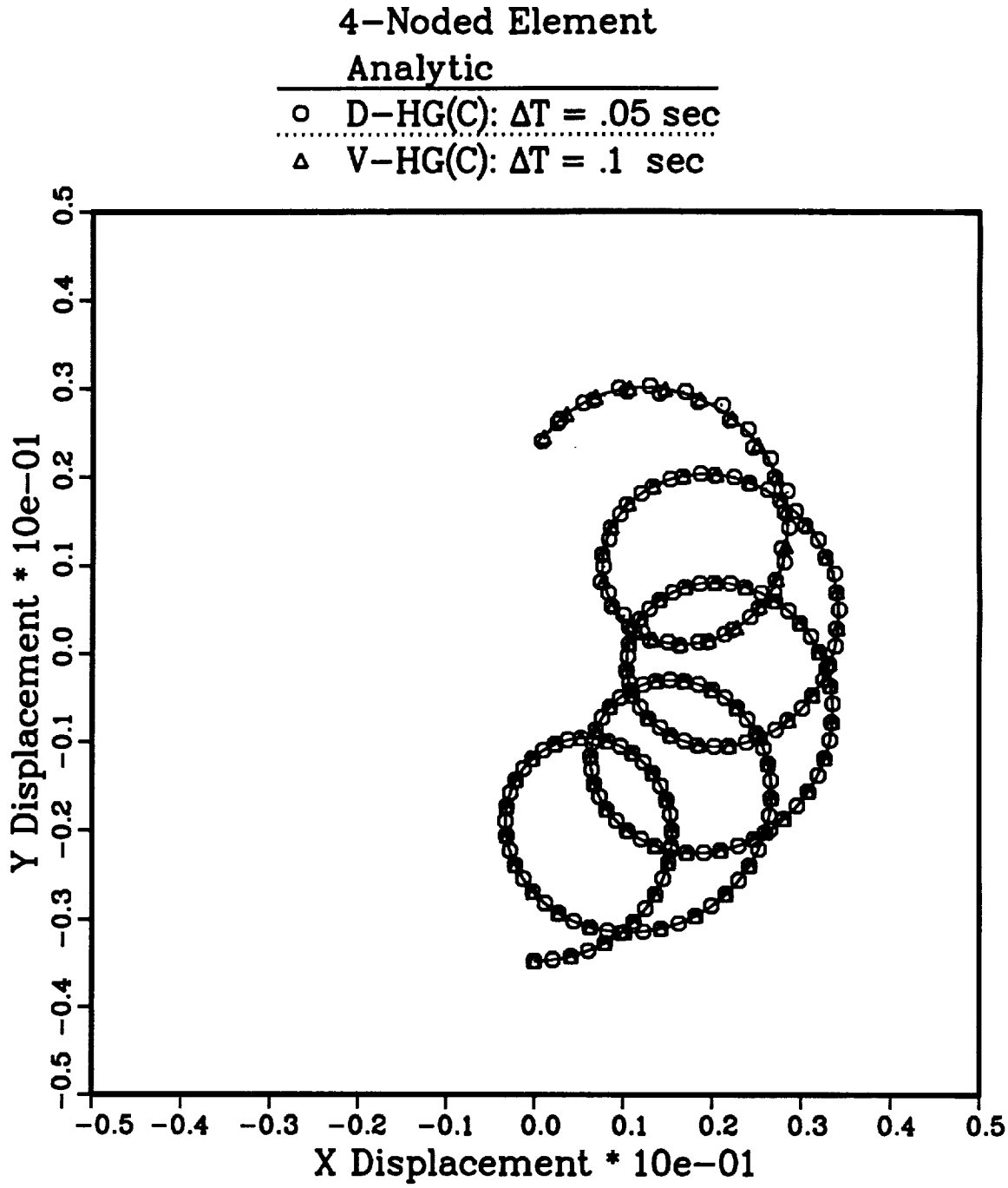

Fig 5.7 Spinning Top Case 2

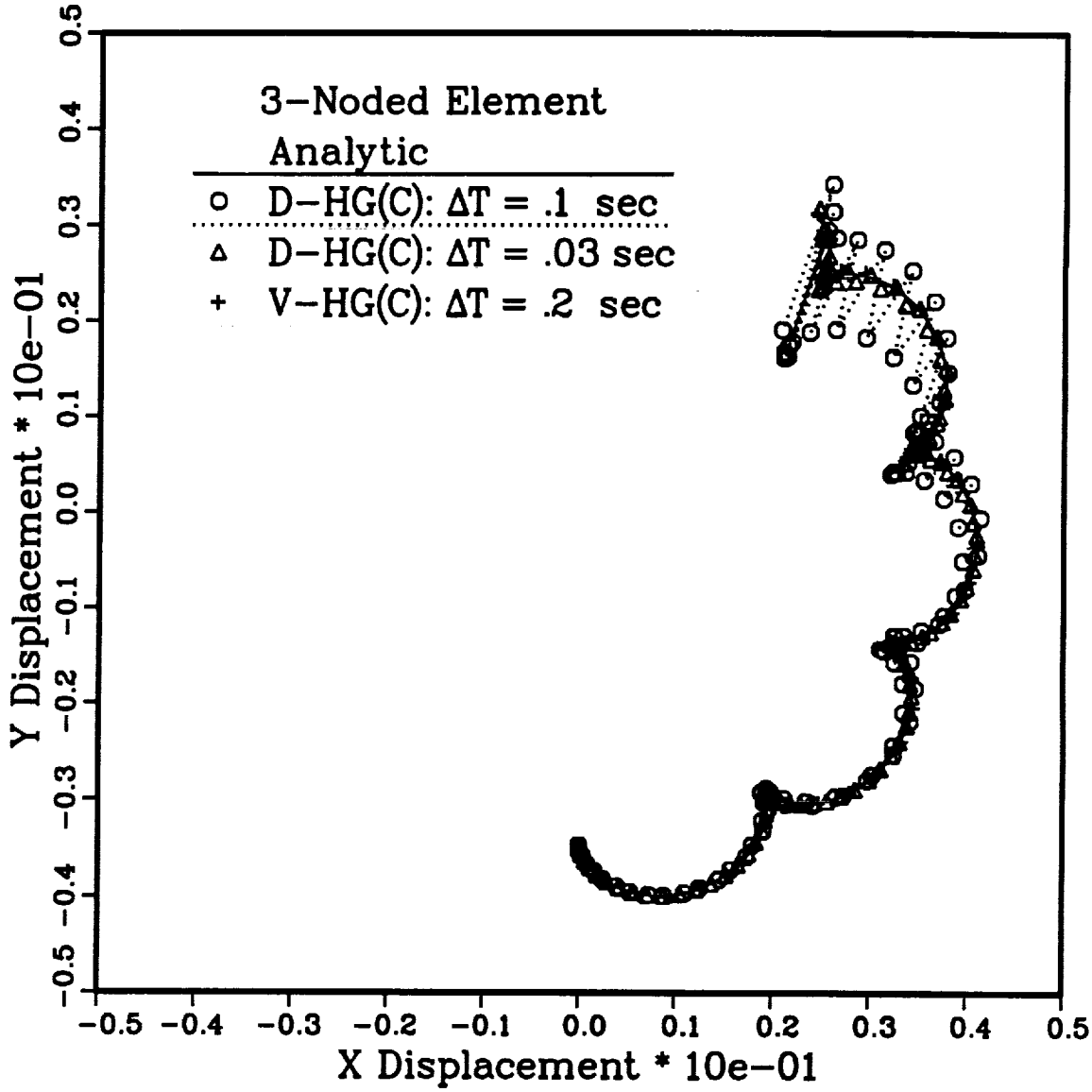

Fig 5.8 Spinning Top Case 3

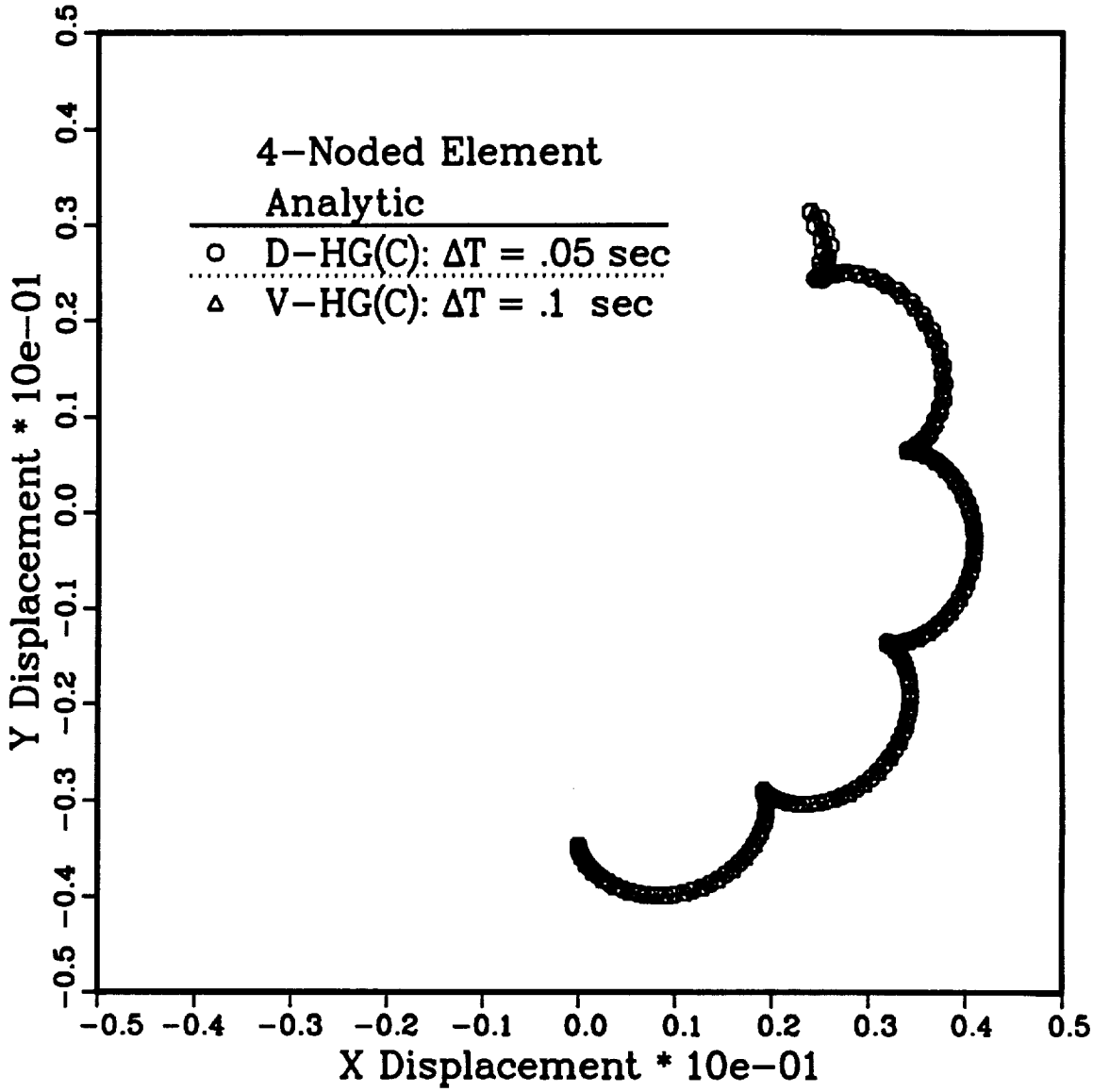

Fig 5.9 Spinning Top Case 3

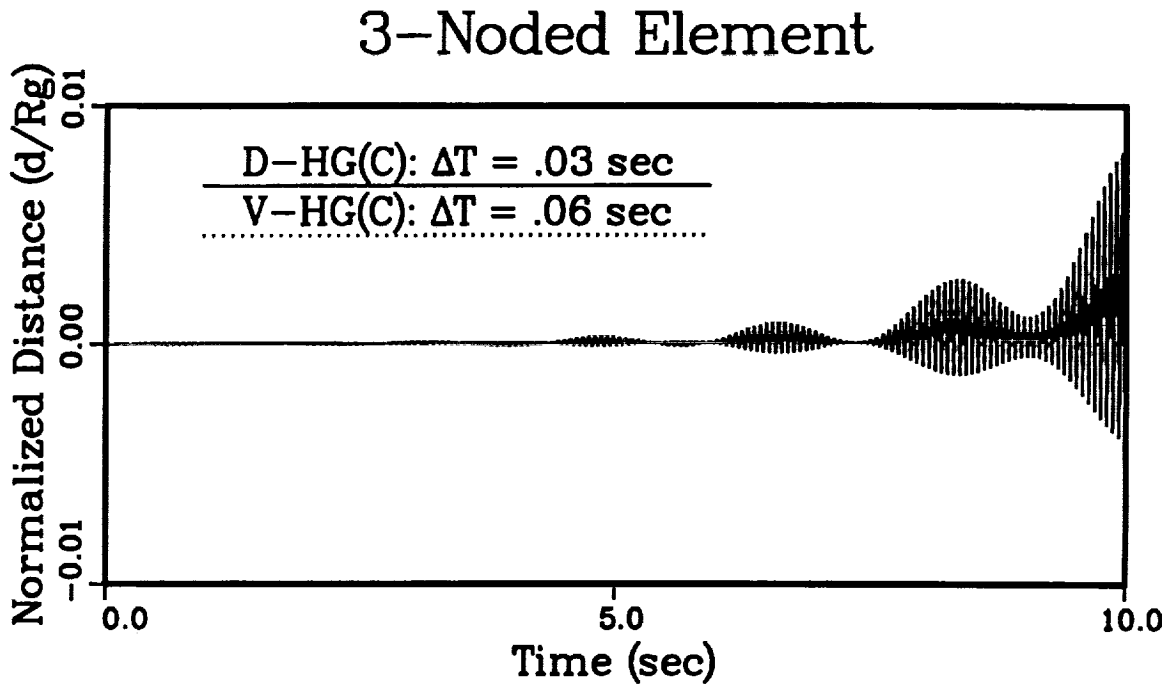

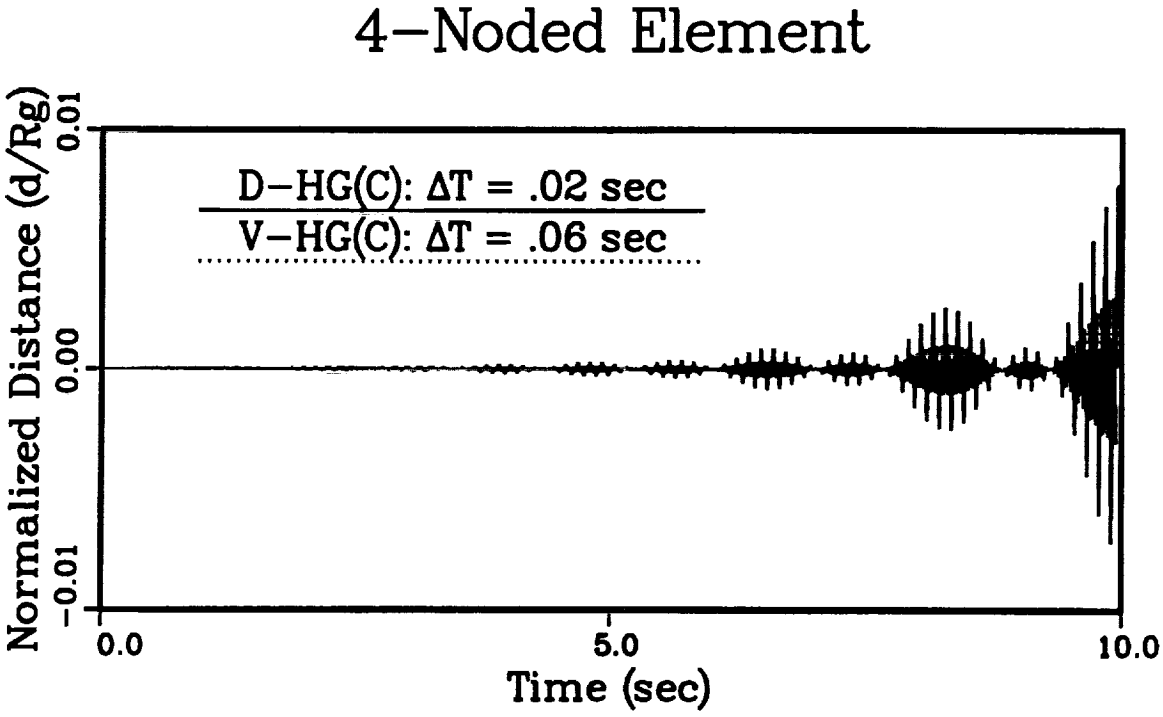

Fig 5.10 Relative Errors at The Hinge(Case 1)

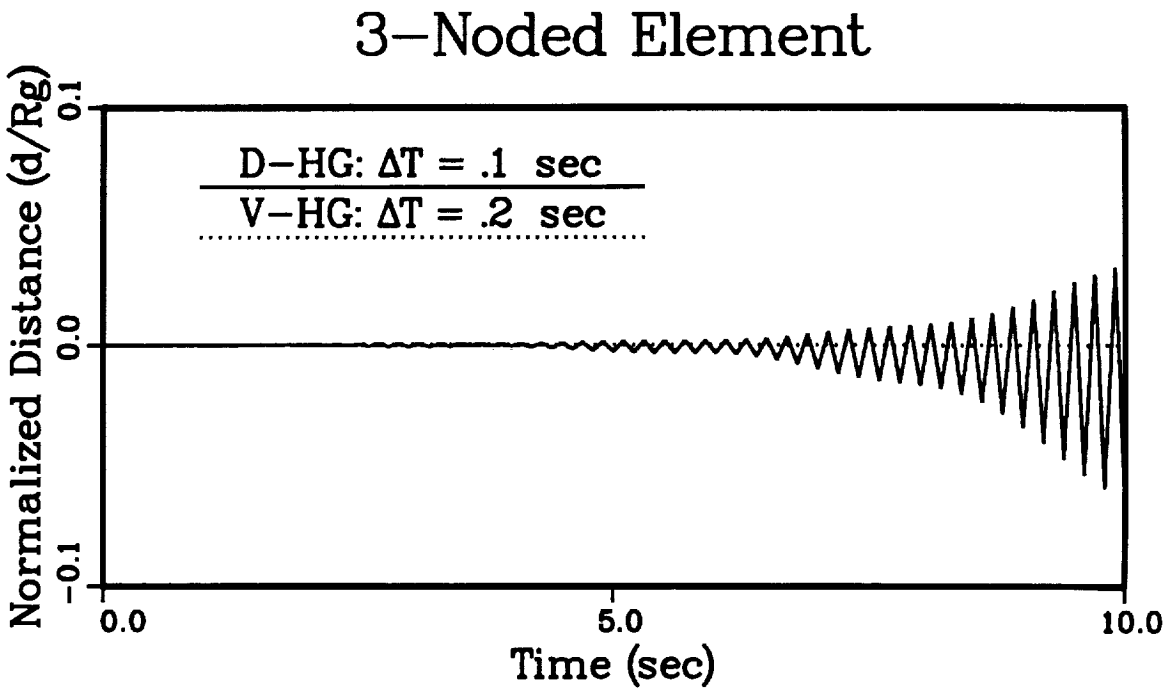

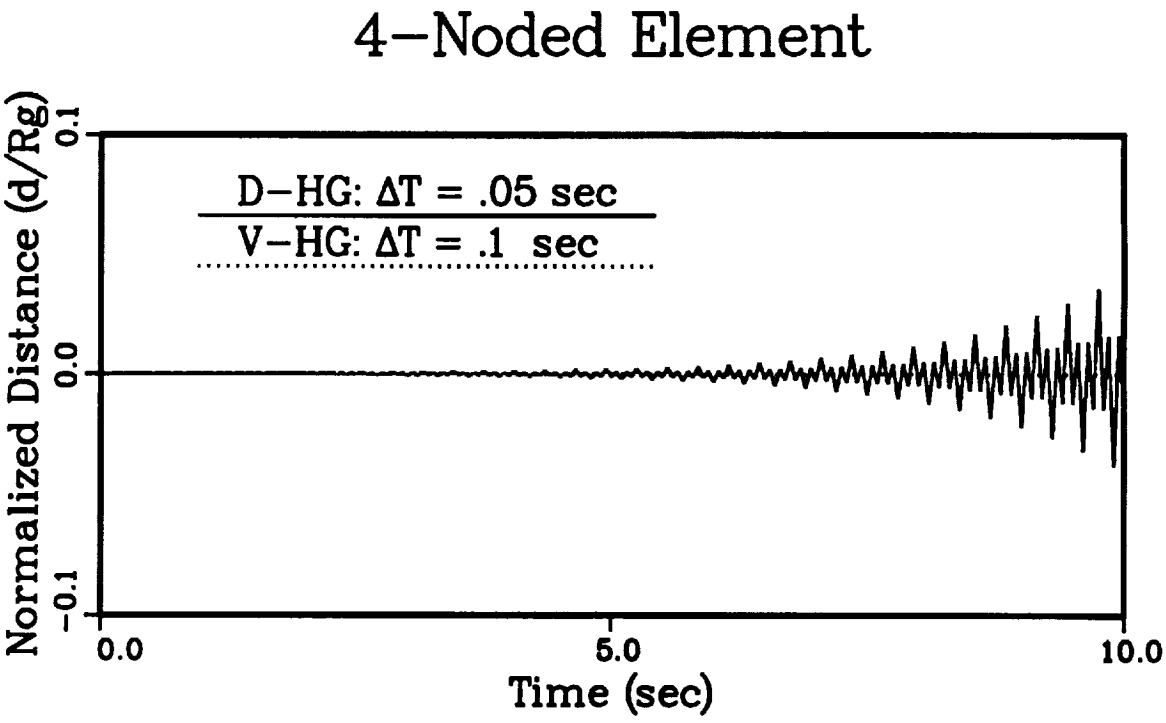

Fig 5.11 Relative Errors at The Hinge(Case 2)

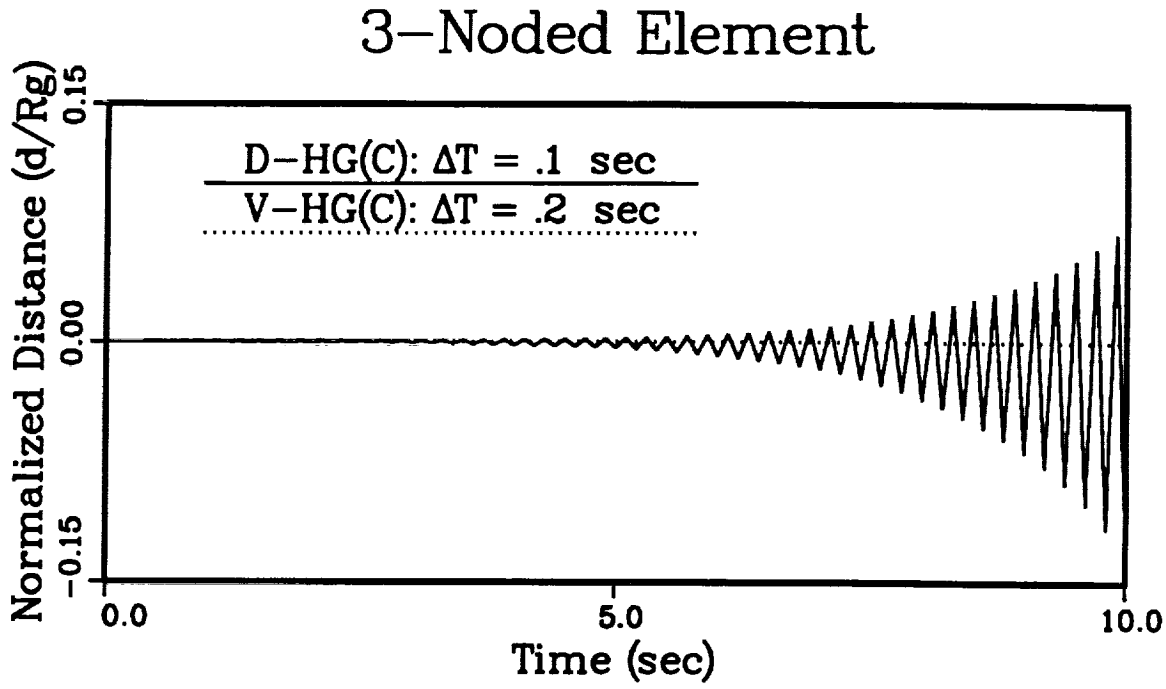

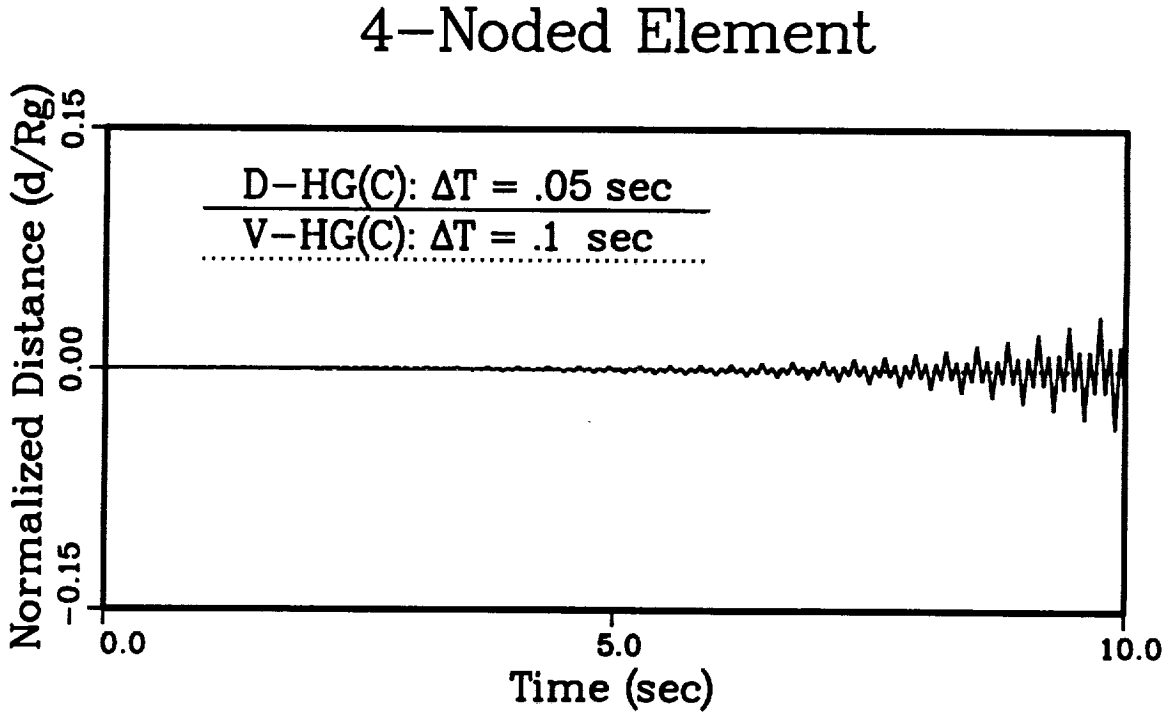

Fig 5.12 Relative Errors at The Hinge(Case 3)

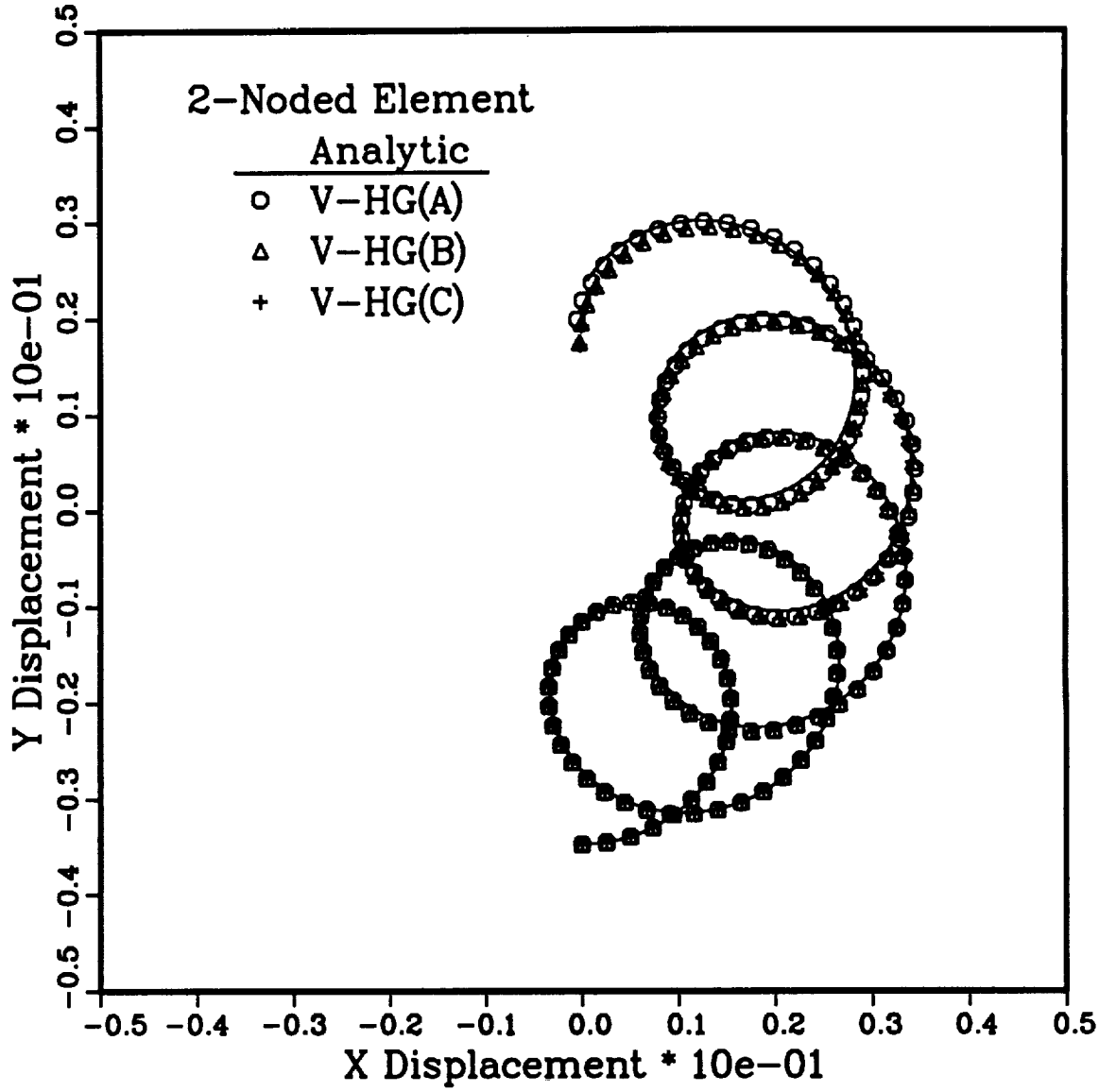

Fig 5.13 Spinning Top Case 2: $\Delta T = .06$ sec

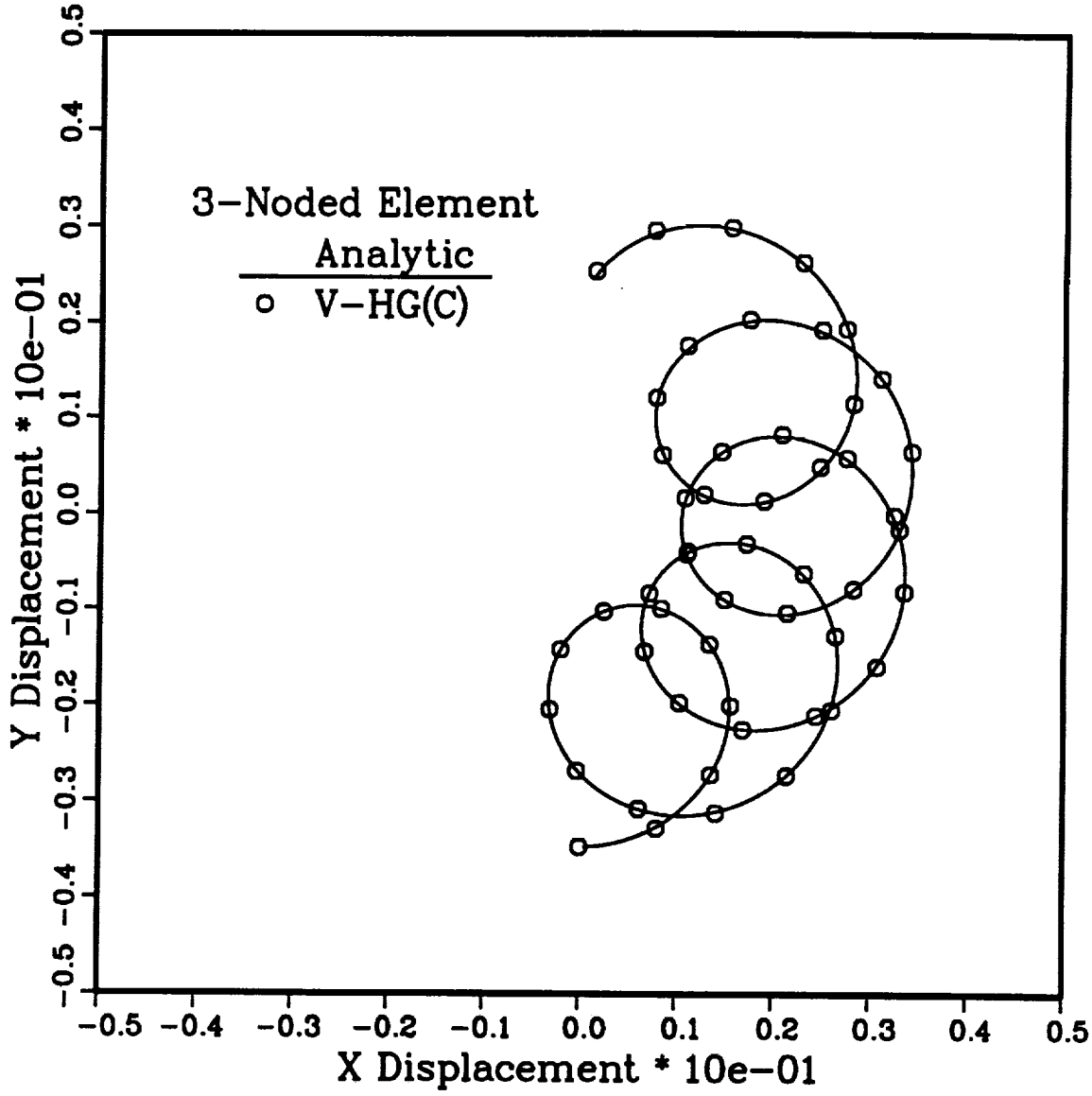

Fig 5.14 Spinning Top Case 2: $\Delta T = .2$ sec

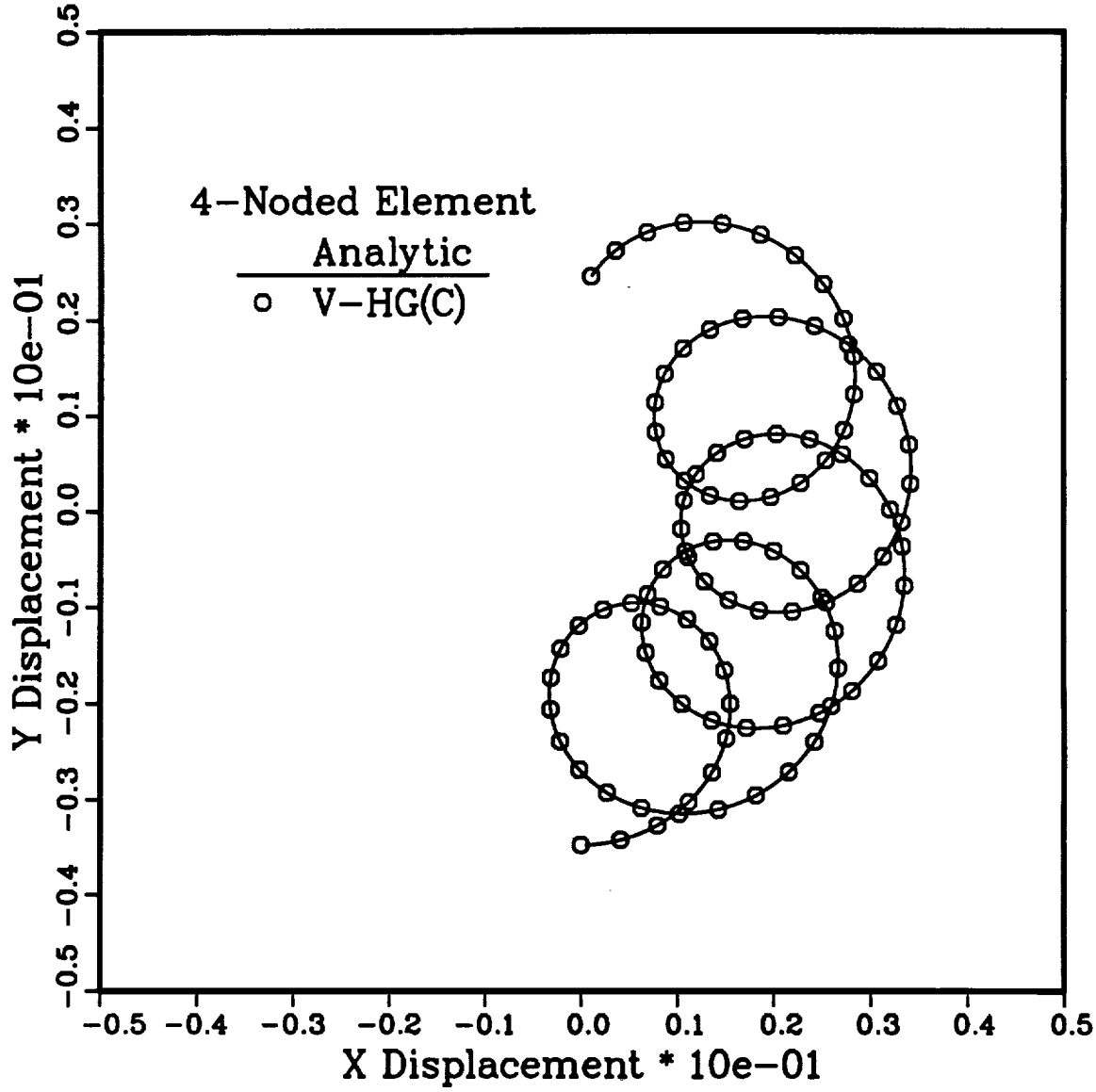

Fig 5.15 Spinning Top Case 2: $\Delta T = .2$ sec

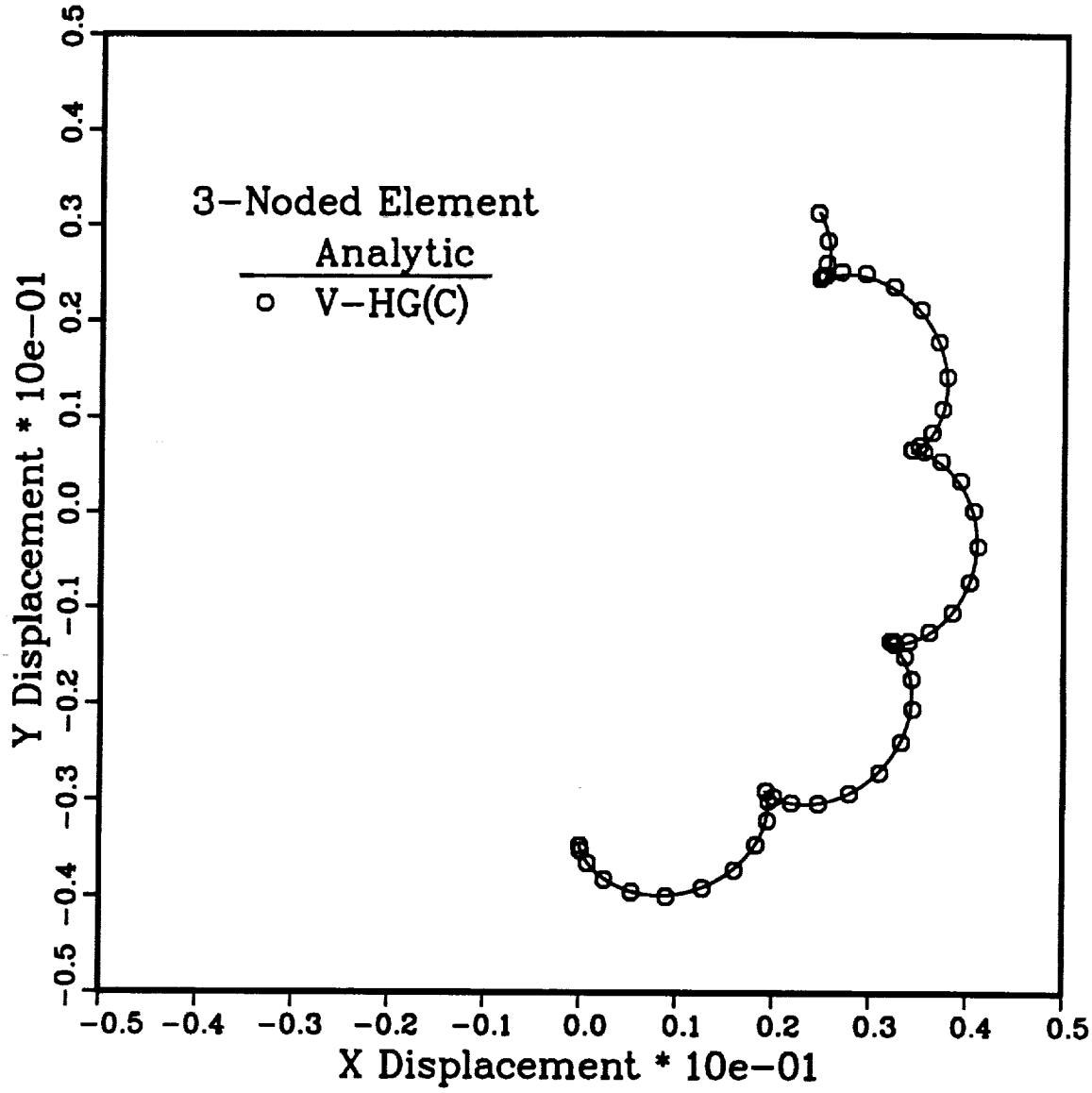

Fig 5.16 Spinning Top Case 3: $\Delta T = .2$ sec

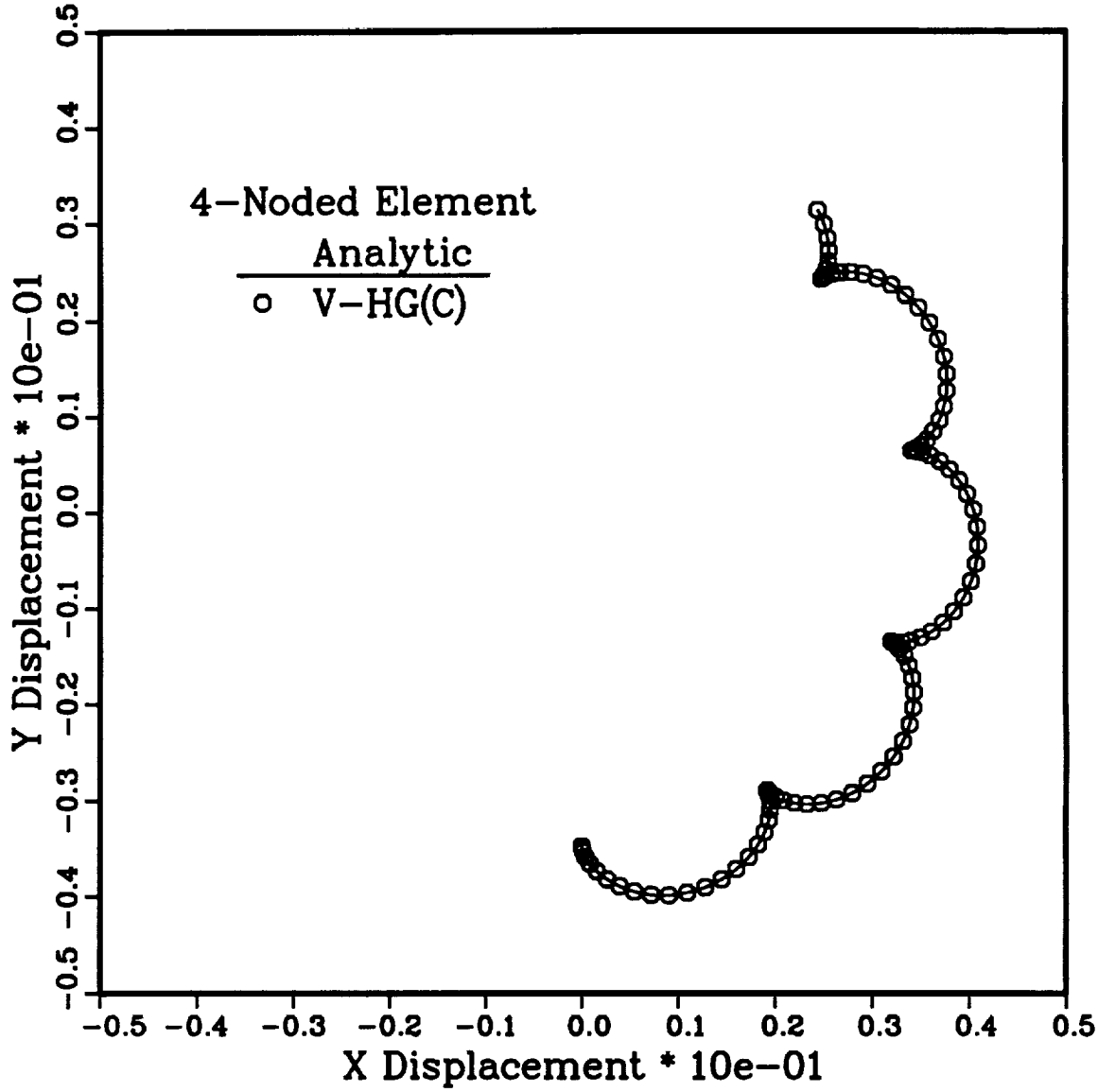

Fig 5.17 Spinning Top Case 3: $\Delta T = .1$ sec

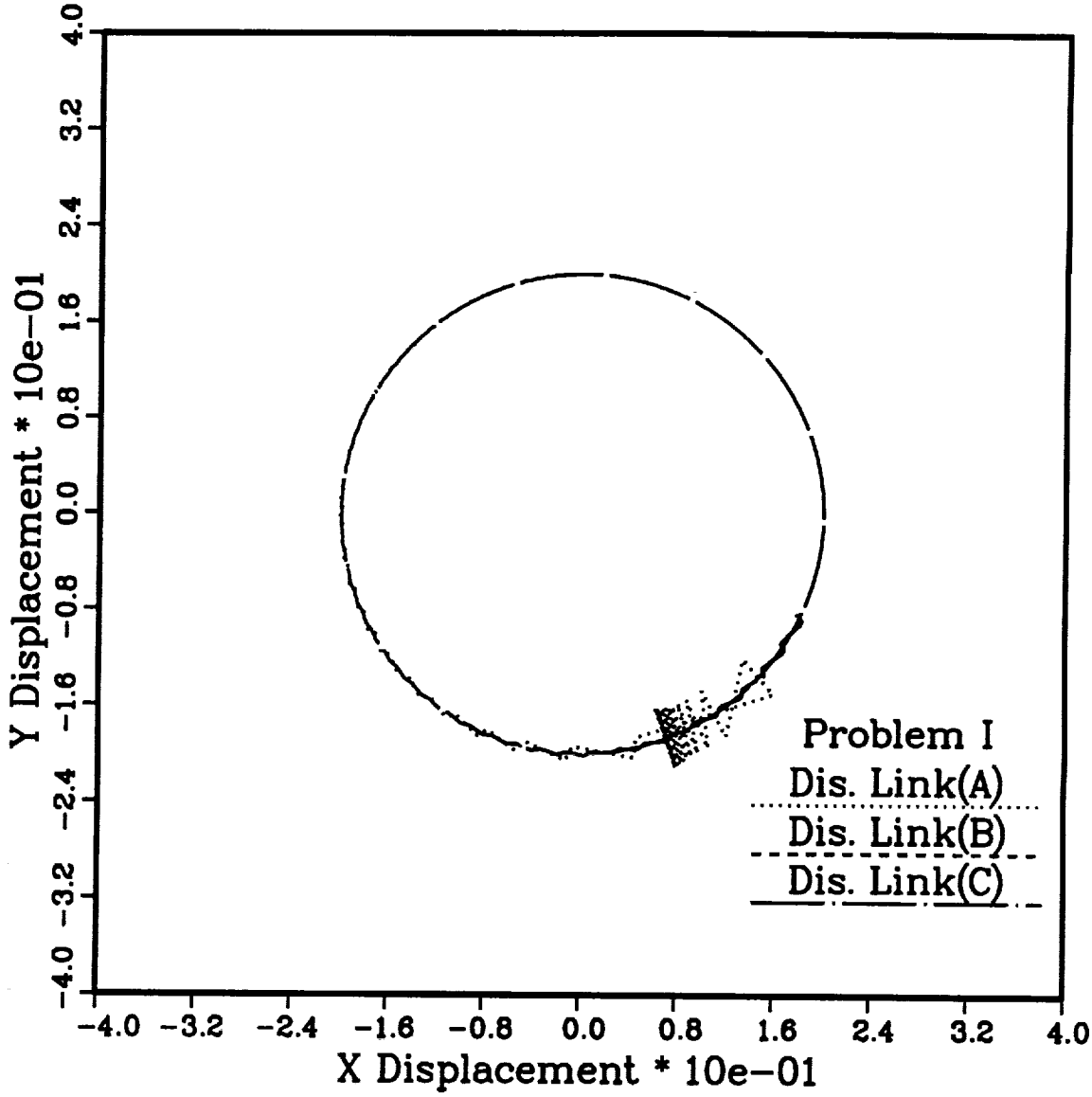

Fig 5.18 Disp. Link : Vi(x) = 1.0 , $\mu g = -1.0$

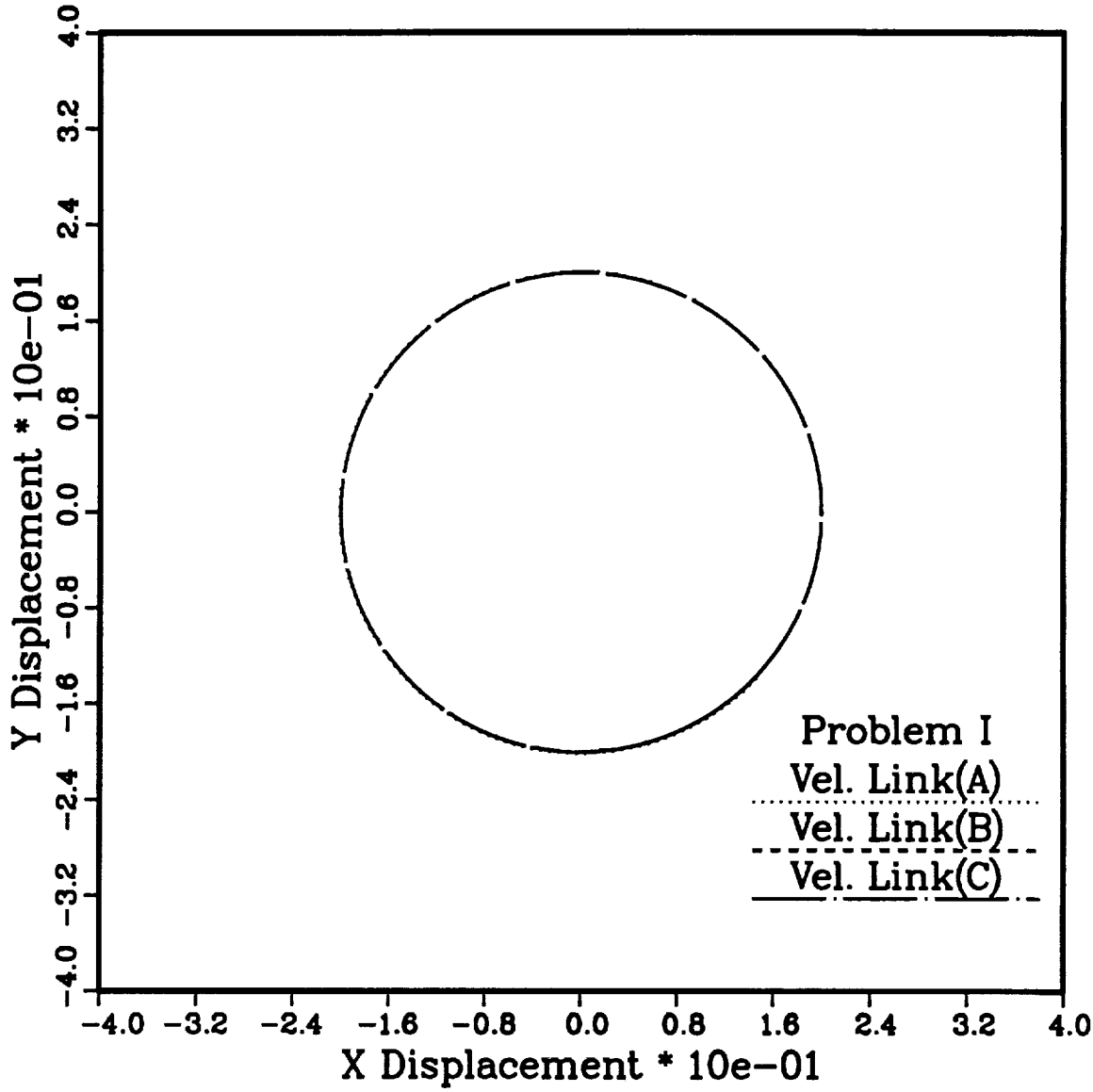

Fig 5.19 Vel. Link : Vi(x) = 1.0 , $\mu g = -1.0$

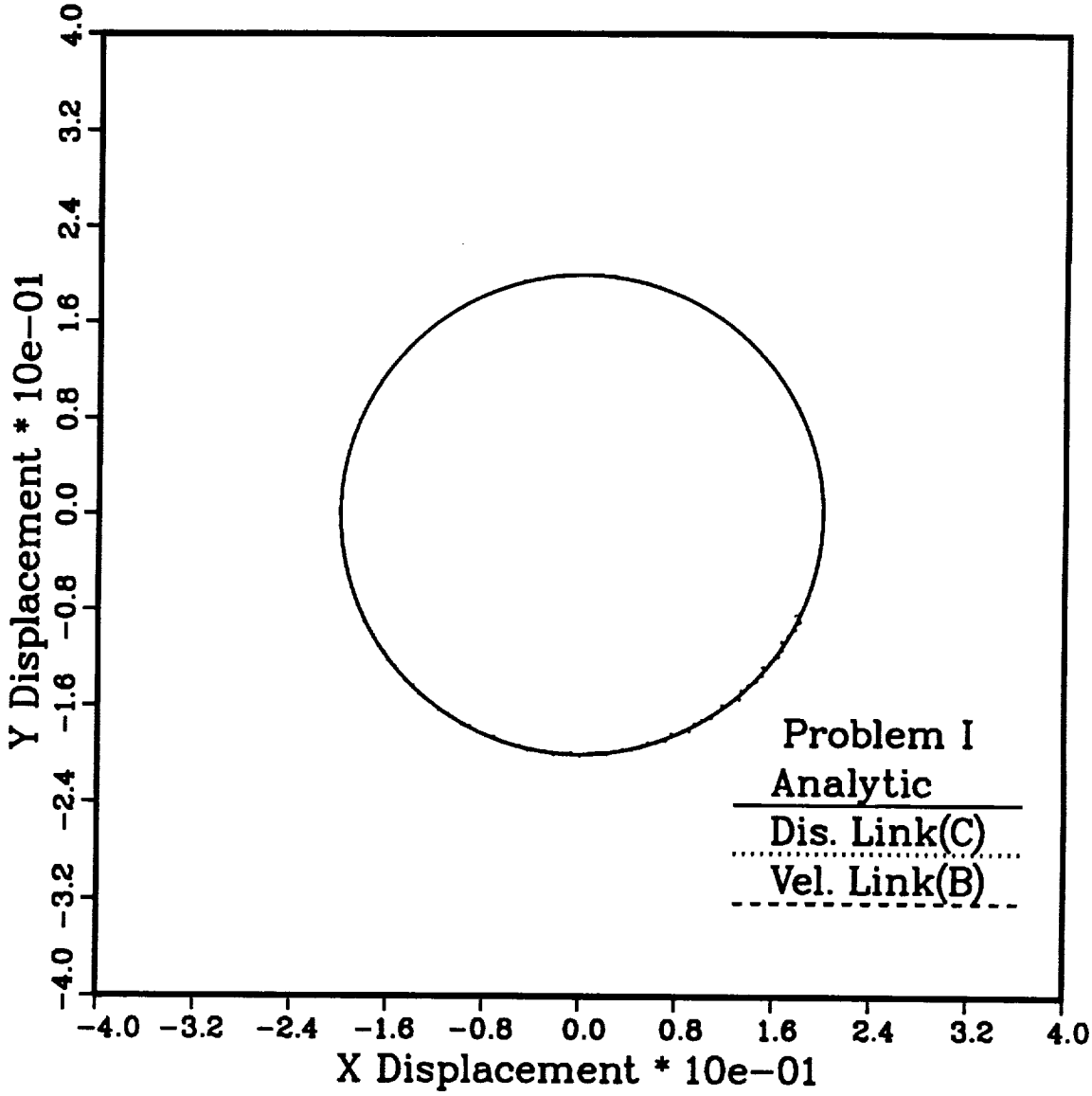

Fig 5.20 Rigid Link : Vi(x) = 1.0 , $\mu g = -1.0$

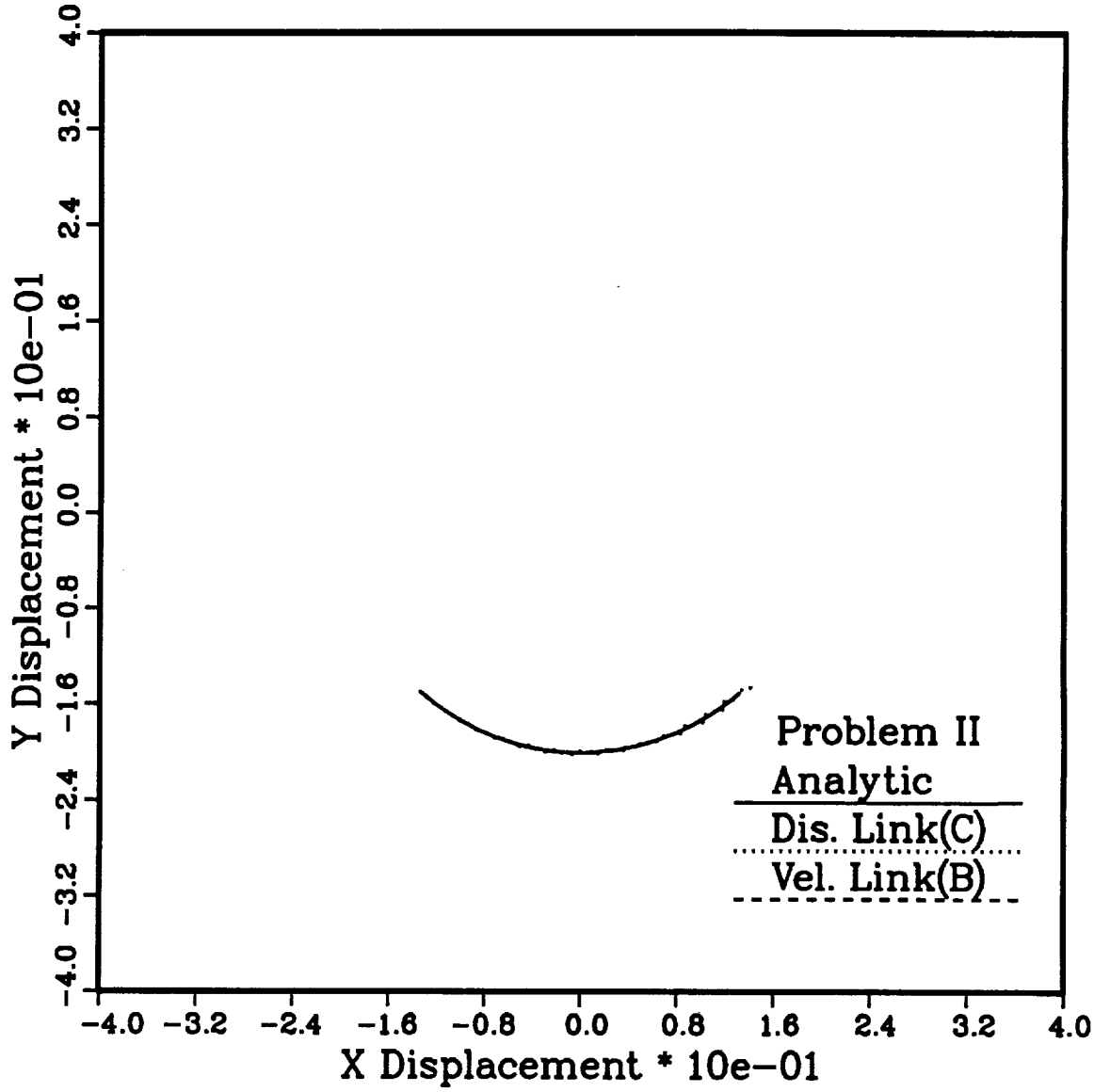

Fig 5.21 Rigid Link : Vi(x) = 1.0 , $\mu g = -10.0$

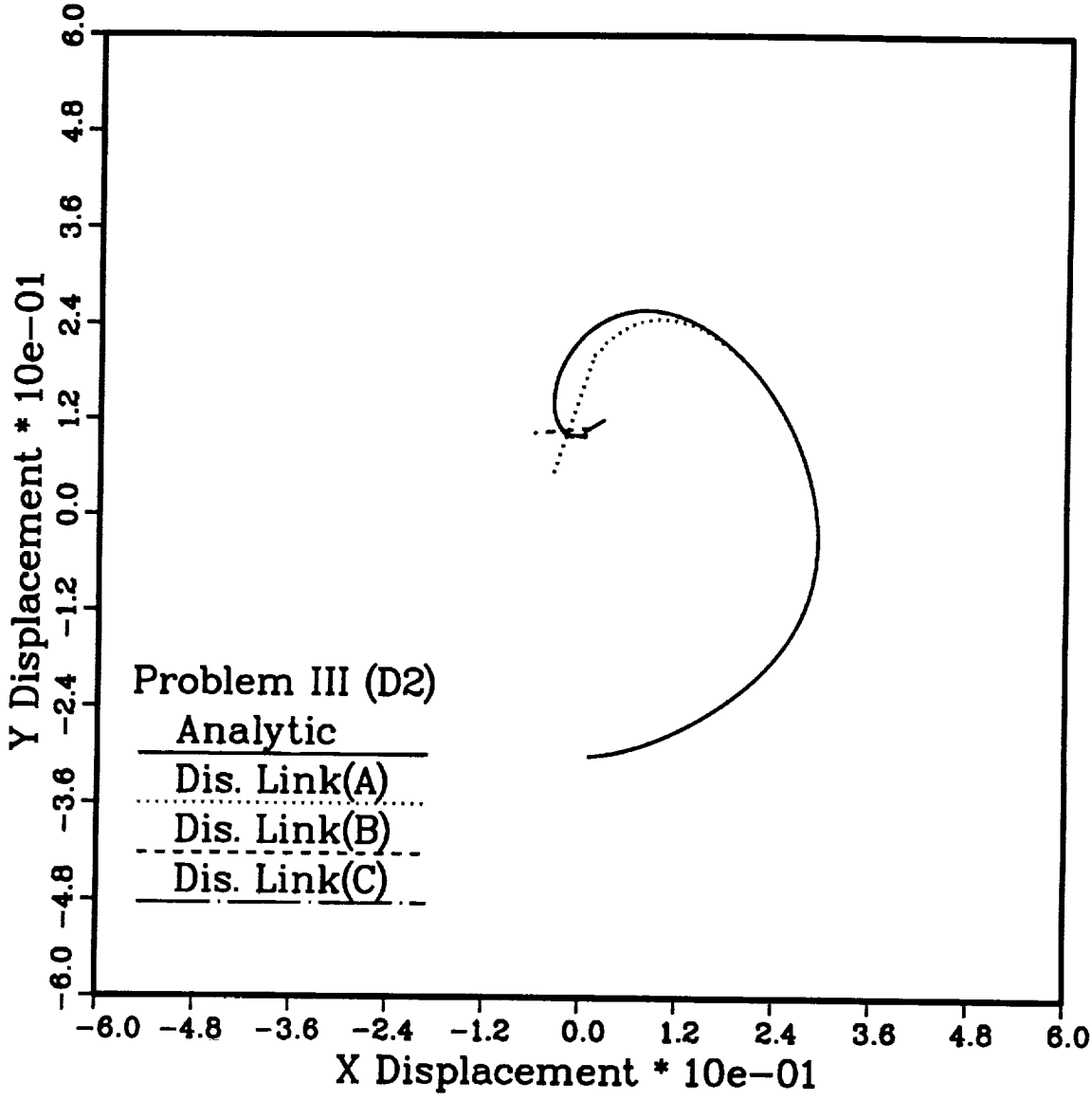

Fig 5.22 Disp. Link : Vi1(x) = 1.0 , $\mu g = -1.0$

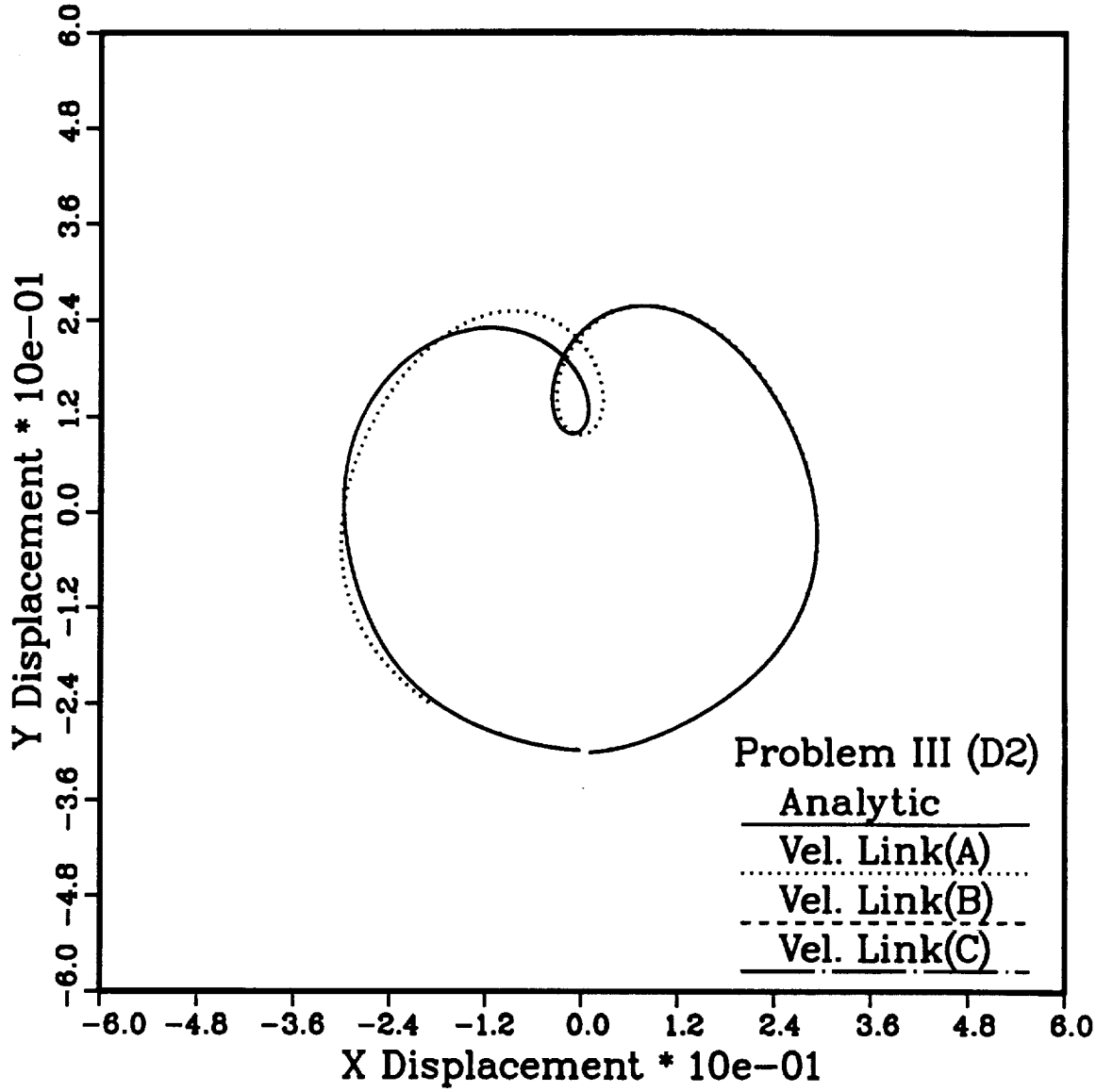

Fig 5.23 Vel. Link : Vi1(x) = 1.0 , $\mu g = -1.0$

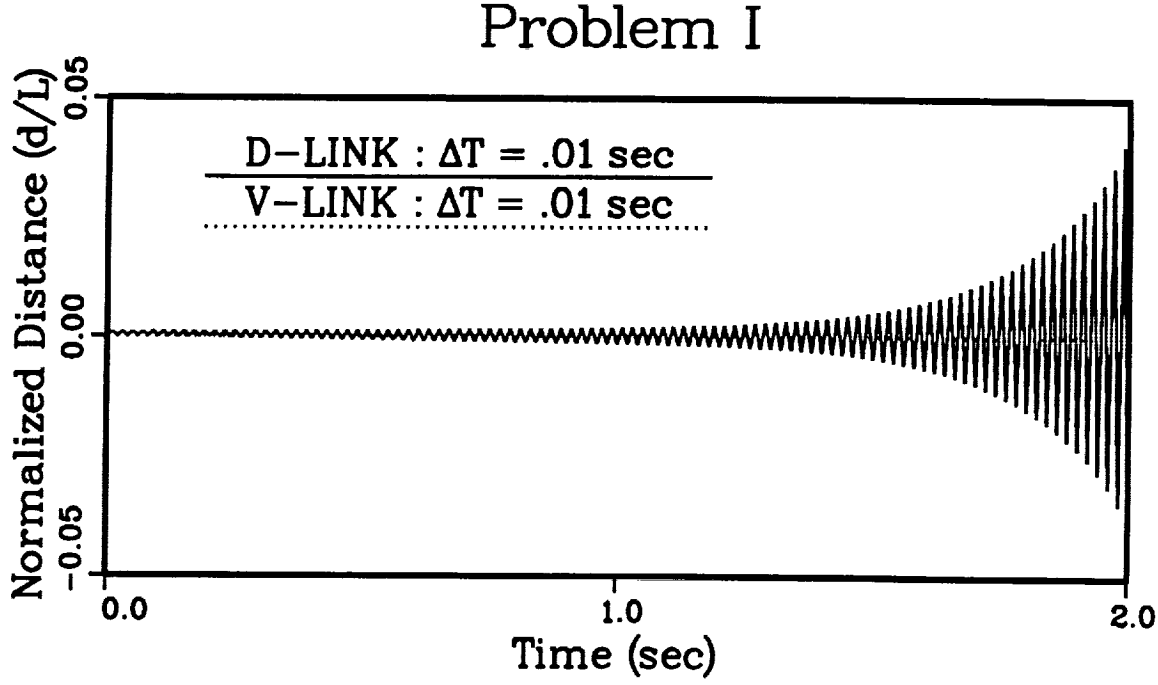

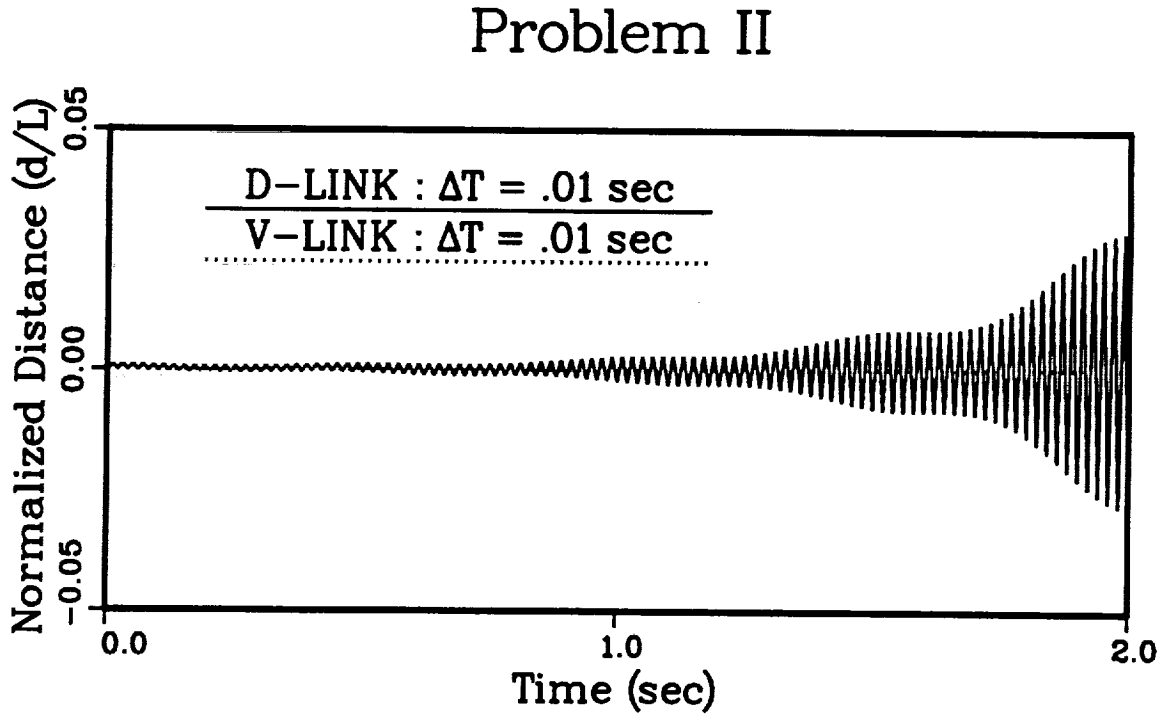

Fig 5.24 Rel. Errors for Length of Link

C-2

Chapter 6

Full Finite Element Modeling

Section 6.1: Introduction

The previous chapters have described the formulation of multibody dynamic problems with a finite element based modal analysis procedure to model each elastic body. This kind of formulation is very cumbersome, as demonstrated by the lengthy derivations and expressions of the last chapters. Furthermore, there is a tremendous overhead associated with modal methods consisting of the management and manipulation of all the coefficients of the modal expansion. This results in an increased computational cost which burdens modal analysis.

An alternate formulation is to deal directly with a full finite element model, such as that used in chapter 4 for determining the reference solution. In this case, there is no need to distinguish between rigid body motion and elastic motion: the actual motion of each node is tracked by the finite procedure. Large rigid body motion results in finite rotations, however, finite rotations were already required to properly model the large elastic rotations. In this effort the Milenkovic parameters were used to model the finite rotations (see appendix A). This representation of the finite rotations is preferable to the Euler parameters as it involves three parameters only as opposed to four. This results in improved computational efficiency.

An additional advantage of the full finite element formulation is that constraint equations ("hinges") between two elastic bodies are much easier to formulate. In deed the constraint only involves the degrees of freedom of two nodes, on of each body. This contrasts with the formulation of constraint equations between elastic bodies modeled with a modal representation which involves all the elastic and rigid degrees of freedom of both bodies. Section 2 describes the formulation of a typical hinge in the full finite element model.

Section 6.2: Hinge Element

Consider a hinge with two components which undergoes a relative rotation. The two components of the hinge are defined by the triads $\vec{e}_n^A$ and $\vec{e}_n^B$, respectively, which are coincident before deformation, i.e. $\vec{e}_n^A \equiv \vec{e}_n^B$. After deformation the triad $\vec{e}_n^A$ has become $\vec{e}_n^{*A}$ (rotation tensor R(a)), and the triad $\vec{e}_n^B$ has become $\vec{e}_n^{*B}$ (rotation tensor R(b)). The relative rotation ϕ, between the two components is shown on Figure 6.1. The finite rotation tensor R(t) defines the initial orientation of the hinge:

$$e_{ni}^A \equiv e_{ni}^B = R_{ij}(t) i_{nj} = e_{nj} \tag{6.2.1}$$

and after deformation, we have:

$$e_{ni}^{*A} = R_{ij}(a) = e_{nj} \; ; \; e_{ni}^{*B} = R_{ij}(b) = e_{nj} \tag{6.2.2}$$

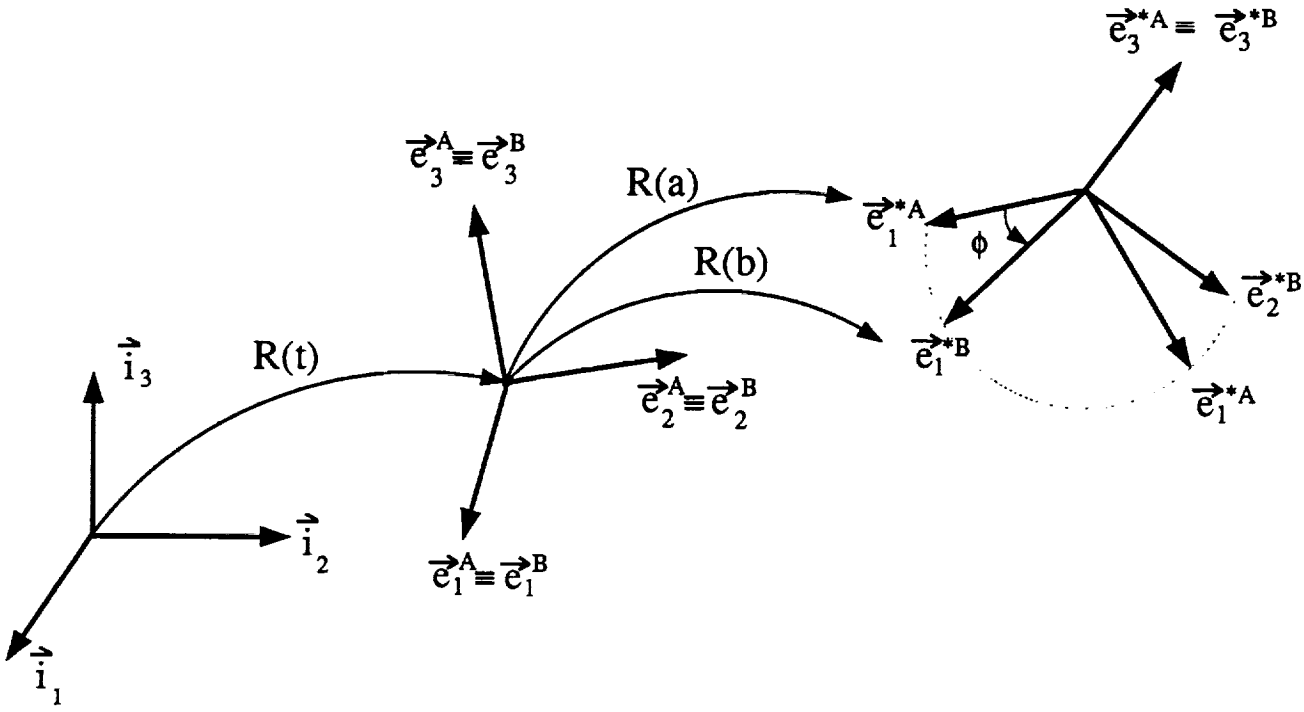

Fig 6.1 Relative Rotation at a Hinge

Since the hinge only allows a relative rotation about $\vec{e}_3^A \equiv \vec{e}_3^B$, the rotation tensor R(a) and R(b) are related by the following constraints:

$$\begin{aligned} C_1 &= \vec{e}_1^{*B} . \vec{e}_3^{*A} = 0 \\ C_2 &= \vec{e}_2^{*B} . \vec{e}_3^{*A} = 0 \end{aligned} \tag{6.2.3}$$

If the value of the relative rotation is desired, it can be obtained from the following constraints:

$$C_3 = 4 \tan^{-1} \frac{1}{4} \left(\vec{r} \cdot \vec{e}^{*A} \right) - \phi = 0 \tag{6.2.4}$$

where $\vec{r}$ is the relative rotation vector, and R(r) the corresponding finite rotation tensor. From (6.2.2), it is clear that

$$e_{ni}^{*B} = R_{ij}(b) R_{kj}(b) e_{nk}^{*A} = R_{ik}(r) e_{nk}^{*A} \tag{6.2.5}$$

or

$$R_{ij}(r) = R_{ik}(b) R_{jk}(a) \tag{6.2.6}$$

This tensor relationship can be expressed in the $\vec{e}_n^{*A}$ triad, as:

$$R\left(r^{[*]}\right) = R\left(b^{[*]}\right) R^T \left(a^{[*]}\right) \tag{6.2.7}$$

The right hand side can be transformed to the $\vec{i}_n$ triad to yield

$$R\left(r^{[*]}\right) = R^T(t)R^T(a)R(b)R(t) \tag{6.2.8}$$

where $\underline{a}$,$\underline{b}$,$\underline{t}$, are the components of the rotation vector in its base triad $\vec{i}_n$. Using the formula for composition of rotation, (Appendix A), the Milenkovic parameter $\underline{r}$ of the relative rotations are found as

$$\underline{r} = \frac{4}{D}R^T(t)\left(a_0\underline{b} - b_0\underline{a} + \tilde{b}\underline{a}\right) \; ; \; D = a_0b_0 + \underline{a}^T\underline{b} + (4-a_0)(4-b_0) \tag{6.2.9}$$

The constraints are now evaluated to yield:

$$\begin{aligned} C_1 &= \underline{e}_1^T R^T(b)R(a)\underline{e}_3 = 0 \\ C_2 &= \underline{e}_2^T R^T(b)R(a)\underline{e}_3 = 0 \\ C_3 &= 4\tan^{-1}\frac{1}{D}\left(a_0\underline{b}^T - b_0\underline{a}^T + \underline{a}^T\tilde{\underline{b}}^T\right)\underline{e}_3 - \phi = 0 \end{aligned} \tag{6.2.10}$$

It is preferable to enforce the two first constraints in a differential form, whereas the last constraint can be enforced as is since it is only used to define ϕ.

$$\begin{aligned} \dot{C}_1 &= \dot{\underline{a}}^T\frac{2G^T}{4-a_0}\tilde{e}_3^*\underline{e}_1 - \dot{\underline{b}}^T\frac{2G^T}{4-b_0}\tilde{e}_3^*\underline{e}_1 = 0 \\ \dot{C}_2 &= \dot{\underline{a}}^T\frac{2G^T}{4-a_0}\tilde{e}_3^*\underline{e}_2 - \dot{\underline{b}}^T\frac{2G^T}{4-b_0}\tilde{e}_3^*\underline{e}_2 = 0 \\ C_3 &= 4\tan^{-1}\frac{1}{D}\left(a_0\underline{b}^T - b_0\underline{a}^T + \underline{a}^T\tilde{\underline{b}}^T\right)\underline{e}_3 - \phi = 0 \end{aligned} \tag{6.2.11}$$

where $\underline{e}_1^* = R(b)\underline{e}_1$, $\underline{e}_2^* = R(b)\underline{e}_2$, $\underline{e}_3^* = R(a)\underline{e}_3$

These constraints could be enforced using a penalty technique:

$$\mathcal{L} = \int_{t_i}^{t_f}\left[\frac{1}{2}\left(\alpha_1\dot{C}_1^2 + \alpha_2\dot{C}_2^2 + \alpha_3\dot{C}_3^2\right) + \frac{1}{2}k\phi^2\right]dt \tag{6.2.12}$$

where α_1, α_2, and α_3 are the penalty coefficients, and k is the stiffness of a torsional spring that can be present in the hinge. It is preferable, however, to use a mixed formulation to enforce the constraint (6.2.12) then transforms to

$$\mathcal{L} = \int_{t_i}^{t_f}\left[F_1\dot{C}_1 + F_2\dot{C}_2 + F_3C_3 + T\phi - \frac{1}{2}\left(\frac{F_1^2}{\alpha_1} + \frac{F_2^2}{\alpha_2} + \frac{F_3^2}{\alpha_3}\right) - \frac{1}{2}\frac{T^2}{k}\right]dt \tag{6.2.13}$$

where F_1, F_2, and F_3 are the Lagrange multipliers associated with the three constraints, and T the torque in the spring.

References

6–1. Geradin M., Cardona, A., "Kinematics and Dynamics of Rigid and Flexible Mechanisms using Finite Elements and Quaternion Algebra," Computational Mechanics, 1987.

Chapter 7

Conclusions and recommendations

Two approaches have been developed to analyze the dynamic behavior of multibody systems. In the first approach, each elastic body is represented in a local, noninertial frame of reference with unknown rigid body motions with respect to an inertial frame, and a finite element based modal analysis methodology is used to model the elastic behavior of the body. Constraint equations are used to model the interaction among the various elastic bodies. In the second approach, all elastic bodies are represented directly in a single inertial frame, and a full finite element methodology (without a modal reduction) is applied. Constraint equations are used again to model the interaction among the elastic bodies.

The following conclusions can be drawn from the study of the finite element based modal analysis methodology:

1. The accuracy of modal methods strongly depends on the choice of the modal basis.
2. Nonlinear kinematic couplings are poorly represented by natural vibration mode shapes. This is easily understood since both phenomena are of a different physical nature: one is a purely nonlinear kinematic phenomenon, the other a purely linear vibratory phenomenon. Even a large number of orthogonal vibration modes do not "synthesize" properly the nonlinear kinematic behavior.
3. Adding perturbation modes to the classical natural mode shapes considerably improves the accuracy of modal methods. Perturbation modes contain information about the nonlinear behavior of structures extracted from higher order derivation of the Lagrangian.
4. The nonlinearities associated with rotational dynamic effects are sometimes poorly respected by both natural vibration mode shapes and perturbation modes, resulting in a poor correlation for the angle of attack.
5. When accurate predictions of rotor behavior is sought, modal analysis should be avoided, and full finite element methods should be preferred.
6. A tremendous amount of overhead is associated with nonlinear modal methods. This involves the storage and manipulation of the many coefficients appearing in the elastic modes. The number of coefficients grows as N^n where N is the number of modes, and n the highest power of the nonlinearities.
7. When rigid body motions are added to the elastic behavior this overhead increases roughly tenfolds. This tremendous overhead is responsible for the very rapid increase in computational effort required to deal with modal methods as the number of modes increases.
8. The computational effort involved in the integration of the full finite element calculations presented in this work does not seem to be prohibitive when compared to that of the modal analysis. This observation should not be generalized. It is clear that as the number of degrees of freedom in the finite element model increases the cost of solution increases as well and will eventually become more expensive than that of the modal

solution. It seems however, that for typical rotorcraft problems the full finite element method is directly competitive with modal solutions.

Two approaches were developed for dealing with the kinematic constraints. In the first approach the kinematic constraints are enforced as is, whereas in the second approach the time derivative of the constraints are enforced. In both cases a Lagrange multiplier technique is used to enforce the constraints within the framework of a mixed formulation.

The following conclusions can be drawn from the study of the constraint equations enforcement:

1. Enforcing the time derivative of the kinematic constraints yields numerical schemes which are far more accurate than those obtained from enforcing the kinematic constraint itself.
2. When kinematic constraints are enforced, the problem becomes very "stiff" due to the presence of the larger fictitious stiffness associated with the constraint. Integration schemes applied to these very stiff problems can easily become unstable, and this behavior was observed in the various examples treated here. When the time derivative of the constraint was enforced, this numerically unstable behavior disappeared.
3. Enforcing the time derivative of the kinematic constraints is only slightly more complex than enforcing the kinematic constraint itself.

The two methods developed in this study for the analysis of multibody dynamic systems differ only by their modeling approach for a single elastic body. The first approach relies on a modal approximation, the other on a full finite element model. The use of a modal approach requires modeling each elastic body in a local coordinate system. A large overhead is associated with nonlinear modal analysis, which puts this approach to a disadvantage when high order nonlinearities are present, and specially in the context of multibody analysis. Furthermore the accuracy of modal methods tend to deteriorate when nonlinearities are prominent. This discussion leads to the following recommendations for future work:

1. For dynamic systems where nonlinear effects are not too pronounced, the finite element based modal analysis option can be pursued, and the following features of the modeling approach could be improved. The order of the nonlinearities could be reduced by ignoring higher order terms in the expression of the Lagrangian expression. For instance, keeping only quadratic terms would result in a linearized modeling of the system, keeping terms up to the third order would correspond to a "moderate rotation" type approximation. Such simplification would considerably decrease the overhead associated with the modal approach and make it much more computationally efficient at the expense of limiting its range of validity.
2. Constraint equations are key to efficient multibody dynamic analysis. Enforcing the time derivative of theses constraints appears to improve numerical stability and accuracy. Further insight could be gained by computing the internal forces associated with the constraints. For instance, in the case of a rigid link, the load in the link is often a quantity of primary interest which can be obtained from the time derivative of the Lagrange multiplier used to enforce the constraint.

3. The full finite element approach should be used in complex multibody dynamic presenting strong nonlinearities. The resulting equations are rather "stiff", even when the kinematic constraints are enforced in a time derivative fashion. To avoid numerical instabilities in the integration process, it is desirable, and probably necessary to use an integration scheme that provides high frequency numerical damping. Finite element in time procedures based on the time discontinuous Galerkin method might be well suited for this type of problems.
4. The determination of the physical stability boundaries of a multibody system is an important problem. With a modal analysis involving a small number of degrees of freedom classical techniques such as the characteristic exponent method or the Floquet theory approach can be readily used. However, with the full finite element approach such method breaks down because of the presence of a large number of degrees of freedom. Innovative methods should be developed to deal with this situation.

Appendix A: Parametrization of Finite Rotations.

Section A.1: The Geometric Representation of Finite Rotation

Consider a finite rotation of magnitude ϕ about an axis $\vec{u}$ (unit vector) and an arbitrary vector $\vec{a}$. Let the rotation $\phi, \vec{u}$ bring this vector to $\vec{b}$. From Figure A.1 it is clear that:

$$\vec{b} = \vec{OC} + \vec{CB} = \| \vec{b} \| \cos\alpha \, \vec{u} + \| \vec{b} \| \sin\alpha \, [\vec{s}\cos\phi + \vec{t}\sin\phi] \tag{A1.1}$$

where the unit vectors $\vec{s}$ and $\vec{t}$ are defined as:

$$\vec{t} = \frac{\vec{u} \times \vec{a}}{\| \vec{u} \times \vec{a} \|}; \qquad \vec{s} = \vec{t} \times \vec{u} = \frac{(\vec{u} \times \vec{a}) \times \vec{u}}{\| \vec{u} \times \vec{a} \|}. \tag{A1.2}$$

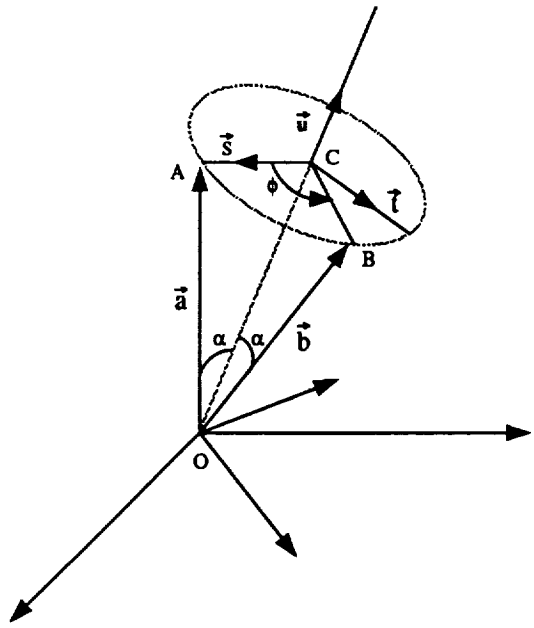

Figure A.1 Change of Basis Viewed as a Single Rotation

The fundamental property of rotation is to preserve length, hence:

$$(\vec{u} \cdot \vec{a}) = \| \vec{a} \| \cos\alpha = \| \vec{b} \| \cos\alpha; \qquad \| \vec{u} \times \vec{a} \| = \| \vec{a} \| \sin\alpha = \| \vec{b} \| \sin\alpha \tag{A1.3}$$

Equation (A1.1) now becomes:

$$\vec{b} = (\vec{u} \cdot \vec{a})\vec{u} + (\vec{u} \times \vec{a}) \times \vec{u}\cos\phi + (\vec{u} \times \vec{a})\sin\phi \tag{A1.4}$$

For a unit vector $\vec{u}$, the following relation can be shown to hold:

$$(\vec{a} \cdot \vec{u})\vec{u} = \vec{a} + \vec{u} \times (\vec{u} \times \vec{a}) \tag{A1.5}$$

so that (A1.4) becomes:

$$\vec{b} = \vec{a} + \sin\phi(\vec{u} \times \vec{a}) + (1 - \cos\phi)\vec{u} \times (\vec{u} \times \vec{a}). \tag{A1.6}$$

Section A.2: The Rotation Tensor

We wish to transform the above geometric notation into a tensor, index notation. For practical implementations it is necessary to work with tensor components in a particular system. The following notations will be used:

Geometric notation	Tensor notation	Tensor component notation
$\vec{u}$	u_i	$\underline{u}$
$\vec{u} \cdot \vec{v}$	$u_i v_i$	$\underline{u}^T \underline{v}$
$\vec{u} \times \vec{v} = -\vec{v} \times \vec{u}$	$S_{ij}(u)v_j = -S_{ij}(v)u_j$	$\tilde{u}\underline{v} = -\tilde{v}\underline{u}$

S_{ij} is a skew symmetric tensor which components are:

$$S_{ij}(u) = \begin{bmatrix} 0 & -u_3 & u_2 \\ u_3 & 0 & -u_1 \\ -u_2 & u_1 & 0 \end{bmatrix} \tag{A2.1}$$

This tensor has the following properties that are readily verified:

$$S_{ij}(u) = -S_{ji}(u), \tag{A2.2}$$

and $S_{ik}(u)S_{kj}(u)$ is a symmetric tensor. When u_i is a unit vector, then

$$S_{ik}(u)S_{kl}(u)S_{lj}(u) = -S_{ij}(u) \tag{A2.3}$$

In tensor notation (A1.6) becomes:

$$b_i = R_{ij}a_j \tag{A2.4}$$

where the rotation tensor R_{ij} is given as:

$$R_{ij}(u) = \delta_{ij} + \sin\phi S_{ij}(u) + (1 - \cos\phi)S_{ik}(u)S_{kj}(u) \tag{A2.5}$$

and

$$R_{ij}(u) = R_{ji}(-u) \tag{A2.5a}$$

An interesting expression can be found by expanding the trigonometric function in series and using (A2.3):

$$R_{ij}(r) = \delta_{ij} + S_{ij}(r) + \frac{1}{2!}S_{ik}(r)S_{kj}(r) + \frac{1}{3!}S_{ik}(r)S_{kl}(r)S_{lj}(r) + \cdots hot \tag{A2.6a}$$

or

$$R_{ij}(r) = exp[S_{ij}(r)] \tag{A2.6b}$$

where the rotation vector r_i is defined as $r_i = \phi u_i$.

The following fundamental property of the rotation tensor can be readily verified:

$$R_{ik}R_{jk} = R_{ki}R_{kj} = \delta_{ij} \tag{A2.7}$$

which implies:

$$det(R_{ij}) = 1 \tag{A2.8}$$

The eigenvalues λ and corresponding eigenvector e_i of the rotation tensor are:

$$\begin{aligned} &\lambda = 1; && e_i = u_i \\ &\lambda = \cos\phi \pm \sqrt{-1}\sin\phi; && e_i = a_i \pm \sqrt{-1}b_i \end{aligned} \tag{A2.9}$$

where a_i is an arbitrary vector normal to u_i, i.e.

$$a_i u_i = 0 \qquad and \qquad b_i = S_{ij}(a)u_j \tag{A2.9a}$$

Section A.3: The Angular Velocity Vector

A time derivative of (A2.7) yields:

$$\dot{R}_{ik}R_{jk} = -\left(\dot{R}_{ik}R_{jk}\right)^T, \tag{A3.1}$$

which implies that this tensor is skew symmetric, hence we can write:

$$S_{ij}(\omega) = \dot{R}_{ik}R_{jk}, \tag{A3.2}$$

where ω_i is the angular velocity vector. With the helps of (A2.5) we find:

$$S_{ij}(\omega) = \dot{\phi}S_{ij}(u) + \sin\phi S_{ij}(\dot{u}) + (1-\cos\phi)\left[S_{ik}(\dot{u})S_{jk}(u) - S_{jk}(\dot{u})S_{ik}(u)\right], \tag{A3.3}$$

where the following identity was used:

$$S_{ik}(u)S_{kl}(\dot{u})S_{lj}(u) = 0. \tag{A3.4}$$

An alternate writing is:

$$\omega_i = \dot{\phi}u_i + \sin\phi\dot{u}_i + (1-\cos\phi)S_{ij}(u)\dot{u}_j. \tag{A3.5}$$

Section A.4: The Virtual Rotation Vector.

The virtual rotation vector can be defined by analogy to the angular velocity vector as:

$$S_{ij}(\delta\psi) = \delta R_{ik} R_{jk}, \tag{A4.1}$$

where $\delta\psi_i$ are the components of the virtual rotation vector. Note that there is no vector ψ_i such that $\delta(\psi_i)$ is the virtual rotation. Taking a variation of A3.2 and a time derivative of A4.1 yields:

$$\begin{aligned} S_{ij}(\delta\omega) &= \delta\dot{R}_{ik} R_{jk} + \dot{R}_{ik}\delta R_{jk} \\ S_{ij}\left(\delta\dot{\psi}\right) &= \delta\dot{R}_{ik} R_{jk} + \delta R_{ik}\dot{R}_{jk}, \end{aligned} \tag{A4.2}$$

which, after subtraction becomes:

$$S_{ij}(\delta\omega) = S_{ij}\left(\delta\dot{\psi}\right) + \dot{R}_{ik}\delta R_{jk} - \delta R_{ik}\dot{R}_{jk}. \tag{A4.3}$$

In view of the orthogonality of the rotation tensor A2.7, this becomes:

$$S_{ij}(\delta\omega) = S_{ij}\left(\delta\dot{\psi}\right) + S_{il}(\delta\psi)S_{lj}(\omega) - S_{il}(\omega)S_{lj}(\delta\psi). \tag{A4.4}$$

The following identity:

$$S_{il}(a)S_{lj}(b) - S_{il}(b)S_{lj}(a) = S_{ij}(S_{kl}(a)b_l) \tag{A4.5}$$

then yields:

$$S_{ij}(\delta\omega) = S_{ij}\left(\delta\dot{\psi}\right) + S_{ij}(S_{kl}(\delta\psi)\omega_l) \tag{A4.6}$$

and finally:

$$\delta\omega_i = \delta\dot{\psi}_i - S_{ik}(\omega)\delta\psi_k. \tag{A4.7}$$

This important relationship relates the variation of the angular velocity vector to the virtual rotation vector and its derivatives.

Section A.5: Change of Basis

Consider a basis b^1 defined by the unit vectors $\vec{b}_1^1, \vec{b}_2^1$ and $\vec{b}_3^1$ and an arbitrary vector $\vec{a}$. Let $R(u^1)$ be a rotation vector applies to each one of these vector to yield basis b^2 defined by $\vec{b}_1^{(2)}, \vec{b}_2^{(2)}, \vec{b}_3^{(2)}$ and the vector $\vec{a}^2$, (A2.4) yields:

$$a_i^2 = R_{ij}(u^1)a_j^1 \tag{A5.1}$$

This tensor relationship can be expressed in component form as:

$$\underline{a}^{2[1]} = R\left(u^{1[1]}\right)\underline{a}^{1[1]} \tag{A5.2}$$

where the notation $()^{[1]}$ is used to express the components of a tensor in the basis b^1.

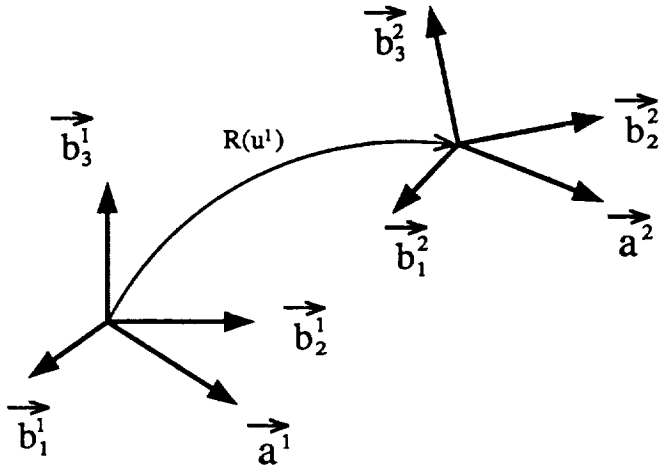

Figure A.2 Change of Basis

It is clear that the components of $\vec{a}^1$ in basis b^1 are identical to the components of $\vec{a}^2$ in the base b^2, i.e.:

$$\underline{a}^{1[1]} = \underline{a}^{2[2]} \tag{A5.3}$$

hence (A4.2) becomes:

$$\underline{a}^{2[1]} = R\left(u^{1[1]}\right)\underline{a}^{2[2]} \tag{A5.4}$$

Since the starting vector $\vec{a}^1$ is arbitrary this relationship holds for any vector, and more generally we can write the transformation law of the components of a vector $\vec{v}$ as:

$$\underline{v}^{[1]} = R\left(u^{1[1]}\right)\underline{v}^{[2]} \quad or \quad \underline{v}^{[2]} = R^T\left(u^{1[1]}\right)\underline{v}^{[1]} \tag{A5.5}$$

It is also clear that the rotation vector has the same components in the two basis, hence:

$$R\left(u^{1[1]}\right) = R\left(u^{1[2]}\right) \tag{A5.6}$$

Consider now a second order tensor such as $T_{ij} = a_i b_j$, where a_i and b_j are two arbitrary vectors. In component form we have:

$$T^{[1]} = \underline{a}^{[1]}\underline{b}^{[1]T}; \qquad T^{[2]} = \underline{a}^{[2]}\underline{b}^{[2]T} \tag{A5.7}$$

With the helps of (A4.5) the transformation law for second order tensor component is found as:

$$T^{[2]} = R^T\left(u^{1[1]}\right)T^{[1]}R\left(u^{1[1]}\right) \tag{A5.8}$$

Finally, consider a set of basis $b^1, b^2 \cdots, b^n$ obtained by successive rotation $R(u^1), R(u^2) \cdots, R(u^n)$ and let $R(r)$ be the rotation from base b^1 to base b^n. Repetitive application of (A4.1) yields:

$$R_{ij}(r) = R_{ik}(u^{n-1})R_{kl}(u^{n-2}) \cdots R_{lm}(u^2)R_{mj}(u^1) \tag{A5.9}$$

In component form, the following expressions hold:

$$R\left(r^{[1]}\right) = R\left(r^{[n]}\right) = R\left(u^{n-1[n]}\right)R\left(u^{n-2[n]}\right) \cdots R\left(u^{2[n]}\right)R\left(u^{1[n]}\right), \tag{A5.10}$$

$$R\left(r^{[1]}\right) = R\left(r^{[n]}\right) = R\left(u^{n-1[1]}\right)R\left(u^{n-2[1]}\right) \cdots R\left(u^{2[1]}\right)R\left(u^{1[1]}\right), \tag{A5.11}$$

$$R\left(r^{[1]}\right) = R\left(r^{[n]}\right) = R\left(u^{1[1]}\right)R\left(u^{2[2]}\right) \cdots R\left(u^{n-2[n-2]}\right)R\left(u^{n-1[n-1]}\right), \tag{A5.12}$$

where the last expression can be obtained from the first or second through repetitive use of the second order tensor component transformation law (A4.8). These various relationships can also be viewed as composition of rotations: the rotations u^1, u^2, ..., u^{n-2}, u^{n-1} are applied successively to yield a single composed rotation r.

Section A.6: Euler Parameters

The rotation tensor (A2.5) is expressed in terms of the rotation vector $\vec{u}$ and the magnitude of the rotation ϕ. An alternate representation is in terms of the Euler Parameters defined as follows:

$$q_0 = \cos\frac{\phi}{2}; \qquad q_i = u_i \sin\frac{\phi}{2}; \qquad i = 1,2,3 \tag{A6.1}$$

to yield the rotation tensor (A2.5) as:

$$R_{ij}(q) = \delta_{ij} + 2q_0S_{ij}(q) + 2S_{ik}(q)S_{kj}(q) \tag{A6.2}$$

or

$$R(q) = \begin{bmatrix} q_0^2 + q_1^2 - q_2^2 - q_3^2 & 2(q_1q_2 - q_0q_3) & 2(q_1q_3 + q_0q_2) \\ 2(q_1q_2 + q_0q_3) & q_0^2 - q_1^2 + q_2^2 - q_3^2 & 2(q_2q_3 - q_0q_1) \\ 2(q_1q_3 - q_0q_2) & 2(q_2q_3 + q_0q_1) & q_0^2 - q_1^2 - q_2^2 + q_3^2 \end{bmatrix} \tag{A6.3}$$

All trigonometric functions have now disappeared from the rotation tensor. It is important to note the redundancy in the representation since four parameters are used when in fact only three parameters are required. This redundancy is clear when considering the definition A6.1 which yields the normality condition:

$$q_0^2 + q_1^2 + q_2^2 + q_3^2 = 1. \tag{A6.4}$$

The angular velocity tensor (A3.3) becomes:

$$S_{ij}(\omega) = 2q_0 S_{ij}(\dot{q}) - 2\dot{q}_o S_{ij}(q) + 2\left[S_{ik}(\dot{q})S_{jk}(q) - S_{jk}(\dot{q})S_{ik}(u)\right] \tag{A6.5}$$

and the corresponding angular velocity vector is:

$$\omega_i = 2q_0\dot{q}_i - 2\dot{q}_0 q_i + 2S_{ij}(q)\dot{q}_j \tag{A6.6}$$

or

$$\underline{w}(q) = 2\begin{bmatrix} -q_1\dot{q}_0 + q_0\dot{q}_1 - q_3\dot{q}_2 + q_2\dot{q}_3 \\ -q_2\dot{q}_0 + q_3\dot{q}_1 + q_0\dot{q}_2 - q_1\dot{q}_3 \\ -q_3\dot{q}_0 - q_2\dot{q}_1 + q_1\dot{q}_2 + q_0\dot{q}_3 \end{bmatrix} = 2H(q)\dot{q} \tag{A6.7}$$

where

$$H(q) = \begin{bmatrix} -q_1 & q_0 & -q_3 & q_2 \\ -q_2 & q_3 & q_0 & -q_1 \\ -q_3 & -q_2 & q_1 & q_0 \end{bmatrix}. \tag{A6.8}$$

The components of the angular velocity vector in the rotating system are found by using (A5.5):

$$\underline{\omega}^*(q) = R^T(q)\underline{\omega}(q) = 2G(q)\dot{\underline{q}} \tag{A6.9}$$

where

$$G(q) = \begin{bmatrix} -q_1 & q_0 & q_3 & -q_2 \\ -q_2 & -q_3 & q_0 & q_1 \\ -q_3 & q_2 & -q_1 & q_0 \end{bmatrix}. \tag{A6.10}$$

These matrices present the following remarkable properties:

$$H(q)H^T(q) = G(q)G^T(q) = I, \tag{A6.11}$$

$$R(q) = H(q)G^T(q); \quad G(q) = R^T(q)H(q); \quad H(q) = R(q)G(q); \tag{A6.12}$$

$$H^T(q)H(q) = G^T(q)G(q) = I_4 - \underline{q}\underline{q}^T; \quad H(q)\underline{q} = G(q)\underline{q} = 0 \tag{A6.13}$$

$$R(\dot{q}) = 2H(q)G^T(\dot{q}) = 2H(\dot{q})G^T(q) \tag{A6.14}$$

$$\tilde{\omega} = R(\dot{q})R^T(q) = 2H(\dot{q})H^T(q); \quad \tilde{\omega}^* = R^T(q)R(\dot{q}) = 2G(q)G^T(\dot{q}); \tag{A6.15}$$

Section A.7: Composition of Rotations with the Euler Parameters

Since all trigonometric functions have been eliminated from the rotation tensor and angular velocity vector when expressed in terms of Euler Parameters, all finite rotation operations can be expressed in

component form using a purely algebraic formalism. This task is eased when the following matrices are defined:

$$A(q) = \begin{bmatrix} q_0 & -q_1 & -q_2 & -q_3 \\ q_1 & q_0 & -q_3 & q_2 \\ q_2 & q_3 & q_0 & -q_1 \\ q_3 & -q_2 & q_1 & q_0 \end{bmatrix} \tag{A7.1}$$

$$B(q) = \begin{bmatrix} q_0 & -q_1 & -q_2 & -q_3 \\ q_1 & q_0 & q_3 & -q_2 \\ q_2 & -q_3 & q_0 & q_1 \\ q_3 & q_2 & -q_1 & q_0 \end{bmatrix} \tag{A7.2}$$

$$C(q) = \begin{bmatrix} q_0 & q_1 & q_2 & q_3 \\ q_1 & -q_0 & q_3 & -q_2 \\ q_2 & -q_3 & -q_0 & q_1 \\ q_3 & q_2 & -q_1 & -q_0 \end{bmatrix} \tag{A7.3}$$

$$D(q) = \begin{bmatrix} 1 & 0 \\ 0 & R(q) \end{bmatrix} \tag{A7.4}$$

Let $\underline{q}^T = (q_0, q_1, q_2, q_3)$ and $\underline{r}^T = (r_0, r_1, r_2, r_3)$ be the Euler Parameters of two rotations in specific axes. The following formulae are readily verified:

$$\begin{gathered} G(q)\underline{r} = -G(r)\underline{q}; \quad H(q)\underline{r} = -H(r)\underline{q}; \\ A(q)B^T(r) = B^T(r)A(q) \end{gathered} \tag{A7.5}$$

$$A(q)\underline{r} = B(r)\underline{q}; \quad A^T(q)\underline{r} = C^T(r)\underline{q}; \quad B^T(q)\underline{r} = C(r)\underline{q}; \tag{A7.6}$$

$$D(q) = A(q)B^T(q) = B^T(q)A(q) = C(q)C(q). \tag{A7.7}$$

Furthermore, the normality condition results in the orthogonality of these matrices

$$\begin{aligned} A^T(q)A(q) = A(q)A^T(q) = I_4; \quad B^T(q)B(q) = B(q)B^T(q) = I_4; \\ C^T(q)C(q) = C(q)C^T(q) = I_4; \quad D^T(q)D(q) = D(q)D^T(q) = I_4. \end{aligned} \tag{A7.8}$$

From the definition of the angular velocity vector we find:

$$\begin{aligned} \underline{\omega} = 2B^T(q)\dot{\underline{q}}; \quad A(\omega) = 2A(\dot{q})A^T(q); \quad B(\omega) = 2B^T(q)B(\dot{q}) \\ \underline{\omega}^* = 2A^T(q)\dot{\underline{q}}; \quad A(\omega^*) = 2A^T(q)A(\dot{q}); \quad B(\omega^*) = 2B(\dot{q})B^T(q) \end{aligned} \tag{A7.9}$$

With the help of the above relationships, the composition of rotation formula A5.12 can be shown to imply:

$$\begin{aligned} A\left(r^{[1]}\right) &= A\left(q^{1[1]}\right)A\left(q^{2[2]}\right)\cdots A\left(q^{n-1[n-1]}\right) \\ B\left(r^{[1]}\right) &= B\left(q^{n-1[n-1]}\right)\cdots B\left(q^{2[2]}\right)B\left(q^{1[1]}\right) \end{aligned} \tag{A7.10}$$

or

$$\begin{aligned}\underline{r}^{[1]} &= A\left(q^{1[1]}\right)A\left(q^{2[2]}\right)\cdots A\left(q^{n-2[n-2]}\right)\underline{q}^{n-1[n-1]}\\ \underline{r}^{[1]} &= B\left(q^{n-1[n-1]}\right)B\left(q^{n-2[n-2]}\right)\cdots B\left(q^{2[2]}\right)\underline{q}^{1[1]}\end{aligned} \tag{A7.11}$$

An alternative representation of composition of rotation such as A5.11 implies:

$$\begin{aligned}A\left(r^{[1]}\right) &= A\left(q^{n-1[1]}\right)A\left(q^{n-2[1]}\right)\cdots A\left(q^{2[1]}\right)A\left(q^{1[1]}\right)\\ B\left(r^{[1]}\right) &= B\left(q^{1[1]}\right)B\left(q^{2[1]}\right)\cdots B\left(q^{n-2[1]}\right)B\left(q^{n-1[1]}\right)\end{aligned} \tag{A7.12}$$

or

$$\begin{aligned}\underline{r}^{[1]} &= A\left(q^{n-1[1]}\right)A\left(q^{n-2[1]}\right)\cdots A\left(q^{2[1]}\right)\underline{q}^{1[1]}\\ \underline{r}^{[1]} &= B\left(q^{1[1]}\right)B\left(q^{2[1]}\right)\cdots B\left(q^{n-2[1]}\right)\underline{q}^{n-1[1]}\end{aligned} \tag{A7.13}$$

Section A.8: Rodrigues' Parameters

Rodrigues' Parameters can be defined in relation to the Euler Parameters as:

$$r_i = 2\frac{q_i}{q_0}, \tag{A8.1}$$

so that their geometric interpretation is:

$$r_i = 2u_i\, tg\frac{\phi}{2}. \tag{A8.2}$$

It is clear that this representation presents an obvious singularity $r_i \to \infty$ when $\phi \to \pm\pi$. Relationship A8.1 can be inverted to yield:

$$q_0 = \frac{1}{(1+r^2/4)^{1/2}}; \quad q_i = \frac{r_i}{2(1+r^2/4)^{1/2}} \tag{A8.3}$$

where:

$$r^2 = r_1^2 + r_2^2 + r_3^2 \tag{A8.4}$$

The rotation tensor follows from A6.3and A8.3:

$$R(r) = \frac{1}{1+r^2/4}\begin{bmatrix} 1+\frac{r_1^2}{4}-\frac{r_2^2}{4}-\frac{r_3^2}{4} & \frac{r_1r_2}{2}-r_3 & \frac{r_1r_3}{2}+r_2 \\ \frac{r_1r_2}{2}+r_3 & 1-\frac{r_1^2}{4}+\frac{r_2^2}{4}-\frac{r_3^2}{4} & \frac{r_2r_3}{2}-r_1 \\ \frac{r_1r_3}{2}-r_2 & \frac{r_2r_3}{2}+r_1 & 1-\frac{r_1^2}{4}-\frac{r_2^2}{4}+\frac{r_3^2}{4} \end{bmatrix} \tag{A8.5}$$

The components of the angular velocity vector are obtained from A6.7 and A8.3:

$$\underline{\omega} = G\dot{\underline{r}} \tag{A8.6}$$

where

$$G = \frac{1}{1+r^2/4}\begin{bmatrix} 1 & -\frac{r_3}{2} & \frac{r_2}{2} \\ \frac{r_3}{2} & 1 & -\frac{r_1}{2} \\ -\frac{r_2}{2} & \frac{r_1}{2} & 1 \end{bmatrix} \tag{A8.7}$$

Section A.9: Milenkovic Parameters

The Milenkovic Parameters can be defined in relation to the Euler Parameters as:

$$a_i = \frac{4q_i}{1+q_0} \qquad i = 0,1,2,3, \tag{A9.1}$$

so that their geometric interpretation is:

$$a_i = 4u_i \tan\frac{\phi}{4}. \tag{A9.2}$$

Note that these parameters present no singularity within the range $-\pi \leq \phi \leq \pi$. Relationship A9.1 can be inverted to yield:

$$q_i = \frac{a_i}{4-a_0} \qquad i = 0,1,2,3. \tag{A9.3}$$

The parameter a_0 can expressed in terms of the other three as:

$$a_0 = (16 - a^2)/8 \tag{A9.4}$$

where

$$a^2 = a_1^2 + a_2^2 + a_3^2 \tag{A9.5}$$

This representation involves 3 parameters only a_1, a_2, *and* a_3, however a_0 is used in the various formulae to simplify the notation.

The rotation tensor follows from A6.3:

$$R(a) = \frac{1}{(4-a_0)^2}\begin{bmatrix} a_0^2+a_1^2-a_2^2-a_3^2 & 2(a_1a_2-a_0a_3) & 2(a_1a_3+a_0a_2) \\ 2(a_1a_2+a_0a_3) & a_0^2-a_1^2+a_2^2-a_3^2 & 2(a_2a_3-a_0a_1) \\ 2(a_1a_3-a_0a_2) & 2(a_2a_3+a_0a_1) & a_0^2-a_1^2-a_2^2+a_3^2 \end{bmatrix} \tag{A9.6}$$

The components of the angular velocity vector are obtained from A6.7 and A9.3:

$$\underline{\omega} = \frac{2}{4-a_0} G\dot{\underline{a}} \tag{A9.7}$$

where

$$G = \frac{1}{4-a_0}\begin{bmatrix} a_0+\frac{a_1^2}{4} & \frac{a_1a_2}{4}-a_3 & \frac{a_1a_3}{4}+a_2 \\ \frac{a_1a_2}{4}+a_3 & a_0+\frac{a_2^2}{4} & \frac{a_2a_3}{4}-a_1 \\ \frac{a_1a_3}{4}-a_2 & \frac{a_2a_3}{4}+a_1 & a_0+\frac{a_3^2}{4} \end{bmatrix}. \tag{A9.8}$$

This matrix has the following remarkable properties:

$$GG = R; \quad GG^T = G^TG = I; \quad G\underline{a} = G^T\underline{a} = \underline{a} \tag{A9.9}$$

The components of the angular velocity vector in the rotating system are then:

$$\underline{\omega}^* = \frac{2}{4 - a_0} G^T \dot{\underline{a}} \tag{A9.10}$$

The matrix G is orthogonal, hence the following properties can be obtained:

$$\begin{aligned} \dot{G}G^T &= \tilde{\gamma}; \qquad \underline{\gamma} = \frac{1}{4 - a_0} H \dot{\underline{a}} \\ G^T \dot{G} &= \tilde{\gamma}^*; \qquad \underline{\gamma}^* = \frac{1}{4 - a_0} H^T \dot{\underline{a}} \end{aligned} \tag{A9.11}$$

where

$$H = \begin{bmatrix} 1 & -\frac{a_3}{4} & \frac{a_2}{4} \\ \frac{a_3}{4} & 1 & -\frac{a_1}{4} \\ -\frac{a_2}{4} & \frac{a_1}{4} & 1 \end{bmatrix}. \tag{A9.12}$$

This matrix has the following properties:

$$GH^T = H; \qquad G^T H = H^T; \qquad H\underline{a} = \underline{a} \tag{A9.13}$$

Other matrix functions of the Milenkovic Parameters also play an important role. The following matrices are defined for an arbitrary vector $\underline{b}$:

$$\begin{aligned} D(\underline{b}) &= \frac{1}{4 - a_0} \left[H^T \tilde{b}^T - \frac{1}{4} \underline{a}.\underline{b}^T \right]; \\ &= \frac{1}{4 - a_0} \left[-\tilde{b} + \frac{1}{4} \left(\tilde{a}\tilde{b} - \underline{a}.\underline{b}^T \right) \right] = \frac{1}{4 - a_0} \left[\frac{1}{4} \widetilde{\underline{a}\underline{b}} - \tilde{b} - \frac{1}{4} \left(\underline{a}^T \underline{b} \right) I \right]; \end{aligned} \tag{A9.14a}$$

$$\begin{aligned} D^*(\underline{b}) &= \frac{1}{4 - a_0} \left[H\tilde{b} - \frac{1}{4} \underline{a}.\underline{b}^T \right]; \\ &= \frac{1}{4 - a_0} \left[\tilde{b} + \frac{1}{4} \left(\tilde{a}\tilde{b} - \underline{a}.\underline{b}^T \right) \right] = \frac{1}{4 - a_0} \left[\frac{1}{4} \widetilde{\underline{a}\underline{b}} + \tilde{b} - \frac{1}{4} \left(\underline{a}^T.\underline{b} \right) I \right] \end{aligned} \tag{A9.14b}$$

and

$$\begin{aligned} E(\underline{b}) &= \frac{1}{4 - a_0} \left[H\tilde{b}^T - \frac{1}{4} \underline{a}.\underline{b}^T \right]; \\ &= \frac{1}{4 - a_0} \left[-\tilde{b} - \frac{1}{4} \left(\tilde{a}\tilde{b} + \underline{a}.\underline{b}^T \right) \right] = \frac{1}{4 - a_0} \left[-\tilde{b} - \frac{1}{4} \left(\underline{a}.\underline{b}^T + \underline{b}.\underline{a}^T - \left(\underline{a}^T.\underline{b} \right) I \right) \right] \end{aligned} \tag{A9.15a}$$

The off-diagonal terms of the D matrices are skew symmetric as can be seen from expanding their definition:

$$D(\underline{b}) = \begin{bmatrix} d_0 & -d_3 & d_2 \\ d_3 & d_0 & -d_1 \\ -d_2 & d_1 & d_0 \end{bmatrix}; \qquad \begin{bmatrix} d_0 \\ d_1 \\ d_2 \\ d_3 \end{bmatrix} = \frac{1}{4 - a_0} \begin{bmatrix} -\frac{a_1}{4} & -\frac{a_2}{4} & -\frac{a_3}{4} \\ -1 & -\frac{a_3}{4} & \frac{a_2}{4} \\ \frac{a_3}{4} & -1 & -\frac{a_1}{4} \\ -\frac{a_2}{4} & \frac{a_1}{4} & -1 \end{bmatrix} \begin{bmatrix} b_1 \\ b_2 \\ b_3 \end{bmatrix}; \tag{A9.16a}$$

$$D^*(\underline{b}) = \begin{bmatrix} d_0^* & -d_3^* & d_2^* \\ d_3^* & d_0^* & -d_1^* \\ -d_2^* & d_1^* & d_0^* \end{bmatrix}; \quad \begin{bmatrix} d_0^* \\ d_1^* \\ d_2^* \\ d_3^* \end{bmatrix} = \frac{1}{4-a_0} \begin{bmatrix} -\frac{a_1}{4} & -\frac{a_2}{4} & -\frac{a_3}{4} \\ 1 & -\frac{a_3}{4} & \frac{a_2}{4} \\ \frac{a_3}{4} & 1 & -\frac{a_1}{4} \\ -\frac{a_2}{4} & \frac{a_1}{4} & 1 \end{bmatrix} \begin{bmatrix} b_1 \\ b_2 \\ b_3 \end{bmatrix} \tag{A9.16b}$$

In contrast the off diagonal terms of the E matrices are not skew-symmetric

These matrices enjoy remarkable properties:

$$\begin{aligned} GD(\underline{b})G^T &= D(G\underline{b}); \quad G^T D(\underline{b})G = D\left(G^T\underline{b}\right); \\ RD(\underline{b})R^T &= D(R\underline{b}); \quad R^T D(\underline{b})R = D\left(R^T\underline{b}\right); \end{aligned} \tag{A9.17a}$$

$$\begin{aligned} GE(\underline{b})G^T &= E(G\underline{b}); \quad G^T E(\underline{b})G = E\left(G^T\underline{b}\right); \\ RE(\underline{b})R^T &= E(R\underline{b}); \quad R^T E(\underline{b})R = E\left(R^T\underline{b}\right); \end{aligned} \tag{A9.17b}$$

$$\begin{aligned} GD^*(\underline{b})G^T &= D^*(G\underline{b}); \quad G^T D^*(\underline{b})G = D^*\left(G^T\underline{b}\right); \\ RD^*(\underline{b})R^T &= D^*(R\underline{b}); \quad R^T D^*(\underline{b})R = D^*\left(R^T\underline{b}\right); \end{aligned} \tag{A9.17c}$$

Furthermore, they are related as follows:

$$\begin{aligned} &D(\underline{b})\underline{c} = E^T(\underline{c})\underline{b}; \quad D^*(\underline{b})\underline{c} = E(\underline{c})\underline{b}; \\ &GD(\underline{b}) = E(\underline{b}); \quad D(\underline{b})G = E\left(G^T\underline{b}\right); \\ &G^T D^*(\underline{b}) = E^T(\underline{b}); \quad D^*(\underline{b})G^T = E^T(G\underline{b}); \\ &E(\underline{b})\underline{c} = D^T(\underline{c})\underline{b} \end{aligned} \tag{A9.18}$$

where both $\underline{b}$ and $\underline{c}$ are arbitrary vectors.

These matrices appear when taking derivative of expressions containing Milenkovic Parameters. For instance, one can readily verify that:

$$\begin{aligned} \underline{b}^T\delta\left(\frac{G}{4-a_0}\right) &= \delta\underline{a}^T D(\underline{b})\left(\frac{G}{4-a_0}\right) = \delta\underline{a}^T E\left(\frac{G^T\underline{b}}{4-a_0}\right); \\ \underline{b}^T\delta\left(\frac{G^T}{4-a_0}\right) &= \delta\underline{a}^T D^*(\underline{b})\left(\frac{G^T}{4-a_0}\right) = \delta\underline{a}^T E^T\left(\frac{G\underline{b}}{4-a_0}\right); \\ \delta\left(\frac{G}{4-a_0}\right)\underline{b} &= \left(\frac{G}{4-a_0}\right)D^{*T}(\underline{b})\delta\underline{a} = E\left(\frac{G\underline{b}}{4-a_0}\right)\delta\underline{a}; \\ \delta\left(\frac{G^T}{4-a_0}\right)\underline{b} &= \left(\frac{G^T}{4-a_0}\right)D^T(\underline{b})\delta\underline{a} = E^T\left(\frac{G^T\underline{b}}{4-a_0}\right)\delta\underline{a}, \end{aligned} \tag{A9.19}$$

Finally, derivatives of these matrices become:

$$\delta(D(\underline{b})\underline{c}) = X(\underline{b},\underline{c})\delta\underline{a} + E^T(\underline{c})\delta\underline{b} + D(\underline{b})\delta\underline{c} \tag{A9.20}$$

where

$$X(\underline{b},\underline{c}) = -\frac{1}{4}\frac{1}{4-a_0}\left[\tilde{\underline{b}}\underline{c} + \left(\underline{b}^T\underline{c}\right)I + (D(\underline{b})\underline{c}).\underline{a}^T\right]. \tag{A9.21}$$

$$\delta(E(\underline{b})\underline{c}) = Y(\underline{b},\underline{c})\delta\underline{a} + D^*(\underline{c})\delta\underline{b} + E(\underline{b})\delta\underline{c} \tag{A9.22}$$

where

$$Y(\underline{b},\underline{c}) = -\frac{1}{4}\frac{1}{4-a_0}\left[\tilde{\underline{b}}\underline{c}^T + \left(\underline{b}^T\underline{c}\right)I + (E(\underline{b})\underline{c}).\underline{a}^T\right]. \tag{A9.23}$$

Composition of rotation is easily obtained from the corresponding relationships for the Euler Parameters. Let f_i *and* g_i be the Milenkovic Parameters of two successive rotations, and a_i the parameters of the resulting rotation, then A7.4 yields:

$$\frac{\underline{a}}{4-a_0} = \frac{A(f)\underline{g}}{(4-f_0)(4-g_0)} \tag{A9.24}$$

Computing a_0 from the first equation we obtain:

$$\underline{a} = \frac{4A(f)\underline{g}}{(4-f_0)(4-g_0) - f_0g_0 - f_ig_i} \tag{A9.25}$$

Other useful relationships can be readily obtained from the corresponding relationships on the Euler Parameters.

Within the range of $-\pi \leq \phi \leq \pi$ the Milenkovic Parameters present no singularities since

$$-4 \leq a_i \leq +4 \quad and \quad 0 \leq a_0 \leq 2, \tag{A9.26}$$

furthermore the orthogonality of the matrix G always yields a well defined angular velocity. However restricting the range of ϕ would limit the range of admissible rotations. Hence, then definition of the Milenkovic Parameters is generalized to allow any magnitude of rotation:

$$\begin{aligned} a_i = & 4u_i\, tg\left(\frac{\phi}{4} + \quad k \quad \frac{\pi}{2}\right) \qquad k\ even \\ & 4u_i\, tg\left(\frac{\phi}{4} + (k-1)\frac{\pi}{2}\right) \qquad k\ odd \end{aligned} \tag{A9.27}$$

where $-\pi \leq \phi \leq \pi$, and due to the following trigonometric identities:

$$\begin{aligned} & tg\left(\frac{\phi}{4} + \quad k \quad \frac{\pi}{2}\right) \equiv tg\left(\frac{\phi}{4}\right), \qquad k\ even; \\ & tg\left(\frac{\phi}{4} + (k-1)\frac{\pi}{2}\right) \equiv tg\left(\frac{\phi}{4}\right), \qquad k\ odd; \end{aligned} \tag{A9.28}$$

it is clear that the bounds A9.16 remain valid. If, at an instant during the motion of the structure, the rotation reaches, let say, the upper bound, i.e.:

$$\phi = \pi + \epsilon \qquad \epsilon \geq 0 \tag{A9.29}$$

or, in terms of the parameters:

$$a^2 \geq 16 \tag{A9.30}$$

one passes from the current state to a complementary one (i.e. from an even state to an odd one) to remain within bounds:

$$\phi \rightarrow \phi' = \phi - 2\pi; \quad k \rightarrow k' = k + 1 \tag{A9.31}$$

The corrected value of the parameters is:

$$\begin{aligned} a_i' &= 4u_i\, tg\left(\frac{\phi'}{4} + (k'-1)\frac{\pi}{2}\right) = 4u_i\, tg\left(\frac{\phi}{4} - \frac{\pi}{2} + k\frac{\pi}{2}\right) \\ &= 4u_i\, tg\left(\frac{\phi}{4} - \frac{\pi}{2}\right) = -4u_i / \, tg\left(\frac{\phi}{4}\right) = -16a_i / \, a^2 \end{aligned} \tag{A9.32}$$

a_0' can be shown to transform similarly so that:

$$a_i' = -16a_i/a^2 \qquad i = 0,1,2,3 \tag{A9.33}$$

and finally:

$$a' = 16/a \tag{A9.34}$$

which clearly shows that the passage to a complementary state decreases the norm of the Milenkovic Parameters.

References

A-1. Kane, T. R., Likins, P. W., and Levinson, D. A., Spacecraft Dynamics, McGraw-Hill Book Company, 1983.

A-2. Geradin, M., Robert, G., and Buchet, P.,"Kinematic and Dynamic Analysis of Mechanisms: a Finite Element Approach Based on Euler Parameters," Finite Element Methods for Nonlinear Problems, edited by P. Bergan et al., Springer-Verlag, 1986.

A-3. Geradin M., Cardona, A., "Kinematics and Dynamics of Rigid and Flexible Mechanisms using Finite Elements and Quaternion Algebra," Computational Mechanics, 1987.

NASA National Aeronautics and Space Administration

Report Documentation Page

1. Report No.	2. Government Accession No.	3. Recipient's Catalog No.
NASA CR-187597		

4. Title and Subtitle	5. Report Date
Nonlinear Dynamic Analysis of Flexible Multibody Systems	July 1991
	6. Performing Organization Code

7. Author(s)	8. Performing Organization Report No.
O. A. Bauchau and N. K. Kang	
	10. Work Unit No. 505-63-36-01

9. Performing Organization Name and Address	11. Contract or Grant No.
Rensselaer Polytechnic Institute Department of Mechanical Engineering, Aeronautical Engineering, and Mechanics Troy, NY 12180-3590	NAG1-1018
	13. Type of Report and Period Covered
12. Sponsoring Agency Name and Address	Contractor Report
National Aeronautics and Space Administration Langley Research Center Hampton, VA 23665-5225	14. Sponsoring Agency Code

15. Supplementary Notes

Langley Technical Monitor: Raymond G. Kvaternik
Final Report

16. Abstract

Two approaches are developed to analyze the dynamic behavior of flexible multibody systems. In the first approach each body is modeled with a modal methodology in a local non-inertial frame of reference, whereas in the second approach, each body is modeled with a finite element methodology in the inertial frame. In both cases, the interaction among the various elastic bodies is represented by constraint equations. The two approaches have been compared for accuracy and efficiency: the first approach is preferable when the nonlinearities are not too strong but it becomes cumbersome and expensive to use when many modes must be used. The second approach is more general and easier to implement but could result in high computation cost for large systems. The constraints should be enforced in a time derivative fashion for better accuracy and stability.

17. Key Words (Suggested by Author(s))	18. Distribution Statement
Flexible Multibody Dynamics Nonlinear Dynamics	Unclassified - Unlimited Subject Category - 39

19. Security Classif. (of this report)	20. Security Classif. (of this page)	21. No. of pages	22. Price
Unclassified	Unclassified	121	A06